Mechanisms of Apoptosis-Driven Carcinogenesis and Caspase 8-Dependent DNA Damage Response

Dissertation

zur

Erlangung der naturwissenschaftlichen Doktorwürde

(Dr. sc. nat.)

vorgelegt der

Mathematisch-naturwissenschaftlichen Fakultät

der

Universität Zürich

von

Yannick Thimotheus Böge

aus Deutschland

Promotionskomitee

Prof. Dr. Adriano Aguzzi (Vorsitz)

Prof. Dr. Mathias Heikenwälder (Leitung)

Prof. Dr. Achim Weber

Prof. Dr. Ian Frew

Zürich 2015

Die vorliegende Arbeit wurde von der mathematisch-naturwissenschaftlichen Fakultät der Universität Zürich auf Antrag von Professor Dr. Adriano Aguzzi als Dissertation angenommen.

1 Abbreviations

aCGH	array-based comparative genomic Hybridization
ALT	alanine transaminase
ALPPS	associating liver partition and portal vein ligation for staged hepatectomy
AOM	azoxymethane
APC	Adenomatous Polyposis Coli
AST	aspartate transaminase
ATM	ataxia telangiectasia mutated
ATR	ataxia telangiectasia and Rad3 related
BHA	butylated hydroxyanisole
BCL2-A1	Bcl-2-related protein A1
BSA	bovine serum albumin
cDNA	copy DNA
Casp8	caspase 8
CD	Crohn`s disease
cl.Casp3	cleaved caspase 3
DAMPs	damage-associated molecular patterns
DDR	DNA damage response
dpi	days post injection
DNA	deoxyribonucleic acid
DNA-PK	DNA-dependent protein kinase
DSS	dextran sulfate sodium
DX	doxorubicin
FCS	fetal calf serum
FFPE	formalin-fixed, paraffin-embedded
FITC	fluorescein isothiocyanate
gDNA	genomic DNA
GPNMB	glycoprotein nmb-like protein (“osteoactivin”)
HBV	hepatitis B virus
HCC	hepatocellular carcinoma
HCV	hepatitis C virus
H/E	Hematoxylin/Eosin staining
HRP	horse-radish peroxidase
IBD	inflammatory bowel disease
IECs	intestinal epithelial cells
IKKβ	inhibitor of nuclear factor kappa-B kinase subunit beta

IL	interleukin
ILC	innate lymphoid cell
i.p.	intraperitoneal
JNK	c-Jun N-terminal kinase
kDa	kilo Dalton
LPS	lipopolysaccharide
LTα	lymphotoxin alpha
LTβ	lymphotoxin beta
MAPK	mitogen-activated protein kinase
Mcl-1	myeloid cell leukemia 1
MDa	mega Dalton
mdr2	multidrug resistance gene 2
min	minute
mRNA	messenger ribonucleic acid
NFκB	nuclear factor kappa B
NVH	non-viral hepatitis
PHX	partial hepatectomy
PBS	phosphate-buffered saline
PBST	phosphate-buffered saline (with) Tween-20
PCR	polymerase chain reaction
PFGE	pulse field gel electrophoresis
PLK1	polo-like kinase 1
qPCR	quantitative PCR (real-time PCR)
Rag1	recombination activating gene 1
RIPK1	receptor-interacting serine/threonine-protein kinase 1
RIPK3	receptor-interacting serine/threonine-protein kinase 3
RNA	ribonucleic acid
ROS	reactive oxygen species
TAK1	TGFβ activated kinase
TGFβ	transforming growth factor beta
TINAG	tubulointerstitial nephritis antigen
TLR	toll-like receptor
TNFα	tumor necrosis factor alpha
TNFR	tumor necrosis factor receptor
UC	ulcerative colitis
WNT	Wnt family int1

2 Summary

Cancer is the second leading cause of death worldwide, accounting for 8.2 million deaths and an estimated 14 million newly diagnosed cases in 2012 [1]. The most common causes of death due to cancers are carcinoma of the lung (1.45 million/year), liver (0.75 million/year), stomach (0.72 million/year) and colon (0.69 million/year). The most important risk factor for cancer development is age and the most modifiable risk factors besides tobacco consumption are chronic infections and unhealthy life style. Patients with chronic diseases of the digestive system such as persistent infections (e.g. hepatitis due to infections with hepatitis B or C virus; chronic gastritis due to Helicobacter pylori infection), inflammatory bowel diseases (IBD) or metabolic disease (alcoholic and non-alcoholic steatohepatitis) are at higher risk to develop carcinoma of the liver, stomach or intestinal tract, respectively. However, the exact molecular, genetic and cellular mechanisms driving carcinogenesis in these chronically diseased organs remain elusive.

1.1 Constant hepatocyte apoptosis triggers proliferation-induced DNA damage and genetic instability in the liver and predisposes towards hepatocarcinogenesis

In the first part of my thesis, I investigated the molecular and genetic mechanisms of tumorigenesis in chronic liver disease.

Hepatocyte cell death is a hallmark of chronic liver disease (CLD), the background on which most hepatocellular carcinoma (HCC) develop [2]. In my doctoral thesis, I was able to show that constantly increased levels of hepatocyte apoptosis in human CLD as well as in several independent murine HCC models correlate with subsequent HCC development. Moreover, hyper-regenerative human and murine livers already revealed proliferation-associated DNA damage and genetic instability long prior the detection of dysplastic changes. Genetic reduction of elevated levels of hepatocyte apoptosis resulted in reduced levels of hepatocyte proliferation, DNA damage, genetic instability and significantly reduced HCC development *in vivo*.

In addition, I uncovered an oncogenic gene expression pattern in regenerating mouse livers, which is highly overlapping and similar to expression patterns found in murine and human HCC. Expression of these genes significantly correlated with patient survival and thus these genes are of potential interest as biomarkers for liver malignancy and tumorigenesis.

These findings suggest that - independent of the underlying etiology - the accumulated amount of apoptotic liver cell death not only correlates with, but is the decisive determinant of liver carcinogenesis.

1.2. A non-apoptotic function of Caspase 8 mediates DNA damage response via JNK1/2

Most interestingly, when studying mechanisms of apoptosis-driven hepatocarcinogenesis, I uncovered a novel DNA damage response (DDR) pathway in hepatocytes. A (dynamic) signaling platform comprising a non-catalytic, scaffolding function of Caspase 8, a kinase-dependent function of receptor interacting protein kinase 1 (RIPK1) and cFLIP controls the activity of c-Jun N-terminal kinase (JNK) and the JNK-dependent phosphorylation of the key component in DNA repair, histone variant H2AX (γH2AX), independent of TNFR1 signaling. Hepatocyte-specific deletion of Caspase 8 or cFLIP, or genetic or pharmacological inhibition of RIPK1 abolished DDR and decreased DDR in mice post partial hepatectomy and genotoxic challenge.

2. Chronic intestinal tissue damage suffices to trigger hyper-proliferation, IBD-like inflammation and carcinogenesis

In the second part of my thesis, I focused on intestinal regeneration and carcinogenesis. Based on the observation that constant hepatocyte cell death suffices to trigger hepatocarcinogenesis, I asked whether the concept of apoptosis-triggered tumorigenesis is also transferable to other regenerative organs, in particular the intestinal tract. Enterocyte-specific knock-out of the anti-apoptotic protein Mcl-1 (Mcl-$1^{\Delta IEC}$ mice) led to disruption of the epithelial barrier, severe consecutive intestinal inflammation, and intestinal carcinogenesis, thus recapitulating central features of inflammatory bowel diseases (IBD)

By germ-free housing and antibiotic treatment I was able to show that the inflammatory reaction was triggered by a leaky intestinal barrier and the influx of microbiota. Using $RAG1^{-/-}$ intercrossings and antibody treatments of Mcl-$1^{\Delta IEC}$ mice, I identified innate lymphoid cells (ILCs) - and not classical B- and T-lymphocytes - as the most important immune cell type responsible for intestinal inflammation upon intestinal barrier disruption. Furthermore, Mcl-$1^{\Delta IEC}$ mice morphologically and genetically recapitulated the well-described adenoma-carcinoma sequence and finally developed invasive carcinoma harboring chromosomal aberrations and mutations in well-described genes of human colorectal cancer. For the first time, I showed that constant enterocyte cell death suffices to drive intestinal carcinogenesis under genotoxic-free conditions.

3 Zusammenfassung

Krebserkrankungen gelten heute als die zweithäufigste Todesursache und die Ursache für 8,2 Millionen Todesfälle und geschätzte 14 Millionen Neuerkrankungen im Jahr 2012. Die meisten Todesfälle, die auf Krebserkrankungen zurückzuführen sind, resultieren aus Krebserkrankungen der Lunge (1,45 Millionen Todesfälle/Jahr), der Leber (0,75 Millionen/Jahr), dem Magen (0,72 Millionen/Jahr) und dem Darm (0,69 Millionen/Jahr). Der Hauptrisikofaktor für eine Krebsentstehung ist das Alter, gefolgt von beeinflussbaren Risikofaktoren wie Tabakkonsum, ein ungesunder Lebensstil und chronische Infektionen.

Patienten mit chronischen Erkrankungen des Verdauungstrakts wie zum Beispiel chronischen Infektionen (HBV/HCV-induzierte Hepatitis, Helicobacter pylori-induzierte chronische Gastritis), chronisch entzündlichen Darmerkrankungen oder chronischen metabolischen Erkrankungen (alkoholische oder nichtalkoholische Steatohepatitis) weisen ein erhöhtes Krebsrisiko für die Leber, den Magen oder den Intestinaltrakt auf. Die genauen molekularen, genetischen und zellulären Mechanismen, die zur Krebsentstehung in diesen chronisch erkrankten Organen führen, sind bisher wenig verstanden.

1.1. Konstanter Hepatozyten-Zelltod führt zu proliferations-induziertem DNA Schaden, genetischer Instabilität und prädisponiert die Leber für eine Krebsentstehung

In dem ersten Teil meiner Doktorarbeit habe ich die molekularen und genetischen Mechanismen der Krebsentstehung in chronisch erkrankten Lebern untersucht.

Chronische Lebererkrankungen sind gekennzeichnet durch eine erhöhte Rate an induzierten Tod von Hepatozyten und bilden somit den Hintergrund, auf dem am häufigsten Hepatozellulären Karzinome (HCC) entstehen. In der vorliegenden Doktorarbeit konnte ich zeigen, dass eine konstant erhöhte Rate von induziertem Zelltod von Hepatozyten in humanen chronischen Lebererkrankungen und in verschiedenen unabhängigen Mausmodellen mit der Krebsentstehung korreliert. Hyper-regenerative humane und murine Lebern zeigten bereits lange Zeit vor dem Nachweis von dysplastischen Veränderungen eine proliferations-assoziierte DNA Schädigung und genetische Instabilität. Eine durch genetische Manipulation reduzierte Rate von Zelltod führte im Mausmodell ebenfalls zu reduzierter Hepatozytenproliferation, DNA Schädigung, genetischer Instabilität und signifikant weniger Lebertumoren.

Zusätzlich habe ich ein Expressionsmuster von Onkogenen in regenerativen Mauslebern gefunden, das sehr ähnlich zu dem Expressionsprofil dieser Gene in humanen und murinen HCC ist. Die Expression dieser Onkogene korrelierte signifikant mit dem Überleben der Patienten, weshalb diese Gene möglicherweise als Biomarker für die Malignität der Leber oder die Lebertumorigenese von Interesse sind.

1.2. Eine nicht-apoptotische Funktion von Caspase 8 vermittelt eine DNA Schadensantwort durch die Aktivierung von JNK

Interessanterweise habe ich bei der Analyse der Zelltod-gesteuerten Mechanismen der Hepatokarzinogenese einen neuen Signalweg der DNA Schadensantwort entdeckt. Eine dynamische Signalplatform, bestehend aus einer katalytischen inaktiven und bindenden Caspase 8, einer Kinase-abhängigen Funktion von Receptor interacting protein kinase 1 (RIPK1) und cFLIP. Dieser Komplex kontrolliert unabhängig vom TNFR Signalweg die Aktivität der c-Jun N-terminal kinase (JNK) und die JNK-abhängige Phosphorylierung der Schlüsselkomponente für die DNA Reparatur, das Histon H2AX (γH2AX) – und ähnelt dem Ripoptosome Komplex. Die Inhibierung des neuen Signalwegs zum Beispiel durch die Deletion von Caspase 8 oder cFLIP, oder die genetische oder pharmakologische Inhibierung von RIPK1 in Hepatozyten vermindert die Antwort auf DNA Schädigung nach partieller Hepatektomie oder genotoxischer Behandlung.

2. Chronischer intestinaler Gewebeschaden reicht aus um eine Hyper-Regeneration, chronische Entzündung und Karzinogenese auszulösen

Basierend auf der Beobachtung der Leberkarzinogenese aufgrund einer konstant erhöhten Rate von induziertem Zelltod in Hepatozyten, habe ich die Frage gestellt, ob das Konzept der Zelltod-gesteuerten Karzinogenese auch auf andere regenerative Organe, insbesondere den Intestinaltrakt übertragbar ist. Der Enterozyten-spezifische Knock-out des anti-apoptotischen Proteins Mcl-1 (Mcl-1$^{\Delta IEC}$ Mäuse) zeigte wesentliche Aspekte von chronisch entzündlichen Darmerkrankungen mit einer Störung der intestinalen Barriere, gefolgt von schwerer intestinaler Entzündung und Karzinogenese.

Ich konnte durch keimfreie Haltung oder die Behandlung von Mcl-1$^{\Delta IEC}$ Mäuse mit Antibiotika zeigen, dass die Entzündungsreaktion von der Störung der intestinalen Barriere und dem Einströmen der Mikrobiota abhängig war. Ich konnte durch eine RAG1$^{-/-}$ Rückkreuzung und Antikörper Behandlungen zeigen, dass nicht die klassischen B- und T-Lymphozyten, sondern innate lymphoid cells die wichtigsten Immunzellen für die intestinale Entzündung nach Barriereverlust sind.

Die Pathologie der Mcl-1$^{\Delta IEC}$ Mäuse spiegelt genetisch und morphologisch die Adenom-Karzinom Sequenz wider, welche zu invasiven Karzinomen mit Mutationen und chromosomalen Aberrationen führt. Zum ersten Mal konnte so gezeigt werden, dass der chronisch induzierte Zelltod von intestinalen Epithelzellen alleine ausreicht, um intestinale Karzinogenese ohne Gabe von genotoxischen Substanzen zu induzieren.

4 The role of hepatocyte apoptosis in DNA damage response and tumorigenesis

Parts of the 'Introduction', 'Material and Methods', 'Results' and 'Discussion' section are reproduced or adapted from the following manuscript (in preparation):

"A novel RIPK1/c-FLIP/CASP8-dependent pathway mediates DNA damage response via JNK signaling in hepatocytes"

Yannick Boege[1], Mohsen Maleh Mir[1], Akshay Ahuja[2], Monika Wolf[1], Mihael Vucur[3], Friederike Böhm[1], Lukas Frick[1], Joachim Mertens[4], Beat Müllhaupt[4], Holger Moch[1], Regina Boger[5], Henning Schulze-Bergkamen[5], Tobias Speicher[6], Susagna Padrissa-Altés[6], Sabine Werner[6], Christiane Koppe[3], Tom Lüdde[3], Massimo Lopes[2], Ricardo Weinlich[5], Douglas Green[5], Christopher Dillon[5], Emmanuel Dejardin[6], Mathias Heikenwälder[1,7]* and Achim Weber[1*]

[1] Institute of Surgical Pathology, University Hospital Zürich, Switzerland
[2] Institute of Molecular Cancer Research, University of Zürich, Switzerland
[3] University Hospital RWTH Aachen, Germany
[4] Institute of Gastroenterology and Hepatology, University Hospital Zürich, Switzerland,
[5] National Center for Tumor Diseases (NCT), University of Heidelberg, Germany
[6] Institute for Molecular Health Sciences, ETH Zürich, Switzerland
[5] St.Jude Children's Research Hospital, Memphis, U.S.A.
[6] GIGA-Research, University of Liège, Belgium
[7] Institute of Virology, Helmholtz Center Munich/TU Munich, Germany
* These authors contributed equally to this work

4.1 Introduction

4.1.1 Introduction: Global burden of cancer

Cancer is one of the leading causes of death worldwide, accounting for 8.2 million deaths accompanied by estimated 14 million newly diagnosed cases in 2012 [3]. In 2014, the latest WHO cancer report predicts a significant increase in cancer incidence, doubling within the next two decades, with approximately 22 million new cases and 13 million deaths due to cancer to be expected per year.

The most common causes of death due to cancer are carcinoma of the lung (1.59 million deaths/year), liver (0.75 million/year), stomach (0.72 million/year), colon (0.69 million/year) and breast (0.52 million/year) (Figure 1), but the most frequent types of cancer differ between men and women. In men, lung cancer was the most common cancer diagnosed in 2012 with 1.18 million/year (16.7% of all cases in men). In women, breast cancer is the most common type of cancer, diagnosed in 1.7 million women in 2012 (25.2% of all new cases) [3].

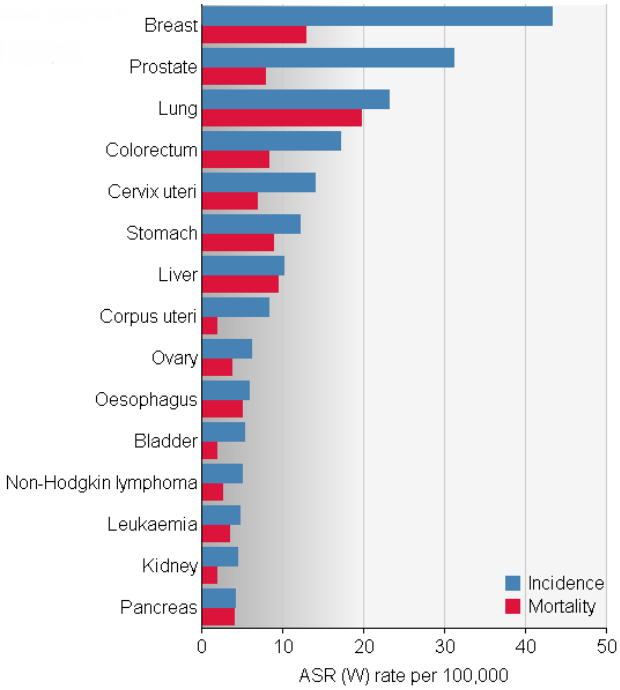

Figure 1: Estimated cancer incidence and mortality rates (both sexes) in 2011. 14 million new cancer cases and 8.2 million cancer deaths are expected to rise up to 22 million new cases within the next 2 decades. Figure from WHO-Cancer Fact Sheet [1].

Tobacco consumption is the most important modifiable risk factor for cancer development, causing 71% of deaths due to lung cancer and 22% of cancer deaths in total. The second most important risk factor for cancer is chronic infection. Persistent infection with Helicobacter pylori, hepatitis B, C and human papilloma virus taken together account for around 1.9 million cases of gastric, liver and cervix uteri cancer per year being responsible for estimated 20% of total cancer-related deaths (Figure 2). Around 30% of all cancer deaths are due to an unhealthy life style combining an metabolic syndrome, low fruit and vegetable intake, lack of physical activity with tobacco and alcohol consumption [3].

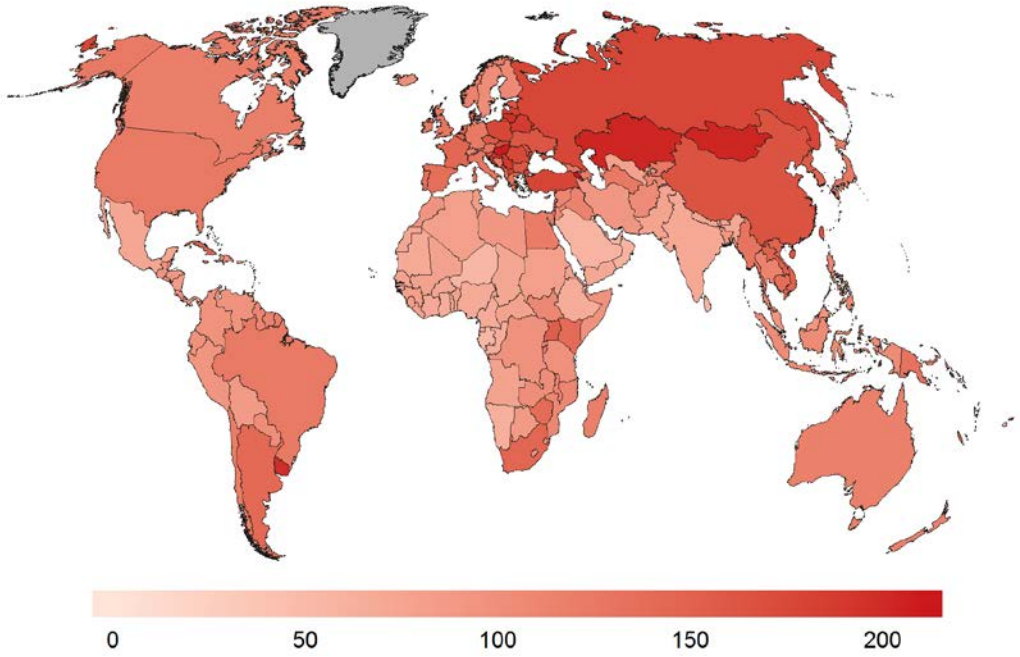

Figure 2: Estimated Cancer Mortality Worldwide in 2012 (only men). In men, the mortality rates are 15% higher in more developed compared to less developed regions in men. The mortality is 8% higher in women compared to men due to high incidence and mortality of breast cancer. In men, the highest rates are in Central and Eastern Europe (173/100.000) and the lowest are in Western Africa (69/100000) Color code: estimated age-standardized rates (world) per 100.000. Figure from WHO-Cancer Fact Sheet [1].

4.1.2 Cancer of the digestive system

All of the above described risk factors directly or indirectly affect the organs of the digestive system. Especially liver, intestine and stomach are at high risk to become affected by infections or inappropriate diet.

The most prevalent risk factor for liver cancer development has been chronic hepatitis, mainly due to persistent infection with hepatitis B or C viruses (HBV or HCV). However, the most common etiology for HCC in Western countries has recently changed from viral infections to obesity and therefore HCC is the most rapidly increasing type of cancer in the U.S., with around 19.000 new cases and 17.000 deaths in 2007 [4]. A strong link between obesity and cancer is well established and a body mass index (BMI) >25 substantially increases the risk for developing cancer [5].

4.1.3 Chronic liver disease and liver cancer

In the majority of cases, liver tumor development is caused by chronic liver disease (CLD), which substantially increases the risk for tumor development independent of their etiology. In most circumstances, CLD are characterized by increased hepatocyte damage and hepatocyte death [6]. Activation of an energy-dependent, apoptotic cell death program is a means of keeping liver homeostasis, resulting in the controlled elimination of damaged hepatocytes, thus preventing accumulation of genotoxic events [7]. Therefore, hepatocyte apoptosis can be considered as hallmark of CLD, independent of etiology.

4.1.4 Parameters for analyzing hepatocyte cell death in patients

The health status of the liver can be assessed non-invasively in serum of patients by measuring various parameters. The most important markers for CLD measured in serum are aminotransferases such as alanine (ALT) or aspartate aminotransferase (AST), alkaline phosphatase, bilirubin and bile acids. Additional markers such as miR-122 or keratin-18 are also used but not frequently applied in clinics.

Aminotransferases are cytoplasmic enzymes that catalyze the transfer of amino groups. Whereas AST is also expressed in cardiac and skeletal muscle, ALT expression is restricted to hepatocytes. ALT and AST are released from dying hepatocytes into the blood stream and can be used as liver-specific markers to monitor acute and chronic liver dysfunction. ALT is the most common and established biomarker for diagnosis and monitoring of CLD and it can be even correlated with the progress of fibrosis and cirrhosis in HBV-positive patients and the liver-specific mortality in the population [8, 9].

4.1.5 Cell death in chronic liver disease

Clinical data and mouse models indicate that hepatocyte death is the key trigger of chronic liver disease and the main reason for the development of inflammation, fibrosis and cirrhosis (Figure 3) [10]. The phenotypical outcome of hepatocyte death largely depends on the different forms of cell death with respect to the inflammatory reaction or regeneration rate. Different forms of cell death have been described during the last years based on their characterization on molecular level, but the three most prevalent forms in the liver are apoptosis, necrosis and necroptosis [11, 12].

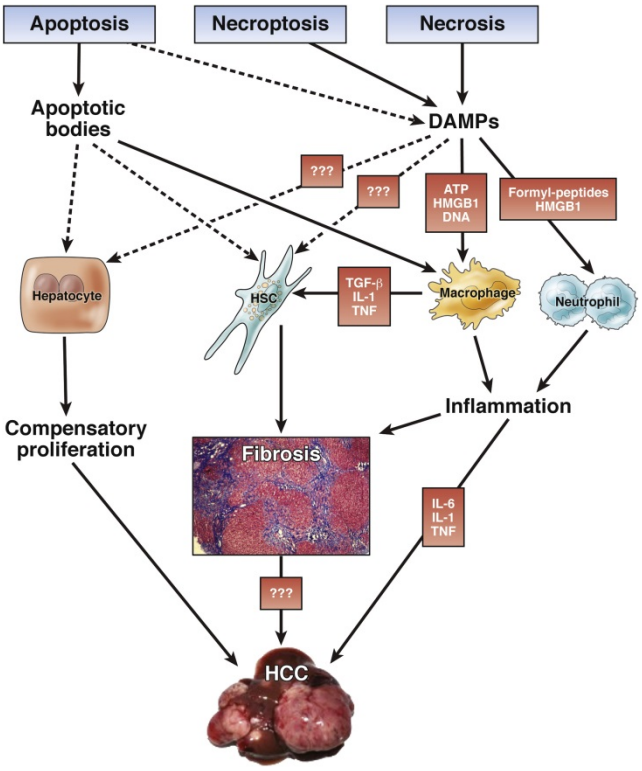

Figure 3: Cell death in chronic liver disease. In chronic liver disease, apoptosis, necroptosis, and necrosis lead to compensatory hepatocyte proliferation, HSC activation, inflammatory cell recruitment and activation. The long term outcomes potentially are fibrosis, chronic hepatitis, cirrhosis and HCC development. Figure from Luedde et al [10].

4.1.6 Apoptosis

Programmed cell death is an active process and plays an important role to maintain liver tissue homeostasis. Apoptosis is a self-protective function of hepatocytes for the clearance of hepatotropic viruses, pathogens and to remove aberrant hepatocytes to prevent the malignant transformation. Hepatocytes express high levels of death receptors and are highly susceptible to death receptor induced cell death (Figure 4) and death receptor mediated apoptosis is a common feature of chronic and acute liver diseases [13]. Apoptosis is tightly controlled and can be actively induced by extrinsic or intrinsic signaling pathways and finally leads to the activation of effector caspase and subsequently to cellular shrinkage, nuclear fragmentation, DNA laddering and formation of apoptotic bodies (Figure 4).

4.1.7 Extrinsic apoptosis

The extrinsic apoptosis pathway is triggered via activation of cell surface bound death receptors through binding of their cognate ligands. All death receptors belong to the tumor necrosis factor receptor superfamily (TNFRSF) and for hepatocytes the expression of the following receptors is known: TNFR1, TNFR2, Fas/CD95, TRAILR and TWEAK [14]. Their ligands (FasL/CD95L, TNFα, and TRAIL) are mainly expressed by cells of the immune system and are crucial for the elimination of virally infected, transformed, or damaged hepatocytes. The ligand binding to the receptor first leads to trimerization and is followed by

the recruitment of several adaptor protein to form the so-called death-inducing signaling complex (DISC) (Figure 4A). First, the TNFR-associated death domain (TRADD) protein is recruited to the cytoplasmic death domain of the death receptor and second the Fas-associated protein with death domain (FADD) binds to TRADD. The association of TRADD and FADD leads to the induction of apoptosis via the recruitment and cleavage of pro-Caspase 8, whereas binding of TNF-associated factor 2 (TRAF2) to TRADD initiates NFκB or JNK signaling pathways [15] (Figure 4D). TNFR complex IIb, also called necrosome, is formed under some cellular conditions such as presence of RIPK3 or reduced Caspase 8 activity in which RIPK3 is recruited to RIPK1 allowing mutual phosphorylation and subsequent activation of necroptosis executer protein MLKL (Figure 4B).

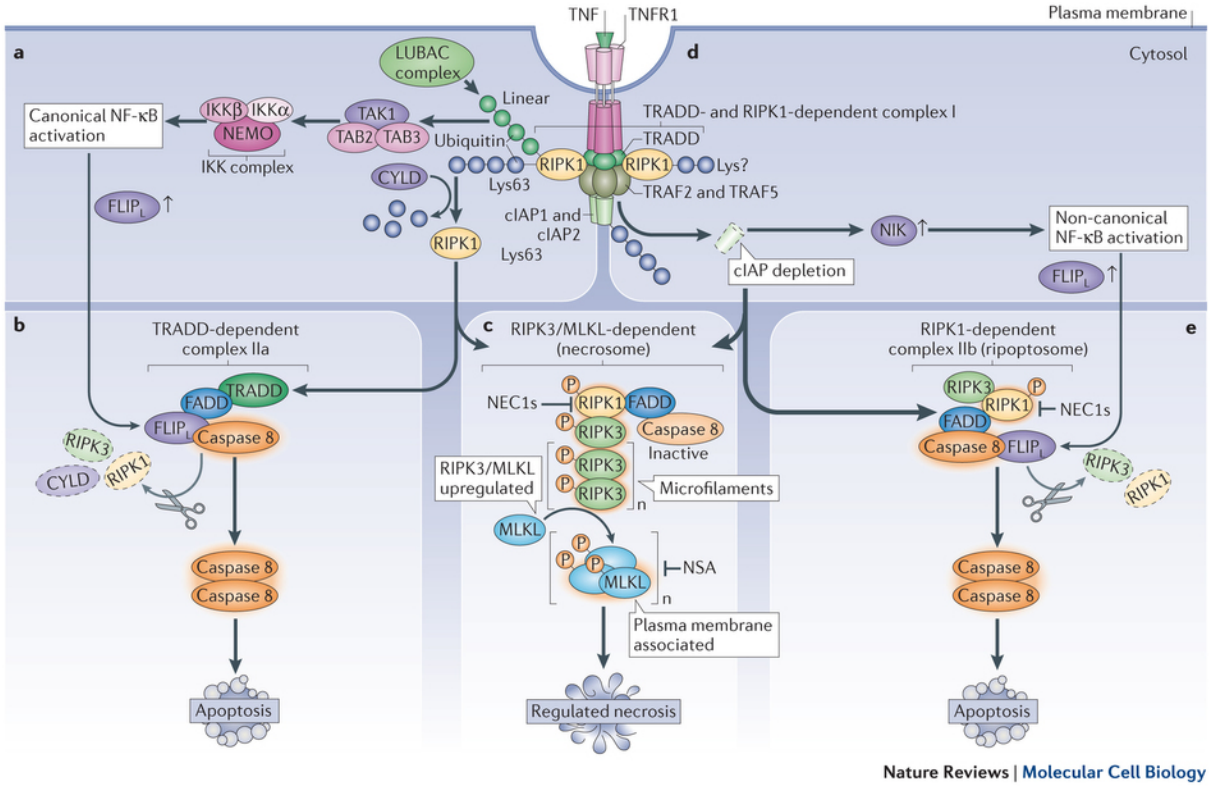

Figure 4: Activation of TNFR can lead to apoptosis, necroptosis or cell survival. Binding of TNFα to TNFR1 lead to its trimerization and recruitment of TNFR-associated death domain (TRADD), TNFR-associated factor 2 (TRAF-2) and receptor-interacting protein 1 (RIPK1) and further binding partners to form the death-inducing signaling complex (DISC), also called TNFR complex I. This complex may activate NF-κB and mediate cell survival by inducing a number of anti-apoptotic molecules (Bcl-xL, cIAPs, cFLIP, A20) and therefore inhibiting apoptosis. After internalization of the DISC, FADD and Caspase 8 are recruited and form the pro-apoptotic TNFR complex IIa or the pro-necroptotic complex IIb (also called necrosome). The complex IIa inhibits RIPK1 and RIPK3 and allows the release of Caspase 8 inhibitory protein cFLIP and subsequent Caspase 8 homodimerization and activation, finally leading to the activation of executioner Caspase 3.
The cytosolic FADD-RIPK1-RIPK3-cFLIP-Caspase 8 complex, also defined as ripoptosome complex, is formed independent of death receptor activation upon cellular stress and eventually leads apoptosis induction or inflammasome activation. Figure from Vanden Berghe et al [16].

4.1.8 Apoptosome-dependent apoptosis (type 2)

The activated Caspases 8 and 10 trigger a proteolytic cascade, leading to activation of effector caspases (Caspase 3, 6, and 7) and finally cleavage and degradation of cellular proteins resulting in cell death (Figure 4B).

There are two different signaling pathways described for the activation of effector pathways, defined as “type 1 death receptor signaling” and “type 2 death receptor signaling”. Whereas type 1 signaling, the direct cleavage of effector caspases through initiator caspases, is mainly taking place in lymphocytes, type 2 signaling occurs in hepatocytes via formation of the cytoplasmic apoptosome [14]. The assembly of the apoptosome complex depends on Cytochrome c released from the mitochondria and dATP to the binding of the cytosolic protein Apaf1, which serves as central scaffold protein [17]. The assembled apoptosome is a heptameric complex of around 1.4 MDa with a seven-fold symmetry structure and a Cytochrome c/Apaf1 ratio of 1:1. Next, the inactive pro-Caspase 9 is recruited as monomer or dimer to the apoptosome complex and activated by auto-cleavage, but the exact mechanisms how the apoptsome serves as platform for autocleavage of pro-Caspase 9 is still poorly understood [17]. Activated Caspase 9 itself leads activation of the caspase cascade by cleavage and therefore activation of the downstream effector caspases 3, 6 [17].

4.1.9 Intrinsic apoptosis

Whereas the extrinsic apoptotic pathway is activated by death receptors on the plasma membrane, the intrinsic apoptotic pathway is initiated by cytochrome c release upon disruption of the outer mitochondrial membrane caused by pro-apoptotic stimuli such as DNA damage, endoplasmic reticulum (ER) stress or the activated pro-apoptotic Bcl-2 family members BAX or BAK [18, 19]. Anti-apoptotic proteins of the Bcl-2 family (Bcl-2, Mcl-1, Bcl-x) prevent the mitochondrial outer membrane permeabilization (MOMP) by binding and neutralization of pro-apoptotic family members [19]. Upon disruption of the outer mitochondrial membrane the released cytochrome c triggers the formation of the apoptosome and the execution of cell death.

4.1.10 Necrosis

Chronic liver diseases do not only show signs of programmed and tightly controlled cell death, but also others forms of cell death are observed, for example in alcoholic livers and non-alcoholic fatty liver disease [20]. Necrosis is defined as an acute form of accidental cell death as a consequence of an extreme cytotoxic stimulus, e.g. physicochemical stress, such as heat, osmotic shock or mechanical stress, which does not share features of apoptosis and autophagy [11, 21]. Necrosis is morphologically characterized by a gain in cell volume

(oncosis), swelling of organelles, plasma membrane rupture and subsequent uncontrolled loss of intracellular contents [11].

4.1.11 Necroptosis

For a long time, necrosis has been considered as an accidental and uncontrolled form of cell death, but pathways regulating the execution of necrosis have been described in the last few years and consequently the term “necroptosis” was defined [22]. Necroptosis is mainly mediated by TNFRSF members or Toll-like receptors (TLR) in a RIPK1-dependent manner (Figure 4C). RIPK1 in the DISC remains inactive through ubiquitination and serves as a scaffold protein and consequently contributes to the survival-promoting effects by mediating TNF-dependent activation of the pro-survival pathways NFκB and MAP kinase. The RIPK1-specific deubiquitinating enzyme CYLD leads to the de-ubiquitination and to the activation of the RIPK1 kinase activity and the recruitment and binding of RIPK1 to RIPK3 and MLKL to form the necrosome complex. The necrosome complex mediates the activation of RIPK3 and MLKL, two crucial downstream mediators of necroptosis, and finally leads to membrane permeabilization to induce necrotic cell death (Figure 4C) [11, 22].

4.1.12 Cell death and inflammatory response

Apoptosis was considered as none or low-inflammatory process in the liver due to the rapid clearance of apoptotic bodies by engulfment through phagocytic cells, i.e. macrophages or granulocytes [11]. But recent studies described the release of intracellular cytokines (e.g. IL1, TNFα) during apoptotic processes as an important mechanism to alert the immune system of tissue damage and to initiate the tissue healing. The cytokine and chemokine secretion under non-infectious conditions has been defined as “sterile inflammation” [23, 24].

In contrast, necrosis and necroptosis are described as highly immune stimulatory events. The uncontrolled release of cellular contents triggers a strong inflammatory response in solid tissues, while the inflammatory reaction itself further promotes cell death, constituting a feed-forward loop [22, 25]. The uncontrolled release of immunogenic molecules called ‘‘damage-associated molecular patterns’’ (DAMPs) and include HMGB1, IL-1a, uric acid, DNA fragments, mitochondrial content and ATP (Figure 5).

It was recently shown that Caspase 8 and FADD suppress a RIPK1 and RIPK3-dependent necroptotic cell death and inflammatory response in murine keratinocytes and murine intestinal epithelial cells. Both, necroptotic cell death as well as subsequent inflammation could be rescued by additional pharmacological inhibition of RIPK1 or genetic deletion of RIPK3 [25]. Stimulation of TNFR1 by TNF triggered necroptotic cell death and chronic ilitis with TNFα being mainly MyD88-dependent produced as response to bacterial infection [25].

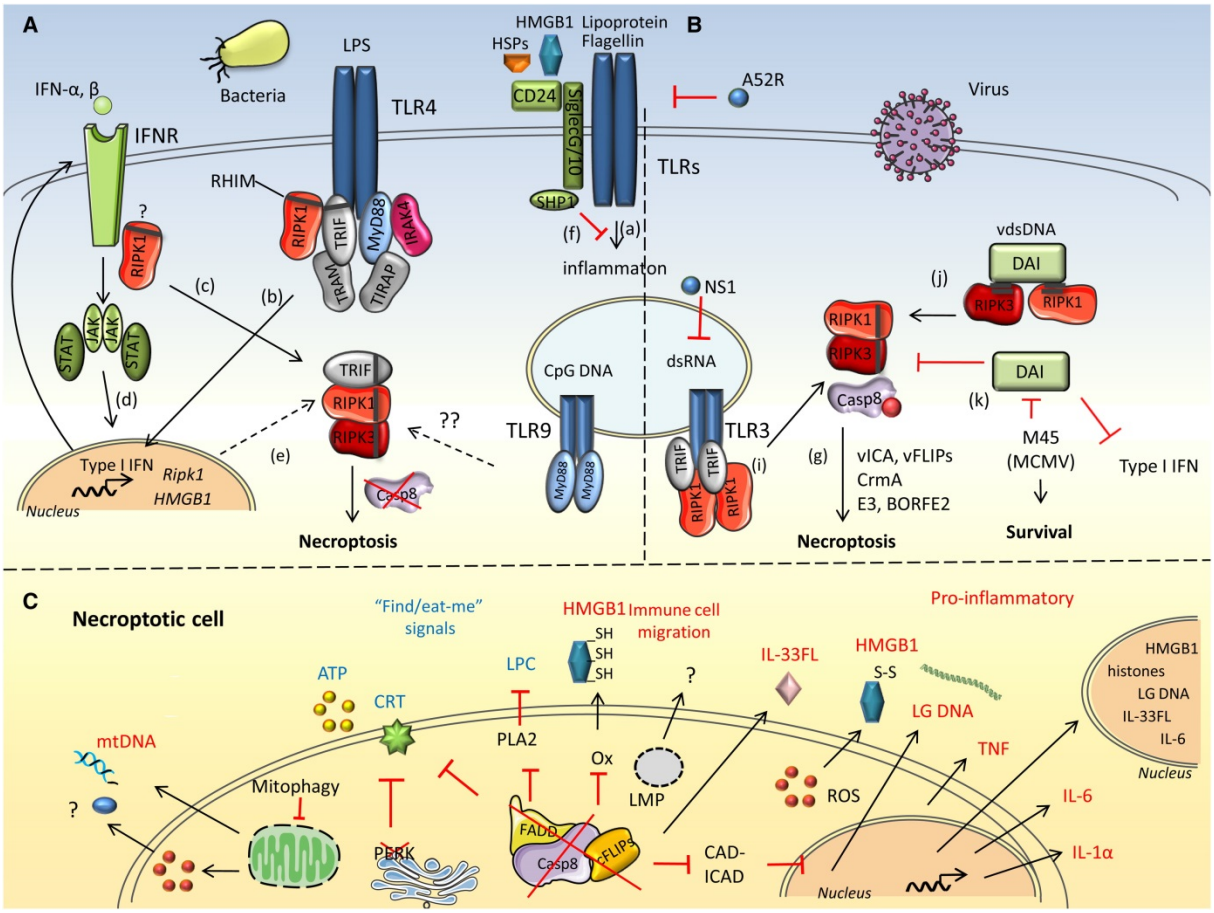

Figure 5: Inflammatory cell death and release of DAMPs. A) and B) Pathogen triggered necroptotic cell death via TLRs when Caspase 8 is inhibited or genetically ablated. Additionally, stimulation of TLRs by PAMPs can provoke inflammatory responses in infected cell C) Necroptotic cell death is highly immune stimulatory due to the widebroad and unspecific release of DAMPs, e.g. HMBG1, IL1, TNFα and ATP. Figure from Kaczmarek et al [25].

4.1.13 Cell death and liver regeneration

Apoptosis contributes to tissue homeostasis in solid and regenerative organs and is needed for the removal of damaged hepatocytes in the liver and to keep the equilibrium between loss and replacement of hepatocytes [10]. Most of the hepatocytes rest in G0 phase and the proliferation and turn-over rate of hepatocytes under normal physiological conditions is very low (about 0.05% of hepatocytes) as reflected by almost undetectable aminotransferase levels. The liver has an unique ability to control regeneration processes and quickly adjust liver tissue regeneration in response to massive hepatocyte death or loss of liver mass [10], as seen in acute liver failure due to toxin or poison uptake or surgical resection of liver mass. But also under non-acute conditions, the constant uptake of food-derived toxins, alcohol consumption or a persistent hepatic inflammation with hepatotropic virus may lead to persistently increased hepatocyte death, as known from patients suffering from chronic HBV

or HCV infection or life-style related chronic liver diseases such as NAFLD, ASH or NASH. In these chronically diseased livers, increased levels of hepatocyte apoptosis and liver tissue regeneration and the promoted development of liver fibrosis, cirrhosis and hepatocarcinogenesis is well known [10].

4.1.14 Liver cancer and hepatocellular carcinoma

Tumors of the liver are classified by the World Health Organization (WHO) due to their origin into epithelial or non-epithelial tumors. Malignant tumors derived from hepatocytes are named hepatocellular carcinoma (HCC) (Figure 6) and account for 75% of all liver cancers, whereas benign tumors are called hepatocellular adenoma. Cholangiocarcinoma, tumors derived from bile ducts account for approximately 6% of primary liver cancers [4, 26].

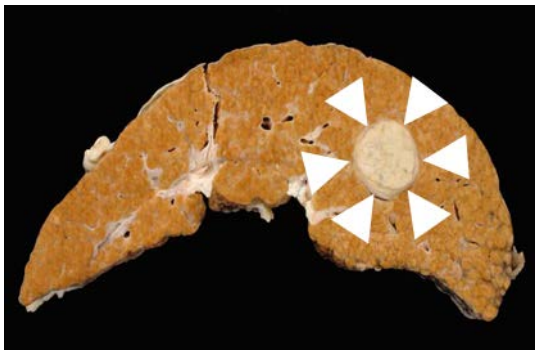

Figure 6: Macroscopic appearance of HCC. HCC are visible macroscopically as clear and distinct nodular structures in in the liver. Figure from Flejou et al. [27].

HCC is the most frequent and clinically significant primary neoplasia, and is almost always lethal. Only 5-9% of patients survive for five years or more from the time point of diagnosis. The incidence of HCC has doubled in the US and Europe in the past four decades. In line, the most common etiology for HCC in industrialized countries has recently switched from viral infections to obesity, making HCC the most rapidly increasing type of cancer in the U.S., with 19,160 new cases and 16,780 deaths in 2007 [4, 26].

HCC have various epidemiologic features including variations among (I) geographic regions, (II) racial and ethnic groups, (III) gender and (IV) environmental risk factors. In almost all populations worldwide males are more likely to be affected by HCC than females (Figure 7) [28]. The male:female ratio persists around 2:1 to 4:1 and is declared to the exposure of risk factors.

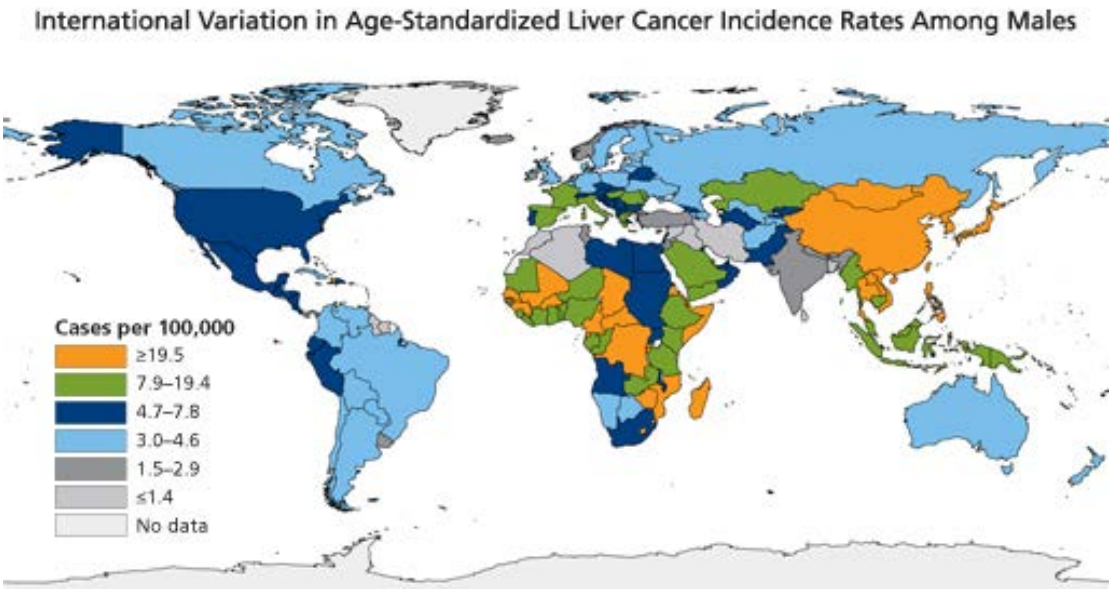

Figure 7: Liver cancer incidence worldwide, only males. For men, the average lifetime risk of getting liver or bile duct cancer is approximately 1 in 100, for women 1 in 250. Liver cancer mainly occurs in less developed regions where 83% of the estimated 782,000 new cancer cases worldwide occurred in 2012 [1, 29].

4.1.15 HCC treatments: diagnosis, resection and transplantation

Non-invasive imaging tests like computer tomography (CT) or magnetic resonance imaging (MRI) made it possible to detect early lesions with more than 2 cm in diameter in the liver because the radiologic changes are related to increased vascularity in the hepatocellular carcinoma and can be detected easily. Additional liver needle biopsies are necessary to validate the tumor finding in case of unclarity. The choice of treatment depends on the cancer stage and different curative or palliative treatments available, but the treatment finally depends on the tumor stage at the day of diagnosis [28]. According to the so-called Milan criteria, patients suffering from an early-stage HCC with less than 5 cm in diameter or up to 3 lesions each less than 3 cm in diameter, with preserved liver function normally undergo surgical transplantation and show a 5-year survival rate of up to 75% [30]. Since the Milan criteria were implemented the numbers of liver transplantation in HCC patients have increased worldwide and currently in Europe around 27% of all patients with solid organ transplantation suffer from HCC [31]. To assess the need for liver transplantation for patients suffering from liver dysfunction due to HCC, the Child-Pugh classification or model for end-stage liver disease (MELD) criteria are used to predict the potential survival of the patient and set the priorities for transplantations.

Systemic therapy with the sorafenib (Nexavar®), a small molecule that inhibits cell proliferation and angiogenesis by inhibiting RAF1 and VEGF, is currently the best option for

advanced HCC. Monotherapy with sorafenib significantly prolonged overall survival of patients and the 1-year survival rates were 44% with sorafenib versus 33% with placebo and also the median time to progression was prolonged to 7.6 versus 2.8 months [32]. A combination therapy of sorafenib plus doxorubicin showed a significantly longer survival of patients (13.7 months) compared to placebo plus doxorubicin treated patients (6.5 months) [33].

4.1.16 Genetic alterations in hepatocellular carcinoma

Various genetic alterations mount up during the process of hepatocarcinogenesis and progressively provoke the malignant transformation of hepatocytes by altering expression of genes controlling cell cycles and cell proliferation [34, 35]. Genetic alterations also decrease the genomic integrity for example by inactivating the machinery of sensing and repairing DNA damage or the correct chromosomal segregation during mitosis, which can lead to aneuploidia.

Malignant hepatocytes in HCC accumulate a large number of chromosomal rearrangements leading to highly complex karyotypes. About 40% of all HCC reveal an aneuploid genome and numerical chromosomal abnormalities [34]. Malignant tumors are in general highly aneuploid, containing an uncommon number of chromosomes. The chromosomal regions involved frequently in structural rearrangements are located on chromosomes 1, 7 and 8 [36] and exhibit structural alterations such as translocations, deletions and amplifications. The first chromosomal abnormality detected in human tumors was the Philadelphia chromosome. This chromosomal aberration is generated by reciprocal translocation involving the ABL oncogene, a tyrosine kinase on chromosome 9. The ABL gene locus is linked close to the BCR (breakpoint cluster region) on chromosome 22, leading to the expression of the BCR-ABL gene product [37]. However, chromosomal alterations provide important evidence to the genetic changes in cancer. The chromosomal alterations in human solid tumors such as carcinoma are heterogeneous and complex. Therefore, the comprehensive knowledge of a broad field of genetic alterations in tumor subtypes and the study of the correlation between these alterations and the different clinical and histological parameters allow to refine the tumor classification and the understanding of the multi-step carcinogenesis process [34] [38].

4.1.17 The role of oncogenes and tumor suppressor genes in tumorigenesis

Hepatocarcinogenesis is tightly linked to chronic liver damage but hardly occurs in healthy liver. One possible driver of carcinogenesis and chromosomal aberrations in hepatocytes is the high proliferation rate occurring in chronic liver damage – also named compensatory proliferation. Multiple genetic mutations can activate oncogenes or disrupt/inactivate tumor

suppressor genes [39]. Mutations or aberrant expression of oncogenes, as well as activation of oncogenic pathways found the basis for the malignant transformation of healthy hepatocytes. Oncogene expression patterns of tumors can differ between various types of cancer and also within the same subclass of cancer. Therefore, expression analysis of oncogenes is a tool to classify tumor subtypes in humans. In human liver cancer, increased expression levels of the ras subfamily, namely H-ras, N-ras and K-ras, have been reported [40]. The RAS proteins are GTPases involved in cell signal transduction and activating mutations lead to the permanently activation of cell growth and cell division. The oncogenic activation links (I) enhanced cell proliferation, (II) resistance to apoptosis and (III) the self-sufficiency in growth signals to the uncoupling of cell growth from extrinsic regulatory signals, finally leading to limitless replication and carcinogenesis [41]. Tumor suppressor genes, or in fact the proteins these genes encode, mediate various functions including the repression of cell cycle promoting genes, sensing of DNA damage and apoptosis.

4.1.18 Hallmarks of cancer

During the multi-step process of hepatocarcinogenesis numerous genetic and cellular alterations select for proliferative and survival advantages of malignant cells [39]. The complexity of cellular and genetic alterations allowing cancer cells to survive, proliferate and disseminate was summarized for the first time in the year 2000 by Douglas Hanahan and Robert Weinberg as the six hallmarks of cancer, namely (I) self-sufficiency in growth signals, (II) evading growth suppressors, (III) resisting cell death, (IV) replicative immortality, (V) inducing angiogenesis and (VI) tissue invasion and metastasis [41]. In addition, inflammation was added as the seventh hallmark of cancer, but inflammation was actually already described by Rudolph Virchow in the year 1863, uncovering the tumor promoting effects of the inflammatory micro-environment [42].

Remarkable progress in cancer research has been achieved in the last years and new observations and conclusions deepened the understanding of cancer biology leading to additional hallmarks of cancer. (VIII) Evading immune destruction, but also (IX) reprogramming of energy metabolism and (X) genome instability & mutations have been added to the classical hallmarks of cancer (Figure 8) [43]. The hallmarks summarize the enabling and emerging characteristics of cancer, but to understand the complex progress of carcinogenesis, one has also to consider the tumor micro-environment, cancer stem or progenitor cells and overlapping signaling networks as important determinants. Furthermore, cell type specific reactions for example due to the differentiation status or tissue environment may lead to different cellular outcome.

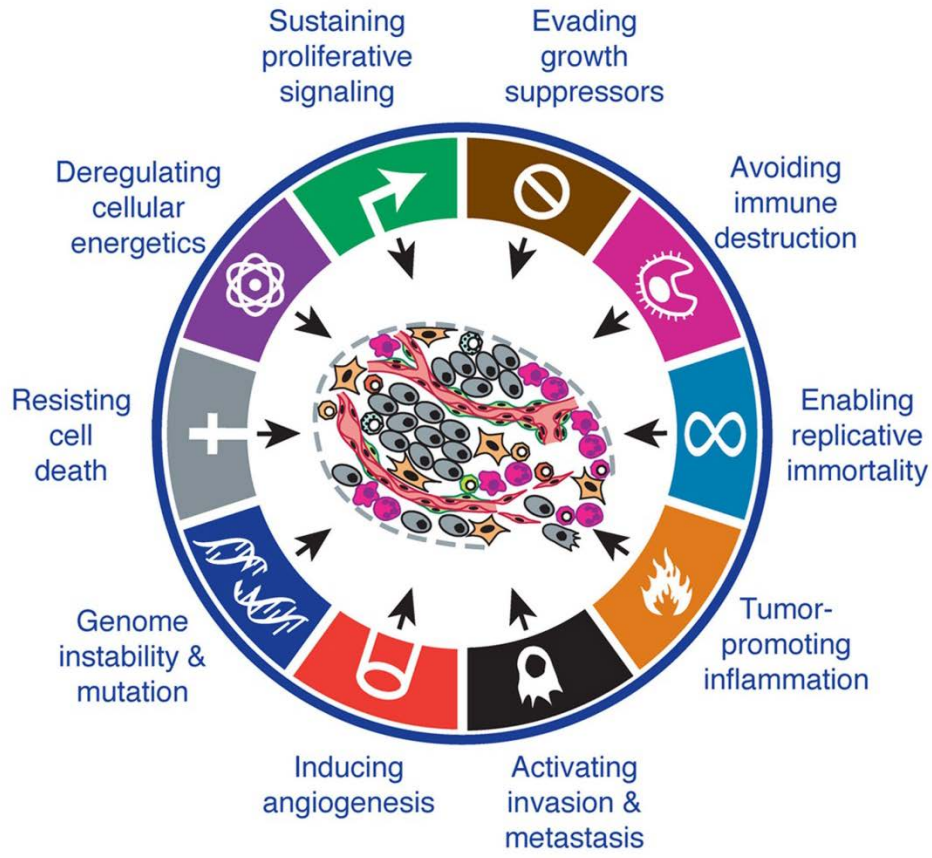

Figure 8: Hallmarks of cancer. The initially described acquired capabilities defining the hallmarks of cancer I) self-sufficiency in growth signals, II) evading growth suppressors, III) resisting cell death, IV) replicative immortality, V) inducing angiogenesis and VI) tissue invasion and metastasis have be complemented. The emerging hallmarks VII) reprogramming energy metabolism and VIII) evading immune destruction as well as the enabling characteristics IX) tumor-promoting inflammation and X) genome instability and mutation have been added. Figure adapted from Hanahan and Weinberg [43].

4.1.19 Mouse models for cell death and hepatocarcinogenesis

The relevance of constant hepatocyte cell loss in driving chronic liver regeneration and hepatocarcinogenesis is very well described in different mouse models for spontaneous development of HCC (Table 1) [44]. Increased hepatocyte apoptosis in non-transformed hepatocytes could be observed in TAK1$^{\Delta hep}$, Mcl-1 $^{\Delta hep}$ as well as Bcl-xl $^{\Delta hep}$ knock-out mice and a causal link to HCC development in relation to hepatocyte apoptosis is already shown [45-48].

The hepatocyte-specific deletion of TAK1 leads to apoptotic and necrotic hepatocyte death, accompanied by enhanced liver cell proliferation and HCC development at 4 months of age. Of note, the additional Caspase 8 knock-out prevented hepatocyte apoptosis and subsequently led to reduced liver regeneration and abrogated tumor development. Whereas the additional knock-out of RIPK3 prevented necrotic cell death, it leads to increased rates of

apoptotic and proliferative hepatocytes resulting in a higher tumor burden. The TAK1$^{\Delta hep}$ mouse model demonstrated that hepatocyte apoptosis-driven liver regeneration and not necroptotic hepatocyte cell death promotes hepatocarcinogenesis [49].

The hepatocyte-specific knock-out of the anti-apoptotic Bcl-2 family members Bcl-xl and Mcl-1 lead to spontaneous induction of hepatocyte apoptosis, accompanied by compensatory hyper-proliferation to restore liver mass and function. Over time, the hyper-apoptotic and hyper-proliferative environment in Bcl-xl$^{\Delta hep}$ and Mcl-1$^{\Delta hep}$ mice leads to spontaneous liver tumor formation, with an incidence of 27% in Bcl-xl$^{\Delta hep}$ and 50% in Mcl-1$^{\Delta hep}$ mice at 12 months and 88% in Bcl-xl $^{\Delta hep}$ and 100% in Mcl-1$^{\Delta hep}$ mice at 18 months. Interestingly, the additional knock-out of the pro-apoptotic counter-player Bak in Mcl-1$^{\Delta hep}$ mice rebalanced hepatocyte apoptosis to a physiological level and finally completely abolished tumorigenesis in Mcl-1$^{\Delta hep}$ mice, showing that tumor development is not a functional consequence of the knock-out of Mcl-1 but rather due to the apoptotic rate in hepatocytes [45]. The following table is adapted from Ringelhan et al. and Weber et al. and shows some of the currently used genetic mouse models to study HCC development *in vivo* [44, 50].

Table 1: Frequently used HCC mouse models. Several mouse models have been established in the past 30 years to study liver tumorigenesis. Some of the most frequently used are listed below. Due to space limitations not all HCC models are listed. Table adapted from Weber et al [44]

Models	Phenotype	Known mechanism
Transgenic models		
AlbLTαβ	Chronic inflammation, fibrosis, dysplasia, HCC at 12 months	Chronic hepatitis, cell damage, apoptosis, compensatory hepatocyte proliferation, genomic instability
Alb-c-myc	Dysplasia, preneoplastic foci, adenoma, HCC at 12–15 months	Apoptosis induction, enhanced proliferation, genomic instability
c-myc/TGFα	Dysplastic and apoptotic changes in hepatocytes multiple focal lesions, HCC at 8 months	Acceleration of neoplastic development compared to single transgenic models
Knockout models		
Mcl-1$^{\Delta hep}$	Apoptoses, architectural disarray, fibrosis, dysplastic nodules and 50% HCC incidence at 12 months	Spontaneous hepatocyte apoptosis leading to chronic liver damage and compensatory proliferation
Mdr2$^{-/-}$	Cholastasis, inflammation, 100% HCC incidence at 10 months, metastasis	Mice are unable to secrete phospholipids into bile leading to liver disease
NEMO$^{\Delta hep}$	Steatohepatitis, liver fibrosis, dysplasia, 100% HCC incidence at 11 months	Increased apoptotic hepatocyte death and subsequent compensatory proliferation
TAK1$^{\Delta hep}$	Steatohepatitis, liver fibrosis, biliary cirrhosis, 100% HCC incidence at 4 months	TAK1 deficiency leads to Caspase 3- mediated apoptosis accompanied by enhanced liver cell proliferation
Dietary models / chemically-induced models		
Choline-deficient high fat diet	Recapitulated key features of human metabolic syndrome, NASH and HCC, 30% HCC incidence at 12 months, –	NKT cell secreted LIGHT mediated steatosis, activated CD8(+) T cells and NKT cell triggered liver damage
Choline-deficient diet	Steatosis, HCC at 11–12 months	Formation of oval cells due to oxidative DNA damage and chromosomal instability finally leading to generation of hepatocytes
DEN wild-type	Acute hepatitis, hepatocyte proliferation, HCC at 8–10 months	Chemically-induced DNA damage leading to genetic mutations
Transgenic models / viral genes		
HBV X protein	Cytoplasmic vacuolations, neoplastic lesions, HCC at 13 months	Transcriptional transactivation of viral genes leading to altered host gene expression and carcinoma
HCV core	Steatosis, HCC at 16 mo	Core protein acts as transcriptional activator affecting the proliferative ability of hepatocytes, ROS production, transcriptional activation of TNF and IL1
SV40 T-Ag	Hyperplastic hepatocytes, dysplasia, HCC at 3 months, lung metastasis	SV40 T-Ag-mediated immortalisation, cell transformation, aberrant DNA replication

4.2 Scientific Questions

As described above, hepatocyte apoptosis seems to be the main driver of hepatocarcinogenesis in chronically diseased human livers and in different mouse models, but the exact molecular mechanisms driving malignant hepatocyte transformation and hepatocarcinogenesis are still poorly understood.

In my doctoral thesis, I aim to understand the molecular mechanisms driving tumor development in chronically diseased livers. More precisely, I aim to answer the following questions:

- Is the Mcl-1$^{\Delta hep}$ mouse a suitable model to study human hepatocarcinogenesis?

- Are the central mechanisms found in the Mcl-1$^{\Delta hep}$ mouse model applicable to human hepatocarcinogenesis?

- What are the molecular mechanisms driving the malignant transformation of hepatocytes in a hyper-apoptotic and hyper-proliferative environment?

4.3 Results

4.3.1 Increased hepatocyte apoptosis and regeneration correlate with DNA damage and genetic instability in human chronic liver diseases

Hepatocyte apoptosis is a hallmark of human chronic liver diseases (CLD) independent of the underlying etiology [6, 10]. Increased levels of hepatocyte apoptosis in CLD correlate with increased levels of proliferating hepatocytes reflecting regeneration. In addition, positivity for the DNA damage marker γH2AX has been described in livers of HBV- and HCV-infected patients, with a sequentially increase in γH2AX positivity from normal to chronic hepatitis, liver cirrhosis, dysplastic nodules and HCC [51, 52].

In the herewith presented doctoral thesis, I observed DNA damage response by γH2AX immunohistochemistry (Figure 9) and immunofluorescence (Figure 10A) in liver tissue from patients independent of etiology. The analyzed etiologies included viral hepatitis (HBV, HCV), autoimmune hepatitis (AIH) and a metabolic disorder, precisely nonalcoholic steatohepatitis (NASH) (Figure 9).

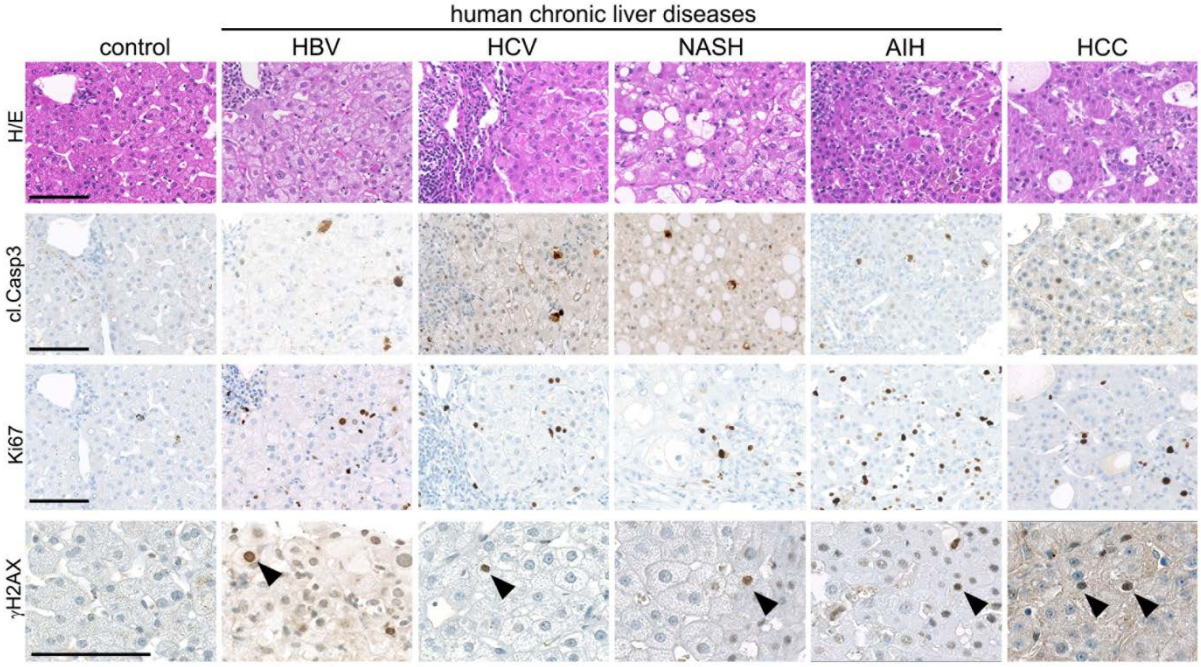

Figure 9: Increased levels of hepatocyte apoptosis, constant regeneration and DNA damage response in chronically diseased human livers and HCC. Human CLD of different etiology including chronic viral hepatitis (HBV, HCV), metabolic (NASH) and autoimmune (AIH) diseases show increased levels of hepatocyte apoptosis (cl.Casp3), proliferation (Ki67) and signs of DNA damage (γH2AX). Scale bars: 100 μm.

Furthermore, I have been able to validate the activation of DNA damage response (DDR) on protein level with immunoblotting for pCHK2 and pCHK1 (Figure 10B), indicating the activation of the two major pathways for single strand and double strand repair (ATR- and ATM-mediated pathways), as well as increased mRNA expression levels of genes of the DNA repair machinery (e.g. Rad51, Exo1, Ddit3) in liver tissue specimen from HBV, HCV and NASH patients (Figure 10C).

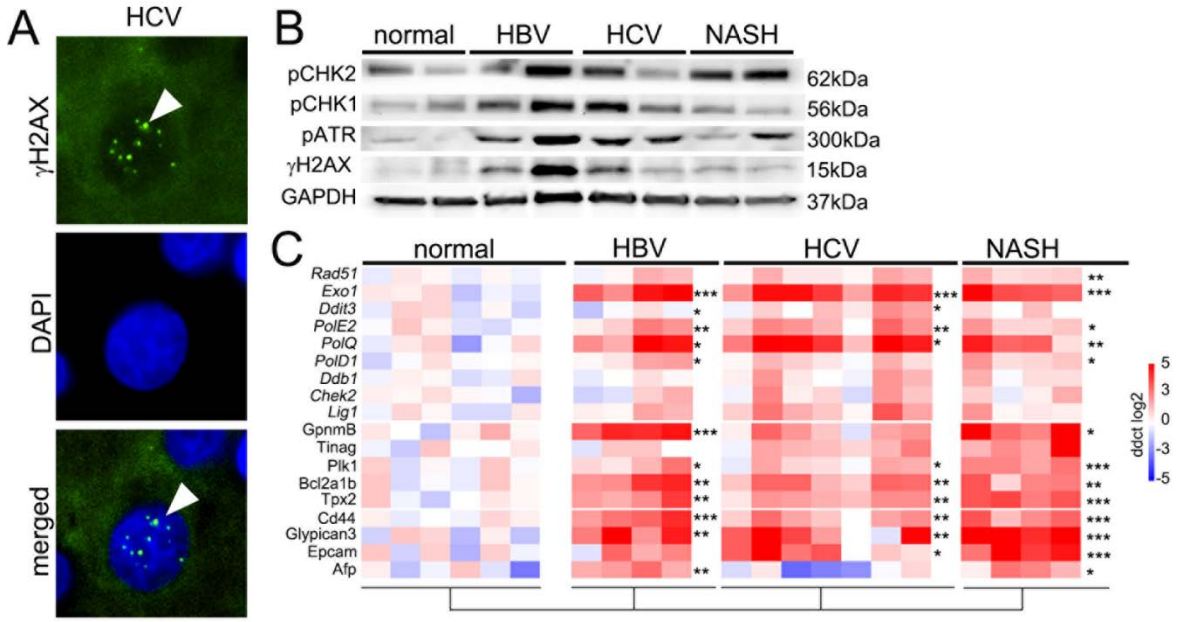

Figure 10: Activation of DNA damage response pathways in CLD tissue. A) Representative immunofluorescence staining demonstrated typical dotted γH2AX foci in the nucleus, indicating DNA damage response. B) Western blots of CLD tissues (liver needle biopsies) revealed activation of proteins associated with DNA repair. C) Increased mRNA expression levels of genes associated with DNA repair in CLD tissue and markers of malignancy analyzed by qPCR. *p < 0.05; **p < 0.01; ***p < 0.001.

The DDR in highly proliferative tissue is considered to reflect replicative stress associated DNA damage, e.g. a stalled or collapsed replication fork and subsequent single or double strand breaks. Therefore, I next addressed the question whether hyper-proliferation in regenerative livers induces genetic instability at chromosomal fragile sites, which are well-known to be susceptible for spontaneous breakage during replication-associated DNA stress and were described to reflect genetic instability in pre-cancerous lesions [53]. I analyzed gDNA from micro-dissected liver tissue of different areas of the same liver needle biopsy by TaqMan copy number assay (Figure 11A) and fragment length analysis (Figure 11B). Interestingly, I could detect significant levels of genetic instability by both methods in chronically diseased livers compared to control patients.

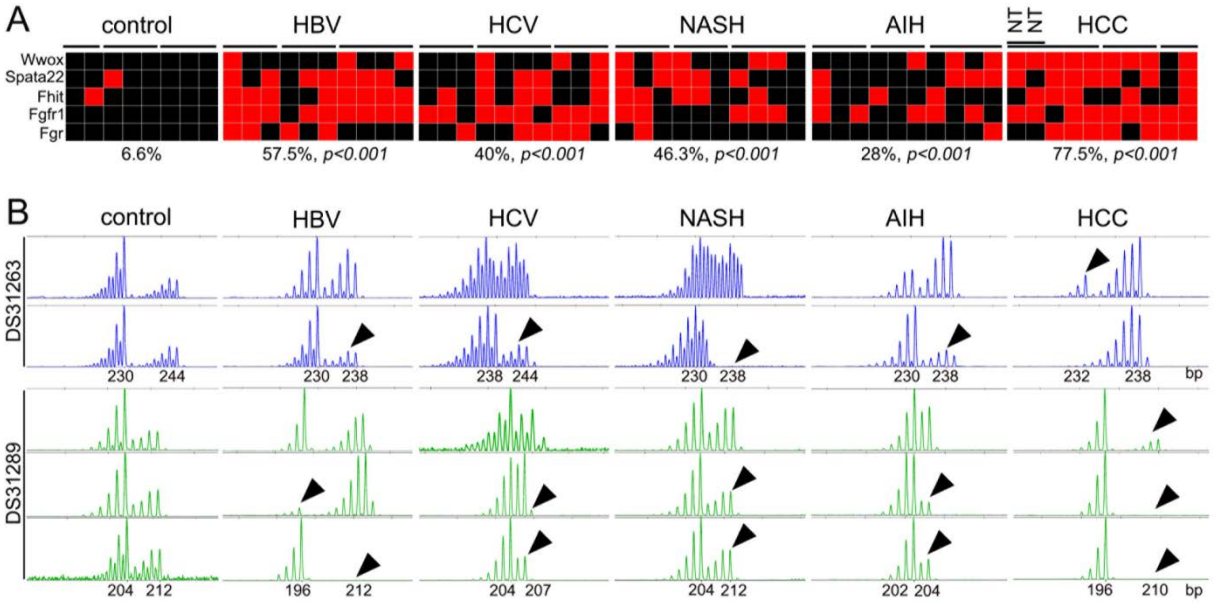

Figure 11: Genetic instability in CLD tissue. A) Increased rates of allelic imbalances (AI) reflecting genetic instability were detected in CLD tissues by TaqMan copy number assay at chromosomal fragile sites. Each square represents one area of microdissected liver tissue and lines indicating different distinct areas of the same liver (red: AI; black: no AI). B) AI was also detected in CLD tissues by fragment length analysis for the loci DS31263 and DS31289 (indicated by arrow heads). A) and B) Representative samples are shown and n=20 control, n=30 HBV, n=22 HCV, n=20 NASH, n=8 AIH, and n=31 HCC and n=6 corresponding non-tumor tissue samples have been analyzed. Statistics calculated by Pearson's Chi-square test compared to control tissue. Chromosomal fragile sites were selected and analyzed according to Gorgoulis et al. [53].

DDR activation and genetic instability were described to correlate with the dysplastic character of pre-cancerous lesions in skin, lung and colon and contribute to tumor progression [53, 54]. In addition, I have been able to detect a shift of gene expression towards a malignant character of chronically diseased HBV, HCV and NASH livers by detecting the significant overexpression of liver malignancy markers Afp, Epcam, Glypican3 and CD44 as well as tumor marker Glypican3 on RNA level.

4.3.2 Increased hepatocyte apoptosis correlates with HCC development in human CLD

Based on the above presented data, I concluded that chronically diseased livers - as reflected by elevated serum transaminase levels (Figure 12) - already possess a pre-cancerous character of early tumor progression and are of high risk for promoting the malignant transformation towards liver tumor development.

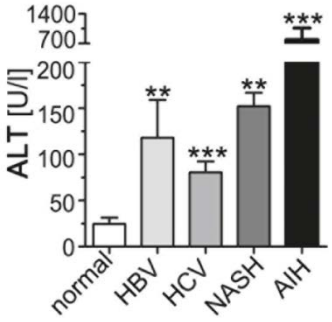

Figure 12: Elevated serum ALT levels detected in human CLD of various etiologies indicating liver damage hepatocyte death. Serum of n=8 normal , n=4 HBV, n=8 HCV, n=4 NASH and n=4 AIH patients was analyzed.

Therefore, I hypothesized that constant hepatocyte death in combination with compensatory proliferation would trigger the malignant transformation of chronically diseased livers and the constant accumulation of genetic and cellular changes over time would significantly contribute to liver tumor development.

To test this hypothesis, I sought for an association between serum transaminase levels and HCC development in a retrospective analysis of patients with HCC versus tumor-free patients and we designed a retrospective cohort study with chronically HCV-infected patients with the defined endpoint HCC diagnosis (Clinic for Gastroenterology and Hepatology/USZ, Prof. Dr. Beat Müllhaupt/ Dr. Joachim Mertens). We compared HCC patients to HCV-positive control patients without HCC development with similar liver function over the years according to their MELD score.

Interestingly, HCC and non-HCC patients did not differ with respect to their serum albumin or bilirubin levels confirming the same liver function, but HCC patients displayed significantly higher ALT and AST levels in the years preceding HCC diagnosis (Figure 13). This finding confirmed the hypothesis that apoptosis-driven hepatocyte death and liver damage significantly contribute to liver tumorigenesis and might be the first and crucial step for tumor initiation and development in chronically diseased livers.

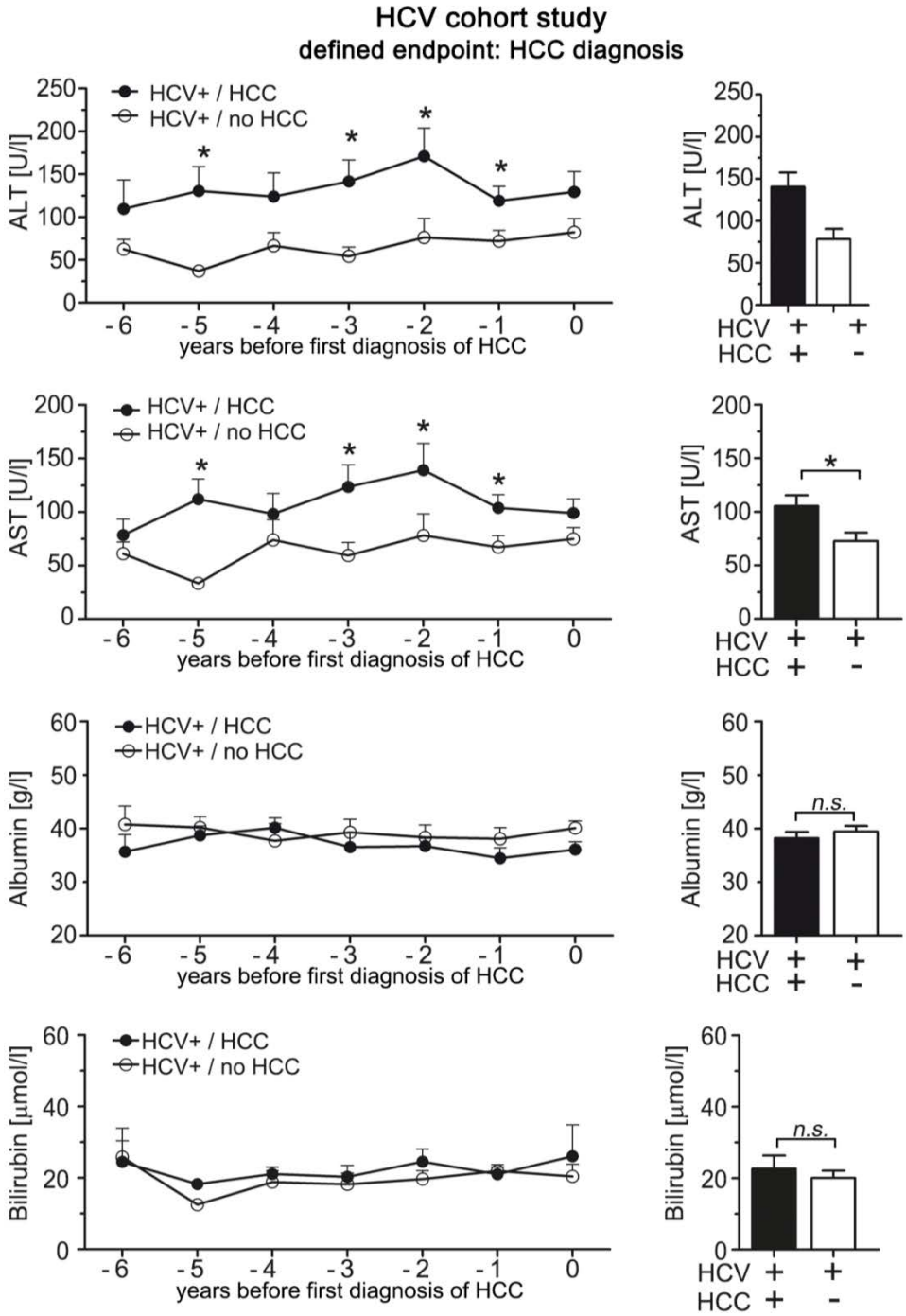

Figure 13: Retrospective cohort study with the defined endpoint of HCC diagnosis. ALT levels in patients with chronic HCV infection and HCC development compared to matched HCV patients without HCC development. n=19 patients were grouped to control patients without HCC development with the same liver function according to the MELD score (based on serum bilirubin, serum creatinine, and the international normalized ratio for prothrombin time (INR). Equal level of serum albumin confirms the same liver function between both groups, whereas patients with HCC development showed significantly elevated ALT levels prior first diagnosis of HCC. Left panel: time course 6 years prior to HCC diagnosis; right panel: mean of values over time.

4.3.3 HCC from Mcl-1$^{\Delta hep}$ mice reveal morphology similar to human HCC

If hepatocyte apoptosis is the first step in driving liver tumorigenesis and if there is a causal link between hepatocyte cell death and HCC development, I hypothesized that the reduction or ablation of hepatocyte apoptosis in the liver would finally reduce tumorigenesis.

To address this question I analyzed the impact of hepatocyte apoptosis on tumor development in Mcl-1$^{\Delta hep}$ mice, as it was shown that this mouse model can be used to analyzed spontaneous liver tumorigenesis in constantly regenerating livers [48, 55]. The hepatocyte-specific deletion of Mcl-1 leads to spontaneous apoptosis of hepatocytes accompanied by compensatory hyper-proliferation, reflecting liver regeneration. Finally, around 50% of knock-out mice develop spontaneously HCC after 12 months of age [48].

To determine to which extend the Mcl-1$^{\Delta hep}$ mouse model mimics human hepatocarcinogenesis, liver tumors and non-neoplastic livers of Mcl-1$^{\Delta hep}$ mice were analyzed on morphological, immunohistochemical and gene expression level.

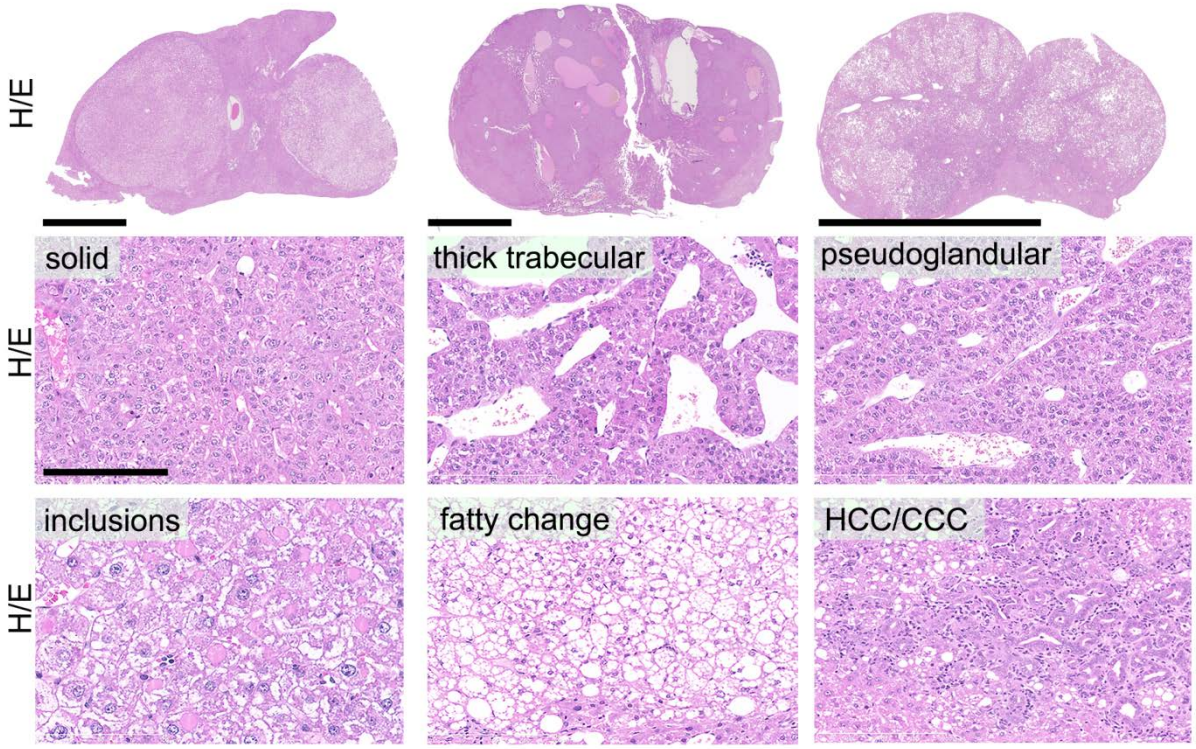

Figure 14: Histology of HCC derived from Mcl-1$^{\Delta hep}$ mice. Histological analysis of HCC derived from Mcl-1$^{\Delta hep}$ mice revealed a histologically and morphologically spectrum of growth patterns found in human HCC. Solid, thick trabecular and pseudoglandular growth patterns, HCC with cytoplasmic inclusions and clear cell and fatty change and combined HCC-CCC could be observed in livers of 12 month-old Mcl-1$^{\Delta hep}$ mice. Upper scale bars = 500 μm, lower scale bar = 500 μm.

Liver tumors developing in Mcl-1$^{\Delta hep}$ mice revealed a broad morphological spectrum displaying all major growth patterns and cytological features found in human HCC [56]: solid, (thick) trabecular, and pseudoglandular growth patterns, clear cell and fatty change, HCC with cytoplasmic inclusions, and also a combined HCC-CCC (hepatocellular-cholangiocellular) carcinoma (Figure 14). Thus, liver tumors developing in Mcl-1$^{\Delta hep}$ mice are morphologically heterogeneous and recapitulate the spectrum of human HCC.

4.3.4 HCC from Mcl-1$^{\Delta hep}$ mice show deregulated oncogene and tumor suppressor gene expression

Furthermore, I screened the mRNA expression of approximately 95 well-known oncogenes and tumor-suppressor genes, which are known to be relevant for human tumor development or described to be deregulated in human or murine HCC [46, 57, 58]. In my analysis,14 HCC-relevant oncogenes and tumor suppressor genes including e.g. *H-Ras*, *Net1*, *Tp53*, and *Mdm2* were significantly deregulated in tumors, and also in corresponding non-tumor tissue of Mcl-1$^{\Delta hep}$ mice compared to wild-type mice (Figure 15). The deregulated expression of oncogenes and tumor suppressor genes described to be relevant for human hepatocarcinogenesis demonstrated the close relation between human hepatocarcinogenesis and the Mcl-1$^{\Delta hep}$ mice on expression level.

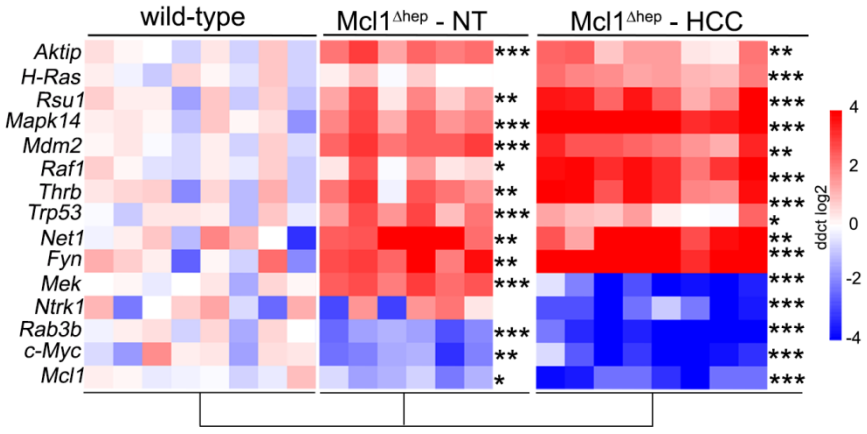

Figure 15: Oncogene expression in HCC and corresponding non-tumor tissue of Mcl-1$^{\Delta hep}$ mice. mRNA expression analysis of HCC and corresponding non-tumor tissue (NT) of 95 oncogenes and tumor suppressor genes performed by qPCR and compared to wild-type controls. Genes were significantly up- and down-regulated in tumor as well as non-tumor tissue. Only significantly deregulated genes are shown for space reasons. Asterisk indicates genes that were significantly up-regulated after multiple comparison (one-way ANOVA, bonferroni-correctd *p<0.05, **p<0.01, ***p<0.001).

Next, I performed a 16-gene expression profiling developed by Cairo et al. to analyze gene expression according to the proliferation and differentiation status initially described for human livers and hepatoblastoma [59]. HCC revealed two signatures, one being indicative of a more aggressive proliferative and less differentiated phenotype, similar to aggressive tumors from c-myc$^{tg/+}$/p53$^{-/-}$ mice, and the other indicative of a less proliferative and more differentiated phenotype, similar to differentiate hepatocytes from control livers. This analysis reflected the heterogeneous character of HCC developed in Mcl-1$^{\Delta hep}$ mice in contratst to several other models (e.g. c-myc$^{tg/+}$/p53$^{-/-}$ mice) in which only particular HCC subtypes develop (Figure 16).

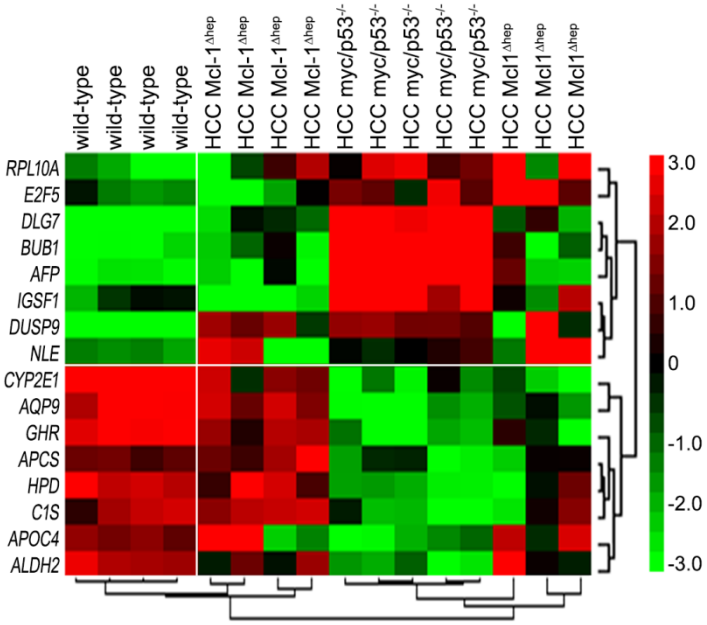

Figure 16: 16-gene profiling analysis of HCC from Mcl-1$^{\Delta hep}$ mice. mRNA analysis by qPCR comparing HCC derived from Mcl-1$^{\Delta hep}$ mice to aggressive liver tumors from c-myc$^{tg/+}$/p53$^{-/-}$ mice [59] and hepatocytes from wild-type livers. Genes above the line indicate a proliferative phenotype and genes below the line represent a less proliferative, but more differentiated phenotype. color code = log2 ratio.

4.3.5 Gene expression analysis in regenerating livers of Mcl-1$^{\Delta hep}$ mice uncovered novel tumor-associated genes

In order to investigate the molecular mechanisms driving tumor initiation during chronic liver regeneration in Mcl-1$^{\Delta hep}$ mice, I performed an unbiased mRNA microarray analysis on liver tissue of two-month-old wild-type, homozygous and hemizygous Mcl-1$^{\Delta hep}$ mice (Figure 17A). The expression of genes found deregulated in mRNA microarray analysis was validated by quantitative RT-PCR. KEGG pathway database analysis revealed that genes which were up-regulated at least two-fold were broadly assigned to variable cellular functions including apoptosis, cell cycle regulation, differentiation, metabolism and DNA damage response (Figure 17B).

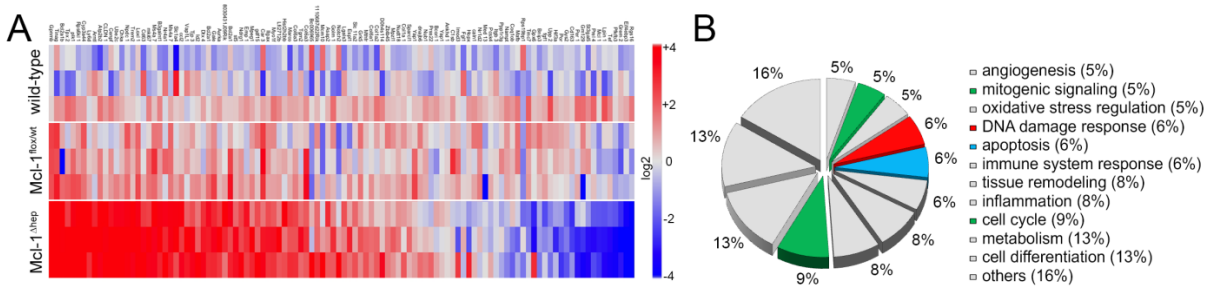

Figure 17: RNA microarray analysis of regenerating livers from Mcl-1$^{\Delta hep}$ mice. A) RNA microarray was performed with RNA isolated from highly regenerative two month-old Mcl-1$^{\Delta hep}$ mice, AlbCre-negative littermates as control mice as wells as hemizygous AlbCre-Mcl-1$^{flox/wt}$ mice with liver damage. B) KEGG pathway analysis revealed an heterogenous expression pattern of pathways (e.g. cell cycle, DNA damage response, angiogenesis), reflecting tissue damage and regeneration.

I performed Gene Set Enrichment Analysis (GSEA) [60] to determine whether livers of Mcl-1$^{\Delta hep}$ mice differ from livers of wild-type mice with respect to several gene sets of interest. Whereas no significant differences were found with respect to a gene set of normal liver, livers of Mcl-1$^{\Delta hep}$ mice were significantly enriched for genes related to apoptosis, proliferation and DNA replication (Figure 18) confirming previous morphological and functional data. Furthermore, livers of Mcl-1$^{\Delta hep}$ mice also displayed a significant enrichment for genes related to wounding, viral infection and alcoholic hepatitis, and despite representing non-neoplastic tissue also to human HCC. RNA microarray datasets performed with RNA from human liver tissue derived from public availably databases.

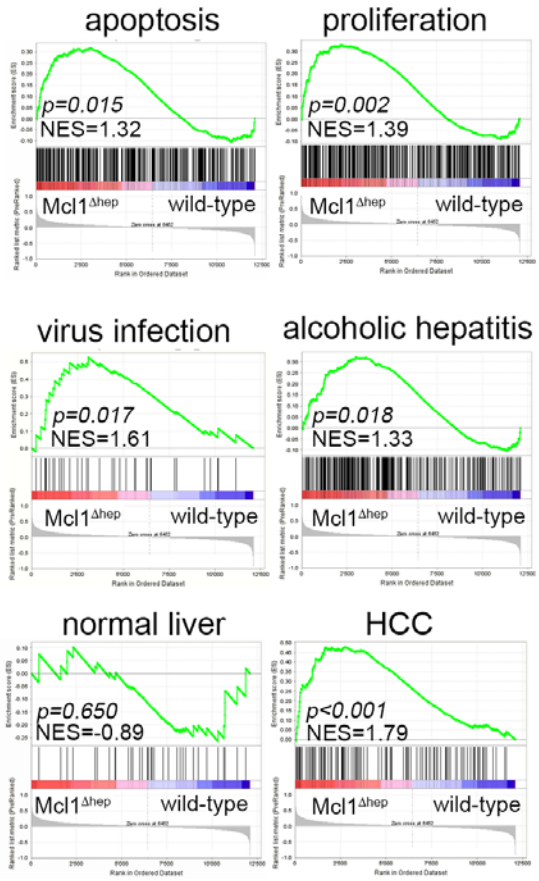

Figure 18: GSEA of RNA microarray data. GSEA to compare all differentially deregulated genes from Mcl-1$^{\Delta hep}$ mice with human gene sets for cellular processes, stress response and normal as well as diseased livers, including HCC. NES= normalized enrichment score.

4.3.6 Uncovered tumor-associated genes are significantly deregulated in other mouse models of HCC

The genes with the strongest up-regulation at two months of age, especially the top five upregulated genes (*Gpnmb*, *Tinag1*, *Plk1*, *Tpx2 and Bcl2a1b*), are indicative for mitotic and regenerative processes in the liver. Because of the overlapping gene expression pattern of livers derived from Mcl-1$^{\Delta hep}$ mice pattern with human HCC found by GSEA, I decided to analyse the gene expression of the newly uncovered genes in tumor and corresponding non-tumor and control livers of 12-month-old Mcl-1$^{\Delta hep}$ mice and could also find a significant over-expression (Figure 19). Therefore I concluded that the expression of these genes is not only related to liver regeneration and tumor initiation but rather also involved in tumor progression. But further experimental approaches would be required to analyze whether these genes causally drive tumorigenesis or are only upregulated as secondary/side-effect.

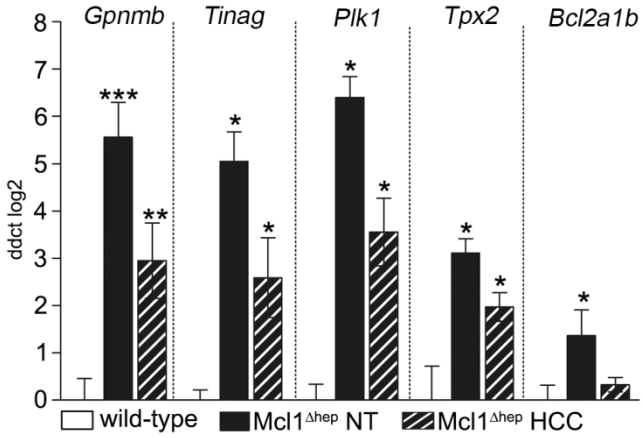

Figure 19: Validation of target gene expression in 12 month-old mice. Top five upregulated genes uncovered in two month-old mice are also significantly upregulated in tumor and non-tumor tissue of 12 month-old Mcl-1$^{\Delta hep}$ mice. *p<0.05, **p<0.01, ***p<0.001.

Next, I asked whether this gene expression of the newly uncovered target genes is specific for Mcl-1$^{\Delta hep}$ mice and therefore analyzed liver tumors derived from c-myc transgenic mice (an oncogene-driven model), LT$\alpha\beta$ transgenic mice (inflammation-driven) and the TAK1$^{\Delta hep}$ mouse model. In brief, the genes of interest were significantly overexpressed in all analyzed mouse models for spontaneous HCC development (Figure 20) but not in chemically, in particular DEN-induced HCC (data not shown), making a similar pathomechanism of spontaneous hepatocarcinogenesis during chronic liver tissue damage and regeneration likely, at least described by this gene expression profile.

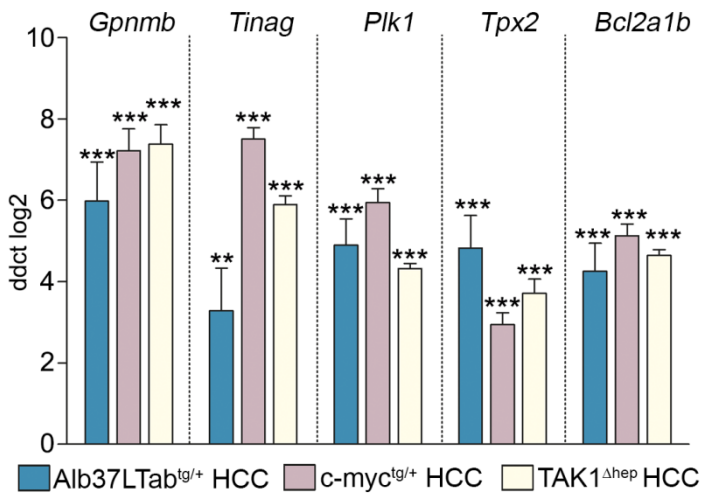

Figure 20: Increased expression of target gene in HCC derived from further mouse models. Top five upregulated genes were also detected by qPCR to be significantly deregulated in HCC of an inflammatory mouse model (Alb37LTαβ), an oncogene-driven mouse model (c-myc$^{tg/+}$) and the TAK1$^{\Delta hep}$ mouse model. n=4 to 8 HCC were analyzed. *p<0.05, **p<0.01, ***p<0.001.

4.3.7 Uncovered tumor-associated genes are significantly deregulated in human HCC and relevant for human hepatocarcinogenesis

Next, to test whether the tumorigenic gene expression profile initially uncovered in livers of Mcl-1$^{\Delta hep}$ mice reveals further similarities with human HCC, expression of genes showing the strongest up-regulation in livers of Mcl-1$^{\Delta hep}$ compared to wild-type mice was analyzed in human HCC of different etiology. Indeed, significantly up-regulated mRNA levels of *TINAG*, *PLK1*, and *TPX2* were found by qPCR in HCC independent of etiology (Figure 21A). Expression of *Gpnmb* was not detectable with different primer sets in human livers tissue and excluded for further analysis. Finally, overexpression of *TINAG1*, *PLK1*, and *TPX2* was confirmed by data mining in several published HCC expression data sets by cand.doc. Lukas Frick (Figure 21B).

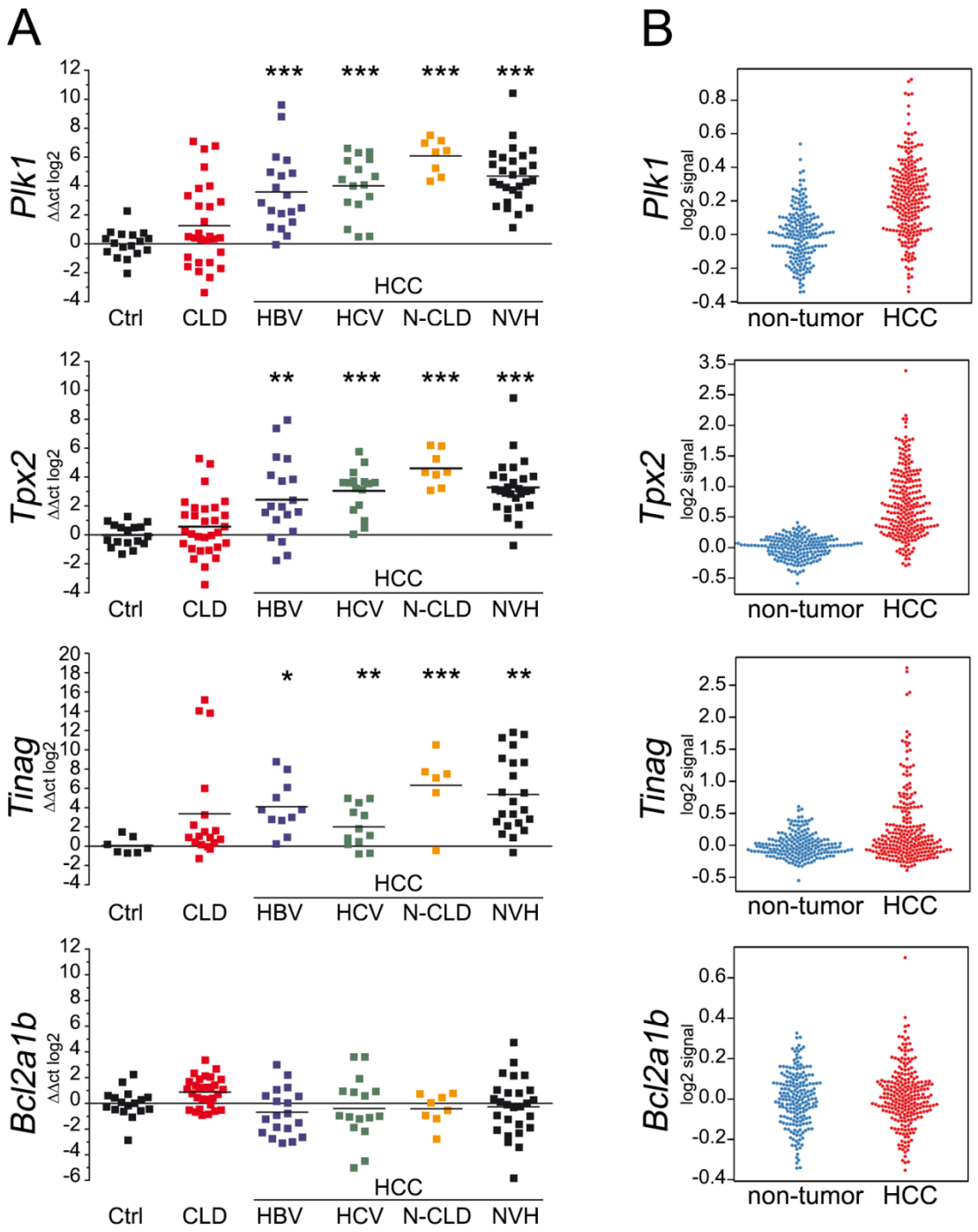

Figure 21: RNA expression analysis of target genes in human tumor and non-tumor liver tissue. A) Expression analysis by qPCR in naïve human liver tissues of CLD and HCC of diverse etiologies revealed elevated expression by tendency in non-tumorous liver tissue of CLD. Expression levels of Plk1, Tpx2, and Tinag, respectively, were significantly upregulated on HCC, independent of etiology. B) Overexpression of Plk1, Tpx2, and Tinag in human HCC could be confirmed in public available microarray expression datasets representative shown for a cohort pf primary HCC from patients treated with surgical resection or liver transplantation and without chemotherapy [61]. Asterisks indicate genes that were significantly up-regulated after multiple comparison, one-way ANOVA, bonferroni-corrected *p<0.05, **p<0.01, ***p<0.001.

As next step, I analyzed together with the help of Dr. Juliane Friemel the protein expression of target genes. Enhanced expression of TINAG, PLK1, TPX2, and BCL2A1 was demonstrated in primary HCC (independent of the underlying etiology) by immunohistochemistry (Figure 22A). In addition, significant overexpression of TINAG, TPX2, and BCL2A1 was observed by quantifying tissue microarray containing human HCC (Figure 22B and C).

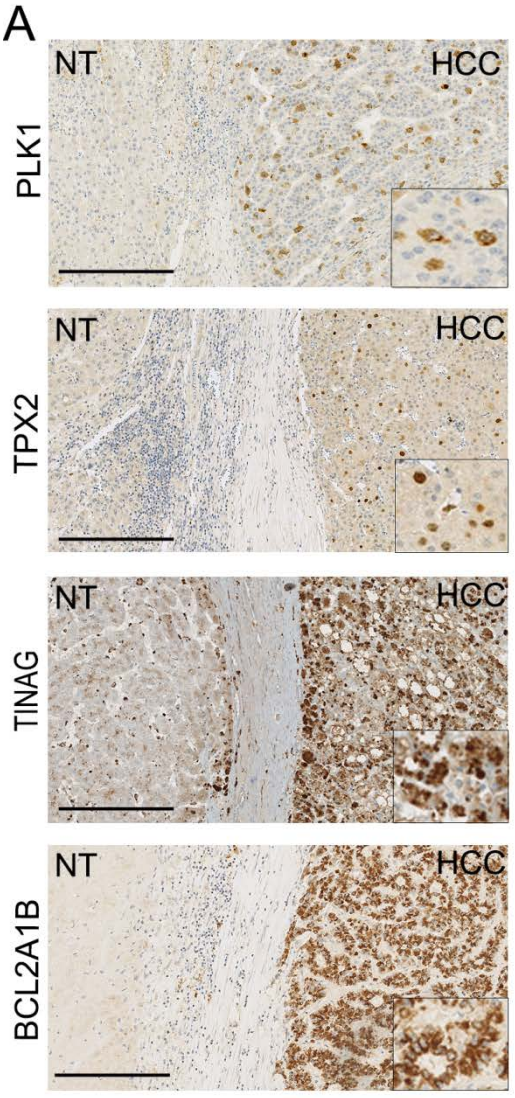

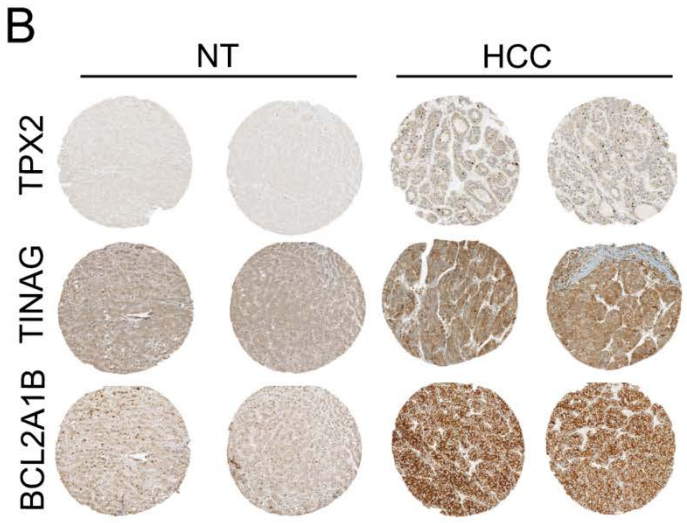

C

expression

		none/weak	moderate	strong	Fisher`s test
BCL2A1B	HCC	19	36	37	*p=0.007*
	NT	12	34	9	
TINAG	HCC	13	52	25	*p=0.034*
	NT	40	15	0	
TPX2	HCC	0	55	37	*p<0.0001*
	NT	0	53	0	

Figure 22: Elevated protein expression of target genes in human HCC. A) B) and C) Semi-quantitative immunohistochemical analysis using tissue microarrays (TMA) containing HCC (duplicates of n=95 HCC specimen) as well as non-tumorous liver tissue (duplicates of n=58). Analysis revealed statistically significant higher protein levels of TPX2, TINAG, and BCL2A1B in HCC, compared to non-HCC liver tissue. PLK1 was not quantified due to inconsistent staining pattern.

Finally, we correlated the protein expression with the patient survival and were able to observe a significant correlation for TPX*2* and TINAG (Figure 23), but not for BCL2A1. A strong expression of TPX2, a kinase involved in mitosis, that is required for AuroraKA activation and mediates chromosome segregation [62], significantly correlated with a short survival and poor outcome of patients. In contrast, the overexpression of poorly described extracellular matrix protein TINAG [63] in HCC significantly correlated with a prolonged survival of patients, compared to low or medium TINAG expression in HCC

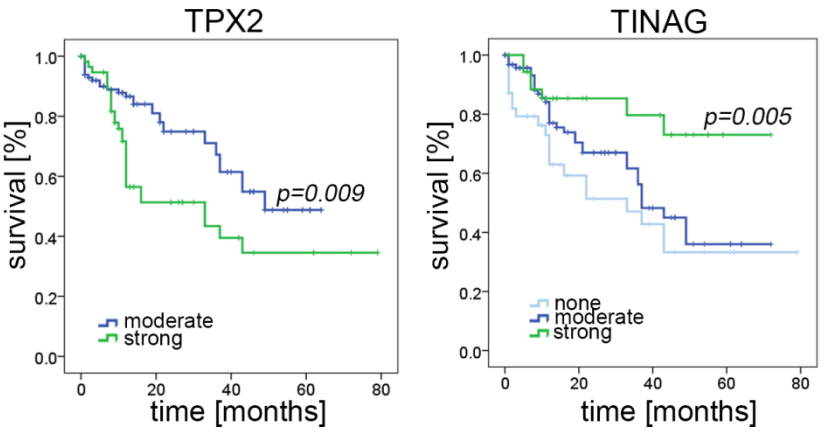

Figure 23: TPX2 and TINAG protein expression correlated with clinical prognosis. Strong expression TPX2 with a poor prognosis, whereas a strong expression of TINAG correlated with a good prognosis and prolonged survival, compared to patients with negative or low expression. Kaplan-Meier survival curved were generate based on semi-quantitative immunohistochemical analysis of TMA, .p-values were calculated by the log-rank test.

In summary, I uncovered novel genes which were poorly (Plk1, Tpx2) or not yet described (Bcl21ab, Tinag, Gpnmb) to be involved in human hepatocarcinogenesis. These genes were initially discovered to be deregulated in highly regenerative livers of 2 month-old Mcl-1$^{\Delta hep}$ mice and are apparently associated with early tumor initiation, tumor progression as well as survival of patients and thus are potentially of interest as therapeutically targets or as biomarkers for liver malignancy and tumor development.

Thus, tumors developing in Mcl-1$^{\Delta hep}$ mice are not only highly similar to human HCC on morphological and immunohistochemical level, but livers of Mcl-1$^{\Delta hep}$ mice also reveal a gene expression pattern highly overlapping with other mouse models for liver tumorigenesis and human HCC. These findings are indicative of a common underlying pathophysiological mechanism and suggest that the Mcl-1$^{\Delta hep}$ model recapitulates central features of human hepatocarcinogenesis and represents a very useful tool to study human hepatocarcinogenesis.

4.3.8 Risk of HCC correlates with apoptotic hepatocyte death in Mcl-1$^{\Delta hep}$ mice

As mentioned above, I hypothesized that hepatocyte cell death is the main stimulus of tumorigenesis and the amount of hepatocyte cell death over-time directly influences tumor development. Therefore, I decided to first correlate basic clinical parameters before analyzing the regenerating livers on molecular level.

At two months of age, Mcl-1$^{\Delta hep}$ mice showed moderate to severe hepatocyte death rates when applying a standard human scoring system for disease activity [64], and a statistically significant positive correlation between the percentage of hepatocyte apoptosis and ALT levels (Figure 24A-C), confirming that apoptotic hepatocyte death is the major source of increased serum transaminase levels in this model.

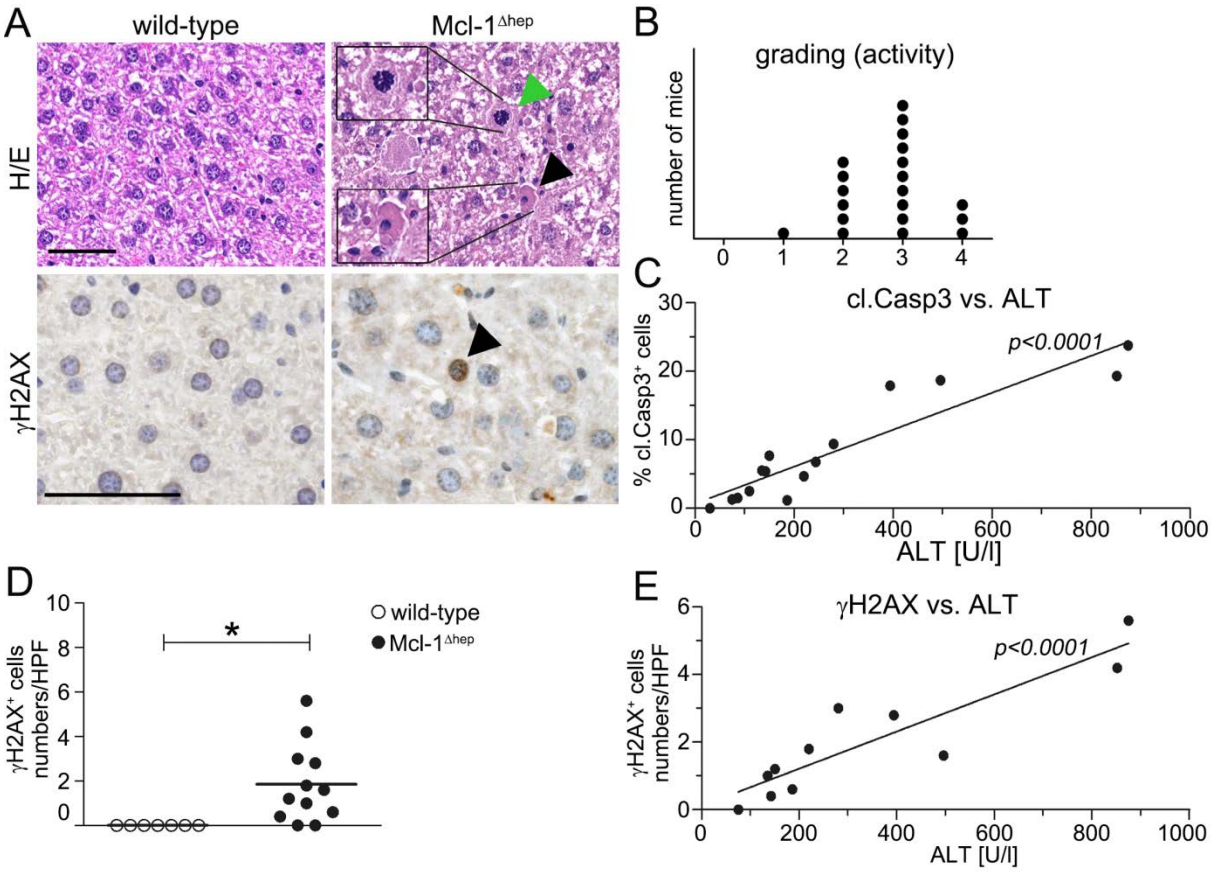

Figure 24: Elevated hepatocyte cell death and signs of DDR in livers Mcl-1$^{\Delta hep}$ mice. A) Hepatocyte apoptosis (black arrow) and signs of DNA damage (γH2AX) in livers of Mcl-1$^{\Delta hep}$ mice (scale bar, upper panel: 50 μm) and B) grading of disease activity in livers of Mcl-1$^{\Delta hep}$ mice. C) ALT levels reflecting liver damage significantly correlate with the rate of apoptotic hepatocytes in livers of Mcl-1$^{\Delta hep}$ mice. D) Significantly increased numbers of hepatocytes per high power field (HPF) positive for γH2AX in livers of Mcl-1$^{\Delta hep}$ mice significantly correlate with D) ALT levels measured non-invasively and reflecting liver damage. A) - E) Livers of 2 month-old Mcl-1$^{\Delta hep}$ or wild-type mice.

Similar to human CLD, livers of 2-month-old Mcl-1$^{\Delta hep}$ mice not only revealed increased levels of proliferating hepatocytes [55], but also a substantial number of γH2AX-positive hepatocytes when compared to age-matched wild-type mice (Figure 24D). Notably, the number of γH2AX-positive hepatocytes positively correlated with ALT levels indicating an association between the amount of hepatocyte apoptosis and DNA damage (Figure 24E).

Next, we asked whether a correlation between the level of hepatocyte apoptosis and HCC development also does exist. To this aim, Mcl-1$^{\Delta hep}$ and wild-type mice were prospectively monitored over time for serum transaminase levels, before they were killed at 12 months of age. Similar to what was reported before [48], 50% of Mcl-1$^{\Delta hep}$ developed liver tumors after one year. Remarkably, Mcl-1$^{\Delta hep}$ mice with HCC had constantly higher serum ALT (and also AST, not shown) levels compared to Mcl-1$^{\Delta hep}$ mice without HCC (Figure 25A). ALT levels were statistically significantly elevated at the age of 2 months (Figure 25B), i.e. the time-point when I also observed elevated numbers of regenerating hepatocytes, which is long before tumors or dysplastic changes were observable (Figure 25C). Thus, the association between elevated transaminase levels indicative of hepatocyte apoptosis and HCC development, which was observed in human patients, could be recapitulated in an *in vivo* model of hepatocarcinogenesis.

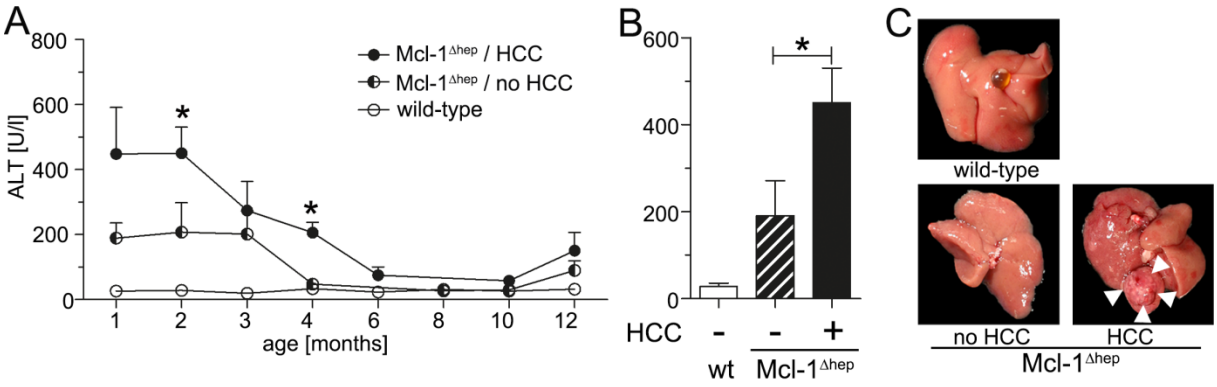

Figure 25: The risk of HCC development correlates with levels of apoptotic cell death in Mcl-1$^{\Delta hep}$ mice. A) Time course of transaminase levels shown for ALT revealing constantly elevated ALT levels throughout life in Mcl-1$^{\Delta hep}$ mice which developed an HCC at 12 months compared to tumor-free Mcl-1$^{\Delta hep}$ mice. B) ALT levels were significantly different at the age of 2 months. C) Macroscopy of livers of 12-month-old wild-type and Mcl-1$^{\Delta hep}$ mice (with and without HCC development).

4.3.9 Inhibition of TNFR1 signaling reduces apoptosis, proliferation and tumor development in Mcl-1$^{\Delta hep}$ mice

Based on the strong link between hepatocyte death and HCC development in Mcl-1$^{\Delta hep}$ mice and the idea that constant hepatocyte apoptosis is the first and crucial step in a cascade leading to liver tumorigenesis, I hypothesized that the reduction or ablation of hepatocyte apoptosis in the liver would finally reduce tumorigenesis. Therefore, I took advantage of mice which systemically lack the pro-apoptotic TNFR signaling pathway and intercrossed TNFR1$^{-/-}$ mice to Mcl-1$^{\Delta hep}$ mice (Mcl-1$^{\Delta hep}$/TNFR1$^{-/-}$ mice) aiming to reduce the extrinsic apoptotic signaling pathway via TNFR1.

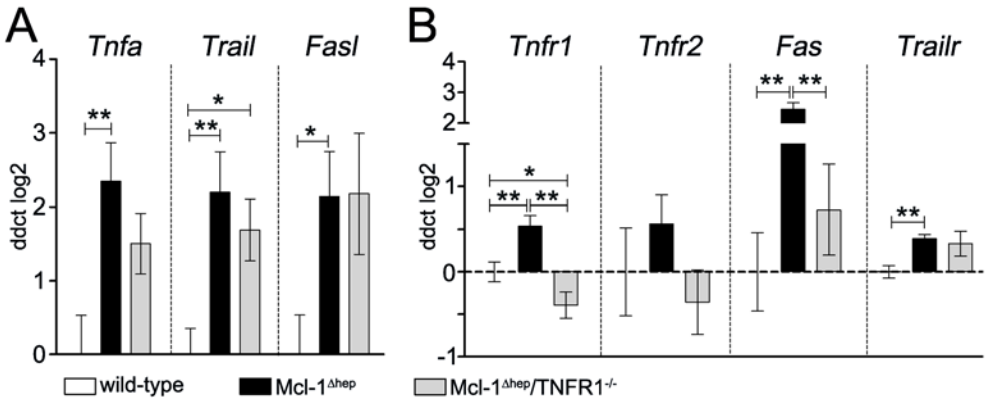

Figure 26: Expression of death receptors and ligands in Mcl-1$^{\Delta hep}$/TNFR1$^{-/-}$ mice. Increased expression of A) death receptors (*Tnfr1, Fas, Trailr*) and B) ligands (*Tnfα, Trail, Fasl*) in livers of 2-month-old Mcl-1$^{\Delta hep}$ compared to Mcl-1$^{\Delta hep}$/TNFR1$^{-/-}$ and wild-type mice. Statistics analyzed by one-way ANOVA, *p<0.05, **p<0.01, ***p<0.001.

TNFα-induced cell death via TNFR1 is known to be one of the most important pathways causing hepatocyte apoptosis in a wide range of chronic and acute liver diseases [65, 66]. Mcl-1$^{\Delta hep}$ mice showed enhanced expression of death receptors (*Tnfr1, Fas, Trailr*) and associated ligands (*Tnfα, Trail, Fasl*) (Figure 26). Interestingly no activation of the downstream pro-survival pathway NFκB was observed (Figure 27).

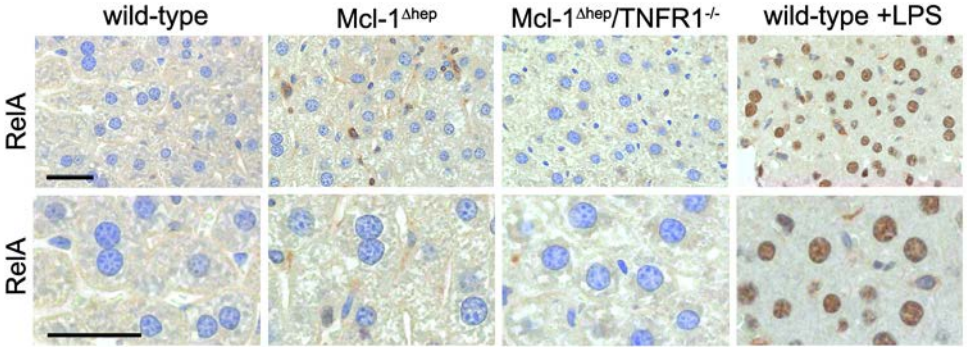

Figure 27: NFκB signaling in Mcl-1$^{\Delta hep}$ mice. RelA staining shows no obvious RelA translocation, indicating NFκB signaling in livers of Mcl-1$^{\Delta hep}$. Scale bar = 50 μm.

Two-month-old Mcl-1$^{\Delta hep}$/TNFR1$^{-/-}$ mice revealed a lower amount of serum transaminases (statistically significant for AST) and an increased liver to body weight ratio compared to age-matched Mcl-1$^{\Delta hep}$ mice (Figure 28A and B).

Liver histology and protein blotting revealed that Mcl-1$^{\Delta hep}$/TNFR1$^{-/-}$ mice had not only significantly lower levels of apoptotic hepatocytes, but also of proliferating hepatocytes compared to Mcl-1$^{\Delta hep}$ mice (Figure 28C, Figure 29). Therefore, I concluded that TNFR1 signaling is crucial for hepatocyte cell death and significantly influences tumor development in Mcl-1$^{\Delta hep}$ mice.

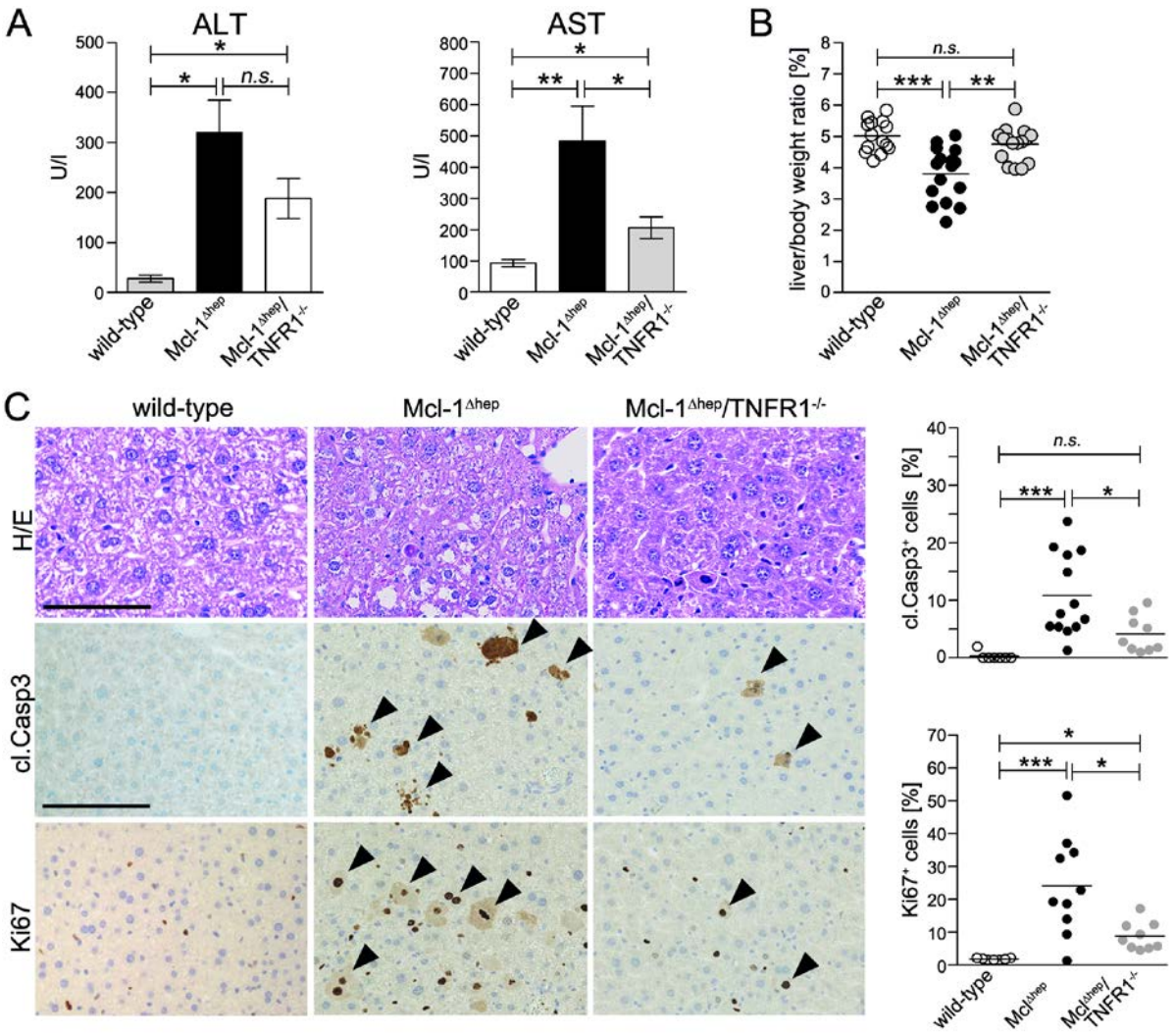

Figure 28: Reduced liver damage, hepatocyte apoptosis and proliferation in Mcl-1$^{\Delta hep}$/TNFR1$^{-/-}$ mice. A) Transaminase (AST, ALT) and B) liver/body weight ratio in Mcl-1$^{\Delta hep}$, Mcl-1$^{\Delta hep}$/TNFR1$^{-/-}$ and wild-type mice at 2 months of age. C) Immunohistochemistry and quantification for cleaved Caspase 3 and Ki67 showing significantly reduced hepatocyte apoptosis and proliferation in Mcl-1$^{\Delta hep}$/TNFR1$^{-/-}$ mice compared to Mcl-1$^{\Delta hep}$ mice at 2 months of age. Upper scale bar = 100 μm, lower scale bar = 200 μm.

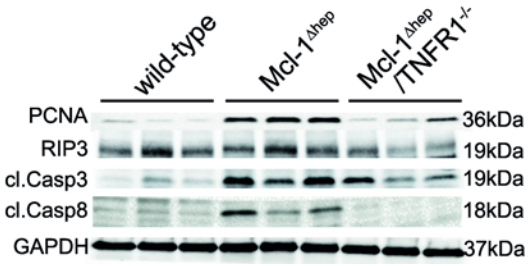

Figure 29: Western blotting confirmed reduced proliferation and apoptosis in livers Mcl-1$^{\Delta hep}$/TNFR1$^{-/-}$ mice compared to age-matched Mcl-1$^{\Delta hep}$ mice. Activated Caspase 8 blotting indicates Caspase 8 dependent cell death in Mcl-1$^{\Delta hep}$, abolished in Mcl-1$^{\Delta hep}$/TNFR1$^{-/-}$ mice.

To analyze the inflammatory reaction in Mcl-1$^{\Delta hep}$ and Mcl-1$^{\Delta hep}$/TNFR1$^{-/-}$ mice I isolated intrahepatic immune cells and flow cytometry analysis (together with Dr. Monika Wolf) revealed a mild increase in CD11^{+}/Ly6G^{+} immune cells in livers of Mcl-1$^{\Delta hep}$ mice, indicating a contribution of granulocytes and/or neutrophils in the clearance of apoptotic hepatocytes. No alteration in numbers of other immune cells, i.e. CD45^{+}/CD4^{+}, CD45^{+}/CD8^{+}, or CD11b^{+}/Ly6C^{+} cells, could be found in Mcl-1$^{\Delta hep}$ mice (Figure 30). The increase of CD45^{+}/Ly6G^{+} cells was reduced to wild-type levels in livers of Mcl-1$^{\Delta hep}$/TNFR1$^{-/-}$ mice (Figure 30).

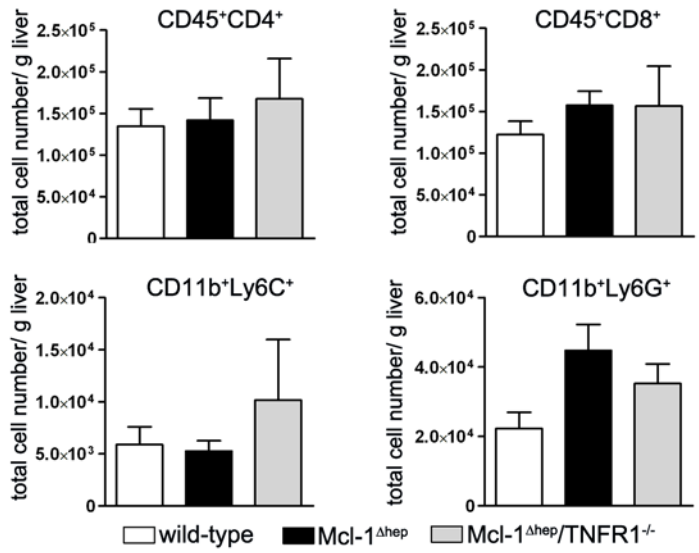

Figure 30: Analysis of intrahepatic immune cells by flow cytometry. No significant changes could be observed in intrahepatic immune cell, but the amount of Ly6G-positive granulocytes has been elevated two fold in Mcl-1$^{\Delta hep}$ compared to wild-type and Mcl-1$^{\Delta hep}$/TNFR1$^{-/-}$ mice (n=3 mice per group, 2 months of age).

Remarkably, significantly deregulated potential oncogenes which I initially found in in livers of 2-month-old Mcl-1$^{\Delta hep}$ mice and HCC were also deregulated in livers of Mcl-1$^{\Delta hep}$/TNFR1$^{-/-}$ mice, indicating that the malignant character in regenerative livers of Mcl-1$^{\Delta hep}$ mice is restored in Mcl-1$^{\Delta hep}$/TNFR1$^{-/-}$ mice (Figure 31).

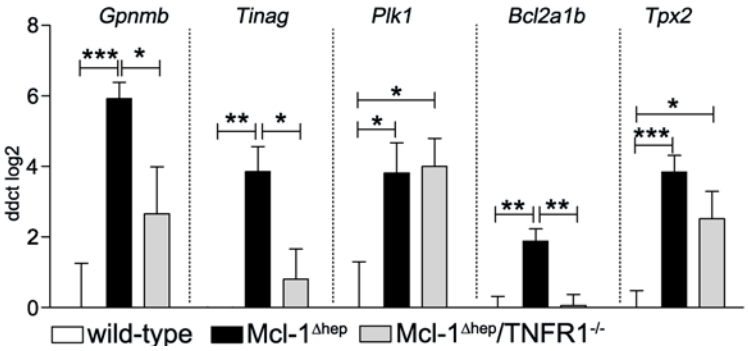

Figure 31: Reduced oncogenic gene expression in Mcl-1$^{\Delta hep}$/TNFR1$^{-/-}$ mice. Previously described by microarray analysis uncovered target genes, reflecting the malignant character of livers on RNA level, were signifcatnly reduced in Mcl-1$^{\Delta hep}$ by TNFR1 deficiency. (n=3 mice per group, 2 months of age).

More important, analysis of the tumor incidence at the age of 1 year revealed a statistically significant reduction of the tumor incidence in Mcl-1$^{\Delta hep}$/TNFR1$^{-/-}$ mice compared to Mcl-1$^{\Delta hep}$ mice (16% versus 50%, $p<0.05$, Figure 32). Of note, Mcl-1$^{\Delta hep}$/TNFR1$^{-/-}$ mice which developed liver tumors at 1 year have had significantly higher transaminase levels at 2 months of age (Figure 32), again showing the same association between high transaminase levels - indicating high apoptotic activity - early in life and tumor development which we already have observed in Mcl-1$^{\Delta hep}$ mice.

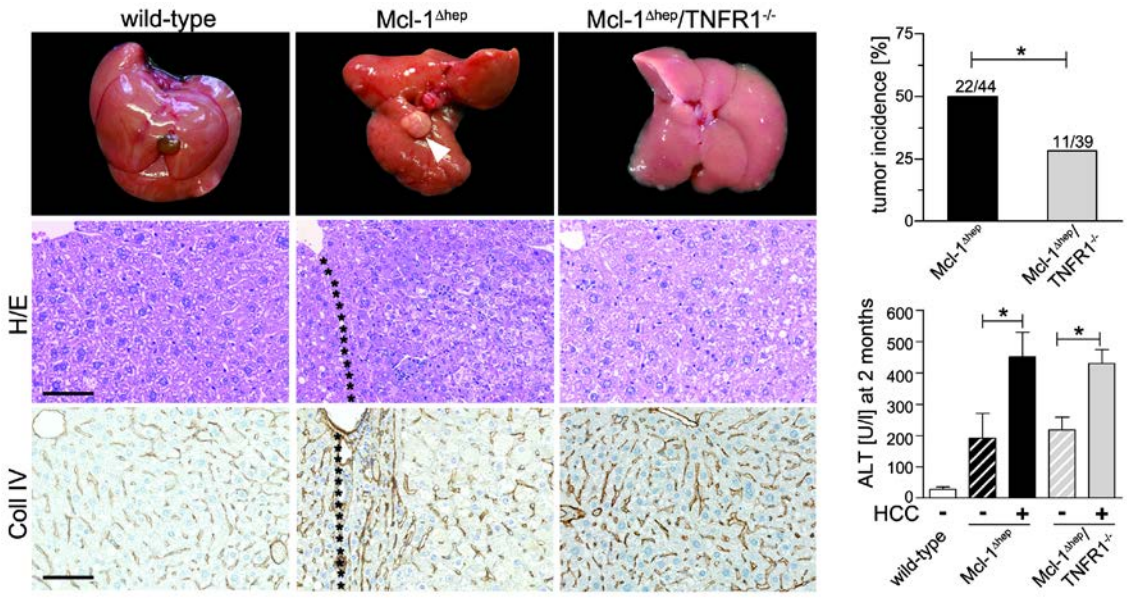

Figure 32: Tumor incidence in 12-month-old mice. Significantly reduced tumor development after 12 months in Mcl-1$^{\Delta hep}$/TNFR1$^{-/-}$ mice, compared to Mcl-1$^{\Delta hep}$ mice. H/E and Collagen IV stainings demonstrate invasive tumor growth, Tumor borders are marked by asterisks. Tumor development correlated with ALT levels at 2 months (retrospectively analyzed). Scale bar = 100 μm *p < 0.05; **p < 0.01; ***p < 0.001.

In summary, these results indicate that the depletion of the pro-apoptotic TNFR signaling in regenerative livers derived from Mcl-1$^{\Delta hep}$ mice reduces hepatocyte death, liver damage and as consequence the malignant character and finally tumorigenesis.

4.3.10 Inhibition of TNFR1 signaling and Caspase 8 reduces the DNA damage response and genetic instability in Mcl-1$^{\Delta hep}$ and TAK1$^{\Delta hep}$ mice

Next, I wanted to address whether apoptosis contributes to tumor initiation and progression in hepatocarcinogenesis in general or whether the findings are only specific for the Mcl-1$^{\Delta hep}$ model. Therefore, I took advantage of the TAK1$^{\Delta hep}$ mouse model [49] in which the hepatocyte-specific knock-out of TAK1 causes hepatocyte apoptosis and necrosis and mice show an early onset of tumorigenesis at around 35 weeks of age. As published by Vucur et al, the additional knock-out of Caspase 8 prevented hepatocyte apoptosis, liver damage and tumorigenesis, whereas the additional knock-out of RIPK3 prevented necroptosis, but leads to high levels of hepatocyte apoptosis and proliferation resulting in increased tumor burden [49].

In line with my results from the Mcl-1$^{\Delta hep}$ model, I expected to find a correlation between hepatocyte apoptosis, DNA damage and genetic instability in TAK1$^{\Delta hep}$ mice and intercrossings.

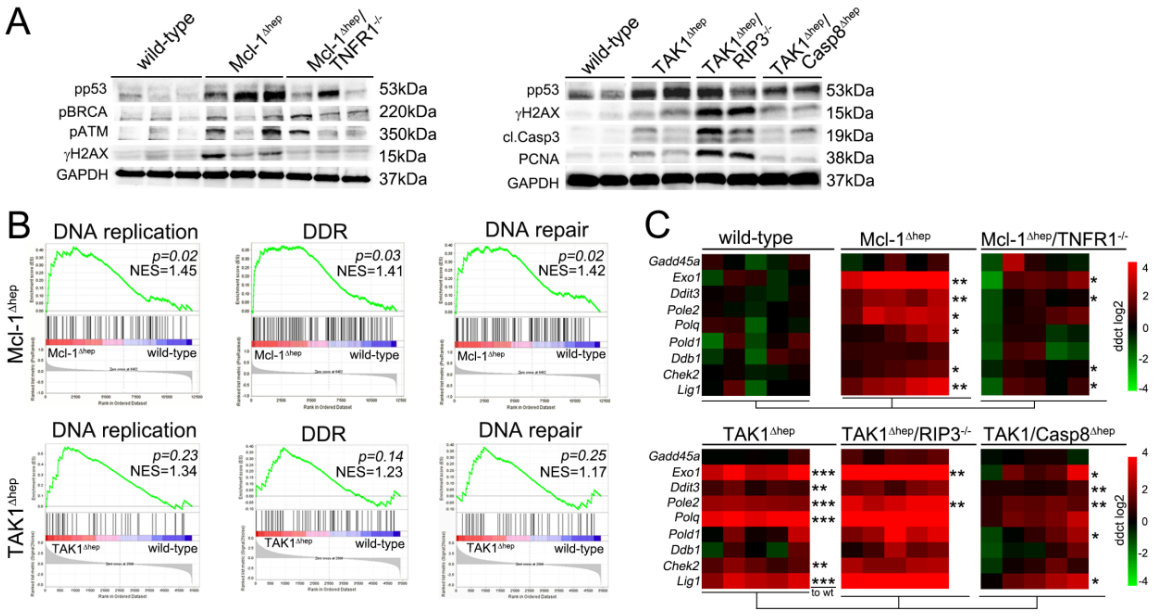

Figure 33: DNA damage response in Mcl-1$^{\Delta hep}$ and TAK1$^{\Delta hep}$ mice. Western blotting revealed activation of DNA damage reponse pathways. Reduced levels of activated DNA damage proteins (e.g. phosphorylated p53) were detected in livers of Mcl-1$^{\Delta hep}$/TNFR1$^{-/-}$ mice compared to Mcl-1$^{\Delta hep}$ and in livers of TAK1/Casp8$^{\Delta hep}$ mice compared to TAK1$^{\Delta hep}$. B) GSEA of RNA microarrays revealing statistically significant enrichment of gene associated with DNA replication, DNA damage response

and DNA repair. NES = normalized enrichment score. C) Heat map showing reduced expression of DNA damage and DNA repair-associated genes by qPCR in livers of Mcl-1$^{\Delta hep}$/TNFR1$^{-/-}$ mice and TAK1/Casp8$^{\Delta hep}$ mice compared to single knock-out mice. *p < 0.05; **p < 0.01; ***p < 0.001. A) – C) Mcl-1$^{\Delta hep}$ mice analyzed at 2 months and TAK1$^{\Delta hep}$ at 6 weeks of age.

First, I analyzed the activation of the DDR pathways on protein and RNA level in highly regenerative livers of two-month-old Mcl-1$^{\Delta hep}$ and 6-week-old TAK1$^{\Delta hep}$ mice and intercrossings. I observed a strong activation of the DDR pathways by immune blotting in livers from Mcl-1$^{\Delta hep}$, TAK1$^{\Delta hep}$ and TAK1$^{\Delta hep}$/RIP$^{-/-}$ mice, but not in Mcl-1$^{\Delta hep}$/TNFR1$^{-/-}$ and TAK1/Casp8$^{\Delta hep}$ mice (Figure 33A). This finding could be confirmed by qPCR for genes involved in DNA repair and by GSEA, suggesting a persistent activation of DNA damage response pathways in regenerating livers of Mcl-1$^{\Delta hep}$ and TAK1$^{\Delta hep}$ mice (Figure 33B,C).

To analyze the DNA damage response in hepatocyte specific, we performed together with Dr. Akshay Ahuja (Institute of Molecular Cancer Research, Prof. Massimo Lopes) single cell flow cytometry analyses for the intracellular DNA damage markers γH2AX and RPA, a protein that binds to single-stranded DNA during DNA repair. Therefore we isolated primary hepatocytes from TAK1$^{\Delta hep}$ mice and TAK1/Casp8$^{\Delta hep}$ mice and interestingly, a substantial amount (~15%) of hepatocytes from TAK1$^{\Delta hep}$ mice showed signs of DNA damage, whereas DNA damage was completely reduced in TAK1/Casp8$^{\Delta hep}$ mice and not detectable in wild-type mice (Figure 34). This confirmed the above mentioned findings that livers from TAK1/Casp8$^{\Delta hep}$ are not only completely rescued from apoptotic cell death and hyper-regeneration but also from DDR.

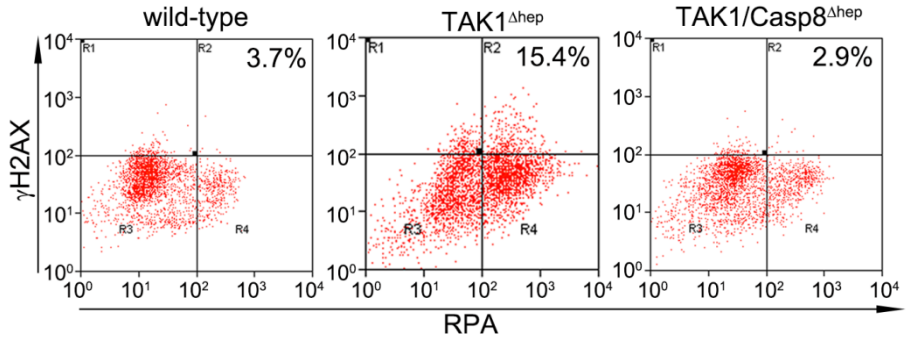

Figure 34: Intracellular analysis of DNA repair by flow cytometry. Isolated primary hepatocytes were analyzed by flow cytometry for γH2AX and RPA showing reduced DNA damage in TAK1/Casp8$^{\Delta hep}$ mice compared to TAK1$^{\Delta hep}$. 2-4 mice per genotype analyzed at the age of 6 weeks,; average percentage of γH2AX+/RPA+ cells indicated.

Next, addressed the question whether livers from Mcl-1$^{\Delta hep}$ and TAK1$^{\Delta hep}$ mice showed genetic instability as described before in human chronically diseased livers and how the knock-out of TNFR1 or Caspase 8 would influence genetic instability. I performed Taqman copy number assay by qPCR for the same chromosomal fragile sites as previously analysed in human tissue and I could detect allelic imbalance in liver tissue from Mcl-1$^{\Delta hep}$, TAK1$^{\Delta hep}$ and TAK1$^{\Delta hep}$/RIPK3$^{-/-}$ mice (Figure 35). Interestingly, allelic imbalance was significantly reduced in Mcl-1$^{\Delta hep}$/TNFR1$^{-/-}$ compared to Mcl-1$^{\Delta hep}$ mice and in TAK1/Casp8$^{\Delta hep}$ compared to TAK1$^{\Delta hep}$ mice. Conclusively, the pro-apoptotic TNFR1 as well as Caspase 8 signaling significantly contributes to genetic instability in regenerative murine livers.

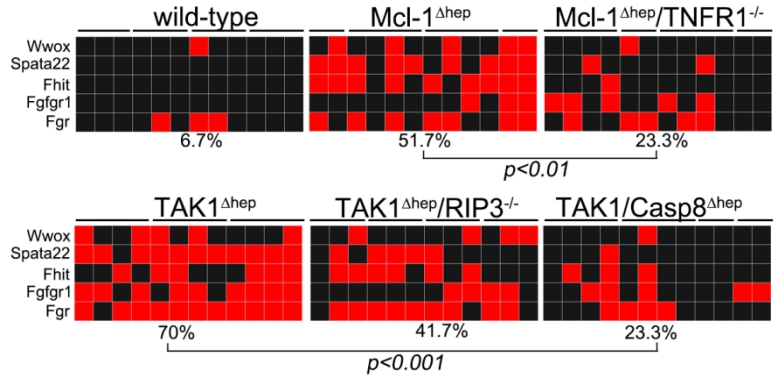

Figure 35: Genetic instability in regenerating livers of Mcl-1$^{\Delta hep}$ and TAK1$^{\Delta hep}$ mice**.** Statistically lower rate of allelic imbalances (AI) in Mcl-1$^{\Delta hep}$/TNFR1$^{-/-}$ mice and TAK1/Casp8$^{\Delta hep}$ compared to Mcl-1$^{\Delta hep}$ and TAK1$^{\Delta hep}$ mice, respectively. Each square represents one area of microdissected liver tissue and lines indicating different areas of the same liver. AI analyzed by Taqman copy number assay, red = AI; black= no AI. A) - C): *p < 0.05; **p < 0.01; ***p < 0.001. Mcl-1$^{\Delta hep}$ mice and intercrossings analyzed at 2 months; TAK1$^{\Delta hep}$ mice and intercrossings analyzed at 6 weeks of age.

4.3.11 Proliferation triggers DNA damage in regenerative livers of Mcl-1$^{\Delta hep}$ and TAK1$^{\Delta hep}$ mice

As described before, I detected DDR on RNA and protein level as well as increased DNA damage by immunohistochemical staining for γH2AX in hepatocytes. To gain insight into the source of DNA damage in hyper-apoptotic and hyper-proliferative livers, I next addressed the question whether DNA damage derived from apoptotic, proliferative or unaffected/senescent hepatocytes. Therefore, I analyzed γH2AX co-stainings with cleaved Caspase 3 (cl.Casp3) as apoptosis marker and Ki67 as proliferation marker.

First, co-staining for γH2AX and cl.Casp3 revealed hepatocytes double-positive for γH2AX and cl.Casp3, whereas γH2AX signals in nuclei resulted from fragmentation during the apoptotic process. I also detected a substantial amount of hepatocytes positive for γH2AX but negative for cl.Casp3. γH2AX single positivity illustrated non-apoptotic hepatocytes carrying DNA damage. Immunofluorescence (IF) staining for γH2AX revealed the typical nuclear staining pattern in the nucleus (Figure 36).

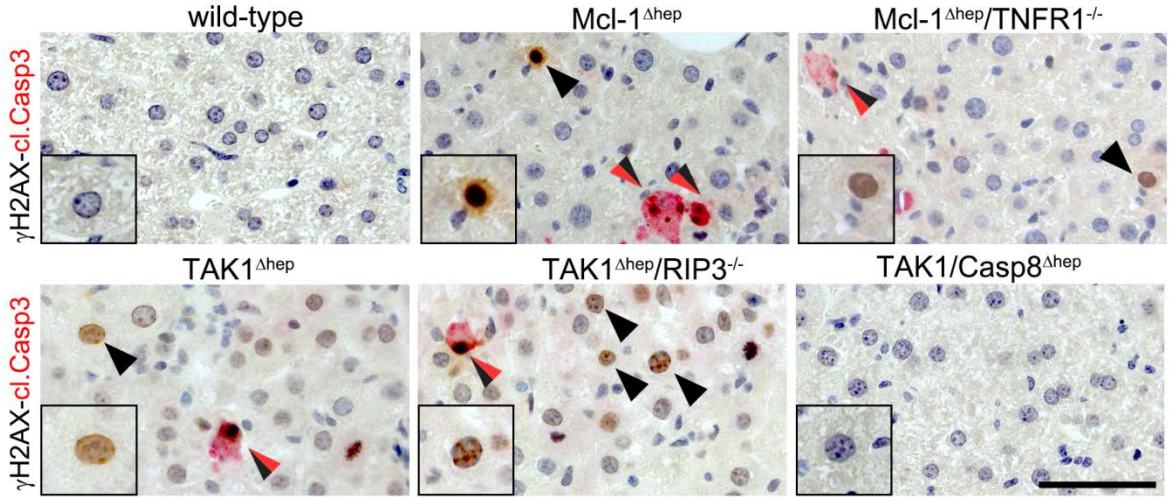

Figure 36: DNA damage in Mcl-1$^{\Delta hep}$ and TAK1$^{\Delta hep}$ mice. Immunohistochemical co-staining for γH2AX (brown, indicated by black arrow haeds) and cleaved Caspase 3 (red, indicated by red arrow haeds) revealed single and double positive hepatocytes, indicating non apoptotic hepatocytes carrying DNA damage in regenerating livers of 6 weeks old mice. Scale bar = 100 μm.

Second, I analyzed IF co-stainings for γH2AX and Ki67 on livers of Mcl-1$^{\Delta hep}$ and TAK1$^{\Delta hep}$ mice and found a substantial proportion of γH2AX and Ki67 double positive hepatocytes (about 10% and 15%, respectively) (Figure 37). Remarkably, the percentage of γH2AX-double positive hepatocytes was significantly reduced in Mcl-1$^{\Delta hep}$/TNFR1$^{-/-}$ mice compared to Mcl-1$^{\Delta hep}$ mice, and also in TAK1$^{\Delta hep}$/Casp8$^{\Delta hep}$ mice compared to TAK1$^{\Delta hep}$ mice, but not in TAK1$^{\Delta hep}$/RIP3$^{-/-}$ mice.

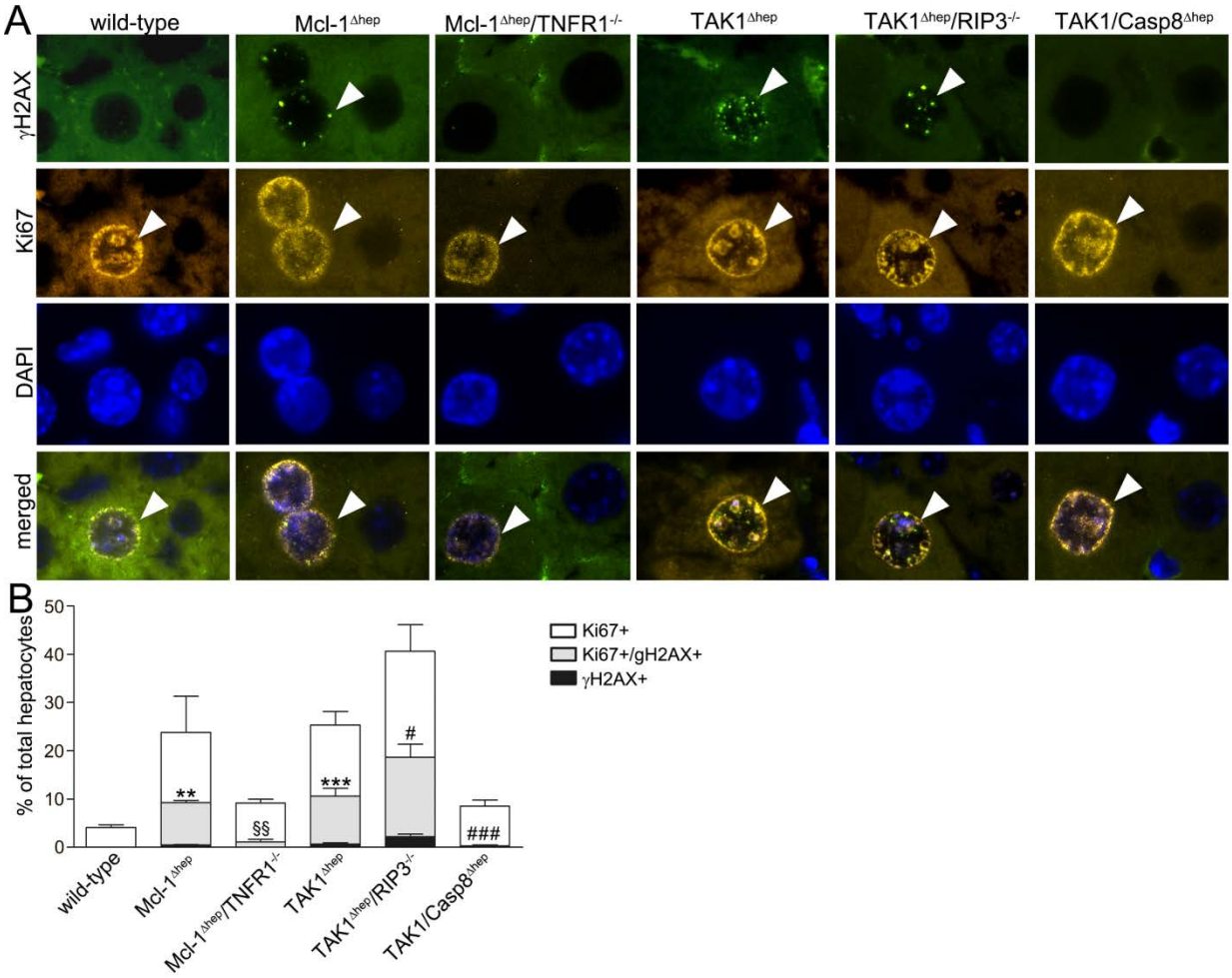

Figure 37: Proliferation-associated DDR in Mcl-1$^{\Delta hep}$, TAK1$^{\Delta hep}$ and TAK1$^{\Delta hep}$/RIP3$^{-/-}$ mice. IF co-staining for γH2AX and Ki67 and quantification revealed statistically reduced numbers and rate of Ki67-single positive and Ki67/γH2AX-double positive hepatocytes in Mcl-1$^{\Delta hep}$/TNFR1$^{-/-}$ mice und TAK1/Casp8$^{\Delta hep}$ compared to Mcl-1$^{\Delta hep}$ and TAK1$^{\Delta hep}$ mice, respectively. Arrow heads indicate positive nuclei. Statistics shown for Ki67/γH2AX double-positivity. * compared to wild-type, § compared to Mcl-1$^{\Delta hep}$ and # compared to TAK1$^{\Delta hep}$ mice. Mcl-1$^{\Delta hep}$ mice were analyzed at 2 months and TAK1$^{\Delta hep}$ at 6 weeks of age.

Of note, I found only a very low proportion (approximately 1-3%) of γH2AX single positive hepatocytes in murine livers (Figure 37B). In summary, γH2AX-staining strongly correlated with Ki67-positivity of hepatocytes pointing to hyper-proliferation as the main source of DNA damage in Mcl-1$^{\Delta hep}$ and TAK1$^{\Delta hep}$ mice.

4.3.12 DNA damage in livers of Mcl-1$^{\Delta hep}$ and TAK1$^{\Delta hep}$ mice is independent of oxidative stress

The accumulation of reactive oxygen species (ROS) in proliferative cells is well known [67] and also ROS as trigger of DNA damage is very well described [68]. Furthermore, ROS as driver of steatohepatitis and liver damage has been described recently in NEMO$^{\Delta hep}$ mice and could be prevented by feeding mice with the antioxidant butylated hydroxyanisole (BHA) [69]. Livers of Mcl-1$^{\Delta hep}$ and TAK1$^{\Delta hep}$ mice showed signs of oxidative stress within hepatocytes as characterized by 8-OHdG staining (Figure 38A). Therefore, I wanted to gain insight into the contribution of oxidative stress in DNA damage under proliferative conditions and decided to analyze Mcl-1$^{\Delta hep}$ and TAK1$^{\Delta hep}$ mice which were kept for four weeks on diets supplemented with the antioxidants BHA or vitamin E. Antioxidant feeding resulted in a reduction of 8-OHdG-positive hepatocytes in both genotypes (Figure 38A), indicative of reduced oxidative stress in murine livers.

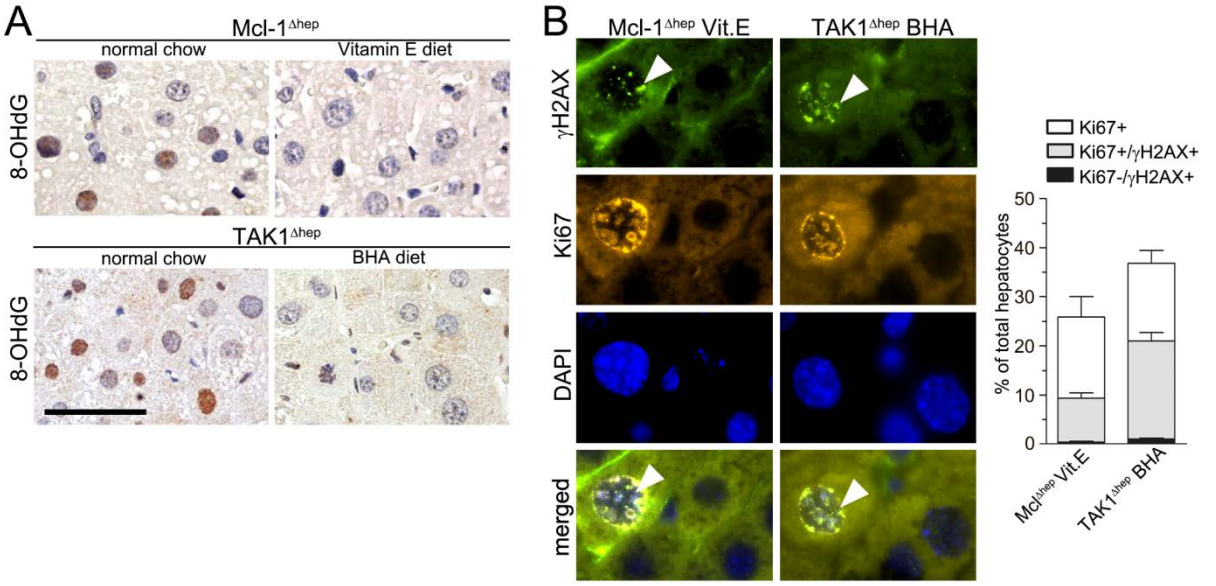

Figure 38: Antioxidant treatment of mice does not reduce proliferation-associated DDR. A) Livers of Mcl-1$^{\Delta hep}$ and TAK1$^{\Delta hep}$ mice on normal chow but not on antioxidant diets showed 8-OHdG positive hepatocytes, indicating oxidative stress. B) and C) Livers of mice kept for four weeks on antioxidant diet, Mcl-1$^{\Delta hep}$ on a Vitamin E supplemented and TAK1$^{\Delta hep}$ on a BHA supplemented diet showed no reduction of hepatocytes proliferation or γH2AX positivity. Arrow heads indicate positive nuclei.

As next step, I analyzed the liver sections for γH2AX and Ki67 co-staining and found no obvious reduction in hepatocyte proliferation in antioxidant-fed mice versus control mice on normal diet. In addition, the rate of proliferating hepatocytes positive for γH2AX was also not altered compared to knock-out mice on normal diet (Figure 38B).

I concluded that ROS does not contribute to hepatocyte proliferation in Mcl-1$^{\Delta hep}$ and

TAK1$^{\Delta hep}$ mice and even more important that oxidative stress is not crucial for hepatocyte-specific DNA damage. Therefore, I concluded that proliferation is the main source of DNA damage in livers of Mcl-1$^{\Delta hep}$ and TAK1$^{\Delta hep}$ mice, most probably due to replicative stress trigged DNA damage, e.g. replication fork stalling and collapse and subsequent DNA strand breaks [70, 71].

4.3.13 Proliferation-associated replicative stress causes DNA damage in murine and human regenerating livers, independent of apoptosis

DDR activation in HCC and corresponding non-tumor tissue has been described in human hepatitis B and C infected livers [51], as wells as activation of DDR in hyper-proliferative livers of mice upon partial hepatectomy. But in this study, partial hepatectomy was performed in 9-month-old mdr2$^{-/-}$ mice at a time-point when livers are strongly inflamed and show pre-neoplastic lesion [72].

To address the question whether proliferation per se - independent of apoptosis - is able to trigger DNA damage in hepatocytes of regenerating wild-type livers, we performed partial hepatectomy in collaboration with the laboratory of Prof. Sabine Werner (ETH Zürich) and I analyzed livers for DNA damage response in respect to hepatocyte proliferation.

Indeed, DDR was detectable by immunoblotting, immunohistochemical and IF staining for γH2AX in livers of wild-type mice correlating with proliferative activity peaking at 48 hours post PHX, whereas no sign of apoptosis could be detected (Figure 39).

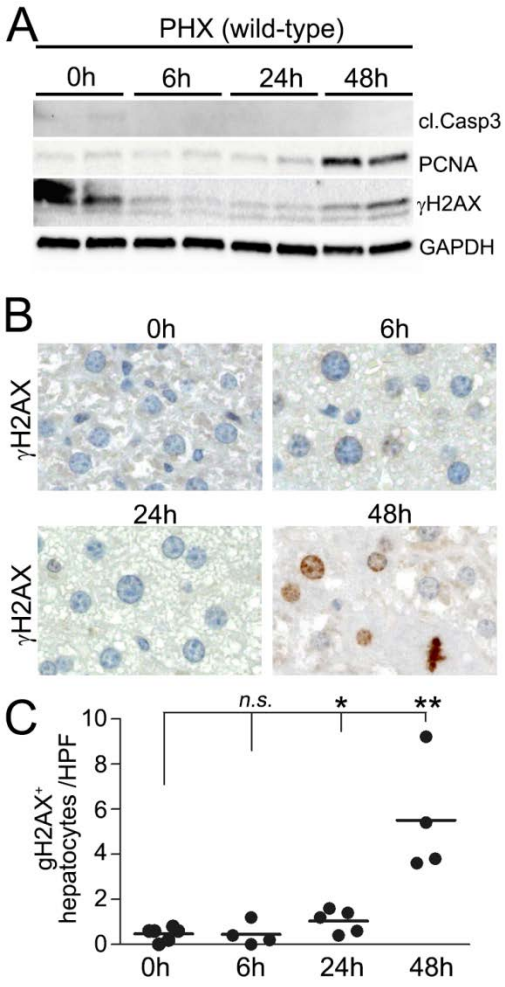

Figure 39: Proliferation-driven DDR in a non-apoptotic environment of acute regenerating wild-type livers. A) Western blotting and B) IHC staining for γH2AX revealed DDR-positive hepatocytes. C) Quantification confirmed significantly elevated numbers of γH2AX-positive hepatocytes at proliferative peak at 48h post PHX. Wild-type mice at the age of 2 months were analyzed at indicated time-points post 2/3 PHX.

Hyper-proliferation-induced DNA damage in hepatocytes was confirmed by γH2AX and BrdU co-stainings following BrdU incorporation in mice after PHX. Almost 75% of all BrdU-positive hepatoctyes in regenerating livers showed γH2AX signals and only very few γH2AX single positive cells could be detected (Figure 40). This pointed out that almost exclusively actively replicating hepatocytes show DNA damage response.

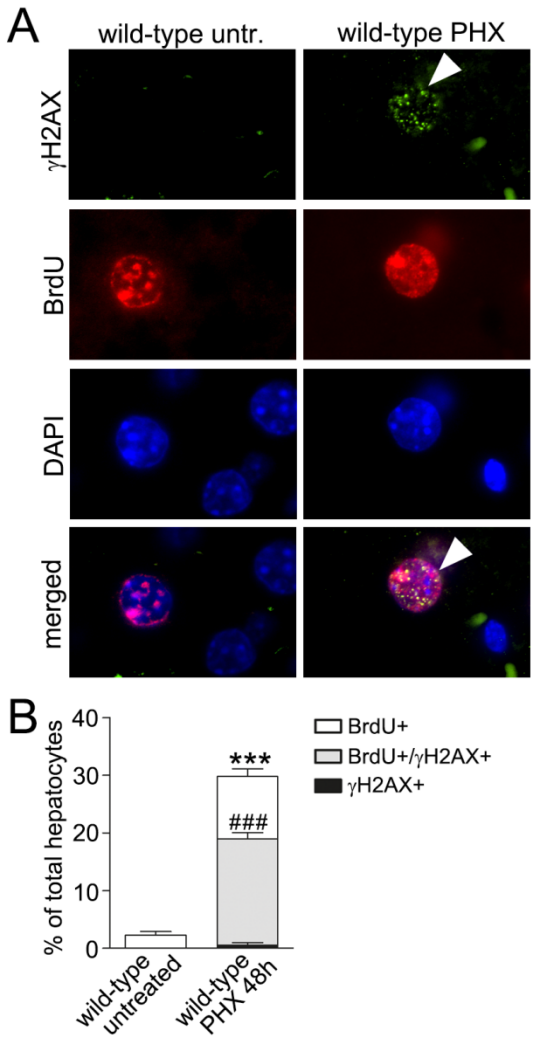

Figure 40: Proliferation-associated DDR in actively replicating cells confirmed by BrdU incorporation. A) and B) BrdU incorporation combined with γH2AX staining demonstrated proliferation-associated DNA damage in replicating hepatocytes. Arrow heads indicate positive nuclei. *p < 0.05; **p < 0.01; ***p < 0.001. *comparing Ki67-single positive cells, #comparing double-positive cells of untreated and operated wild-type mice.

To further investigate whether hyper-proliferative hepatocytes indeed show DNA strand breaks and γH2AX is a robust marker for DNA damage in proliferating hepatocytes, and does not only occur during replication independent of DNA damage, pulse field electrophoresis (PFGE) was performed and clearly demonstrated DNA strand breaks in hepatocytes of PHX mice (Figure 43).

Next, I wanted to find out whether this finding of proliferation-induced DDR in artificially increased proliferation rates of hepatocytes in PHX mice is also transferable to human liver regeneration. Therefore, I analyzed liver specimen from patients who underwent two-step hepatectomy called ALPPS (associating liver partition and portal vein ligation for staged hepatectomy). ALPPS is usually performed in patients with extensive tumors in the liver, e.g. colorectal metastasis to avoid postoperative liver failure due to insufficient functional liver mass. Precisely, during the first step to stimulate liver hypertrophy of the left lobe, the left and right liver lobe is split and the right portal vein is ligated. After 2 weeks, the right liver lobe carrying the initial tumor is resected [73].

I analyzed γH2AX-Ki67 co-stainings of liver needle biopsies of the right and left liver lobes of step1 and step2 of ALPPS patients and I could detect a strong correlation of γH2AX and Ki67 positivity in liver sections derived from the left lobe (Figure 40).

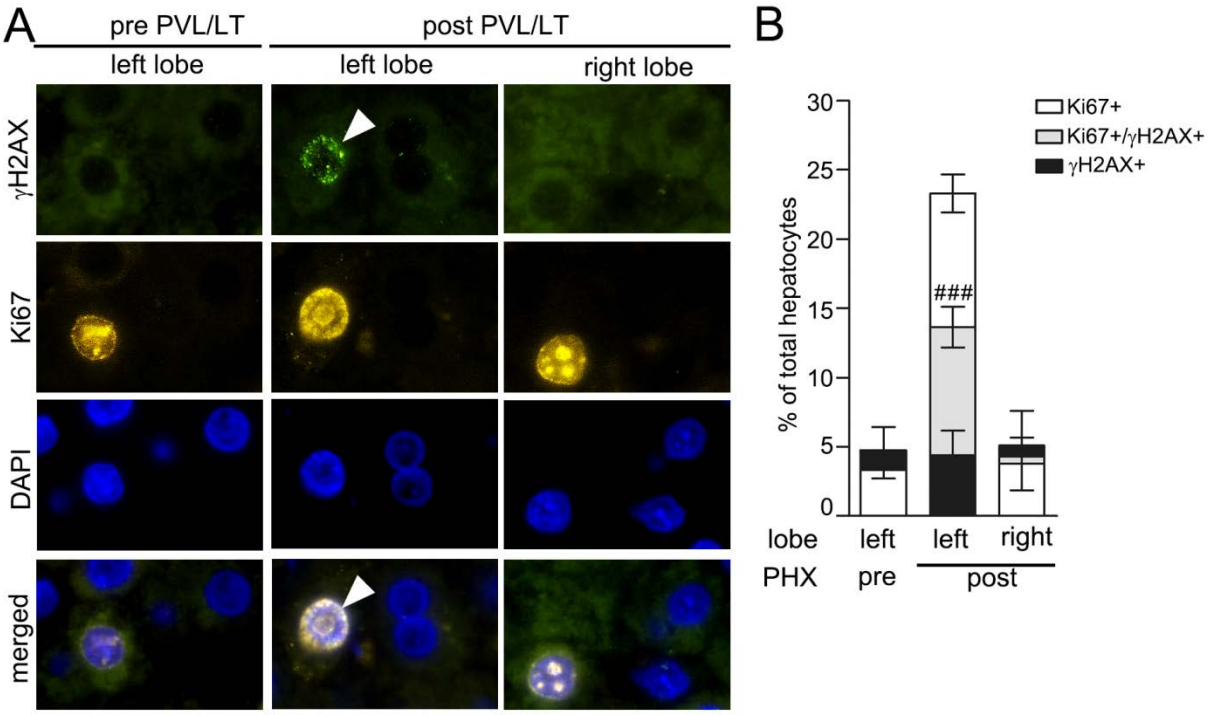

Figure 41: Proliferation-associated DDR in acute regenerating human livers. A) and B) IF co-staining for γH2AX and Ki67 and quantification demonstrated a substantial amount of γH2AX-positive and proliferating hepatocytes. in the acute regenerating left liver lobe. Liver biopsies of each liver lobe of n=6 patients prior to and after (right) portal vein ligation and liver transsection (PVL/LT) were analyzed. Arrow heads indicate positive nuclei. *p < 0.05; **p < 0.01; ***p < 0.001. *comparing Ki67-single positive cells, #comparing double-positive cells.

4.3.14 Impaired DDR of proliferation-induced DNA damage in Caspase 8-deficient hepatocytes

As described above, TAK1/Casp8$^{\Delta hep}$ mice were completely lacking DDR at 6 weeks of age and Mcl-1$^{\Delta hep}$/TNFR1$^{-/-}$ mice show reduced DDR whereas livers from Mcl-11$^{\Delta hep}$, TAK1$^{\Delta hep}$ and TAK1$^{\Delta hep}$/RIP3$^{-/-}$ were strongly positive. Comparing different genotypes also uncovered different rates of hepatocyte proliferation, potentially leading fo fals-positive conclusion about proliferation-induced DDR in analyzed murine livers. Therefore, to address the question whether Caspase 8 or further proteins directly contribute to DDR or whether the proliferation rate of hepatocytes in the different genotypes is responsible for proliferation-associated DDR.

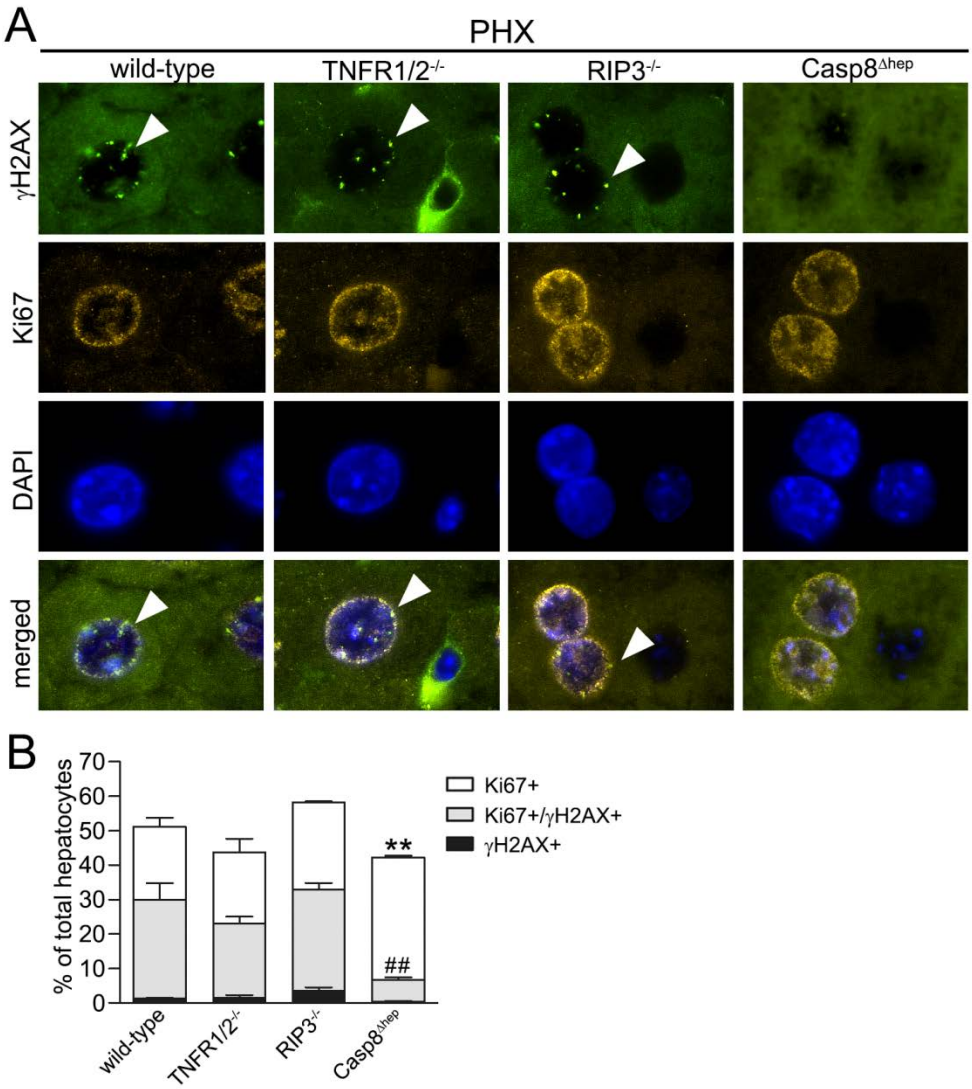

Figure 42: Hyperproliferation-induced DDR is significantly impaired in Casp8$^{\Delta hep}$ mice. A) and B) IF staining for Ki67 and γH2AX and quantification revealed a significant reduction γH2AX-positive proliferating hepatocytes in Casp8$^{\Delta hep}$ mice, compared to wild-type and RIPK3$^{-/-}$ and TNFR1$^{-/-}$ mice. n=3-6 mice analyzed 48h post PHX. Arrow heads indicate positive nuclei. *p < 0.05; **p < 0.01; ***p < 0.001. *comparing Ki67-single positive cells, $^{\#}$comparing double-positive cells.

I analyzed livers of Casp8$^{\Delta hep}$ mice for DNA damage and DDR 48h post PHX. By PFGE quantification, DNA strand breaks were detectable in livers of Casp8$^{\Delta hep}$ mice to a similar level as in wild-type mice (Figure 43). Additionally, Ki67 staining revealed slightly reduced hepatocyte proliferation in Caspase 8 deficient livers (~40%), compared to wild-type livers (~50%) (Figure 42B). Most strikingly, γH2AX/Ki67 co-staining revealed significantly less than 10% of γH2AX-positive proliferating hepatocytes in Casp8$^{\Delta hep}$ mice compared to 30% in wild-type mice (Figure 42A). In summary, these findings indicated the presence of DNA strand breaks in Caspase 8-deficient hepatocytes under proliferative conditions, but an impaired DDR.

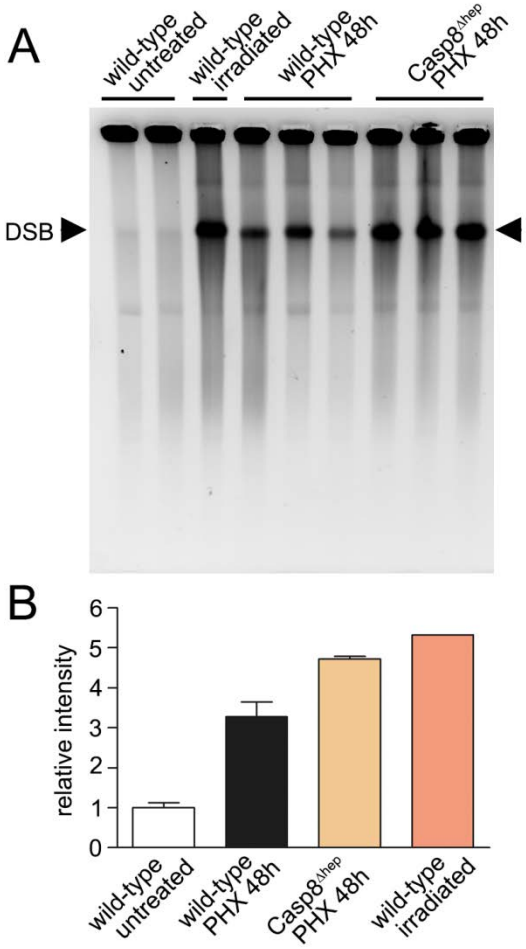

Figure 43: DNA strand breaks (DSB) detectable 48h post PHX. A) and B) PFGE analysis revealed DSB in livers derived from wild-type mice 48h post PHX compared to untreated mice. The amount of DSBs (black arrow) was increased in hepatocytes from Caspase 8 deficient livers.

4.3.15 Impaired DDR in Casp8$^{\Delta hep}$ livers upon chemical induction of DNA strand breaks

I next asked whether Caspase 8 is directly or indirectly involved in DDR upon induction of DNA strand breaks - independent of apoptotic or proliferating stimuli. Therefore, I decide to treat mice with the genotoxic agent doxorubicin (DX) which leads to the intercalation of doxorubicin into the DNA, blockage of DNA topoisomerases, disaggregation of the enzyme-DNA complex and subsequently to DNA double strand breaks in hepatocytes [74, 75].

Wild-type mice treated with doxorubicin showed a strong DDR 12h post treatment in hepatocytes reflected by almost 100% positivity for γH2AX (Figure 44A). Strikingly, Caspase 8-deficient hepatocytes were negative for γH2AX 12h after chemical induction of DNA strand breaks (Figure 44A and B), whereas γH2AX-positivity could be detected in Kupffer cells.

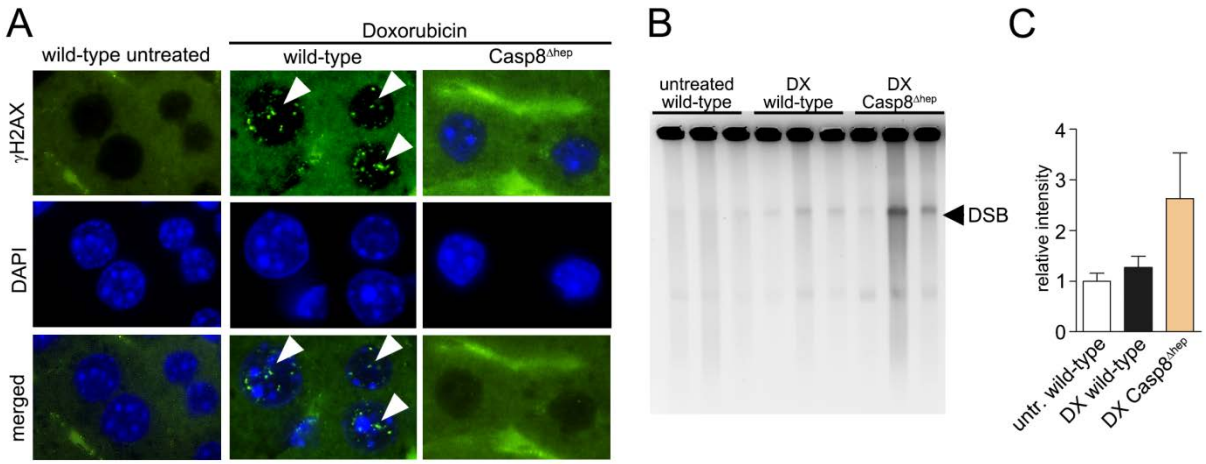

Figure 44: Caspase 8 is crucial for DDR in hepatocytes. A) Hepatocytes of Casp8$^{\Delta hep}$ mice are negative for γH2AX following doxorubicin (DX)-induced DNA damag, but B) and C) demonstrate DNA strand breaks by PFGE. No significant difference in γH2AX staining between untreated and pan-caspase inhibitor (QVD-OPH)-treated wild-type mice.

Of note, doxorubicin at this concentration was not hepatotoxic and no apoptotic hepatocytes or elevated aminotransferase levels 12h post injection could be observed (Figure 45). In addition doxorubicin-induced DDR could be detected in several other organs of wild-type and Casp8$^{\Delta hep}$ mice (Figure 46).

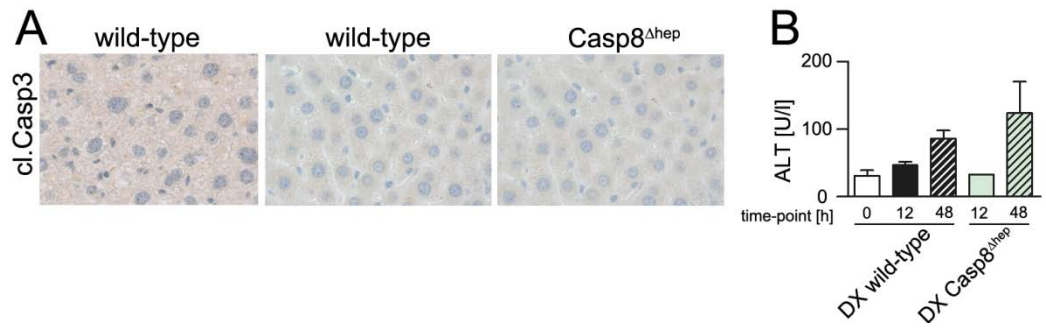

Figure 45: DX treatment does not lead to hepatocyte cell death 12h post treatment. A) Liver sections of treated mice were analyzed by cleaved Caspase 3 staining and B) aminotransferase levels determined.

Next, I addressed the question whether Caspase 8 is directly involved in the execution of DNA strand breaks upon doxorubicin treatment or in the recognition of DNA strand breaks and the subsequent activation of the DNA repair machinery.

Indeed, livers of wild-type as well as Casp8$^{\Delta hep}$ mice showed DNA strand breaks in PFGE and interestingly the amount of DNA strand breaks in Caspase 8-deficient livers as analyzed by semi-densitometric quantification were higher compared to wild-type mice (Figure 43). This indicated the inducation of DSBs but impaired DDR in Caspase 8-deficient hepatocytes. Eventually, DNA strand breaks in wild-type hepatocytes were already repaired whereas Caspase 8-deficient cells still carried the doxorubicin-induced and unrepaired DNA strand breaks post doxorubicin treatment. γH2AX is phosphorylated by the key mediators ATM, ATR and DNA-PK for the induction of the DNA repair machinery, thus my results clearly showed that DNA strand breaks were induced in Caspase 8-deficient hepatocytes, but not recognized and apparently not repaired by the cell intrinsic DNA repair machinery in the same time-frame as seen in wild-type hepatocytes.

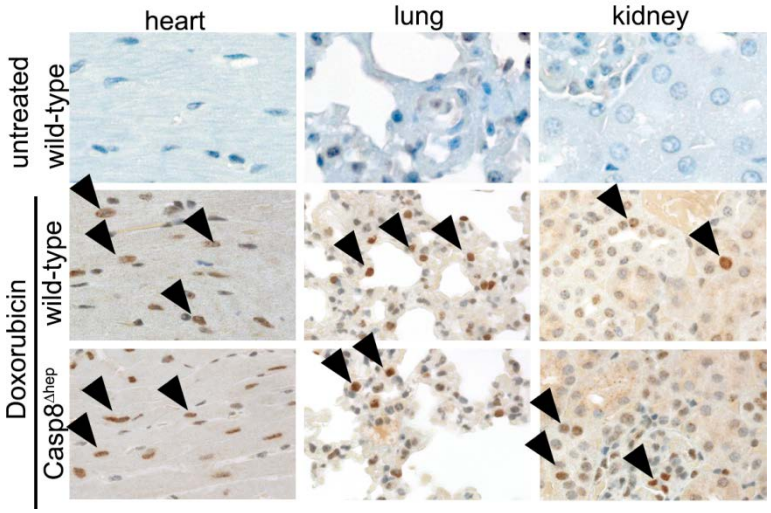

Figure 46: DX-induced DDR in other organs. Upon DX-treatment, γH2AX positive cells (black-arrow heads) were detectable in heart, lung and kidney of wild-type and Casp8$^{\Delta hep}$ mice 12h post injection.

4.3.16 Catalytic activity of Caspase 8 is not required for sensing of DNA damage

Caspase 8 is originally described as an initiator caspase for apoptotic cell death in response to activated death-inducing TNF family receptors. Caspase 8 is initially produced as an inactive monomeric pro-caspase that requires dimerization and cleavage into a large and a small catalytic active subunit for activation.

Assembly into dimers or multi-protein complexes, e.g. death-inducing signaling complex (DISC) or ripoptosome, is facilitated by various adapter proteins that bind to specific regions in the pro-domain of the pro-Caspase 8. The inactive DISC is bound to the intracellular domain and upon death receptor activation the Casp8/RIPK1/RIP3/FADD complex leads to the induction of apoptosis in the cytoplasm [76] .

Binding of cFLIP to Caspase 8 in this complex blocks Caspase 8 activity and leads to the activation of RIP3 and subsequent necroptosis – the latter complex is also described as necrosome [16]. However, the Casp8/RIPK1/RIP3/FADD complex can also be formed independent of death receptors signaling upon cellular stress and can lead to the induction of both, apoptosis or necroptosis and is referred as ripoptosome [77].

Based on this knowledge on Caspase 8 and its function as a scaffolding protein in a multimer complex as well as catalytic protein, I first investigated the role of the catalytic subunit in doxorubicin-induced DNA damage. Therefore, I treated wild-type mice 1h before doxorubicin injection with the pan-caspase inhibitor QVD-OPH to block the catalytic activity of the small Caspase 8 subunit and I analyzed liver tissue 12h post treatment. In a second experiment, I also pre-treated mice with QVD-OPH and repeated the treatment 24h post doxorubicin injection and collected liver tissue after 48h. The quantification of γH2AX positive hepatocytes revealed almost 100% positivity and I could not detect a difference to doxorubicin-treated wild-type mice (Figure 47).

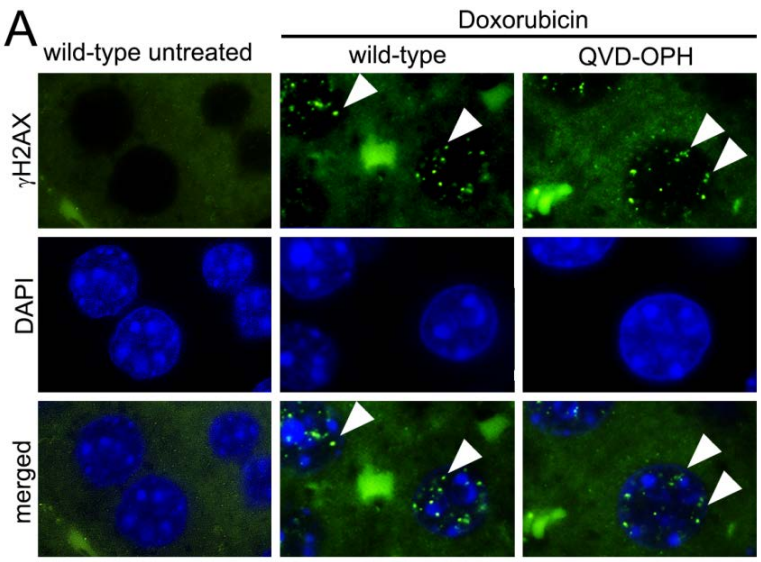

Figure 47: Catalytic activity is not involved in DDR in hepatocytes. Blocking the catalytic subunit of caspases with pan-caspase inhibitor QVD-OPH in wild-type mice does not influence DDR upon DX-treatment. Arrow heads indicate positive nuclei.

Of note, the pan-caspase inhibitor QVD-OPH does not prevent cleavage of Caspase 8 but directly blocks the catalytic domain of all caspases. Pre-treatment of wild-type mice with QVD-OPH successfully rescued LPS/D-Gal induced hepatocyte apoptosis (data not shown).

In conclusion, the catalytic active small subunit of Caspase 8 did not contribute to DDR in hepatocytes, pointing towards a potential role of Caspase 8 as catalytic-inactive protein in DDR. Therefore, I aimed at gaining insight into the role of the binding partners of Caspase 8 and focused on the ripoptosome complex with RIPK1 as central kinase.

4.3.17 TNFR and NFκB signaling do not contribute to the initiation of DDR

The formation of the pro-apoptotic TNFR signaling complex comprising Caspase 8 and RIPK1 and the activation of Caspase 8 largely depends on active TNFR signaling. Thus, I next addressed the question whether TNFR signaling is required for DDR.

In addition, the pro-survival NFκB pathway has been linked to DDR. Upon genotoxic stress and DDR activation, ATM-dependent phosphorylation and translocation of NEMO into the cytoplasm has been shown to stimulate cell survival via NF-κB -dependent expression of pro-survival genes [78, 79]. ATM-dependent activation of IKKβ and nuclear translocation of activated IKKβ was shown to be essential for prolonged ATM activation in the late phase of DNA repair in cells treated with alkylating agents [80]. Based on these results, I addressed the question whether IKKβ is required for the initiation of DNA repair and besides is essential for the prolongation of DNA repair in hepatocytes.

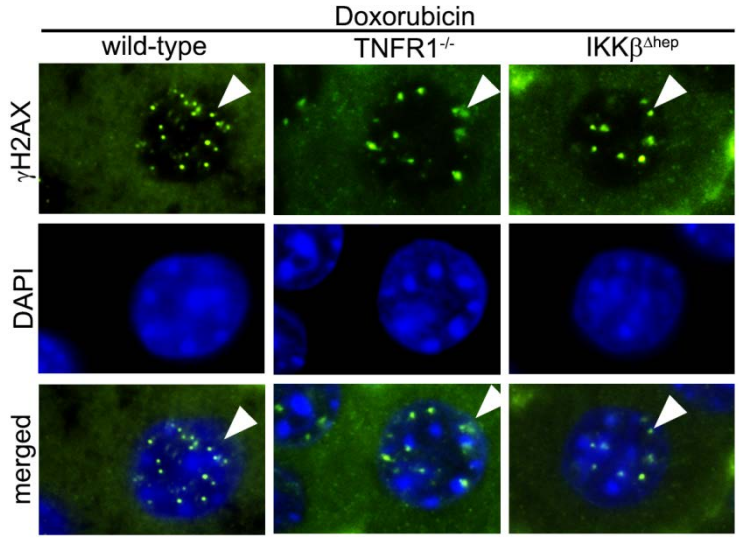

Figure 48: TNFR1 and NFκB signaling does not contribute to DDR upon DX treatment. Genetically inhibited TNFR1 or NFκB signaling by challenging TNFR1$^{-/-}$ and IKKβ$^{\Delta hep}$ mice, with DX does not influence DDR. γH2AX staining revealed no difference in the staining pattern of hepatocytes 12h post treatment. Arrow heads indicate positive nuclei.

Interestingly, treatment of IKKβ$^{\Delta hep}$ and TNFR1/2$^{-/-}$ mice with doxorubicin had no effect on γH2AX positivity at 12h and 48h post treatment as already seen in treated wild-type mice (Figure 48, Figure 51). Therefore, I concluded that IKKβ and the TNFR complex or signaling via TNFR and IKKβ are not required for the initiation of DDR.

4.3.18 RIPK1 is a direct binding partner of Caspase 8 and contributes to the initiation of DDR

Next, I focused on RIPK1 in doxorubicin-induced DNA damage to uncover its potential role in DNA damage. RIPK1 knock-out mice are embryonic lethal and conditional knock-out mice were not available. Thus, I used the Necrostatin1 (Nec1), regarded RIPK1-specific inhibitor which binds and stabilizes RIPK1 in an inactive conformation and therefore protects the phosphorylation site from activation [81].

I pre-treated wild-type mice with Nec1 before doxorubicin injection and repeated the treatment after 24h, respectively. Interestingly, treatment with Nec1 abolished γH2AX positivity of hepatocytes in wild-type mice at 12h as well as 48h post doxorubicin injection (Figure 49, Figure 51), whereas DSB were observed by PFGE (Figure 50). γH2AX negativity indicated that DNA strand break are not recognized because the γH2AX phosphorylation certainly did not occur in the presence of inhibited RIPK1.

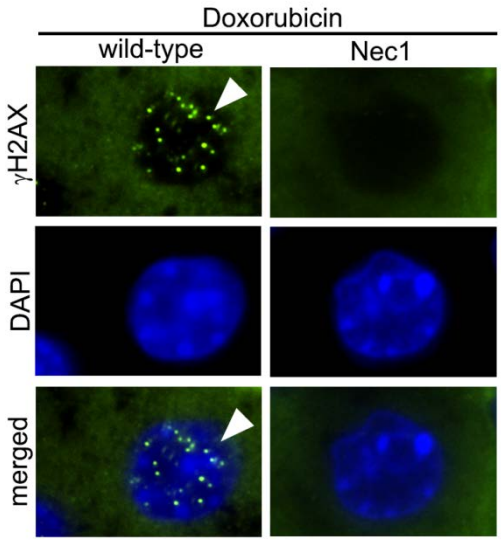

Figure 49: Pharmacological inhibition of RIPK1 abrogates DDR in hepatocytes. Livers of wild-typemice, pre-treated with Nec-1, are negative for γH2AX 12h post DX treatment, compared to inhibitor-free and DX treated wild-type mice. Arrow heads indicate positive nuclei.

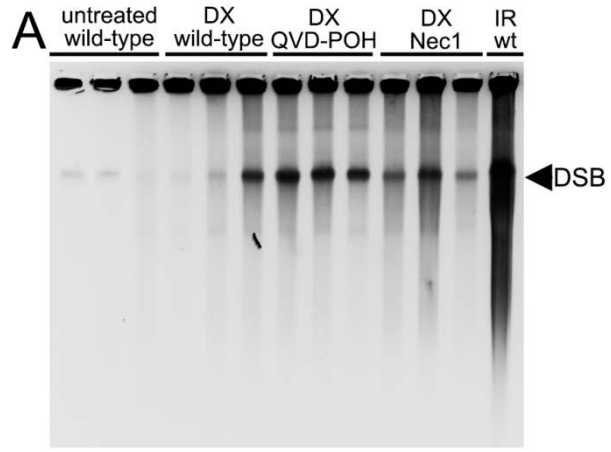

Figure 50: DSB in livers of QVD-OPH or Nec-1 treated and DX challenged wild-type mice. A) and B) Inhibitor pre-treatment has no impact on the induction of DSB (black arrow haed) in wild-type livers. Livers from lethally irradiated wild-type mice (IR, 20 Gray) were used as positive controls.

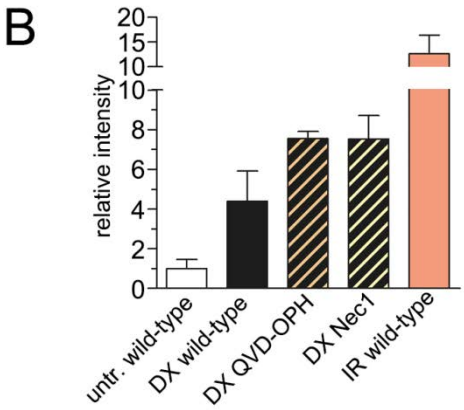

At the later time-point 48h post doxorubicin treatment, wild-type hepatocytes showed a decrease in γH2AX positivity and about 75% of hepatocytes were found γH2AX positive indicating the gradually fading of the DNA repair process (Figure 51). In contrast, Caspase 8 deficient hepatocytes and Nec1-treated mice showed an onset of γH2AX positivity 48h post treatment and a maximum of around 30% of hepatocytes were found to be positive for γH2AX. This suggests a delayed DDR in Caspase 8-deficient and RIPK1 inhibited hepatocytes and later time-points have to be analyzed *in vivo* and further experiments are planned.

In summary, the results obtained from the Nec1 experiments and the known function of Caspase 8 and RIPK1 as direct binding partners led me hypothesize that these proteins contribute to DNA repair as a complex and not as monomers.

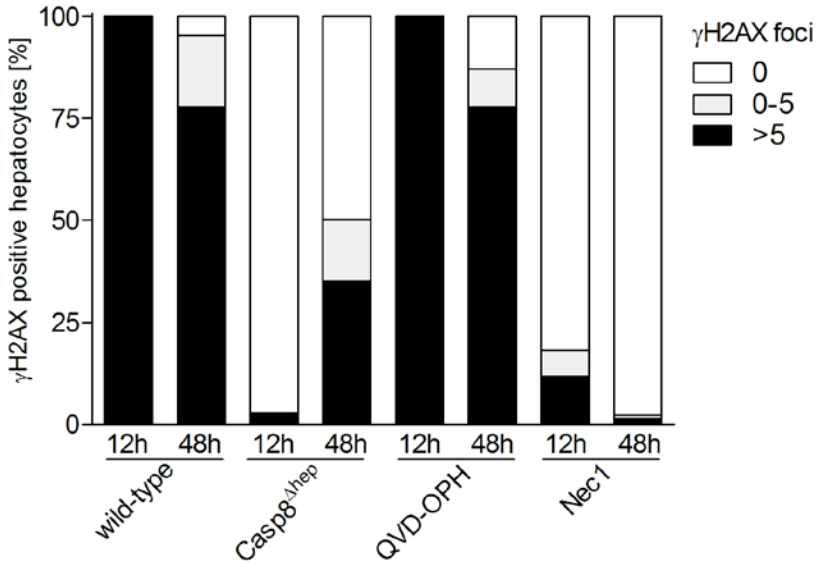

Figure 51: Quantification of γH2AX-positive hepatocytes of DX-treated Casp8$^{\Delta hep}$ or inhibitor treated mice. Liver sections were analyzed 12h and 48h post DX treatment and the amount γH2AX-positive hepatocytes calculated. Nuclei carrying >5 γH2AX-positive foci were counted as positive, negative and nuclei with 0-5 γH2AX-positive foci were counted negative for DDR. The percentage of γH2AX-positive hepatocytes was calculated related to all counted hepatocytes and percentage plotted at the y-axis. Wild-type mice were pre-treated 1h prior the experiment with QVD-OPH or Nec1. Inhibitor treatment was repeated after 24h for the analysis of the 48h time-point. n=3 of Casp8$^{\Delta hep}$ mice were analyzed at 12h and 48h, n=6-8 mice were used all other conditions.

4.3.19 RIPK1 kinase activity and cFLIP but not RIPK3 are required for DDR

Next, I investigated whether other potential binding partners of Caspase 8 or molecules that are related to Caspase 8 and RIPK1 might contribute similarly to DDR.

As described above, pro-Caspase 8 is part of the TNFR signaling complex IIa and IIb, mainly consisting of the binding partner RIPK1, FADD and cFLIP. It has been previously reported that the RIPK1 is required for the DDR *in vitro*, and that *in vitro* knock-down of RIPK1 in different lung cancer cell lines leads to a decreased and delayed response of the DNA repair proteins [82]. Pharmacological inhibition of RIPK1 by Nec1 in doxorubicin-treated wild-type mice resulted in a significantly decreased rate of γH2AX-positive hepatocytes compared to mice without necrostatin treatment. However, Nec1 inhibits RIPK1 scaffolding as well as kinase activity at the same time [81] and I took advantage of kinase-dead knock-in mice, carrying the intact full length but kinase inactivated RIPK1 ($RIPK1^{KI\text{-}DK}$ mice). Indeed, $RIPK1^{KI\text{-}DK}$ mice showed significantly reduced DDR 12h post treatment (Figure 52), clearly indicating the kinase activity and not the scaffolding function of RIPK1 as crucial for DDR.

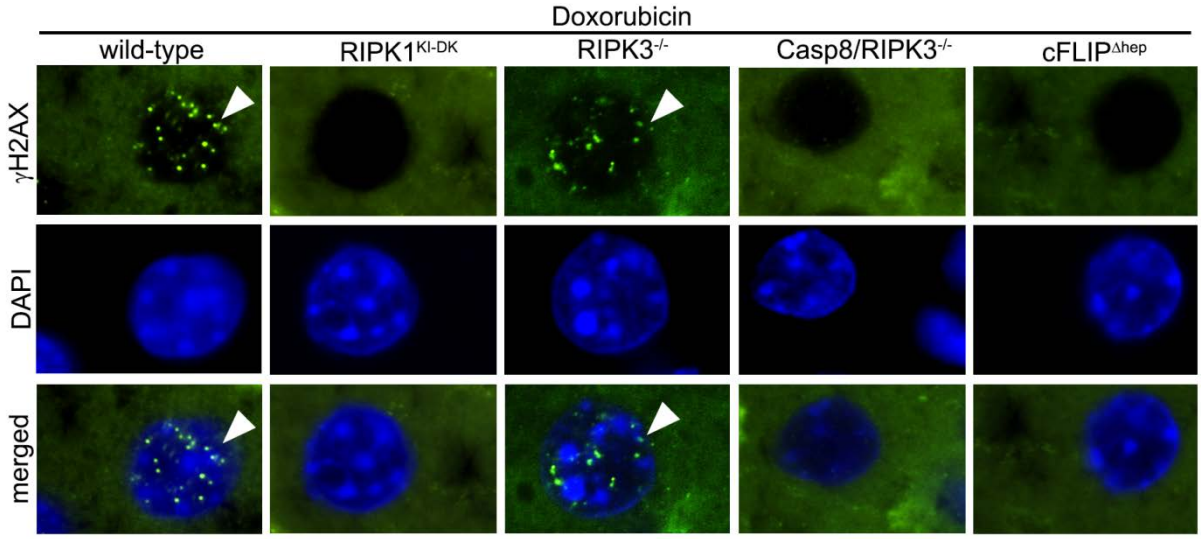

Figure 52: Genetic inactivation of RIPK1 kinase domain and cFLIP, but not RIPK3 abrogates DDR. RIPK1 kinase activity and cFLIP full length protein are required for DDR in hepatocytes upon DX-induced DSB and genetic inhibited or deficient hepatocytes are negative for γH2AX. DX-treated $RIPK3^{-/-}$ mice showed a typical dotted pattern of γH2AX-positive as seen in wild-type hepatocytes and RIPK3 is apparently not involved in DDR. Arrow heads indicate positive nuclei.

In the cellular context, the kinase function of RIPK1 is only activated in the presence of inactivated Caspase 8 and as described above, the catalytic activity is not essential for DDR. Caspase 8 is mainly inhibited by its master regulator and inhibiting binding partner cFLIP. Therefore, I decided to treat mice with a hepatocyte-specific knock-out of cFLIP (cFLIP$^{\Delta hep}$ mice) and I observed again significantly impaired DDR 12h post injection (Figure 52).
Furthermore, I challenged mice devoid of RIPK3$^{-/-}$, the essential binding factor of the necrosome to discriminate between the pro-apoptotic TNFR signaling complex IIa, the ripoptosome (both complexes devoid of RIPK3) and TNFR signaling complex IIb, called necrosome. RIPK3$^{-/-}$ mice showed clear evidence for DDR 12h post treatment and no difference was detectable compared treated wild-type mice (Figure 52, Figure 53).

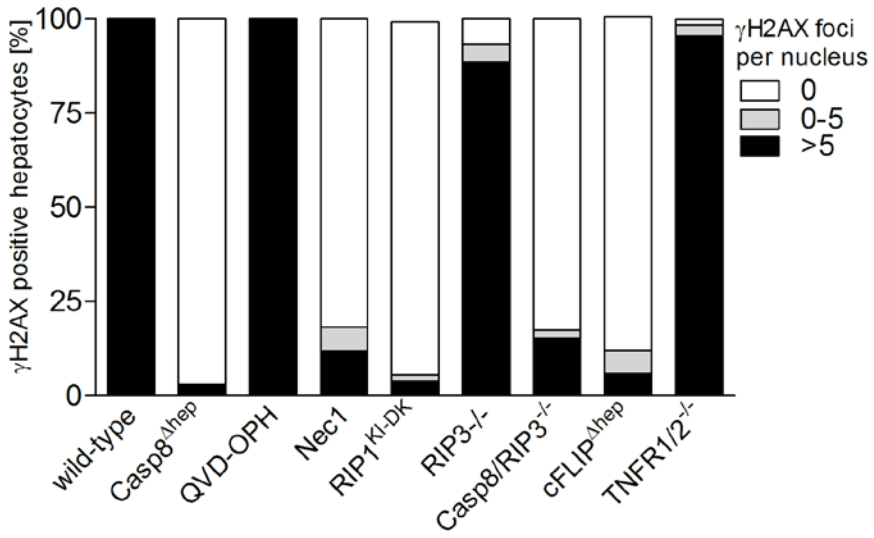

Figure 53 DDR in DX-treated mice under all genetic and pharmacological conditions. Quantification of γH2AX IF staining on livers sections of mice post DX-induction of DSBs. Nuclei carrying >5 γH2AX-positive foci were counted as positive and nuclei with 0-5 γH2AX-positive foci were counted negative for DDR. The percentage of γH2AX-positive hepatocytes was calculated related to all counted hepatocytes and percentage plotted at the y-axis. n= 3 Casp8$^{\Delta hep}$, n=6 QVD-OPH or Nec treated wild-type mice, n=5 of RIPK1^{KI-DK} mice, n=5 RIPK3$^{-/-}$, n=4 Casp8/RIPK3$^{-/-}$, n=3 cFLIP$^{\Delta hep}$ and n=6 TNFR1/2$^{-/-}$ mice were analyzed.

In summary, I uncovered central molecules of the ripoptosome and TNFR signaling complex IIa, comprising of Caspase 8, RIPK1 and cFLIP [77, 83], to be involved in DDR, potentially executing a function as dynamic signaling platform in response to genotoxic stress. Based on the previous observation that DDR is taking place independent of TNFR signaling but TNFR complex IIa and IIb formation depends on TNFR activation, I hypothesized that most likely the ripoptosome complex is crucial to mediate DDR upon DSB.

4.3.20 JNK as downstream mediator of Caspase 8 and RIPK1-dependent DDR in hepatocytes

Next, I sought to identify the signaling pathways involved in the downstream signaling of the newly identified DDR mechanism. To this aim, livers of doxorubicin-treated mice were stained for the downstream signaling candidates pCHK2 and pCHK1, indicating activated ATM or ATR signaling, respectively.

Due to the RIPK1 kinase dependent DDR, I decided to also analyze the activity of JNK, because studies provided evidence that JNK might be regulated by RIPK1 [82, 84] In addition, JNK activity has been linked recently to DDR and H2AX described as substrate for JNK *in vitro* [85, 86]. Therefore I decided to analyze the nuclear translocation of the JNK-target c-Jun (cJun) as indirect marker of JNK activity.

No substantial number of pCHK2, pCHK1, or pcJUN-positive hepatocytes was found in livers of untreated wild-type mice under steady-state conditions. After doxorubicin treatment of wild-type mice, no pCHK2- or pCHK1-positive hepatocytes were found indicating inactive ATM and ATR signaling upon doxorubicin-induced DNA strand breaks. Strikingly, livers of wild-type mice revealed pcJUN positivity in hepatocytes upon doxorubicin treatment, whereas Caspase 8 and cFLIP deficient and RIPK1 inhibited hepatocytes were negative for pcJUN as well as for pCHK2 and pCHk1 (Figure 54).

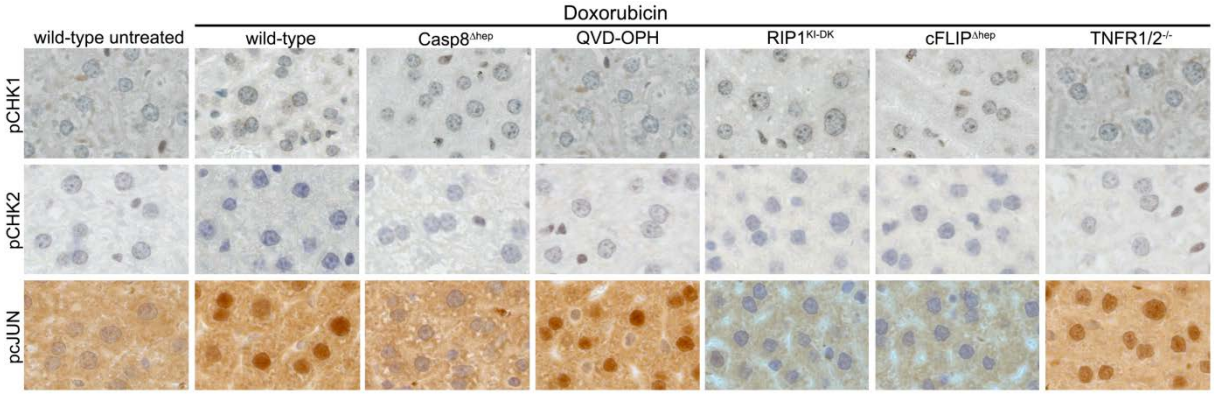

Figure 54: DNA damage signaling in livers of DX-treated mice. Stainings for downstream kinases pCHK1 (indicative for ATR signaling), pCHK2 (indicative for ATM signaling) and pcJUN (indicative for JNK signaling) demonstrated exclusively activated JNK signaling 12h post DX-induced DNA damage in wild-type mice. JNK signaling was abolished in Caspase 8, cFLIP and RIPK1 kinase inhibited mouse livers.

QVD-OPH treatment did not abrogate pcJUN staining and JNK signaling appeared to be downstream of the non-catalytic, full length Caspase 8. As expected, pcJUN-positive hepatocytes were detectable after doxorubicin treatment in RIP3$^{-/-}$ mice and TNFR1/2$^{-/-}$ mice, indicating that JNK activity upon doxorubicin treatment is exclusively downstream of Caspase 8 or downstream of a conceivable Caspase 8/RIPK1/cFLIP signaling complex.

Next, I addressed the question whether JNK directly phosphorylates H2AX at Ser139 and subsequently induces DDR and I analyzed IF double-stainings for phosphorylated JNK as well as γH2AX. Stainings revealed a strong co-localization of activated JNK and γH2AX (Figure 55), clearly indicating JNK as responsible kinase for the induction of DDR in hepatocytes upon DNA damage.

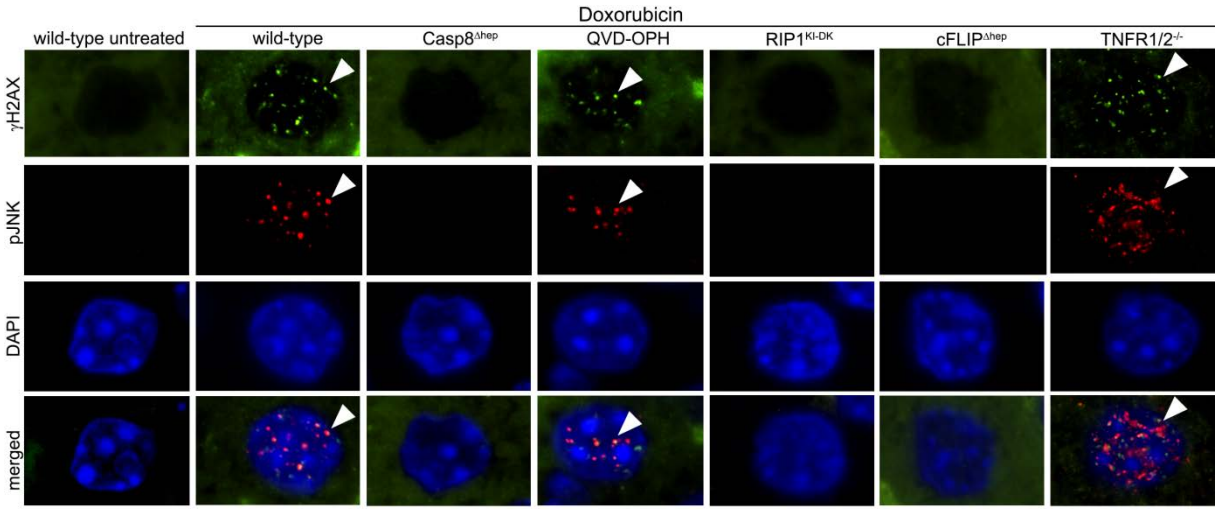

Figure 55 Activated JNK co-localizes with γH2AX during DDR. IF co-staining for pJNK and γH2AX revealed a strong co-localization in wild-type livers 12h post induction of DSB. Activation of pJNK and γH2AX was abolished in Caspase 8, cFLIP and RIPK1 inhibited mouse livers.

Next, to finally prove whether JNK is indeed mediating DDR, I decided to treat mice that lack both c-JUN N-terminal kinases 1 and 2 specifically in hepatocytes (JNK1/2$^{\Delta hep}$ mice) with doxorubicin and analyzed for DDR. Indeed, in line with my hypothesis, JNK1/2$^{\Delta hep}$ mice showed impaired DDR and significant less γH2AX-positive hepatocytes, compared to Cre-negative control littermates (Figure 56).

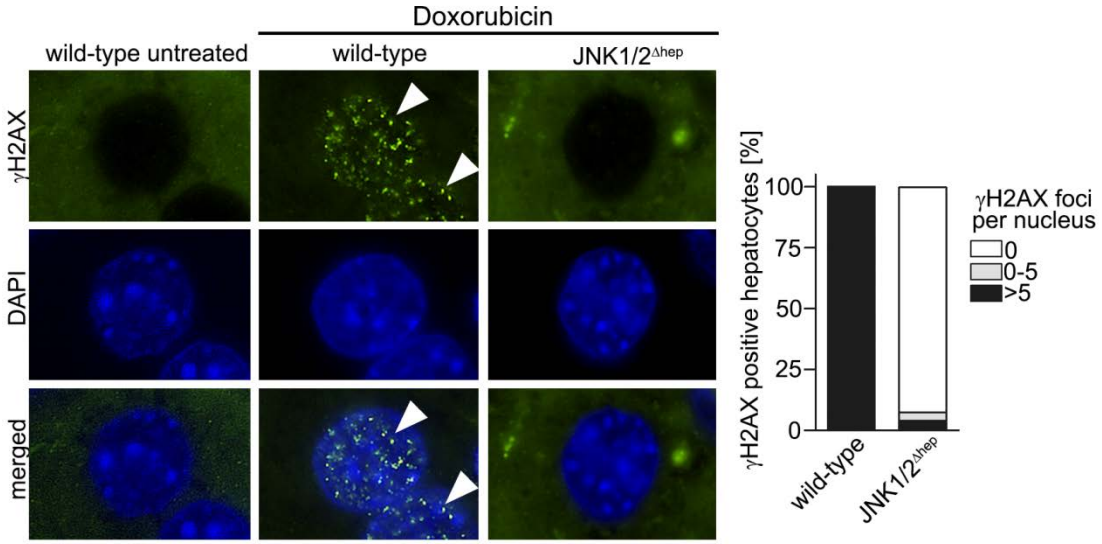

Figure 56: DDR is abolished in JNK deficient hepatocytes Livers of DX-challenged JNK1/2$^{\Delta hep}$ mice are negative for DDR marker γH”AX 12h post treatment. Arrow heads indicate positive nuclei.

Taken together, these data suggested that JNK activation and JNK-dependent phosphorylation of H2AX at Ser139 is downstream of the RIPK1/Caspase 8/cFLIP signaling platform. This signaling platform comprising a non-catalytic, scaffolding function of Caspase 8 and its master repressor cFLIP and a kinase-dependent function of RIPK1 but not RIPK3 and TNFR1, potentially illustrates the ripoptosome complex and represents a hithero unknown ATM- and ATR-independent DDR pathway.

Here, I could show that signaling via the Casp8/RIPK1/cFLIP-JNK axis is essential to initiate DNA repair in response to DSBs in murine hepatocytes.

4.3.21 JNK mediated DDR is detectable in regenerative human livers

Finally, I addressed the question whether the concept of JNK-mediated DDR is transferable from the doxorubicin mouse model to the human liver.

Indeed, pJNK/γH2AX staining revealed a strong co-localization in hepatocytes in constantly regenerating livers of CLD patients (HBV, HCV, NASH and AIH) as well as in acute regenerating livers of patient after two-step hepatectomy (ALPPS) (Figure 57).

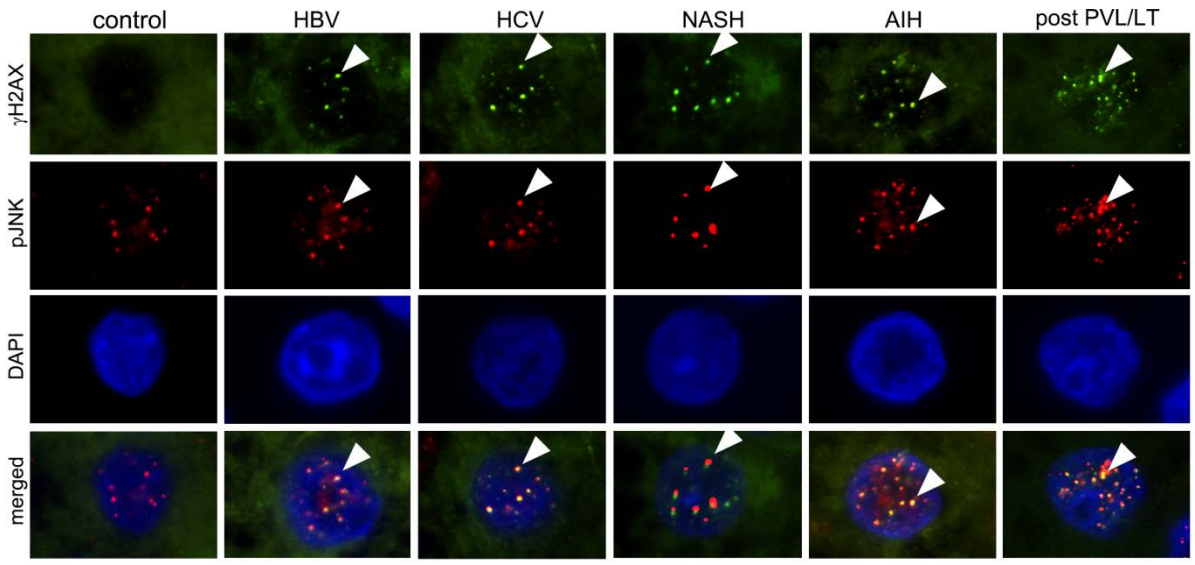

Figure 57: Co-localization of pJNK and γH2AX in tissue of regenerating human liver tissue. IF co-staining for pJNK and γH2AX revealed a strong co-localization in chronically (HBV,HCV,NASH, AIH) and acute (post PVL/LT) regenerating livers, but not in control livers. Arrow heads indicate positive nuclei.

In summary, starting from human CLD and using several genetic and experimental *in vivo* approaches (knock-out mouse models, PHX and doxorubicin challenge), I uncovered a novel DNA repair mechanism in hepatocytes. I could show a crucial non-apoptotic function of Caspase 8 as part of a complex comprising Caspase 8/RIPK1/cFLIP, indicative of signaling platform called ripoptosome, mediating DNA repair of DSB via JNK signaling.

4.3.22 Caspase 8 is required for DDR in U2OS cells

Based on the previously described results, I next addressed the question whether Caspase 8 is required for the initiation of DDR in general or whether the mechanism is hepatocyte-specific effect. Therefore, I decided to perform *in vitro* experiments using a U2OS cell, an osteosarcoma cell line expressing wild-type p53 which is a well-established cell line to study DNA repair *in vitro* [87].

Strikingly, doxorubicin-induced DSB led to the activation of γH2AX and JNK 15min post doxorubicin challenge, but not for ATM or ATR activation. At the same time, pre-treatment with a JNK inhibitor (SP600125) or Caspase 8 knock-down showed significantly decreased levels of γH2AX (Figure 58, red boxes) as well as JNK activation, compared to treated control cells. Of note: preliminary time course experiments showed a delayed activation of ATM and pCHK2 signaling 4h post doxorubicin treatment pointing towards a Caspase 8/JNK-dependent early phase-DDR mechanism in combination with ATM/pCHK2 responsible for late-phase response. Additionally, very long exposure revealed a weak ATM activation in Caspase 8-knock-down or SP600125 treated control cells, indicating a causal relationship and a cross-link between Caspase 8/JNK and ATM/pCHK2 signaling pathways (Figure 58). However, further *in vitro* experiments have to be performed to understand this relationship.

In summary, I could show that the Caspase 8/JNK-mediated DDR is not only limited to hepatocytes and potentially presents a common mechanism for the repair of DSB.

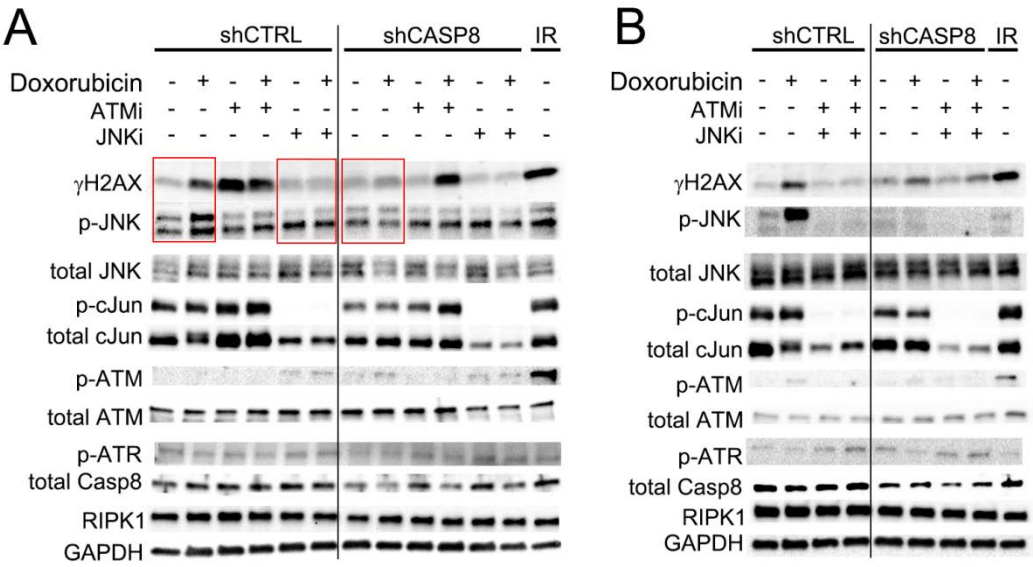

Figure 58: Impaired JNK signaling and DDR in Casp8 knock-down cells. Lentiviral knock-down of Caspase 8 in U2OS cells reduced pJNK and γHAX signals 15min post DX-treatment (1mM). Pharmacological inhibition of JNK (JNKi, SP600125) but not inhibition of ATM (ATMi, Ku-55933) of control cells prevented an increase in γH2AX upon DX treatment. Irradiated control cells (10Gray, 2h prior to the experiments) were used as positive controls.

4.3.23 Caspase 8 does not contribute to irradiation-induced DDR

Based on the previously described results about the control of ATM by Caspase 8/RIPK1 in DDR, I next addressed the question whether Caspase 8/RIPK1 contribute to DDR in general. ATM as “guardian of the genome” [88] is mainly activated upon detection of DSB and is also cross-activated via ATR in single strand breaks (SSB) repair, but not in irradiation (IR)-induced DNA damage. IR induced DNA damage lesions, e.g. inter-strand crosslinks, pyrimidine dimers, are repaired by non-homologous end joining (NHEJ) mediated by DNA-PK. In contrast, DSB are repaired by ATM-mediated homologous recombination (HR) [88], showing a high degree of redundancy and collaboration between ATM and ATR mediated repair of SSB.

I analyzed livers of wild-type as well as Casp8$^{\Delta hep}$ mice 30min post irradiation with 1Gy. Interestingly, quantification of γH2AX staining of Casp8$^{\Delta hep}$ mice showed no difference in the numbers of γH2AX positive hepatocytes compared to wild-type mice (Figure 59).

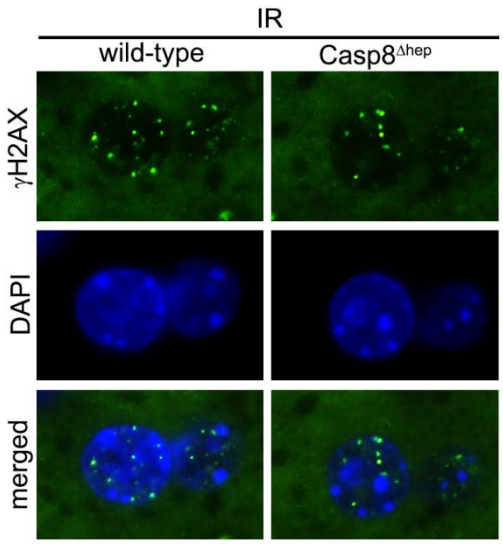

Figure 59: IR induced DNA damage in wild-type and Caspase 8-deficient hepatocytes. Analysis of γH2AX stainings of whole body irradiated (1Gy) mice revealed positive hepatocytes in Casp8$^{\Delta hep}$ and wild-type mice. n=3 Casp8$^{\Delta hep}$ and n=6 wild-type mice were analyzed 30min post irradiation.

In conclusion, Caspase 8-deficiency did not affect DDR in hepatocytes upon IR with 1Gy. IR-induced DNA damage mainly leads to base damage (base loss and change, base oxidization, pyrimidine dimers, DNA cross links) and DNA-protein cross-links which are repaired by mismatch or nucleotides excision signaling pathways (e.g. mediated by DNA-PK) and only low level of double strand breaks are induced and repaired by homologous recombination

Finally, this finding suggested that exclusively DSB are repaired by the Caspase 8/cFLIP/RIPK1-JNK axis.

4.4 Discussion

In this study, I uncovered a novel and unexpected role of the cell death executer molecules Caspase 8, cFLIP and RIPK1 in maintaining genetic integrity by controlling JNK activation and JNK-dependent repair of DSBs. Precisely, I described a doubled-edged function of Caspase 8 in hepatocytes by driving apoptosis-dependent hyper-proliferation and tumorigenesis on one hand and by mediating DDR and activation of JNK representing an anti-tumorigenic mechanism for Caspase 8 on the other hand.

The involvement of Caspase 8` binding partners and the TNFR-independent function suggest the ripoptosome complex as responsible multi-protein complex. Most probably, the catalytic inactive pro-form of Caspase 8 serves as a binding partner for cFLIP and especially RIPK1, in contrast to its catalytic function which promotes tumor development by creating a hyper-proliferative and genotoxic environment in regenerating livers [49]. RIPK1 requires Caspase 8 as scaffold partner to stabilize its kinase active conformation [89].

This finding indicates a novel pro-survial function of the ripoptosome complex as dynamic signaling platform, controlling cell fate in response to cellular stress (Figure 60).

4.4.1 Hepatocyte apoptosis in regenerative livers of CLD patients and murine livers correlates with DDR, genetic instability and tumor development

It is well known that increased levels of apoptosis are a hallmark of many liver diseases including viral hepatitis and a protective mechanism to eliminate potentially damaged hepatocytes [6, 7, 90, 91]. Recently, it was shown in mouse models that HCC development occurs in an environment of chronically increased levels of hepatocyte apoptosis [45, 48, 49], and in humans with chronic HBV infection it has been shown that ALT levels – reflecting (apoptotic) hepatocyte death - are independent predictors of risk for HCC development [92].

Here, I provide arguments, in human as well as in mice, that chronically increased levels of hepatocyte apoptosis are not only associated with liver tumor development, but might be a major, potentially most relevant determinant of HCC development: 1) Mcl-1$^{\Delta hep}$ mice which developed liver tumors at 1 year had higher transaminase levels early in their life reflecting higher levels of hepatocyte apoptosis, compared to Mcl-1$^{\Delta hep}$ mice without tumor development. 2) Genetically reducing levels of hepatocyte apoptosis in Mcl-1$^{\Delta hep}$/TNFR1$^{-/-}$ mice resulted in reduced tumor incidence, similarly as also reported for Mcl-1$^{\Delta hep}$ mice with reduced apoptosis due to additional BAK deficiency [45], or shown for TAK1$^{\Delta hep}$ mice with ablation of apoptosis due to additional Caspase 8 deficiency [49]. 3) As observed in Mcl-1$^{\Delta hep}$ mice, also Mcl-1$^{\Delta hep}$/TNFR1$^{-/-}$ mice revealed a strong correlation between transaminase levels early in their life and later tumor development. 4) Retrospective analyses of a patient cohort with chronic HCV infection revealed that patients who developed HCC during the

course of their disease had higher transaminase levels compared to case-control matched pairs respectively. Taken together, these findings strongly suggest that the accumulated amount of liver cells apoptosis quantitatively determines the risk of HCC development.

Interestingly, it has been explained just recently in a mathematical approach that the number of stem cell divisions is more likely the reason for 2/3 of all cancer types due to stochastic (replicative) factors versus environmental and inherited factors, counting only for 1/3 of cancer types [93]. By plotting the lifetime incidence of various cancers against the estimated number of normal stem cell divisions in the corresponding tissues over a lifetime, they found a strong correlation especially in regenerative organs. HCC in HCV-infected patients showed the fifth highest correlation and colorectal cancer in FAP patients the highest correlation [93]. Therefore, they concluded that the majority of cancer is due to "bad luck," meaning random mutations arising during DNA replication in normal, noncancerous stem cells [93]. In my own study, showing HCC development in patients with elevated aminotransferase levels (apoptotic cell death) in the cohort of HCV-infected patients (MELD study) as well as several mouse models including intercossings, I could show experimentally that is possible to manipulate the previous defined stochastic event called “bad luck”. Since hepatocyte apoptosis is driving compensatory hyper-proliferation (reflecting liver regeneration) and proliferation-associated DNA damage, I concluded that hepatocyte apoptosis is the major, potentially most relevant determinant of HCC development.

4.4.2 Mcl-1$^{\Delta hep}$ mice – a suitable model to study hepatocarcinogenesis

To study to the impact of hepatocyte apoptosis in regenerative livers and hepatocarcinogenesis in more detail, I took advantage of the Mcl-1$^{\Delta hep}$ mouse model. Mcl-1$^{\Delta hep}$ mice were published to develop HCC with a 50% incidence after 12 months of age and 100% after 18 months of age [48]

Interestingly, Mcl-1 could be seen as tumor-suppressing protein in the liver only by inhibiting hepatocyte apoptosis. It has been show that the genetic deletion of the pro-apoptotic counter player Bak in Mcl-1 deficient hepatocytes completely rescued liver tumorigenesis [45]. This finding also implicates that Mcl-1 has no anti-carcinogenic function besides preventing hepatocyte apoptosis which eventually lead to liver tumor development due to increased rates of hepatocyte cell death and hyper-regeneration. Based on this observation, one could define Mcl-1 as tissue-specific or environmental tumor suppressor.

Furthermore, the additional knock-out of the tumor suppressor and anti-apoptotic protein p53 does not only accelerated tumor development in Mcl-1$^{\Delta hep}$ mice, Mcl-1$^{\Delta hep}$/p53$^{-/-}$ mice also showed embryonic lethality due to liver failure and some animals that did survive to adulthood showed increased hepatocyte apoptosis, severe liver damage and 100% tumor

burden [94].

Taken together, the analysis of the Mcl-1$^{\Delta hep}$ mouse model suggests that chronically increased apoptosis in hepatocytes is carcinogenic and inhibition of apoptosis may suppress liver carcinogenesis in CLD [94]. Therefore, I concluded that the Mcl-1$^{\Delta hep}$ mouse model is a suitable model to study apoptosis-dependent liver damage and hepatocarcinogenesis.

Indeed, by analyzing the expression of well-known oncogenes in murine HCC, I found a significant deregulation of oncogenes and tumor suppressor genes again indicating the close relationship to the molecular mechanisms of human hepatocarcinogenesis. Also the morphological analysis of murine HCC demonstrated a broad and heterogeneous spectrum of growth patterns of HCC published by the WHO for liver tumors. But exactly this heterogeneous pattern of murine HCC potentially reflects not unique but rather more likely diverse molecular and cellular mechanisms of tumor development. Therefore, one could potentially oversee crucial molecular and cellular events which are essential for the development specific HCC subtypes and are not detectable because RNA or proteins from different HCC are analyzed in the same experimental approach and the results are discarded due to missing statistical significance. It is known that human HCC subtypes pass different molecular events, e.g. mutations of β-catenin has been described in 32%, TP53 in 21%, AXIN1 in 15.2%, CDKN2A homozygous deletions in 8% and APC in 1.6% of human HCC. Interestingly, *TP53* alterations were usually exclusive from *CTNNB1* mutations (P=0.0001), but not from *AXIN1* and *APC* mutations [35, 95]. These data demonstrate the limitation of pooled analyses of heterogeneous tumors, which overall are not statistically significant but are for the individuum potentially biological relevant.

Nevertheless, especially the fact of statistical significant gene expression in a pool of biological heterogeneous murine HCC elucidated the value of the Mcl-1$^{\Delta hep}$ mice for studying human hepatocarcinogenesis. By performing RNA microarray analysis I uncovered genes in regenerating liver of two months-old Mcl-1$^{\Delta hep}$ mice and validated the expression in HCC of several other mouse models as well as human HCC and finally could significantly correlate the protein expression with patients` survival. The novel regeneration and tumor-associated genes were already described (Plk1, Tpx2) or are not yet described (Bcl21ab, Tinag, Gpnmb) during human HCC development. In conclusion, Mcl-1$^{\Delta hep}$ mice resemble fundamental and common features of human hepatocarcinogenesis - independent of HCC subtypes or etiologies - and further studies have to show whether the uncovered tumor-associated genes are of interest as therapeutically targets or as biomarkers for liver malignancy and tumor development.

4.4.3 DDR and genetic instability in regenerative murine and human livers

In deep analysis of the hyper-apoptotic and regenerative livers of patients with chronic liver diseases as well as several mouse models led me to two additional remarkable observations. First, I found of a significant number of γH2AX-positive hepatocytes indicative of DNA damage response. Second, I detected significant levels of allelic imbalances at chromosomal fragile sites by Taqman copy number assay and fragment length analysis, indicating a substantial level of genetic instability in hepatocytes of regenerating livers. Of note, both DNA damage response as well as genetic instability was detectable in hepatocytes already prior to any dysplastic changes or morphological findings indicative of neoplastic transformation.

The obvious question whether DDR and genetic instability were detected as coincidence with a) DNA fragmentation in apoptotic cells or appeared in b) proliferative or c) senescent/quiescent hepatocytes could be answered by γH2AX/cl.Casp3 and Ki67 γH2AX/Ki67 co-stainings. Finally, as experimental proof by analyzing livers of wild-type mice at proliferation peak 48h post PHX, I was able to show for the first time that regenerating livers independent of apoptosis indeed show proliferation-associated DNA strand breaks and DDR.

The most likely causes of proliferation or precisely replication-associated DNA damage are due to inhibited DNA polymerases (e.g. lack of nucleotides, unwinded DNA), disruptive secondary structure in GC rich regions to G-quadruplex structures, stalled replication forks, torsional stress and subsequent physical breakage at common fragile sites [96]. Chromosomal instability especially at chromosomal fragile sites as a result of replication stress is well-known to promote tumorigenesis [97]. Especially the loss of *WWOX* and *FHIT*, which I analyzed in my study and are located in regions of chromosomal fragile sites, were just recently linked to cancer in breast, prostate, ovarian, and lung [97-99].

The thigh correlation of hepatocyte apoptosis and susequent proliferation with later tumor development in several mouse models (Mcl-1$^{\Delta hep}$ and TAK1$^{\Delta hep}$ mice and intercrossings) supported the initial hypothesis. More important, by inducing hepatocyte proliferation in a model of acute regeneration (PHX mice), I demonstrated that hyper-regeneration by itself indeed is able to trigger DNA damage and induced DDR. This was confirmed by showing widespread DDR in human livers, notably restricted to the regenerating part of the liver, while lacking in non-regenerating parts.

4.4.4 Non-apoptotic functions of Caspase 8

By studying mice with a hepatocyte-specific Caspase 8-deficiency, I made a remarkable, at first glance counter-intuitive observation. Since Caspase 8-deficiency had been shown to abolish HCC development in TAK1$^{\Delta hep}$ mice [49], it was surprising to discover that Caspase

8-deficient hepatocytes revealed significantly reduced γH2AX-positive hepatocytes after exposure to cellular stress induced by either partial hepatectomy or doxorubicin treatment, which at the same time led to widespread γH2AX-positivity in wild-type hepatocytes. The simultaneous detection of DNA strand breaks, directly visualized by PFGE, in Caspase 8-deficient hepatocytes revealed that whereas DNA damage occurred, DNA damage response obviously was impaired in Caspase 8-deficient hepatocytes. Finding that pre-treatment with the pan-caspase inhibitor and blocking of the catalytic activity of Caspase 8 did not affect γH2AX signals in hepatocytes after doxorubicin exposure suggested that DDR was not dependent on Caspase 8 catalytic activity, but rather a non-apoptotic and potentially scaffolding function.

Interestingly, the non-apoptotic functions of Caspase 8 are largely unknown and a big "mystery", currently of high interest. Whereas the Caspase 8-dependent inhibition of RIPK1/RIPK3-mediated necroptotic cell death has been described [100, 101], first studies described just recently a role of Caspase 8 in controlling Nlrp3 inflammasome activation [102, 103] or IRF3 activation and IFNγ expression upon viral infection [104]. Strikingly, this non-apoptotic function of Caspase 8 in controlling innate immune signaling occurs independent of signaling mediated through TNFα, IL-1β or TLR receptors and independent of NF-κB signaling (Figure 60) [105]. However, a role of Caspase 8 in DDR, either sensing of DNA damage or transducing DNA repair, is not yet described.

4.4.5 Role of the Caspase 8-dependent ripoptosome complex in DDR

Inactive and non-catalytic proteins of Caspase 8 are always bound at least to one binding partner under normal physiological conditions, e.g. its main repressor and pseudo-caspase cFLIP [106]. But Caspase 8 has also been shown to be an essential part of the multimeric ripoptosome complex, which is formed under cellular stress conditions, e.g. viral infection, pharmacological Caspase 8 blockage or in response to (genotoxic) stress-induced depletion of XIAP, cIAP1 and cIAP2 for maintaining cellular homeostasis (Figure 60) [77]. Based on this, I aimed to gain insights into the role of further molecules of the ripoptosome complex and/or related to non-apoptotic functions of Caspase 8.

First, I have been able to phenocopy my results from genetically Caspase 8-deficient mice to pharmacological inhibited, Nec1 treated wild-type mice. Second, I could show that DDR is taking place in hepatocytes independent of TNFR1 and NF-κB signaling, but dependent on the presence of cFLIP. Since the kinase activity of RIPK1 seemed to be crucial, but not RIPK3, the composition of proteins involved in DDR potentially corresponds to the ripoptosome complex and is here named "RIPairosome" (Figure 61).

In conclusion, not only assembly of the ripoptosome complex in response to genotoxic stress

[77], but additionally the downstream mediation of DDR represents the next layer of complexity of the non-apoptotic functions of Capase8-dependent ripoptosome complex in controlling cell survival and cell fate.

In the past, RIPK1 was shown to control cell fate in response to extensive genotoxic stress, but the study focused on the induction of apoptosis or necroptosis and NF-κB signaling [84], Potentially, the DDR phenotype has been overseen since Caspase inhibitors against the catalytic subunit instead of Caspase 8 knock-out cells have been used. But additionally, a RIPK1-dependent DDR has been published in a paper dealing with glycolysis [82].

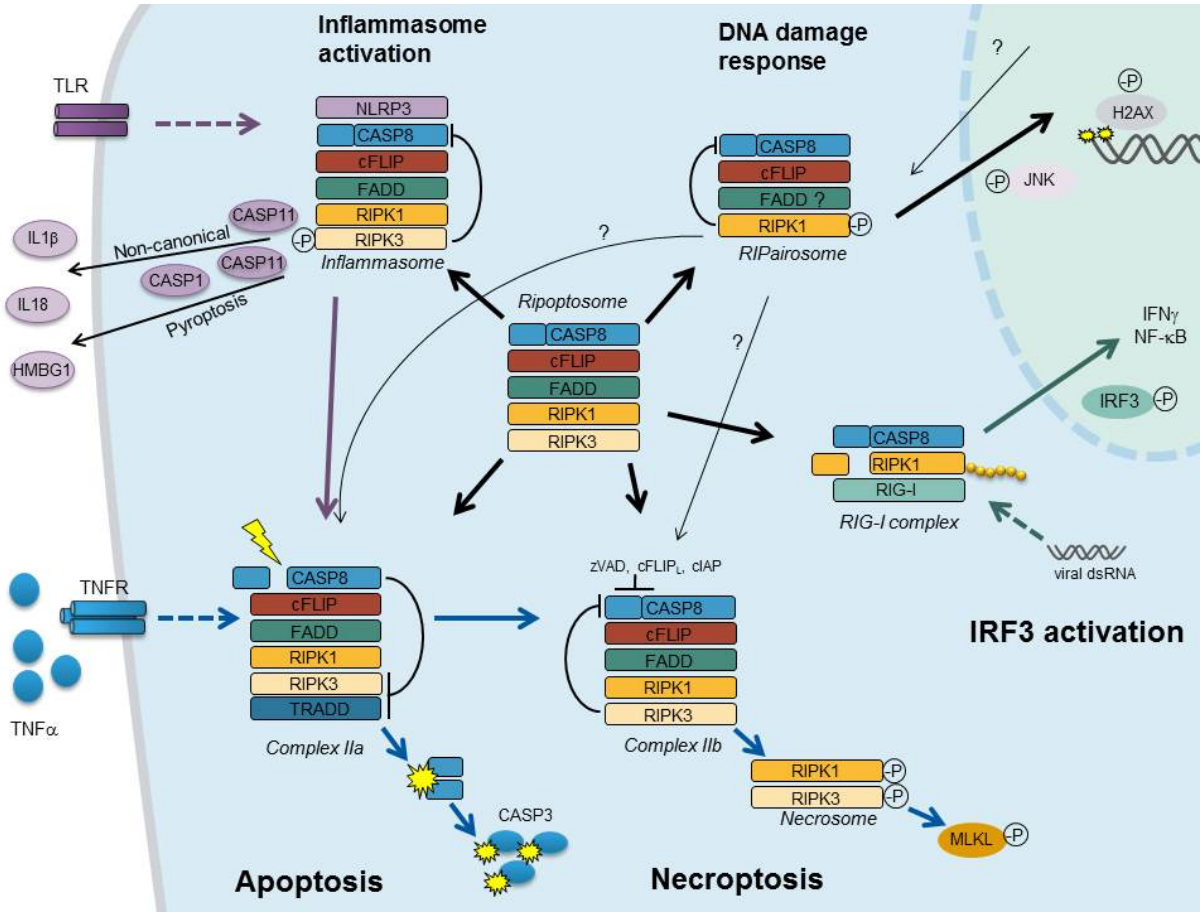

Figure 60: The ripoptosome – a central and dynamic signaling platform controls intracellular stress response. The ripoptosome complex, comprising RIPK1, FADD, cFLIP and Pro-Caspase 8 is highly similar to the TNFR signaling complex II, but the ripoptosome assembly is triggered independent of TNFR signaling upon intracellular stress. The ripoptosome controls intracellular stress response and determines cell fate by the induction of apoptosis, necroptosis, inflammasome or IRF3 activation or as describe in my doctoral thesis to DNA damage response. The regulation of the ripoptosome is highly dynamic and depends on the of the cellular context, posttranslational modifications (phosphorylation or ubiquitination of RIPK1, overexpression or degradation of cIAP or cFLIP isoforms). Figure adapted from Boege et al, unpublished.

Due to technical limitations for Western blotting, the hepatocyte specific knock-out of Caspase 8 in a full organ and technical difficulties with the subcellular fractionation of isolated hepatocytes, I had to characterize the DNA damage signaling pathways in single hepatocytes by IHC. Finding no evidence for ATM or ATR signaling following doxorubicin treatment by analysis of pCHK1 and pCHK2 stainings, but an obviously impaired pcJUN response *in vivo* as well *in vitro* in Caspase 8-knock-down U2OS cells, revealed JNK signaling as responsible pathway in DDR of the newly discovered signaling complex.

The first major breakthrough confirming the existence of a nuclear-cytoplasmic signal transduction described first an ATM- and NEMO-dependent and second an ATM-IKKβ-dependent nucleus-to-cytoplasm signaling responsible for NF-κB activation and cell survival [78, 80]. In contrast, the ripoptosome-dependent and NF-κB signaling independent DDR in my own experiments could be explain due to difference in detailed experimental set-ups (time- and dose-dependent effects) and also cell-type specific mechanisms. In above mentioned studies, DNA damage has been mainly induced by irradiation or etopoiside-treatment exclusively *in vitro* in several cancer cell lines [78, 80] and described an ATM-dependent but also time-dependent DNA repair exclusively [80]. Whereas I could exclude ATM-mediated DNA repair downstream of Capsase8, I could clearly show a convincing co-localization of pJNK and γH2AX in hepatocytes. Interestingly and in line with the published studies, I observed activated ATM signaling in U2OS cell, but this phenotype seemed to be dose and time dependent (4-12h post DX challenge) whereas the JNK-dependent phenotype occurred early between 15min and 30min post treatment.

Furthermore, irradiation experiments with Casp8$^{\Delta hep}$ showed the exclusivity of the novel discovered Caspase 8/cFLIP/RIPK1-JNK axis for the repair of DSB in cells.

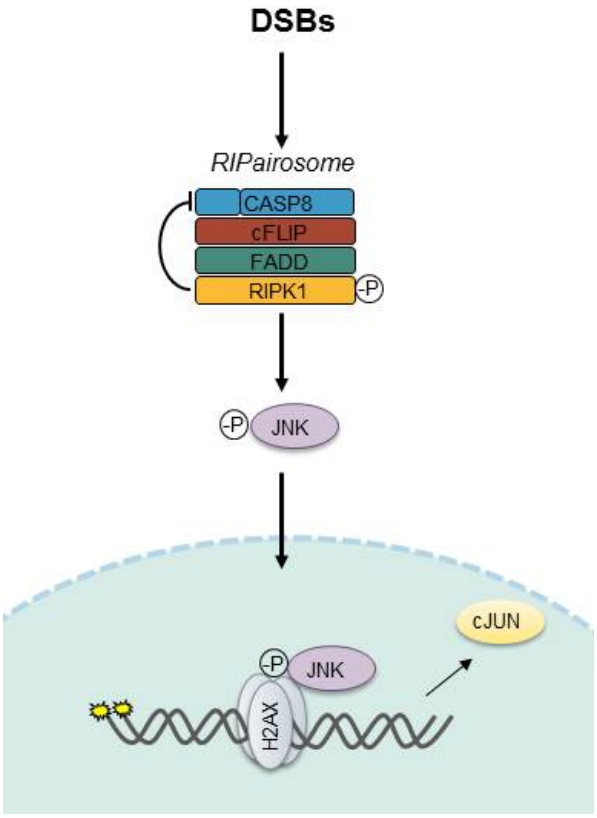

Figure 61 Caspase 8 dependent DDR in hepatocytes. A complex comprising a catalytic inactive Caspase 8, cFLIP, FADD and RIPK1 mediated activation JNK signaling. Activation of JNK depends on the kinase function of RIPK1 and is here named “RIPairosome”. Figure from Boege et al, unpublished.

Further work has to be done to uncover the exact molecular mechanisms mediating a) the activation of the ripoptosome complex in response to genotoxic stimuli and b) the ripoptosome dependent activation of JNK. In addition, I hypothesize that Caspase 8, by mediating DDR in response to DSB, potentially controls the amount of mutations and genetic aberrations and therefore potentially inhibits the malignant transformation of hepatocytes and thereby inhibiting liver tumorigenesis. Caspase 8-dependent hepatocyte apoptosis triggering hepatocarcinogenesis has been shown in several HCC mouse models [49, 107] and the activated, catalytic Caspase 8 protein could be regarded as environmental oncogene in the liver.

In contrast, the catalytic-inactive full length Caspase 8 protein as part of the multimeric ripoptosome could be potentially seen as tumor suppressor for liver tumorigenesis. To answer this question exactly, several experimental approaches are needed to distinguish between apoptotic and non-apoptotic and pro-tumorigenic functions, e.g. by using genetically modified mice carrying a catalytic-inactivated, uncleavable Caspase 8 for different genetic or experimental models of HCC development.

In addition, the hallmarks of cancer proposed by Hanahan and Weinberg described “Genome Instability and Mutation” as enabling hallmark [41, 43]. So called “caretakers” are required for the DNA-maintenance machinery – similar to Caspase 8 and the ripoptosome complex - and these caretakers genes act very much like tumor suppressor genes and their functions can be lost during tumor progression [43]. The loss of these caretakers is gained by inactivating mutations or via epigenetic repression. Interestingly, the epigenetic silencing of Caspase 8 in human HCC has been already shown in two studies [108, 109]. But only HCC and HCC cell lines have been analyzed and it would beof high interest to analyze chronically diseased livers in respect to the loss of Caspase 8, (proliferation-induced) DNA damage, JNK activation and DDR to better understand the contribution of Caspase 8 to hepatocarcinogenesis

5 The role of enterocyte apoptosis in intestinal carcinogenesis

5.1 Introduction:

5.1.1 Intestinal carcinogenesis

As introduced before, the four most common causes of cancer-related death worldwide (lung, liver, stomach, and bowel) account for nearly half (46%) of all cancer deaths (Figure 1) [3] Intestinal, in particular colorectal cancer (CRC) is a common and frequently lethal disease. CRC is among the most frequently diagnosed cancers in the Western world with around 1.36 million new cases and estimated 700.000 deaths per year and affects men and women almost at equal ratios (

Figure 62) [3].

Both, environmental as well as inherited factors influence tumorigenesis in this organ with environmental factors becoming more important in recent years. These environmental risk factors (also called modifiable risk factors) became more important during the last few years, compared to risk factors that cannot be individually controlled, such as age and genetic predisposition. Due to industrialization of developing countries and adaption to a Western life style - i.e. in particular increased intake of energy-dense food with high fat and sugar content, red meat and low intake of dietary fibers, leading to overweight or obesity and physical inactivity – tumor growth in the digestive system is promoted. In particular in countries with a high-income economy that have recently changed from a relatively low-income economy, such Eastern European countries, incidence rates have at least doubled since the mid-1970s [110].

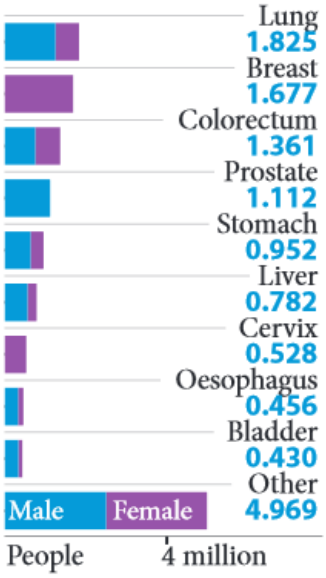

Figure 62: Estimated cancer mortality rates in both sexes in 2011. Colorectal cancer is the third most common cancer worldwide accounting for 1.36 million deaths per year.. Almost 55% of the cases occur in more developed regions, especially in Australia/New Zealand and Europe. Figure from WHO-Cancer Fact Sheet [1].

5.1.2 The Vogelstein scheme

The molecular events driving intestinal and in particular colorectal carcinogenesis are far better characterized than for most other solid tumors. Specific genetic changes that drive the transformation from a normal intestinal epithelial cell to an invasive cancer cell are thought to confer a selective growth advantage, resulting in preferential proliferation of the cell containing a mutation. A lot of our understanding was obtained by the pioneer work of Vogelstein and co-workers and the definition of the adenoma-carcinoma sequence (Figure 63) [111].

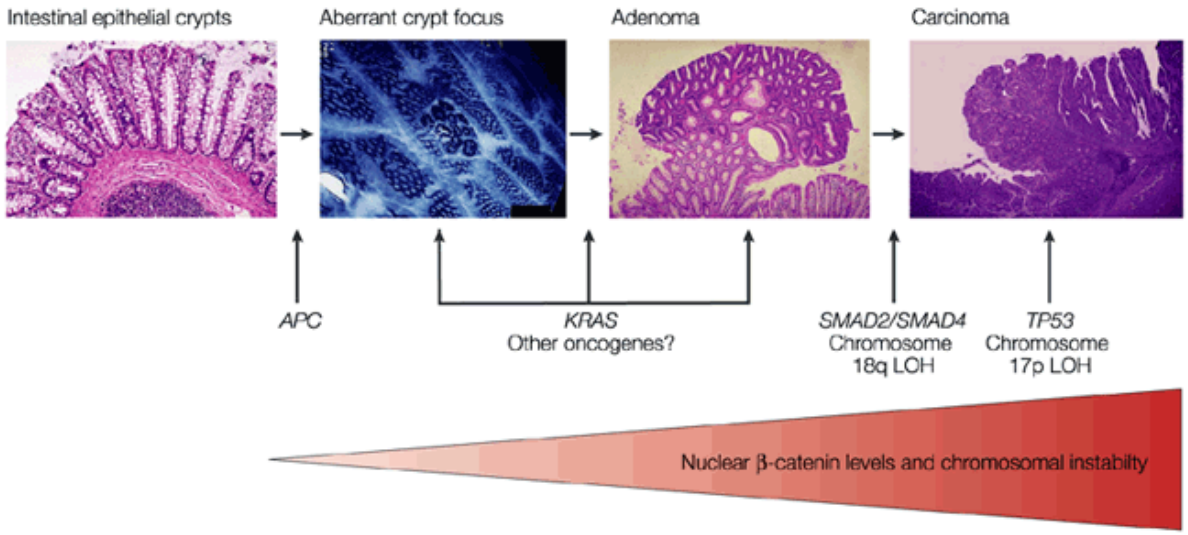

Figure 63: Histopathology of colorectal cancer according of the adenoma-carcinoma sequence known as Vogelstein scheme. Aberrant crypt foci (ACF) are the earliest microscopically detectable colorectal neoplastic lesions. ACF composed of dysplastic cells are prone to become a polyp, a benign tumor. Polyps may progress to adenomatous (dysplastic) polyps and finally invasive-growing carcinoma. Figure from Fodde et al. [112].

Their early model describing genetic changes in genes including APC, β-Catenin, K-ras, and p53 has been refined later. It is now expanded by data from whole tumor genome sequencing efforts including those from the *The Cancer Genome Atlas Network* giving a comprehensive molecular characterization of human colon and rectal cancer [113]. The majority of intestinal cancers progress through an adenoma-carcinoma sequence. Remarkably, there is a strong correlation between the histopathological changes in the intestinal mucosa (normal epithelium → dysplastic changes / adenoma → intramucosal → invasive carcinoma) with the occurrence of genetic changes described in the Vogelstein model [111].

5.1.3 Inflammatory bowel disease

For a long time, it is known and well documented that patients suffering from inflammatory bowel disease (IBD), i.e. Crohn's disease (CD) and ulcerative colitis (UC) are at higher risk to develop intestinal, in particular colorectal carcinoma [114]. Of note, the risk for tumor development in IBD patients depends on the extent, duration, and inflammatory activity of the disease. The pathophysiology of IBD obviously goes along with an abnormal immune response of both, the adaptive and innate immune system. Histopathologically, IBD is characterized by the persistent side by side occurrence of intestinal mucosal damage and inflammation on the one side, and persistent reparation and regeneration on the other side. Thus, the intestinal tract of patients with IBD reveals chronically increased cell death and proliferation of intestinal epithelial cells which are required to keep intestinal homeostasis.

5.1.4 Homeostasis of intestinal epithelium

The intestinal epithelium constitutes a specialized single cell layer with absorptive and secretory functions in the interface between the body and the external environment. In the epithelium, enterocytes are responsible for the absorption of nutrients, ions, vitamins, and water [115-117].

Paneth cells, goblet cells, and enteroendocrine cells comprise the secretory lineage of the intestinal epithelium, playing an important role in the intestinal defense against potentially harmful bacteria and the coordination of intestinal functions by hormone secretion. In close contact with the epithelium lies the lamina propria, a loose connective tissue in which mesenchymal cells and mucosal immune cells are located (Figure 64) [117, 118].

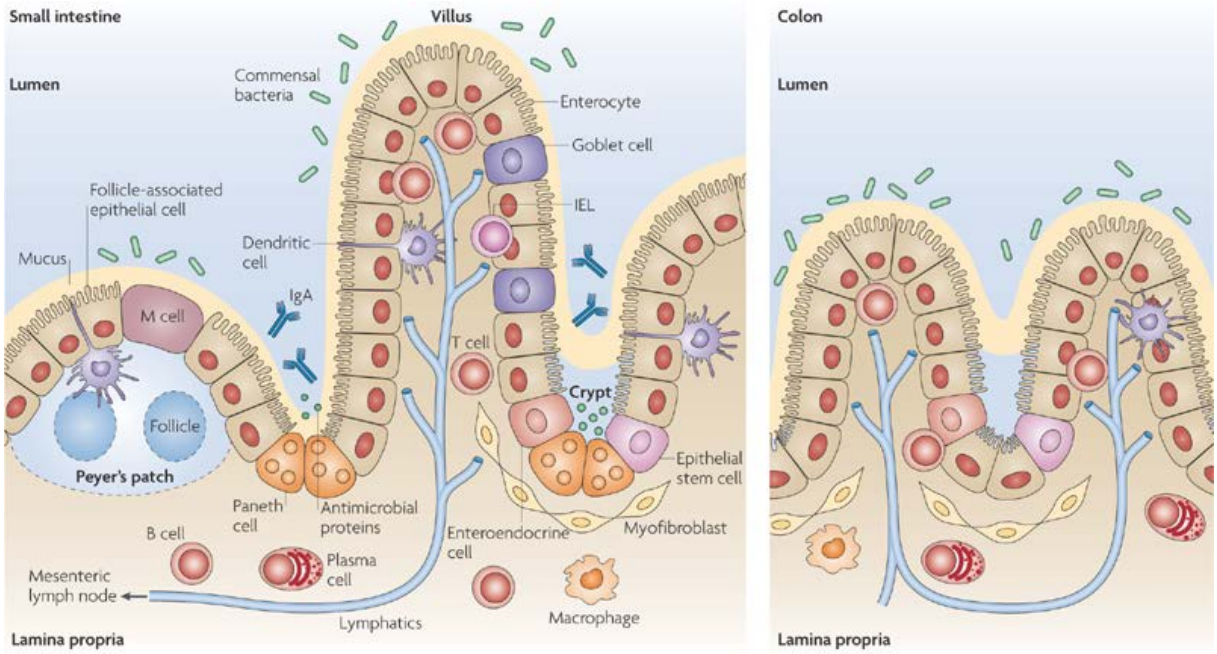

Figure 64: The intestinal epithelium. A single layer of intestinal epithelial cells (IECs)generates a physical barrier that separates the microbiota in the intestinal lumen from the underlying lamina propria. In addition to differentiated enterocytes and goblet cells, progenitor IECs differentiate into both enteroendocrine cells, which secrete enteric hormones, and Paneth cells at the base of the small intestinal crypts [119]. Figure from Abreu et al. [119].

In the large and small intestine, differentiated enterocytes are constantly removed and replaced by new cells originating from undifferentiated adult intestinal stem cells, which are localized in the third or fourth position counted from the base of the crypt [120]. These new cells migrate from the base of the crypt to the apical zone of the intestine undergoing maturation. In the apical zone, these cells survive for about 4-5 days before being shed into the gut lumen. In this single epithelial layer, a tightly regulated equilibrium between cellular proliferation and cell death must be kept in order to maintain the intestinal barrier [117, 121]. Importantly, if cell death in the epithelium is not strictly regulated, it might result in a barrier defect with subsequent microbial invasion and inflammation. Previous studies have shown that epithelial cell proliferation and turnover are accelerated in IBD, with elevated levels of programmed cell death being observed in patients with both CD and UC [117].

5.1.5 Cell death in inflammatory bowel disease

In the normal, healthy intestinal epithelium, apoptosis is needed for tissue homeostasis. Apart from Paneth cells and stem cells, all cells migrate from the base of the crypt to the villus tip where they are shed into the lumen. Cells always undergo apoptosis before shedding and apoptotic bodies are never found in the epithelial monolayer. Interestingly, morphological changes typical of apoptosis are not apparent until the nucleus of the shedding cell has moved above the nuclei of adjacent cells, suggesting that shedding leads to apoptosis [122]. Furthermore, treatment of mice with a broad-spectrum caspase inhibitor blocked almost all shedding events, indicating that Caspase 3 cleavage is critical for cell shedding to occur as revealed by cleaved Caspase 3 staining within the cytoplasm of shedding cells[122]. In addition to cell shedding, rare apoptotic events were observed in the stem cell niche and are believed to contribute to stem cell homeostasis [123].

Under non-physiological conditions, as seen in patients suffering from acute or chronic IBD, high levels of apoptosis have been observed in the intestinal epithelium. Colonic epithelium specimen from patients with UC show higher rates of apoptosis than controls and apoptotic cells are also found in crypts of active UC, suggesting that loss of epithelial cells occurs mainly due to apoptosis in the affected intestine and also in adjacent unaffected areas [52]. In line, apoptotic features in UC patients are significantly more prevalent than in controls but similar to those observed in infectious colitis patients [117, 124, 125].

In CD, the number of apoptotic enterocytes was found to be higher in inflamed compared to non-inflamed areas and normal intestine, with no significant difference found between unaffected and normal mucosa, suggesting that a high rate of enterocyte apoptosis in the intestinal epithelium of CD is associated with intestinal inflammation, being exclusively increased in inflamed areas [126].

Several animal studies describe the central role of apoptosis in the disease mechanisms of IBD. For example, knock-out mice for XBP1 (an endoplasmic reticulum (ER) stress-related transcription factor), develop spontaneous enteritis, associated with Paneth cell dysfunction and subsequent apoptotic cell death. Interestingly, an association between UC and CD with XBP1 variants was identified in humans and replicated as susceptibility genetic factors [127]. In addition, enterocyte-specific inactivation of NFκB signaling was shown to cause apoptosis of colonic epithelial cells with subsequent impaired expression of antimicrobial peptides and translocation of bacteria into the mucosa [128].

The first study showed the role of Caspase 8 in the regulation of necroptosis in the intestinal epithelium. Mice with a conditional deletion of Caspase 8 in the intestinal epithelium spontaneously developed terminal ileitis. These mice showed a loss of Paneth cells, indicating a dysregulated antimicrobial immune cell function of the intestinal epithelium. In addition, epithelial cell death was induced by TNFα and was associated with increased expression of RIP3. More importantly, the authors identified high levels of RIP3 in human Paneth cells and increased necroptosis in the terminal ileum of patients with CD, suggesting a potential role of necroptosis in the pathogenesis of this disease [117, 129].

These findings were confirmed independently in a second study with conditional knockout mice for FADD in intestinal epithelial cells. These mice spontaneously develop epithelial cell necrosis with loss of Paneth cells and bowel inflammation. Inhibition of necroptotic cell death ameliorated intestinal inflammation and tumorigenesis [130].

In addition, a recent study showed a significantly increased expression of the necroptosis executer proteins RIP3 and MLKL, accompanied by a reduction of Caspase 8 expression in biopsy samples from children suffering from IBD. Necroptosis is strongly associated with intestinal inflammation in IBD and contributes to strengthen the inflammatory process [129, 131].

5.1.6 The microbiota promotes intestinal tumorigenesis

Studies with genetically modified mouse models for spontaneous intestinal tumorigenesis have unraveled a fundamental role of the microbiota in tumor promotion. Conditional NEMO knock-out mice or APC transgenic mice showed enhanced intestinal inflammation as well as increased intestinal permeability most probably due to enterocyte apoptosis. Subsequently,

this caused a leaky intestinal barrier, leading to the penetration of microbial products or microbes into the affected mucosal tissue but not into adjacent normal tissue. Germ-free housing of mice significantly reduced the inflammatory response as characterized by IL-23 and IL-17 expression as well as reduced the number of apoptotic enterocytes resulting in a reduced tumor burden under germ-free conditions or antibiotic treatment [132, 133]. This indicates a crucial role of the microbiota for the induction of enterocyte apoptosis under inflammatory conditions and a causal relationship between the microbiota and tumorigenesis. In addition, the tumor promoting effects of the microbiota have been shown in a mouse model for spontaneous intestinal tumorigenesis being accompanied only by mild inflammation. Mice carrying the mutated APC gene were kept under germ-free conditions and the decreased number of tumors was correlated with a reduced expression of TNFα, IL-1β and IL-23 in colonic tumors [134]. Taken together, the tumor promoting effects of the microbiota could be causally linked to intestinal tumorigenesis in mouse models for IBD and the specific IL-23-dependent inflammation pattern was linked to the metastatic spread and overall patient survival [135].

5.2 Scientific Questions

As described above, enterocyte cell death seems to be the main driver of intestinal inflammation in patients suffering from IBD and promotes intestinal tumorigenesis.

In the second project of my doctoral thesis, I aimed at understanding the role of enterocyte cell death in intestinal tissue homeostasis and identifying the molecular mechanisms driving intestinal tumor development in chronically inflamed and regenerating intestinal tissue. More precisely, I aimed to answer the following questions:

- Is it possible to transfer the concept of cell death driven tumorigenesis from to the liver to the intestine?

- Is Mcl-1 required for enterocytes and intestinal tissue homeostasis?

- Do Mcl-1 knock-out mice recapitulate the hallmarks of the Vogelstein scheme?

- Does enterocyte apoptosis lead to an inflammatory and regenerative response?

- Which immune cell type mediates intestinal inflammation in conditional Mcl-1 knock-out mice?

5.3 Results

5.3.1 Generation of enterocyte-specific Mcl-1 knock-out mice (Mcl-1$^{\Delta IEC}$ mice)

To generate conditional Mcl-1 knock-out mice, I intercrossed mice carrying the Mcl-1 loxp sites allele with mice expressing the Cre-recombinase under the enterocyte-specific villin promotor. Mice homozygous for the Mcl-1 flox allele and positive for the Cre-recombinase (further denoted as Mcl-1$^{\Delta IEC}$ mice) were used as knock-out mice and compared in all experiments to Cre-negative littermates serving as age- and gender-matched wild-type controls. I confirmed the conditional knock-out of Mcl-1 in the intestinal epithelium with a specific set of PCR primers for the recombined genetic Mcl-1 locus (Figure 65). For breeding, male mice heterozygous for the Mcl-1 loxP allele were used as breeding males. Homozygous mice – independent of the presence of Cre recombinase - are in contrast to homozygous female mice infertile and therefore not suitable for breeding.

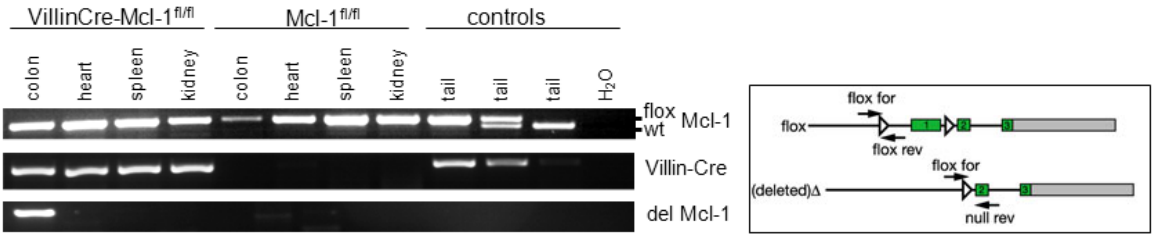

Figure 65: Genotyping PCR for the enterocyte-specific recombination of the Mcl-1 locus. Snap-frozen tissue of indicated organs has been digested with Proteinase K and gDNA was used for PCR reactions. Genotyping PCR primer for the Cre recombinase and the Mcl-1 gene were used as well as a pair of primers specific for the recombined, deleted Mcl-1 locus ("del Mcl-1").

5.3.2 Phenotypically characterization of Mcl-1$^{\Delta IEC}$ mice

Mcl-1$^{\Delta IEC}$ mice were monitored over time by measuring body weight every 4 weeks and Mcl-1$^{\Delta IEC}$ mice showed a reduced body weight compared to age- and gender-matched controls with some mice which had to be euthanized when the criteria for abortion were reached (Figure: 66 and Figure 67).

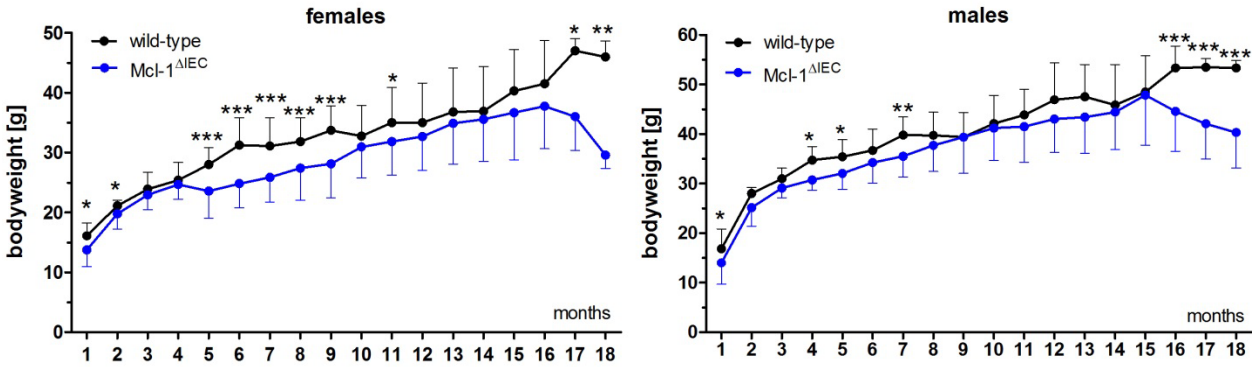

Figure: 66 Monitoring of body weight. Body weight of Mcl-1$^{\Delta IEC}$ mice were monitored over time and compared to gender-matched Cre-negative littermates. Mcl-1 knock-out females (n=39) as well as males (n=41) showed significantly reduced body weight.

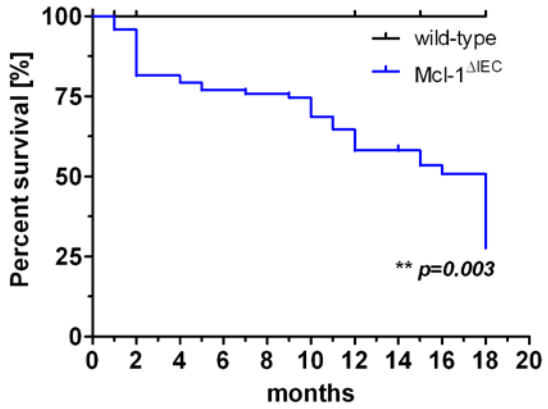

Figure 67: Monitoring of survival. Mcl-1$^{\Delta IEC}$ mice showed significantly reduced survival compared to Cre-negative control littermates.

In addition, I collected stool for the analysis of fecal calprotectin by ELISA. Calprotectin, a protein consisting of a S100A8/S100A9 dimer, strongly correlates with intestinal inflammation as it is released from activated monocytes and granulocytes and therefore it is widely used as a reliable marker for diagnostic purposes in patients suffering from IBD and monitoring disease activity [136]. In addition, some Mcl-1$^{\Delta IEC}$ mice started to develop diarrhea and indeed, I could find enrichment of calprotectin in stool samples of Mcl-1$^{\Delta IEC}$ mice and an enhanced expression of S100A8 and S100A9 on mRNA level in colonic tissue (Figure 68).

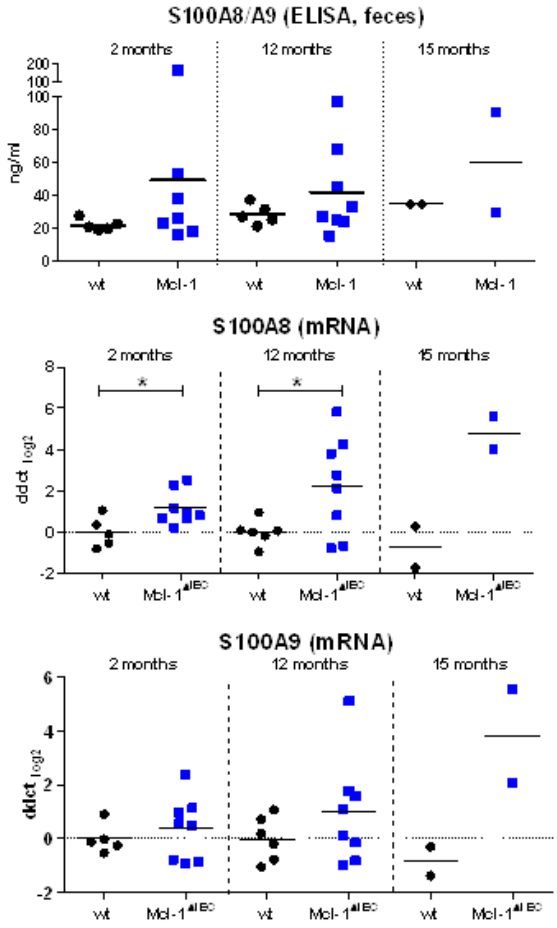

Figure 68: Calprotectin is enriched in Mcl-1$^{\Delta IEC}$ mice. The amount of Calprotectin was assessed by ELISA in feces of mice at indicated time-points or the expression of the S100A8 and S100A9 analyzed by qPCR on colonic tissue.

Due to the spontaneous loss of body weight, I decided to sacrifice and analyze Mcl-1$^{\Delta IEC}$ mice already at young age and collected tissue from 4 weeks-old animals for a detailed morphological analysis. First, a patchy pattern of affected and unaffected mucosal tissue (Figure 72) could be observed throughout the whole intestinal tract, characterized by increased apoptosis of intestinal epithelial cells (IECs) and epithelial damage accompanied by increased IEC proliferation and a strong inflammatory reaction (Figure 69, Figure 70).

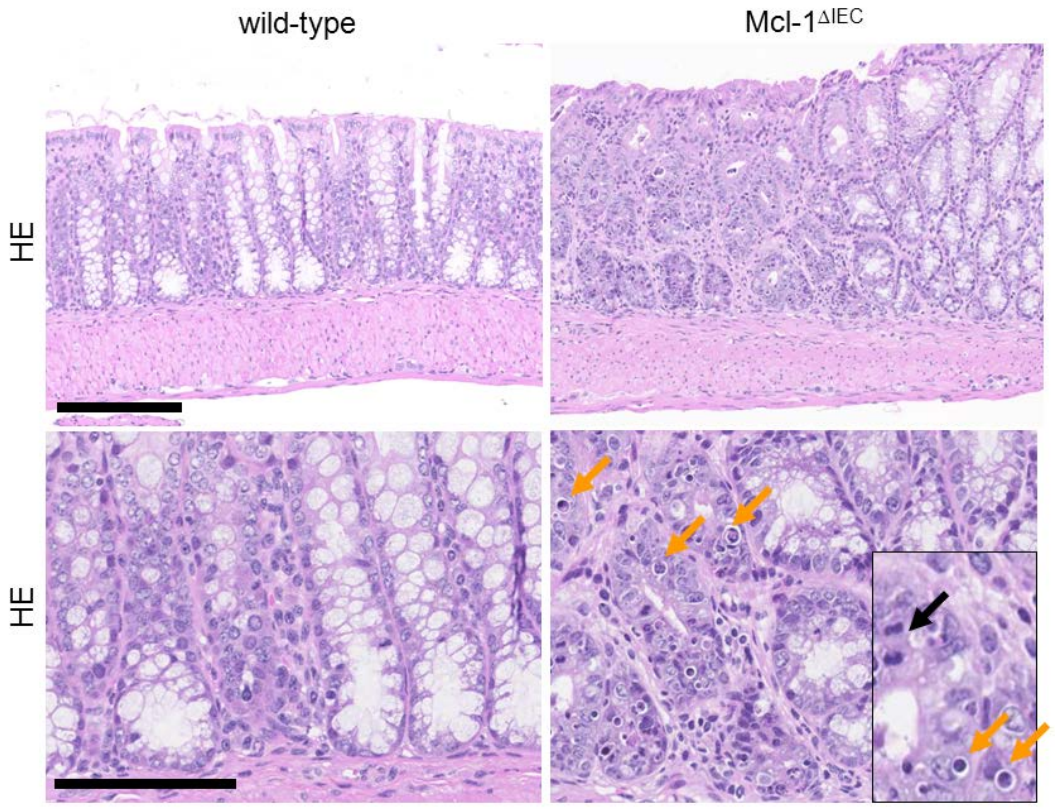

Figure 69: Histology of colonic tissue of mice at the age of eight weeks. Histological analysis revealed enterocyte apoptosis (yellow arrows) as well as enterocyte mitosis (black arrow). Intestinal tissue damage and loss of the regular intestinal architecture could be observed throughout the intestinal tract. Scale bar = 200 μm.

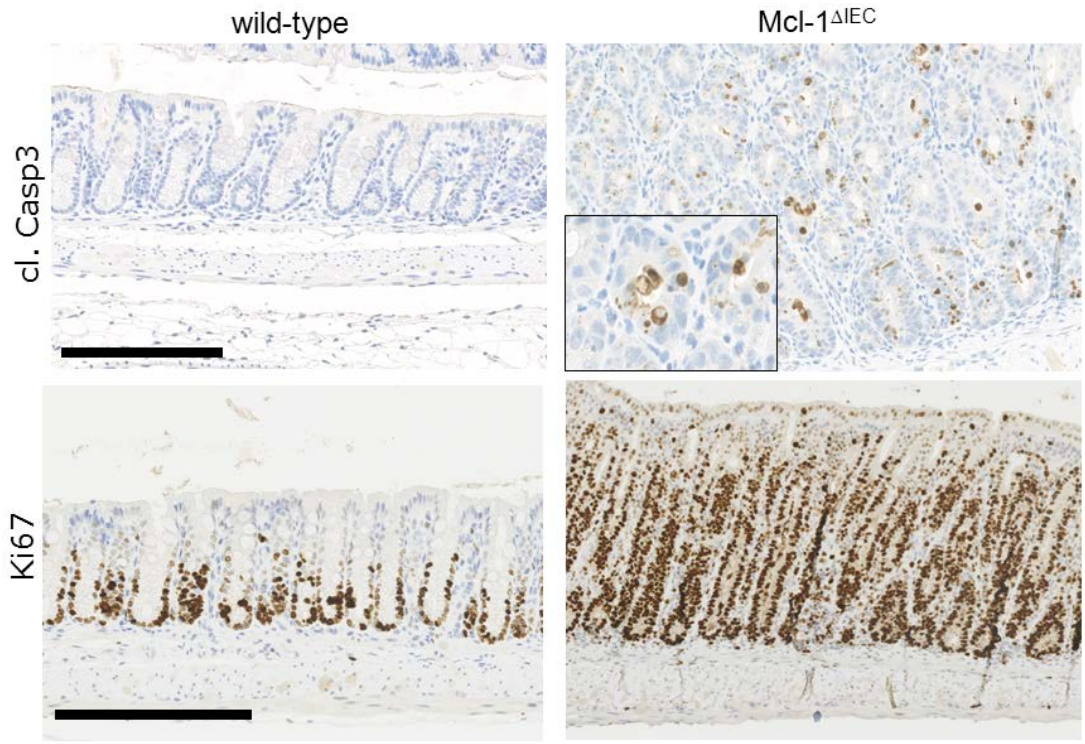

Figure 70: High levels of enterocyte apoptosis and proliferation. Immunohistochemical stainings revealed high levels of enterocyte apoptosis and proliferation in colonic tissue of 8 weeks old mice, indicating strong intestinal tissue damage and compensatory hyper-proliferation. Scale bar = 500 μm.

In addition, we observed a loss of differentiated enteroendocrine cells. Paneth cells in the small intestine as well as mucin-secreting Goblet cells in the colon were lost in affected areas of Mcl-1$^{\Delta IEC}$ mice (Figure 71). These observations already indicate that the anti-apoptotic protein Mcl-1 is a crucial pro-survival factor of enterocytes and needed for intestinal tissue homeostasis.

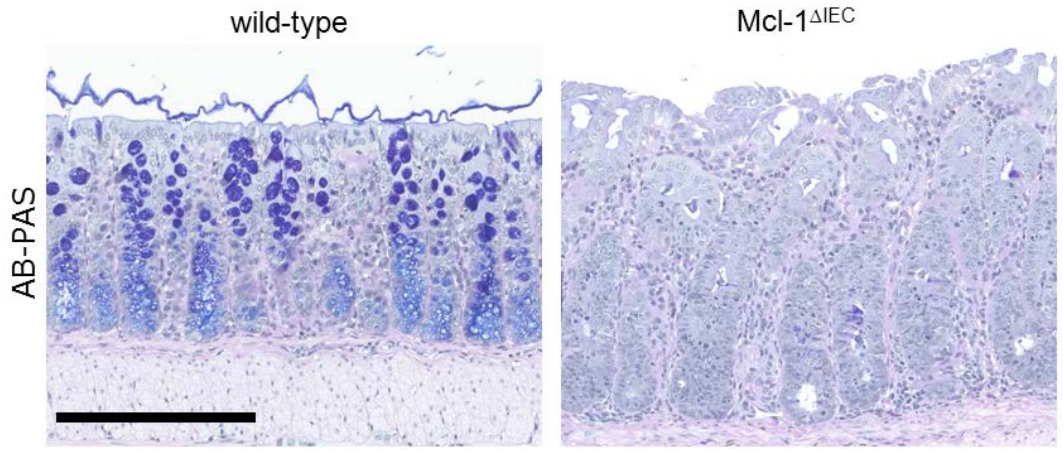

Figure 71: Loss of Goblet cells Mcl-1$^{\Delta IEC}$ mice. Differentiated Goblet cells are lost in affected and highly regenerative colons of Mcl-1 deficient mice. Scale bar = 250 μm.

Interestingly, the distribution of affected and hyper-apoptotic areas throughout the intestinal tract differed substantially between individual animals, being suggestive of an uneven deletion of the Mcl-1 protein. Therefore, we decided to perform a PCR analysis for the recombined genomic locus of the Mcl-1 flox allele on affected and unaffected intestinal tissue (Figure 72), isolated by laser micro dissection of scrapings from FFPE cuttings. Indeed, apoptotic areas showed a signal for the recombined genomic locus whereas gDNA from unaffected and healthy tissue showed no PCR product, indicating no genomic recombination in these regions. This is consistent with previous reports showing a patchy expression pattern of the Cre-recombinase in the Villin-Cre mouse line we used [129, 137, 138]. Whereas in the original publication the Villin-Cre mouse strain was shown to have an active Cre-recombinase throughout the intestinal tract by using a lacZ reporter system, the genomic locus of the Mcl-1 gene might play a crucial role in the recombination of DNA [139].

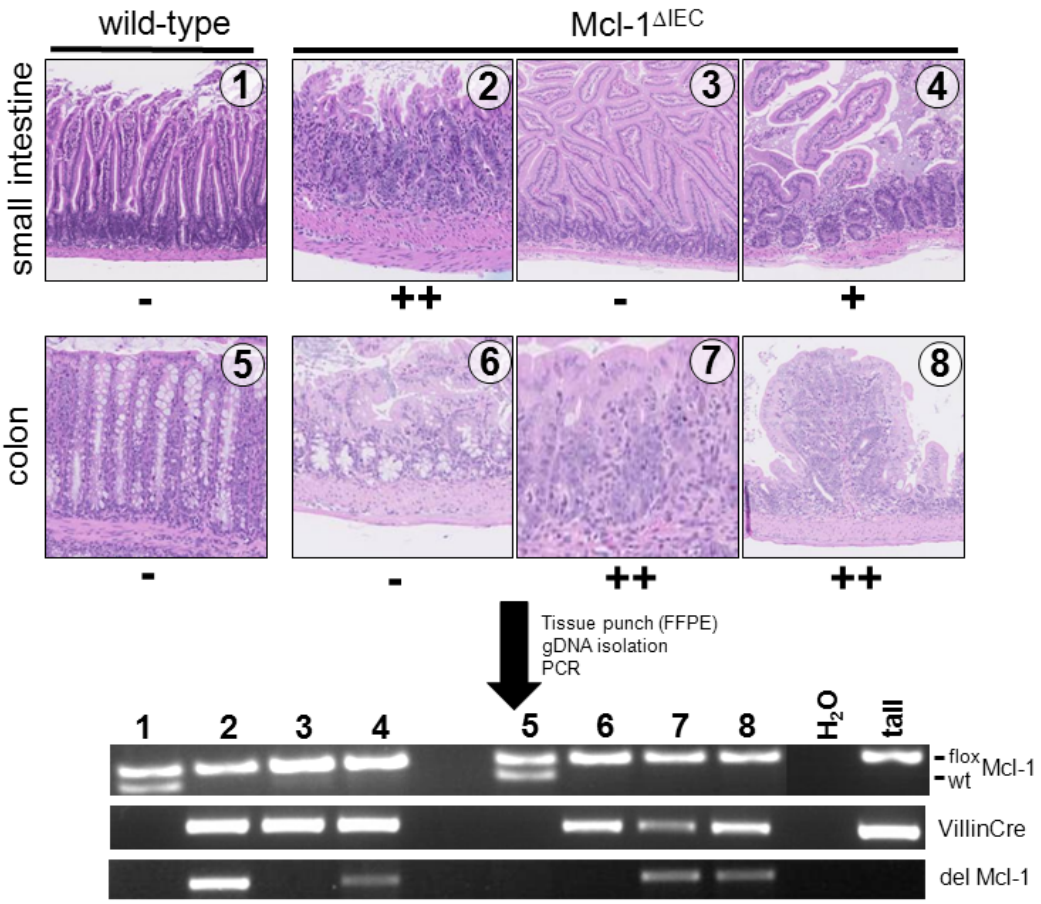

Figure 72: Patchy distribution of Mcl-1 knock-out lesions in Mcl-1$^{\Delta IEC}$ mice. Affected and unaffected areas of interest were defined on histological sections and gDNA was isolated by scrapings. Unaffected lesions of Mcl-1$^{\Delta IEC}$ mice (3,6) showed no genetic deletion of Mcl-1 gene, compared to moderate (4) or severe affected lesions (2,7,8) of the same animal.

5.3.3 Tumor development

As the knock-out of Mcl-1 caused a strong phenotype and Mcl-1$^{\Delta IEC}$ mice had to be monitored thoroughly over time, we decided to analyze the health of the animals on a weekly basis and mice with a loss of body weight were euthanized. We collected tissue of mice at 2, 4, 6 and 12 months of age and also performed colonoscopy to monitor potential tumor development in the colon *in vivo* (Figure 73).

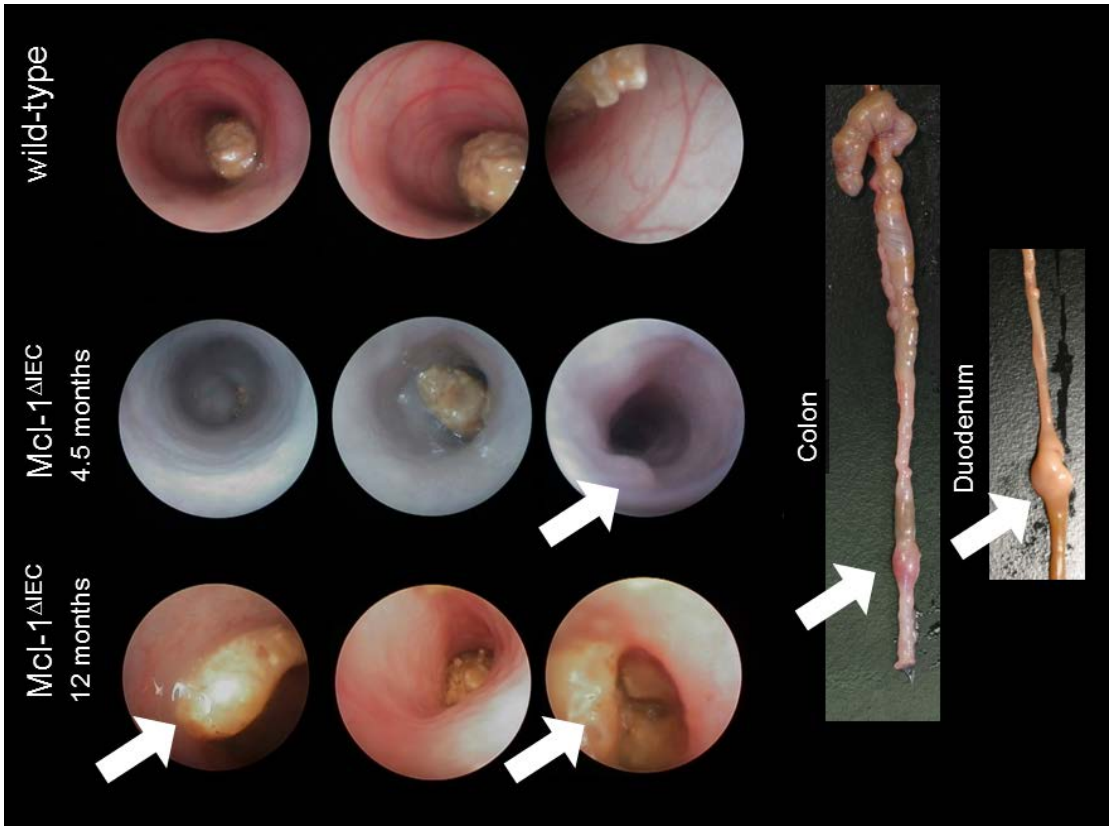

Figure 73: Endoscopy and macroscopy of Mcl-1$^{\Delta IEC}$ mice. Animals were monitored by endoscopic examination at various time-points of age and representative images of a fibrotic colon at 4.5 months of age and polyps in 12 month-old Mcl-1$^{\Delta IEC}$ mice. Macroscopically visible tumors were found in the colon as well as in the small intestine of Mcl-1 deficient mice.

Because mice at the age of four weeks already showed hyperplastic intestinal lesions, the entire intestinal tract of Mcl-1$^{\Delta IEC}$ mice was thoroughly examined for tumor lesions. Based on H&E morphology, tumors were quantified and categorized according to well-established criteria [140] including the following categories: (1) hyperplasia; (2) adenoma - subcategories: adenoma with low grade dysplasia (LGD), adenoma with high grade dysplasia (HGD), and (3) carcinoma, subcategories: intramucosal carcinoma, and carcinoma with invasion beyond muscularis mucosae. In addition, regional lymph nodes and distant organs, in particular lung and liver, were monitored for metastases. Mcl-1$^{\Delta IEC}$ mice (n=30) with carcinoma at the age of 9 months and older were analyzed but no metastases were

found.

Remarkably, Mcl-1$^{\Delta IEC}$ mice developed adenoma as well as carcinoma with an invasive growth pattern. Low grade adenoma were observed in Mcl-1$^{\Delta IEC}$ mice at the age of 6 months and high grade adenoma and carcinoma in Mcl-1$^{\Delta IEC}$ mice with weight loss at the age of 9 months. At 12 months of age, adenoma could be observed in approximately 80% of Mcl-1$^{\Delta IEC}$ mice, including 25% carcinoma (Figure 74). At 18 months of age, adenoma were found only in 50% of Mcl-1$^{\Delta IEC}$ mice, including 30% carcinoma, but due to the reduced survival of Mcl-1$^{\Delta IEC}$ mice and the following bias, this percentage has to be considered carefully.

Histological analyses revealed a spectrum of pathological changes including hyperplastic lesions, intraepithelial neoplasia (adenomas with LGD and HGD), and also invasive carcinoma in the small intestine as well as in the colon. Carcinoma of the colon were macroscopically visible and could be detected by colonoscopy.

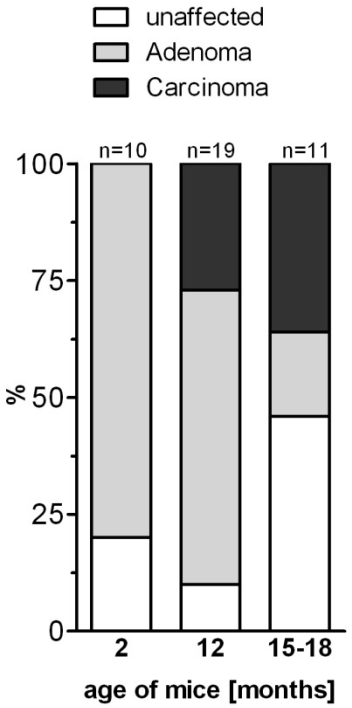

Figure 74: Tumor quality by histological analysis. The whole intestinal tract were analyzed thoroughly and the most affected region of scored for each individual animals.

I could confirm the invasiveness of carcinoma with an immunohistochemical staining for the epithelium-specific marker cytokeratin (CK) which showed CK-positive cells within the muscularis propria (Figure 75). Whereas these cells were negative for αSMA, a marker for smooth muscle cells and defining the muscularis propria, the CK-positive cells showed a typical crypt-like growth pattern within the muscularis propria indicating an epithelial origin of these invasively growing cells.

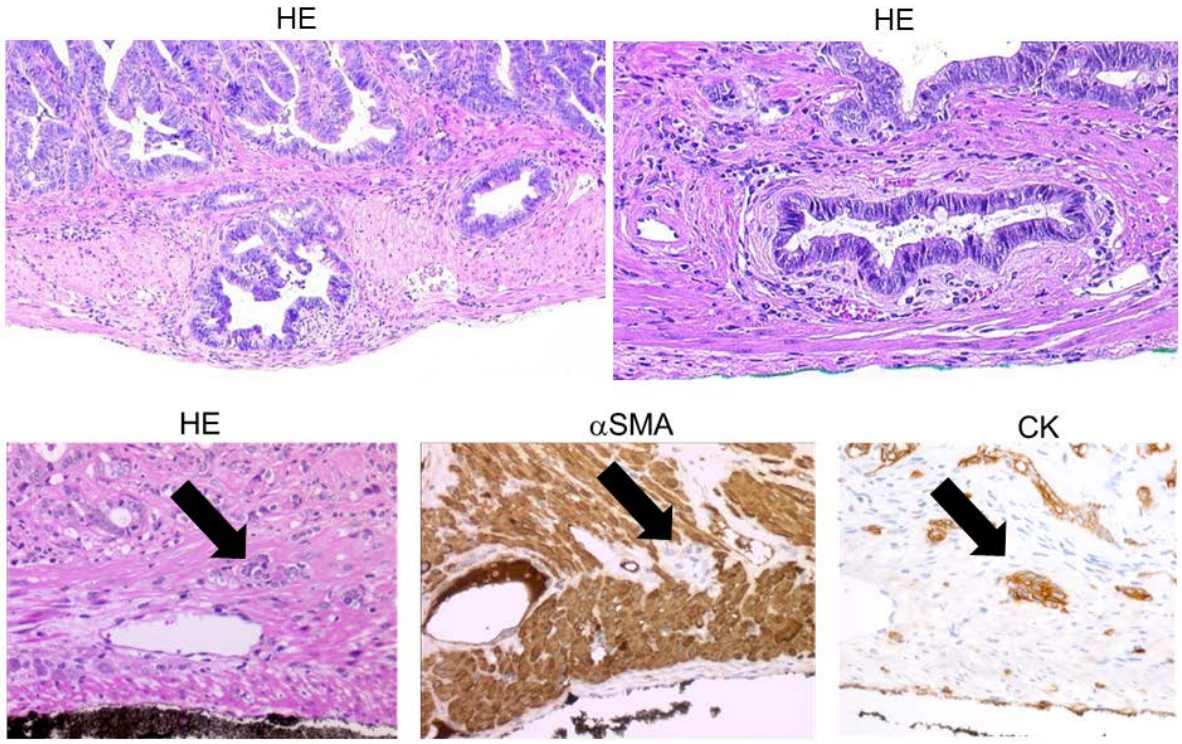

Figure 75: Invasive tumor growth in Mcl-1$^{\Delta IEC}$ mice. Ileum (upper row) and duodenum (lower row) sections of Mcl-1$^{\Delta IEC}$ mice at the age of 18 months and 12 months, respectively, showing invasive growth of tumors into the muscularis propria. Tumor cells stained positive for the epithelium-specific marker cytokeratin (CK) but negative for alpha-smooth muscle actin (αSMA).

Interestingly, immunohistochemical characterization revealed nuclear localization of β-catenin suggesting activated Wnt/β-catenin signaling in invasive carcinoma indicating parallels to human intestinal carcinogenesis (Figure 76). In summary, tumors derived from Mcl-1$^{\Delta IEC}$ mice revealed macroscopically the same adenoma-carcinoma sequence which is characteristic for human intestinal carcinogenesis. In addition, I observed neoplastic lesions in young mice at the age of 4-8 weeks and low grade adenoma as well as high grade adenoma and invasive carcinoma in mice as early as 8 months of age.

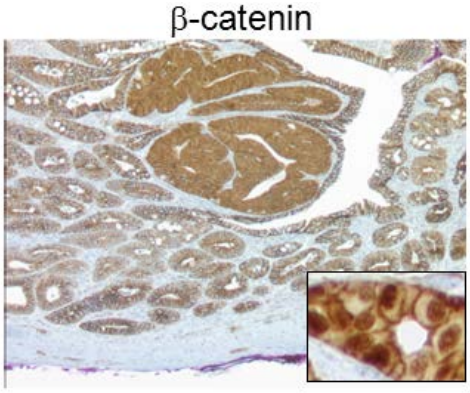

Figure 76: Nuclear β-catenin translocation in carcinoma. Translocation of β-catenin from the membrane into the nucleus could be observed in carcinoma from Mcl-1$^{\Delta IEC}$ mice, suggesting activated Wnt/β-catenin signaling.

5.3.4 Genetic analysis of tumors by Sanger sequencing

Due to the translocation of β-catenin in carcinoma of Mcl-1$^{\Delta IEC}$ mice, we expected to find mutations in the wnt pathway as described by Vogelstein and colleagues, because tumors evolving from benign to malignant lesions acquire a series of mutations over time, a sequence that has been particularly well studied in colorectal tumors [141]. For studying the presence of mutations and chromosomal instability in the Mcl-1$^{\Delta IEC}$ mouse model, we decided to analyze selected genes by Sanger sequencing. The protocols and work-flow was established together with Simone Büehler, who spent six months in lab of Prof. Achim Weber as a master student and helped in generating the sequencing results.

Based on a literature research the following well-known oncogenes and tumor suppressor genes, which were described to accumulate driver mutations during intestinal tumorigenesis at specific hot-spots were selected: APC, β-catenin, Fbxw7, B-Raf, N-Ras, K-Ras, p53, PIK3CA, Smad4 [141].

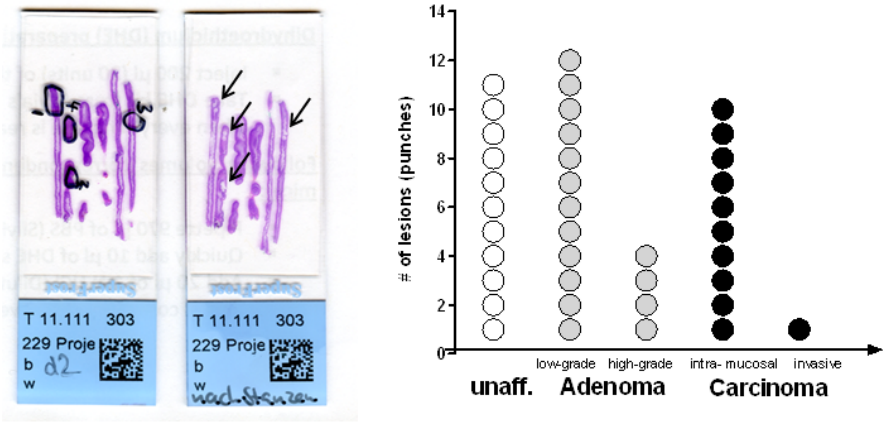

Figure 77: Mutational analysis of tumor and non-tumor tissue from Mcl-1$^{\Delta IEC}$ mice. Histology was examined and tumor lesions of different tumor quality defined and micro-dissected and gDNA for sequencing PCRS isolated from FFPE blocks.

Neoplastic and non-neoplastic tissue from Mcl-1$^{\Delta IEC}$ mice and tissue from control mice was selected according to the tumor stage and gDNA was isolated from micro-needle punches obtained from paraffin blocks (Figure 77). gDNA was used to establish the PCR reaction for the genomic region of interest and the PCR products were sent to Microsynth/Balgach for Sanger sequencing and analyzed using the CLC Workbench software.

Mutations for Catenin-1β were found in exon 2 in three individual punches from intramucosal carcinoma derived from different animals. All mutations were heterozygote mutations ($T_C/^TT$) at Codon 33 (NM_007614.3:c.98C>T, p.Ser33Phe), which led to an amino acid substitution of serine with phenylalanine. Codon 33 is one of four evolutionary conserved serine/threonine residues at the amino-terminal region of β-catenin, which constitute the GSK-3 phosphorylation site. GSK-3 is a part of the β-catenin degradation complex. Hence, mutations in this recognition site lead to the accumulation of β-catenin and its translocation to the nucleus consistent with our observation on β-catenin translocation. In line, mutations in Codon 33, 37, 41 and 45 frequently occur in human colorectal cancer.

In exon 1α of the Fbxw7 gene, one homozygous missense point mutation (NM_001177773.1:c 187A>G, p.Asn62Asp) led to an amino acid substitution of asparagine (AAC) with aspartate (GAC) and one homozygous silent point mutation (NM_001177773.1:c.342A>G, p.Glu114Glu) was detected in all samples as well as VillinCrenegative control samples, which is most probably the result of a spontaneous and silent germ-line mutation within the mouse strain compared to the C57BL/6 reference sequence in the database. This mutation is not described in the literature and control mice did not develope intestinal pathology or tumors.

Analysis of p53 exon 5-8, Smad4 exon 5 & exon 6, Braf, APC exon 15, N-Ras exon 1 & exon 2 and K-Ras exon 1 & exon 2 did not reveal mutations within the analyzed regions. However, it cannot be excluded that mutations in tumor tissue were missed due to biological or technical reasons. Due to technical limitations of the analyses performed by Microsynth, small (< 150bp) PCR products were not readable by the automated sequencer, thus sequences of N-Ras exon 1 (86bp), K-Ras exon 1 (98bp) could not be analyzed. Several attempts for the amplification of Apc exon 15A failed, most likely due to small molecular size of the isolated gDNA undergoing immense DNA fragmentation during formalin fixation when compared to native DNA.

Cancer, especially CRC, results from the accumulation of inherited and somatic mutations in oncogenes and tumor suppressor genes. These genes encode proteins that function in many regulatory pathways as summarized by Hanahan and Weinberg [41, 43]. These pathways also control genetic stability and chromosomal instability (CIN) is a feature of most human cancers [41, 43, 142]. To analyze genetic instability, I performed array comparative genomic hybridization analysis (aCGH) with gDNA isolated from intramucosal carcinoma, also used for mutational analysis by Sanger sequencing. Software based analysis performed by Dr. Kristian Unger (Helmholtz Zentrum/TU München) revealed chromosomal aberrations, with chromosomal gains and chromosomal losses being randomly distributed throughout the chromosomes and showing no recurrent pattern (Figure 78).

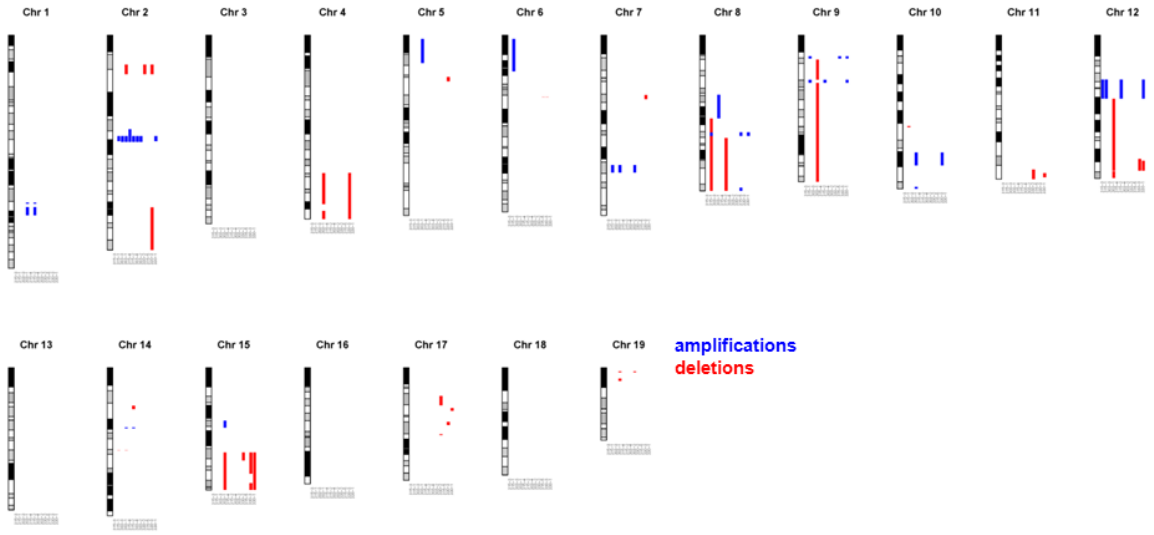

Figure 78: Chromosomal aberration in tumors derived from Mcl-1$^{\Delta IEC}$ mice. Isolated gDNA from tumor tissue which was used for Sanger sequencing was also used to analyze chromosomal aberrations by aCGH analysis. A random pattern of chromosomal amplifications (indicated in blue) and deletions (indicated in red) were detected.

5.3.5 Characterization of intestinal inflammation in Mcl-1$^{\Delta IEC}$ mice

The morphological analysis of 4-week-old Mcl-1$^{\Delta IEC}$ mice revealed besides the hyper-apoptotic and hyper-plastic lesions also a strong inflammatory reaction throughout the intestinal tract. The inflammatory phenotype is consistent with observations in patients suffering from acute or chronic IBD, in which high levels of apoptosis are accompanied by inflamed lesions in the intestinal epithelium [117].

To characterize the inflammation in Mcl-1$^{\Delta IEC}$ mice in more detail and to better understand the pathophysiological mechanisms, I first analyzed immunohistochemical stainings for B- and T-cells and macrophages. I could observe inflammatory aggregates which were positive for the B-cell marker B220 and also an increase in numbers of CD3^{+} T-lymphocytes in the small intestine and the colon (Figure 79).

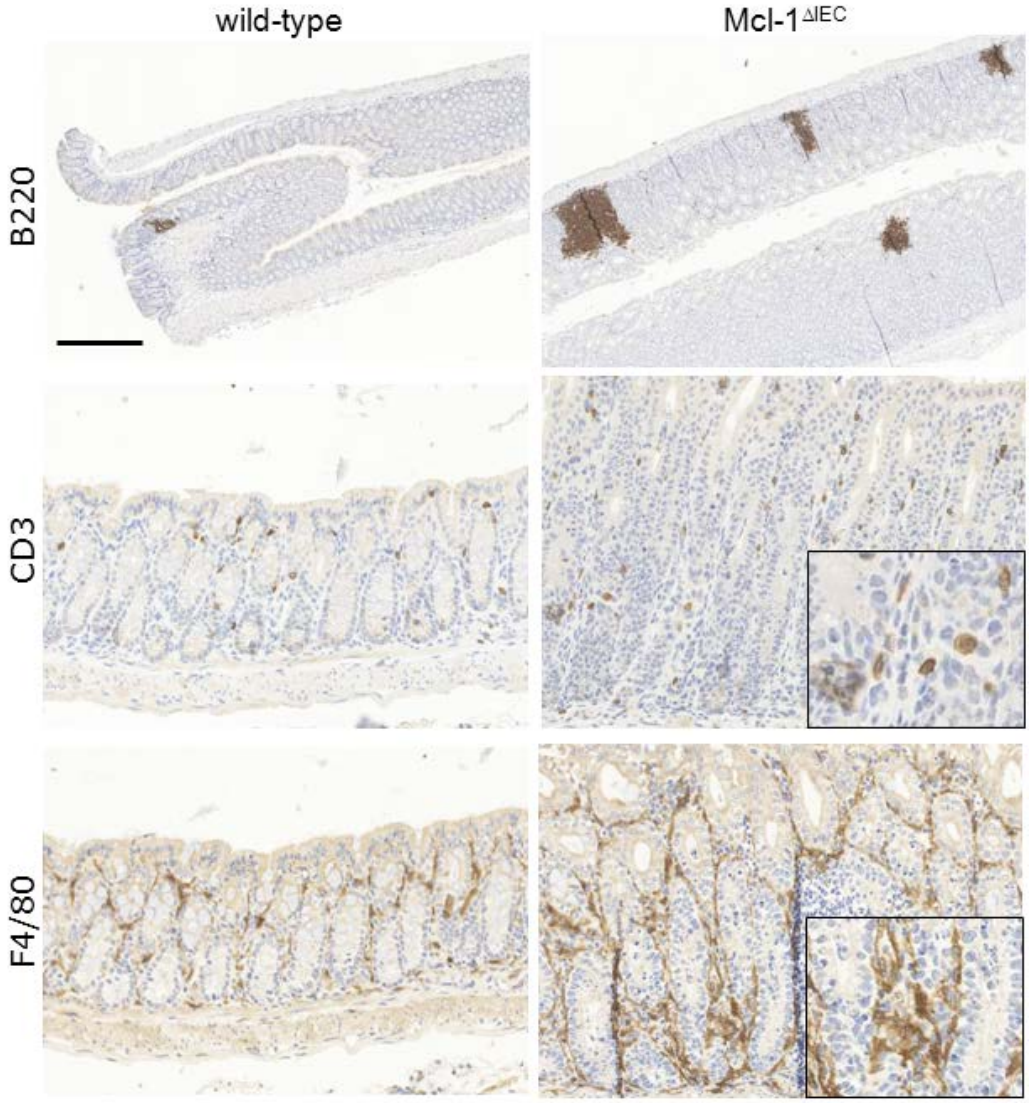

Figure 79: Immunohistochemical analysis of inflamed colons of two-months-old Mcl-1$^{\Delta IEC}$ mice. Staining with B220 revealed B-lymphoyctes in inflammatory aggregates and an increased number of T-lymphocytes (CD3) and macrophages (F4/80).

Second, in collaboration with Dr. Lubor Borsig, we performed a flow cytometry analysis of immune cells isolated from the lamina propria of 8-week-old Mcl-1$^{\Delta IEC}$ mice. We observed a significantly increase in CD19-positive B-cells as well as increase of Ly6C-positive pro-inflammatory monocytes and a Mac1-positive cell population of macrophages and neutrophils. Strikingly, we detected a significant decrease in CD3-positive T-cells, especially in the CD8-positive subset of T-cells (Figure 80). This was in contrast to our previous finding based on immunohistochemical analyses. Due to the experimental set-up chosen for the quantification of intraepithelial immune cells by flow cytometry, we calculated relative numbers of positive cells within the population of CD45-positive cell and due to the explosive increase of B-cells in inflamed intestines, all other analyzed cell types within the CD45-positive cell populations were most likely artificially decreased and we used the data only carefully to draw any conclusions.

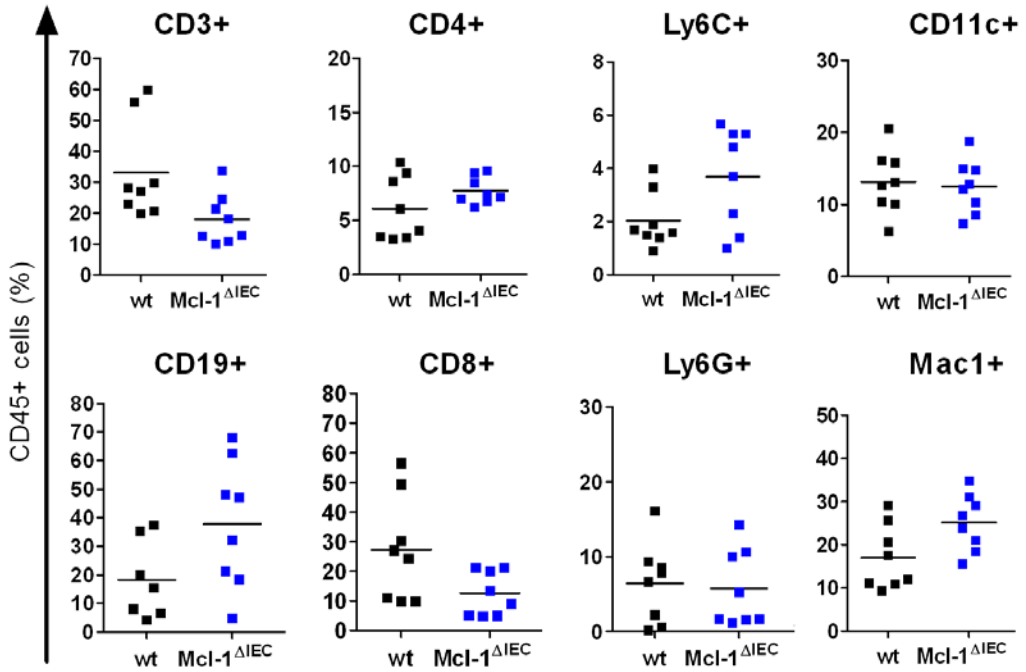

Figure 80: Analysis of inflammatory cells by flow cytometry. Colonic immune cells were isolated from the lamina propria of two month-old Mcl-1$^{\Delta IEC}$ and control mice and an increase in CD19-positive B-lymphocytes, Ly6C-positive monocytes and Mac1-positive macrophages was observed. The percentage of CD3- and CD8-positive T-lymphocytes was reduced.

Due to the strong inflammatory phenotype of Mcl-1$^{\Delta IEC}$ mice and the potential role of immune cells and immune cell-derived cytokines in promoting intestinal tumorigenesis, I next wanted to address the role of B- and T-cells in mediating intestinal pathology and their contribution to tumorigenesis. Therefore, I decided to genetically deplete mature B- and T-cells by intercrossing Mcl-1$^{\Delta IEC}$ mice with RAG1$^{-/-}$ deficient mice.

Interestingly, the Mcl-1$^{\Delta IEC}$/RAG1$^{-/-}$ was very difficult to establish and the breeding did not give birth according to the expected Mendelian ratio. The number of expected Mcl-1$^{\Delta IEC}$/RAG1$^{-/-}$ mice was reduced and a substantial proportion of Mcl-1$^{\Delta IEC}$/RAG1$^{-/-}$ mice was growth retarded and had to be euthanized quickly after weaning and the survival of Mcl-1$^{\Delta IEC}$/RAG1$^{-/-}$ mice was significantly reduced compared to Mcl-1$^{\Delta IEC}$ and wild-type mice (Figure 81).

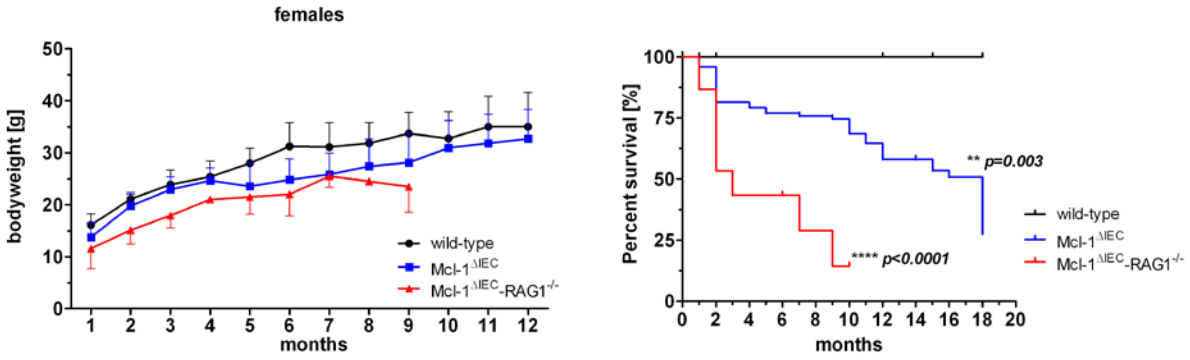

Figure 81: Body weight and survival of Mcl-1$^{\Delta IEC}$/RAG1$^{-/-}$. The body weight of female Mcl-1$^{\Delta IEC}$/RAG1$^{-/-}$ mice was reduced, compared to wild-type and Mcl-1$^{\Delta IEC}$ mice. Only females are shown due to the smal number of males obtained. The survival of Mcl-1$^{\Delta IEC}$/RAG1$^{-/-}$ was significantly reduced compared to Mcl-1$^{\Delta IEC}$ mice and only ~20% of mice reached the age of 10 months.

Histological analysis of intestinal sections derived from 4- and 8-week-old Mcl-1$^{\Delta IEC}$/RAG1$^{-/-}$ mice revealed a similar histopathology as observed in Mcl-1$^{\Delta IEC}$ mice. With respect to the epithelial compartment, I found a histological spectrum including hyperplastic lesions, intraepithelial neoplasia and a loss of highly differentiated Paneth and Goblet cells. The patchy phenotype of affected and unaffected regions in the intestine was observed in Mcl-1$^{\Delta IEC}$/RAG1$^{-/-}$ mice and could potentially explain the survival of less affected Mcl-1$^{\Delta IEC}$/RAG1$^{-/-}$ mice (Figure 82).

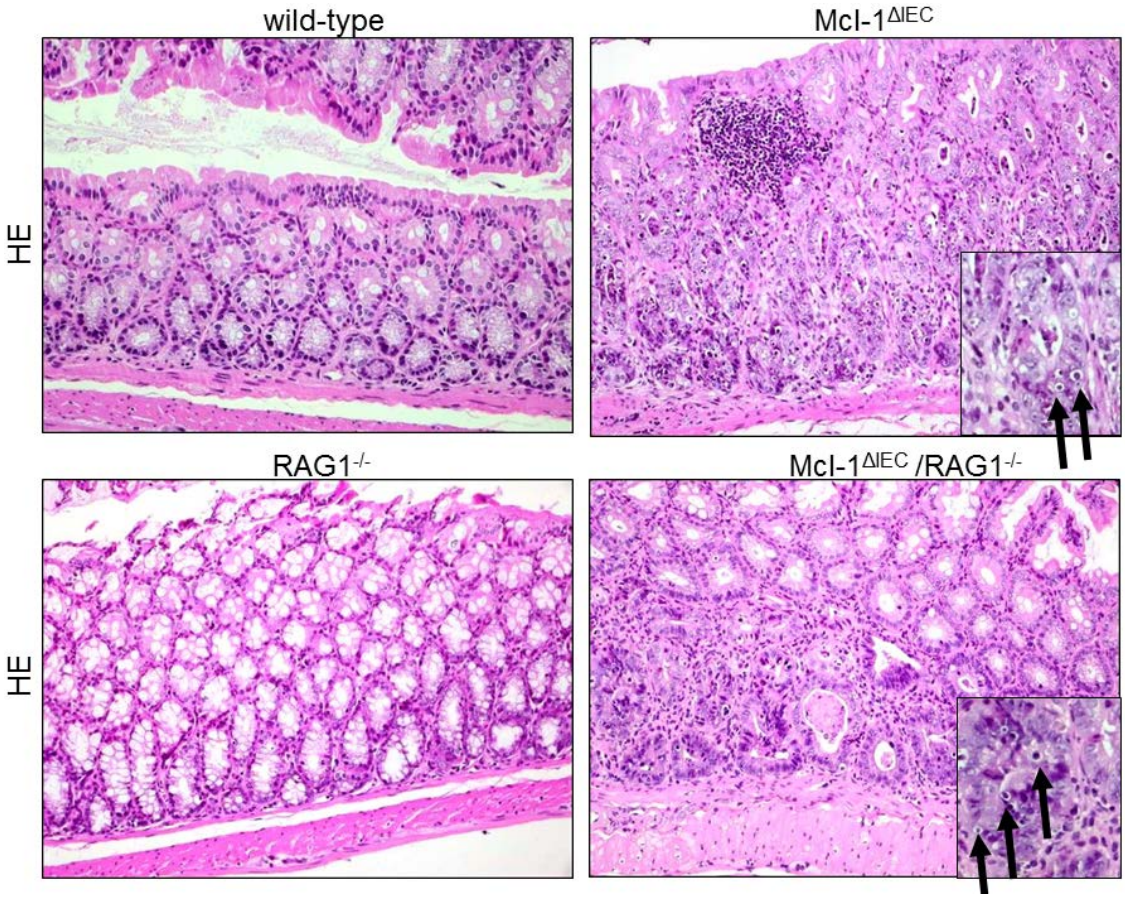

Figure 82: Histology of Mcl-1$^{\Delta IEC}$/RAG1$^{-/-}$ mice. Histopathological signs of increased enterocyte cell death (black arrows), aberrant crypts and loss of tissue architecture were observed in the whole intestinal tract of Mcl-1$^{\Delta IEC}$/RAG1$^{-/-}$ mice at the age of two months.

As next step, I decided to analyze the cytokine expression in intestinal tissue to better understand the inflammatory reaction and to screen for a B- and T-lymphocyte independent cytokine to get an explanation for the unexpected phenotype in Mcl-1$^{\Delta IEC}$/RAG1$^{-/-}$ mice.

The expression analysis of S100A8/A9 showed increased levels in colons of Mcl-1$^{\Delta IEC}$/RAG1$^{-/-}$ mice compared to Mcl-1$^{\Delta IEC}$ mice and indicated a crucial role of calprotection-secreting granulocytes in the intestinal pathology and inflammatory phenotype of Mcl-1$^{\Delta IEC}$/RAG1$^{-/-}$ mice (Figure 83).

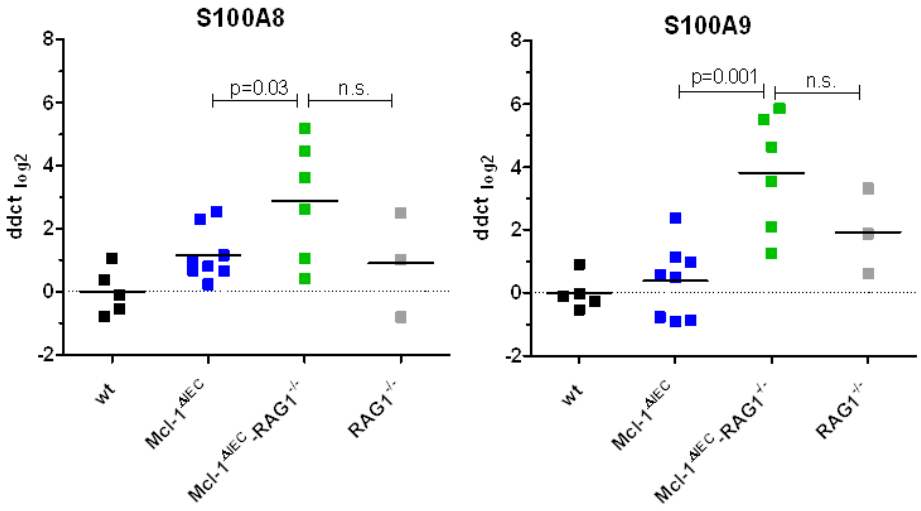

Figure 83: Expression of S100A8/A9 in Mcl-1$^{\Delta IEC}$/RAG1$^{-/-}$ mice. Analysis of S100A8/A9 expression by qPCR revealed significantly increased levels in Mcl-1$^{\Delta IEC}$/RAG1$^{-/-}$ mice compared to Mcl-1$^{\Delta IEC}$ mice. Elevated mRNA levels in RAG1$^{-/-}$ control mice suggest an altered immune cells composition in the colon due to the lack of B- and T-lymphocyte.

Interestingly, the most important cytokines described to be relevant in IBD (e.g. IL-17, IL-22, IL-23) were not detectable on RNA level neither in RNA isolated from whole tissue lysates nor in intestinal epithelial scrapings (data not shown). Therefore, I established an *ex vivo* colon culture system initially developed in the lab of Richard Flavell [143]. Shortly, primary intestinal tissue was harvested, washed and chopped and cultured for up to 72h in specific cell culture medium. Released cytokines are enriched in the cell culture supernatant and I performed a multiplex ELISA to analyze the cytokine profile of intestinal tissue derived from Mcl-1$^{\Delta IEC}$ and Mcl-1$^{\Delta IEC}$/RAG1$^{-/-}$ mice.

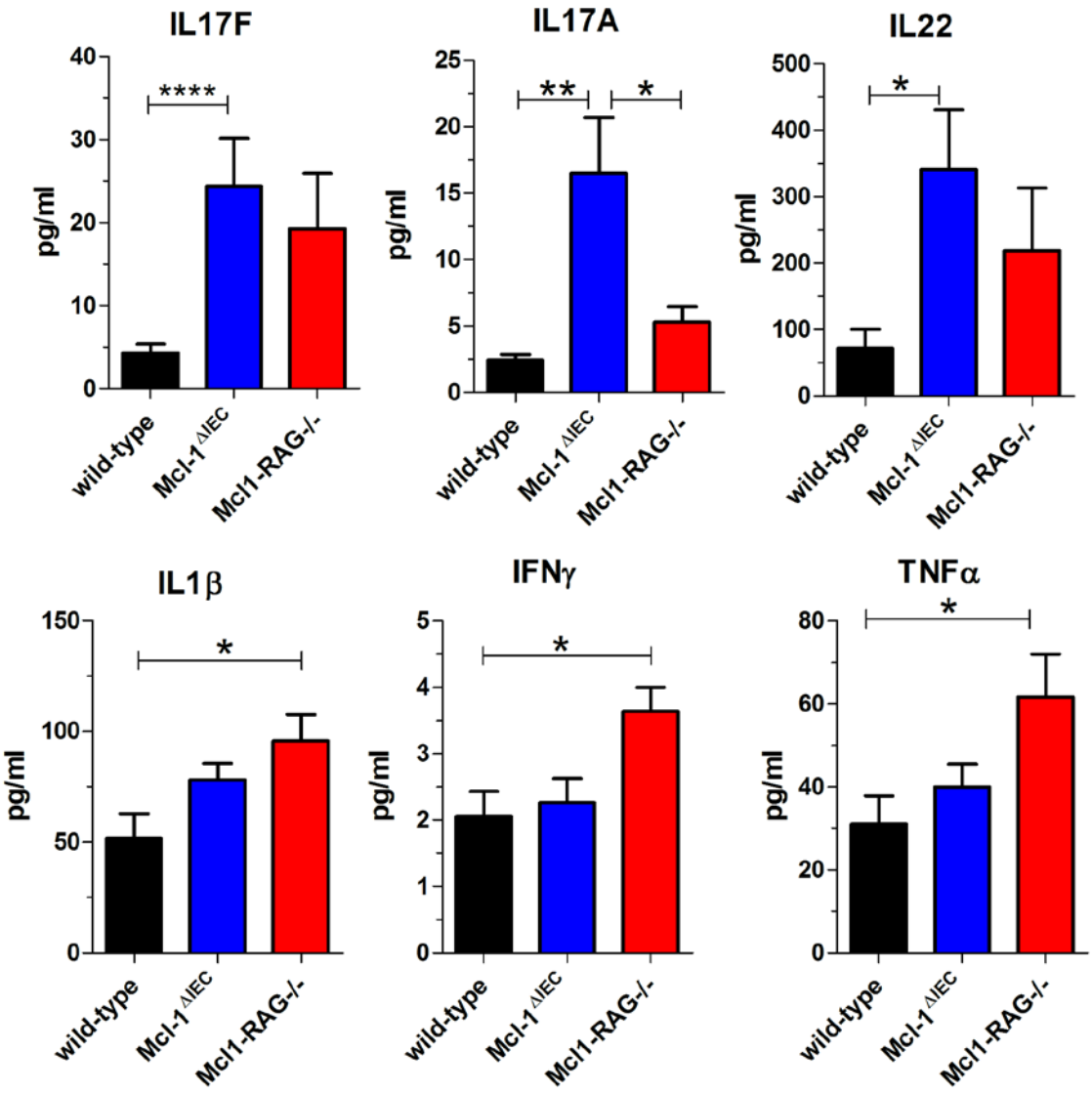

Figure 84: *Ex vivo* cytokine analysis in cell culture supernatant. The most relevant cytokines (IL17A, IL17F, IL22) for IBD were detected significantly enriched in cell culture supernatant from Mcl-$1^{\Delta IEC}$ and Mcl-$1^{\Delta IEC}$/RAG$1^{-/-}$ mice 48h after *ex vivo* incubation.

Indeed, I could detect an enrichment of IBD-related cytokines in the cell culture supernatant. Besides the pro-inflammatory cytokines IL-1β, TNFα and IL-6, I found IL-22, IL-17F and IL-17A (Figure 84). Especially IL-22 was of interest, as it is well-known to be released by TH17 cells, is strongly linked to chronic inflammation in IBD and has a pro-proliferative stimulus on enterocytes to drive intestinal tissue regeneration [144]. TH17 cells were first defined by their expression of IL-17A, but have later been shown to also express IL-22, IL-17F and IL-21 [143]. Also IL-23 is described to be crucial for TH17 cell differentiation and maintenance [145]. Taken together, the enhanced expression of these IBD-related cytokines confirmed the IBD phenotype of Mcl-$1^{\Delta IEC}$ mice. However, the increased expression of cytokines released by TH17 cells in intestinal tissue in Mcl-$1^{\Delta IEC}$/RAG$1^{-/-}$ mice was contradictory and could not be

explained, because TH17 cells like all other B- and T-cells should be depleted in RAG1$^{-/-}$ mice due to the lack of the recombination activating gene 1 (RAG1) which is required for immunoglobulin V-D-J recombination.

Therefore, I went back to the literature and searched for an explanation of a TH17 expression profile in RAG1$^{-/-}$ mice and indeed found a paper, published at the same time by Prof. S. Leibundgut (ETH Zürich) dealing with an IL-17-dependent clearance of *Candida albicans* upon oral infection in RAG1$^{-/-}$ mice [146]. According to this paper, fungal clearance is not mediated via IL-17 released by conventional TH17 cells, but instead IL-17-dependent immunity is mediated by a non-conventional and IL-17-producing immune cell type called innate lymphoid cells (ILCs) and not by classical TH17 cells.
ILCs lack rearranged antigen-specific receptors and the maturation of ILCs is therefore not affected by the deletion of Rag1 gene in mice [147]. As the role of ILCs is currently of high interest but first studies were only limited to pathogen-induced mouse models for intestinal inflammation [148], there was no study showing the causal relationship between ILC-dependent inflammation and intestinal tumorigenesis. Consequently, I aimed to study the role ILCs in the Mcl-1$^{\Delta IEC}$ mouse models and depleted ILCs with an anti-Thy1 antibody in Mcl-1$^{\Delta IEC}$ mice. Because the Mcl-1 and the RORc gene locus were located on the same chromosome, a genetic knock-out of ILCs was not possible. But due to the strong inflammatory phenotype of Mcl-1$^{\Delta IEC}$ mice, I expected to see a potential effect early after antibody treatment.
To study the role of ILCs in tumor initiation, I started to treat Mcl-1$^{\Delta IEC}$ mice at the age of one month for four weeks. In addition, to investigate the role of ILCs in tumor progression in old mice with established IBD, I additionally treated mice at the age of eleven months for four weeks.

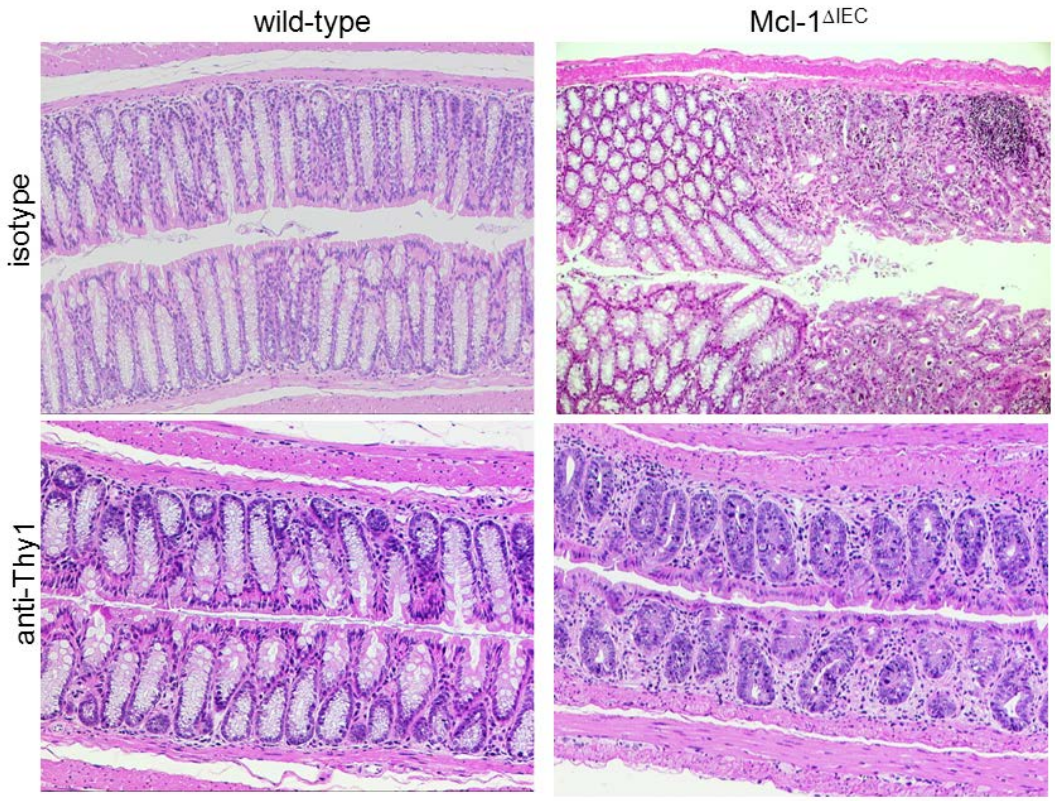

Figure 85: Histology of colons 4 weeks post anti-Thy1 treatment. Histological analysis of intestinal tissue revealed decreased inflammatory infiltrates, reduced tissue damage and intestinal tissue healing after 4 weeks of treatment in Mcl-1$^{\Delta IEC}$ mice at the age of 3 months.

Interestingly, the anti-Thy1 treatment completely abolished the inflammatory phenotype in the small intestine as well as in the colon of Mcl-1$^{\Delta IEC}$ mice (Figure 85). *Ex vivo* cytokine analysis of anti-Thy1 treated mice showed a significantly reduced cytokine expression pattern in Mcl-1$^{\Delta IEC}$ and Mcl-1$^{\Delta IEC}$/RAG1$^{-/-}$ mice. Especially the ILC-specific cytokines IL-17A, IL-17F and IL-22 were reduced to wild-type levels (Figure 86) and I could also detect a significant reduction of the cytokines IL-10, IL-1β and TNFα indicative of attenuated inflammation and tissue regeneration processes. In addition, histology confirmed the positive outcome of the anti-Thy1 treatment. Immunohistochemical stainings for CD3 confirmed the absence of T-cells and also B-cell infiltrates were eliminated (data not shown). Furthermore, morphological analysis showed mucosal healing and a restoration of the intestinal architecture (Figure 85).

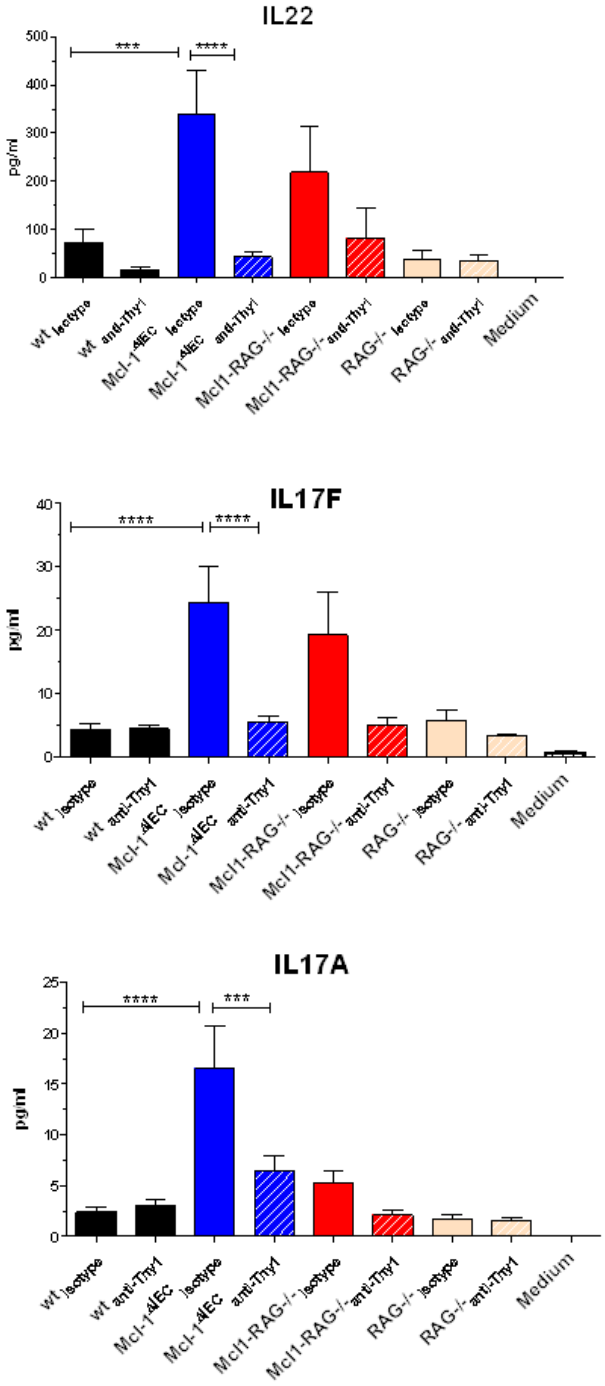

Figure 86: *Ex vivo* cytokine analysis of anti-Thy1 treated mice. Four weeks treatment significantly reduced the amount of released cytokines from colon tissue of anti-Thy1 treated Mcl-1$^{\Delta IEC}$ mice and Mcl-1$^{\Delta IEC}$/RAG1$^{-/-}$ mice compared to isotype control treated animals

5.3.6 Intestinal inflammation in Mcl-1$^{\Delta IEC}$ mice is promoted by the microbiota

Next, I addressed why the inflammatory phenotype in Mcl-1$^{\Delta IEC}$ mice depends on ILCs and how inflammation is initiated in these mice. I hypothesized that the strong inflammatory reaction a) is due to a leaky intestinal barrier and that the inflammation is promoted by bacteria or their products and an elimination of the microbiota would reduce the inflammatory phenotype, and b) the inflammatory environment significantly accelerates tumor development and a depletion of inflammatory cells would also reduce tumorigenesis. First, I analyzed intestinal barrier dysfunction by performing a Limulus amebocyte lysate (LAL) assay and observed an increase of endotoxin levels in serum of in two-month-old Mcl-1$^{\Delta IEC}$ mice (Figure 87A). Second, I orally administered FITC-labeled dextrane to two-month-old Mcl-1$^{\Delta IEC}$ and control mice and analyzed the amount of diffused dextran non-invasively 4h post administration in serum of mice. I detected significantly elevated levels of FITC-labeled dextrane in serum of Mcl-1$^{\Delta IEC}$ and therefore was able to confirm the leaky intestinal barrier (Figure 87B).

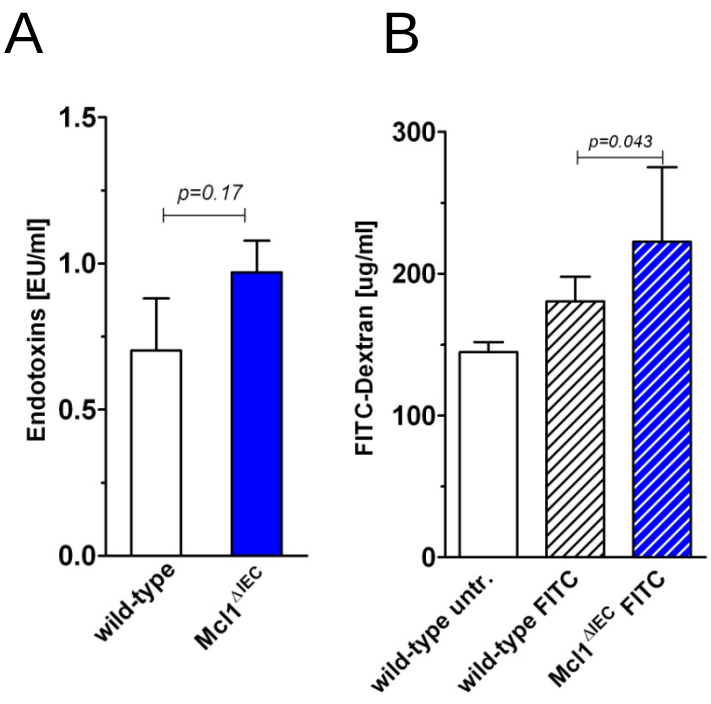

Figure 87: Intestinal barrier disruption in Mcl-1$^{\Delta IEC}$ mice. A) Analyzed endotoxin levels in sera were elevated by tendency and B) FITC-labeled dextran significantly elevated upon oral gavage of two-month-old Mcl-1$^{\Delta IEC}$ mice (n=6) indicating a leaky intestinal barrier.

Thus, Mcl-1$^{\Delta IEC}$ mice were embryo-transferred into the germ-free facility of Prof. Andrew Macpherson at the University of Berne to uncover the role of the microbiota in intestinal

inflammation and its contribution in tumorigenesis. Due to the time-consuming embryo-transfer and difficulties in maintaining the mouse colony under germ-free conditions, we decided in addition to treat the Mcl-1$^{\Delta IEC}$ mice in our mouse facility with broad-spectrum antibiotics.

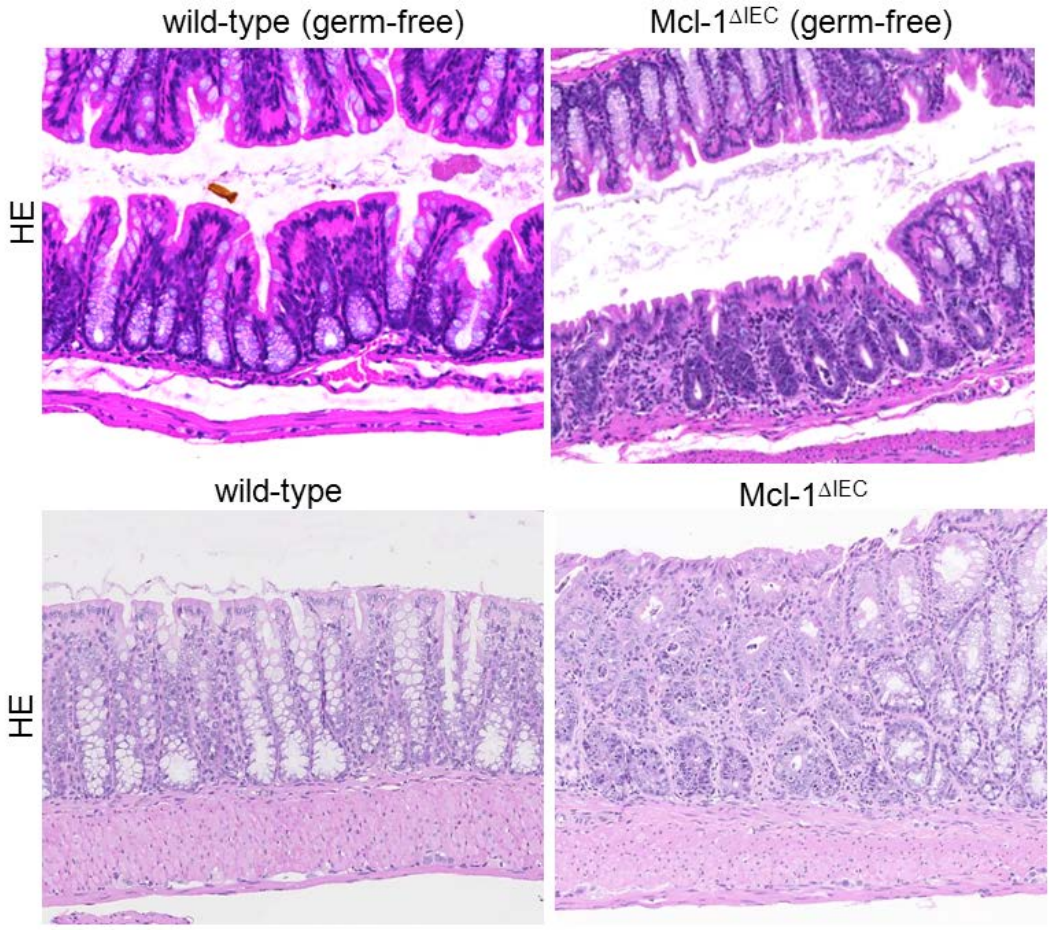

Figure 88: Histology of Mcl-1$^{\Delta IEC}$ mice after four week under germ-free housing. Histological analysis of colonic tissue revealed reduced inflammation, intestinal tissue healing and restoration of intestinal tissue architecture in Mcl-1$^{\Delta IEC}$ mice.

Germ-free housing as well as antibiotic treatment significantly improved and reduced inflammation and apoptosis in Mcl-1$^{\Delta IEC}$ mice at the age of 2 months (Figure 88). In addition, cytokine analyses showed a completely normal cytokine expression pattern (Figure 89). ILC-specific cytokines as well as additional cytokines (e.g. IL-1β, TNFα, IL-6 and IL-10) were completely reverted to wild-type levels in supernatant of colonic and ileal tissue. These results clearly indicated that bacterial colonization and subsequent initiation of inflammatory processes - especially the activation of ILCs in the intestine - significantly contribute to the inflammatory phenotype of Mcl-1$^{\Delta IEC}$ mice.

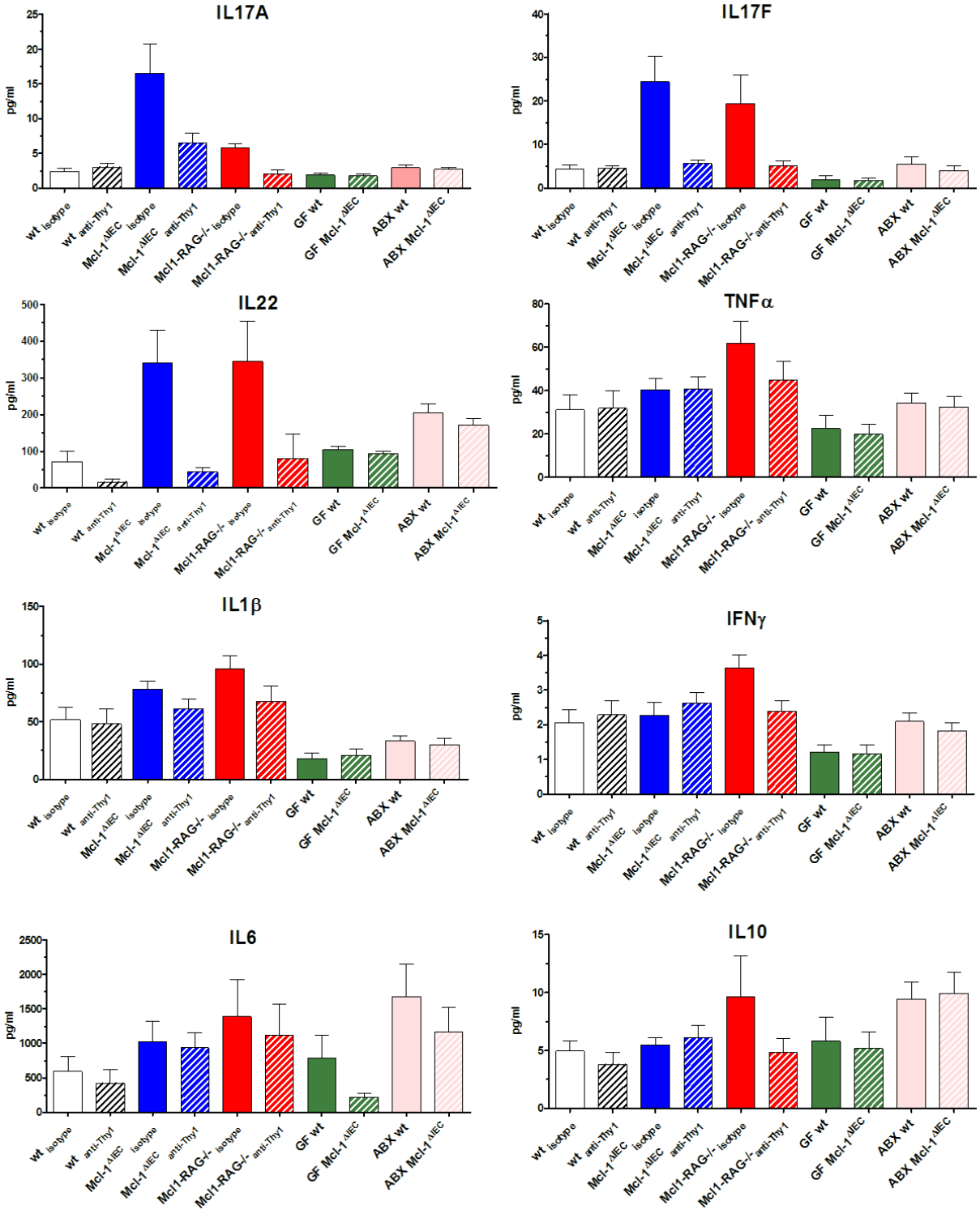

Figure 89: Cytokine analysis in serum of Mcl-1$^{\Delta IEC}$ mice. Pro-inflammatory cytokines IL1β and TNFα as well as IL17A, IL17F and IL22 were significantly reduced in cell culture supernatant 48h post incubation of colonic tissue derived from Mcl-1$^{\Delta IEC}$ mice after four weeks under germ-free housing or antibiotic treatment, compared to mice under conventional housing. n= 4 - 8 mice were analyzed per group.

To investigate the contribution of the bacterial colonization with respect to tumor

development in Mcl-1$^{\Delta IEC}$ mice, we collected organs from mice under germ-free housing and antibiotic-treatment at the age of 12 months. Due to the attenuated breeding of mice under germ-free conditions and the late starting-point of this experiment, these experiments are still under progress and organs of mice at the age of 12 months are periodically collected for future analysis. Until now, only two germ-free and six antibiotics-treated Mcl-1$^{\Delta IEC}$ mice could be collected at the late time-point and no macroscopic visible tumors or distinct carcinoma could be observed at morphological level. Due to the small number of mice and the phenotypically patchiness, this promising observation has to be considered carefully.

5.4 Discussion

5.4.1 Mcl-1$^{\Delta IEC}$ mice recapitulate important aspects of human intestinal carcinogenesis

The second project of my PhD thesis is focusing on the role of intestinal apoptosis and its impact on intestinal inflammation and carcinogenesis. By deleting the anti-apoptotic Mcl-1 in intestinal epithelial cells (Mcl-1$^{\Delta IEC}$ mice), I developed and characterized a novel mouse model for studying intestinal inflammation and carcinogenesis.

So far, the gold standard for colorectal cancer research and the experimental basis for the Vogelstein adenoma-carcinoma-sequence are mice carrying an initially chemically-induced mutation in the APC gene [149, 150]. These mice develop multiple intestinal neoplasia (APC^{min}) in the small intestine and colon due to the genetic defect, but tumors do not spontaneously develop under inflammatory conditions as seen in IBD patients and recapitulated in Mcl-1$^{\Delta IEC}$ mice. APC^{min} mice actually resemble only a small spectrum of human colorectal cancer and are limited to human familial adenomatous polyposis (FAP) showing adenoma, nevertheless being still widely used. Until today, genetically modified versions of the APC^{min} mice are created and mice carrying different APC mutations e.g. APC^{1638N}, APC$^{\Delta 716}$ or conditional APC^{loxP} are used for research [133, 151, 152].

In contrast to APC^{min} mice which develop phenotypically homogenous and non-invasive adenoma, tumors developing in Mcl-1$^{\Delta IEC}$ mice show invasive growth patterns and are genetically and histologically heterogeneous. Invasive carcinoma were randomly distributed in the small intestine and colon and were not limited to any specific site of the intestinal tract. Furthermore, as the germline-stable APC mutation was initially induced by chemical treatment of wild-type mice with ethylnitrosourea (Enu) to generate APC^{min} mice [150], mutations of oncogenes und tumor suppressor genes in carcinoma of Mcl-1$^{\Delta IEC}$ mice occurred spontaneously. However, I could not detect mutations in the APC gene in the analyzed exons of interest in tumor tissue of Mcl-1$^{\Delta IEC}$ mice by Sanger sequencing, but significantly decreased mRNA expression of Apc as well as β-catenin translocation are highly suggestive for APC dysfunction in tumors derived from Mcl-1$^{\Delta IEC}$ mice. Further mutational analyses of tumor tissue from Mcl-1$^{\Delta IEC}$ mice are needed for a better understanding of genetic changes during carcinogenesis.

Although, one of the most important tumor suppressors FBXW7 in colorectal carcinogenesis is commonly mutated in human colorectal cancer, no mutations were detected in APC^{min} mice [153, 154]. Of note, carcinoma derived from Mcl-1$^{\Delta IEC}$ mice showed missense as well as silent point mutations for FBXW7 and therefore revealed the strong correlation between human colorectal carcinogenesis and carcinogenesis in the Mcl-1$^{\Delta IEC}$ mouse model on genetic level.

As mentioned before, adenoma in APC^{min} mice develop due to a specific genetic mutation and not on the background of chronic inflammation as known from IBD patients and as described in Mcl-$1^{\Delta IEC}$ mice. To study colorectal carcinogenesis under inflammatory conditions, the combined treatment with azoxymethane (AOM) and dextran sulfate sodium (DSS) is currently used as a common model of colitis-associated colorectal cancer in mice [155, 156]. The DSS/AOM approach is very prominent due to its high reproducibility, low costs, practicable handling and tumor development within 10 weeks, without intercrossing to a specific tumorigenic strain. In general, it is described as model for “inflammation-driven colorectal tumorigenesis” being somehow imprecise as the main driver of tumorigenesis is the genotoxic agent AOM and not DSS-induced inflammation. Therefore, the DSS/AOM approach is precisely a model for genotoxin-driven and inflammation-associated colorectal tumorigenesis.

In contrast, tumors in Mcl-$1^{\Delta IEC}$ mice develop in the environment of constant intestinal tissue damage and regeneration without the artificial stimulus of genotoxic agents or DSS-mediated destruction of the full mucus layer. Adenoma are first detectable in 4 week or 8-week-old animals and carcinoma development in Mcl-$1^{\Delta IEC}$ mice are first detectable at eight months of age. Therefore, the Mcl-$1^{\Delta IEC}$ mouse model represents a more physiological model recapitulating the adenoma-carcinoma sequence, compared to the acute AOM/DSS-dependent model.

5.4.2 Inflammation-driven intestinal carcinogenesis

IBD patients have an increased risk of colon cancer with cancer development and chronic inflammation often sharing the same molecular pathways [157]. However, the tumor-driving immune cells and cytokines are poorly understood. Grivennikov et al. recently published a milestone paper describing a key role of IL-23 in driving aberrant TH17 response and subsequent IL-17 and IL-22 cytokine production as main driver of tumor-elicited inflammation and tumor growth progression [133]. Furthermore, they describe that IL-23 is mainly produced by tumor-associated myeloid cells that are activated by penetrated microbial products into the tumor tissue due to intestinal barrier defects. Although it is hard to believe and unlikely that IL-23R deficiency or antibiotic treatment is able to rescue tumorigenesis in a mouse model for genetic mutation of the APC gene, their argumentation and data are conclusive and describe a novel microbiota dependent IL-23 and followed IL-17 cytokine expression as main tumor driving mechanism [133].

Since we observed intestinal barrier disruption and deranged microbiotic colonization in Mcl-$1^{\Delta IEC}$ mice early in the beginning of the project, we decided to house Mcl-$1^{\Delta IEC}$ mice under germ-free conditions. Indeed, in line with the Grivennikov paper, we also observed a

reduction of IL-23, IL-17 and especially IL-22 as main driver of epithelium proliferation in Mcl-$1^{\Delta IEC}$ mice under germ-free housing or antibiotic treatment. In addition, we also observed a reduced tumor burden and mucosal healing reflecting advanced tissue regeneration, confirming the role the microbiota and the penetrance of microbial products into disrupted intestinal tissue as driver of tumor progression. Based on this observation, we aimed to identify not only the cytokines but rather the responsible immune cell type.

Strikingly, the knock-out of conventional B and T-cells in the $RAG1^{-/-}$ intercrossing did not rescue the inflammatory phenotype in Mcl-$1^{\Delta IEC}$ mice and surprisingly but undoubtedly excluded TH17 immune cells as responsible cell type. Interestingly, the antibody-mediated depletion of an unconventional T-cell population called innate lymphoid cells (ILCs) rescued the inflammatory phenotype of Mcl-$1^{\Delta IEC}$ mice and also reduced the tumor burden, finally revealing an essential role of ILCs in the progression from colitis to intestinal cancer.

At the same time a paper published in the lab of Prof. F. Powrie showed exactly the same causal relationship and the role of ILCs in promoting colon cancer in a different mouse model. They took advantage of an AOM mouse model and used Helicobacter hepaticus (Hh)-driven colitis in genetically susceptible 129SvEv.$RAG^{-/-}$ mice and induced tumorigenesis by AOM treatment. By antibody depleting experiments, they showed the strongest reduction in tumor development by depleting ILCs or inhibiting ILC-derived IL22, compared to less remarkable anti-IL17 or anti-IFNγ treatments [157].

The published data can be seen as confirmation of our own finding and furthermore approved the Mcl-$1^{\Delta IEC}$ mouse model as useful tool to study human colonic carcinogenesis, but also showed the disadvantage of time consuming breeding time of Mcl-1 mice compared to easy to handle and process of infectious models. On the other hand, the finding of identifying the responsible immune cell type driving colonic cancer and the meaning for the anti-inflammatory treatment of human patients was published in an acute and AOM-dependent mouse model [157] and the exact role and function of ILCs in a chronic model are still poorly understood.

Although the responsible immune cell type is now known, the question still remains elusive how ILCs are activated upon intestinal barrier disruption. A recent publication described a co-stimulation by IL-23 and IL-1 essential for ILC activation and subsequent IL-17 secretion. Not only IL-23 but also IL-1 secretion is controlled by the Nod/Ripk2 pathway in activated dendritic cells and therefore controls colitis and colorectal carcinoma in this model [158]. In contrast, a second paper published at the same time described CX3CR1-positive mononuclear phagocytes in integrating microbial signals to regulate colonic ILC-mediated cytokine secretion and colitis in murine and human inflamed intestinal tissue. They explicitly show the importance of CX3CR1-positive mononuclear phagocytes compared to CD103-

positive dendritic cells [159]. Both groups argue conclusively based on the data obtained from their mouse models. But exactly the difference in both models, spontaneous colitis in T-bet$^{-/-}$RAG2$^{-/-}$ mice [158] and *C. rodentium* infection of Cx3cr1DTR^{+} mice with a specific depletion of colonic lamina propria mononuclear cells [159] is most reasonable the explanation for slight differences in the phenotypically outcome and the different drawn scientific conclusion. Thus, more research has to be carried out to understand the cellular an molecular mechanism driving ILC activation and subsequent intestinal inflammation and carcinogenesis.

5.4.3 Mcl-1 as key regulator of intestinal homeostasis and carcinogenesis

First of all, Mcl-1 emerged as a key regulator of homeostasis and immunity in intestinal barrier tissue. Whereas many studies are focusing at the inhibition of Mcl-1 for potential tumor therapies especially in hematological malignancy such as acute myelogenous leukemia (AML) [160]. Here, I uncovered a novel function of Mcl-1 as tumor-suppressor for intestinal carcinogenesis.

It is very well accepted that inhibition of cell death is essential for tumorigenesis and according to the Vogelstein adenoma-carcinoma sequence and the hallmarks of cancer, the loss of pro-apoptotic genes and overexpression of anti-apoptotic factors like Mcl-1 is very common during tumor progression [43, 161]. Abnormal expression of Mcl-1 as well as Bax and Bcl-xL has been described during colorectal cancer progression and overexpression of anti-apoptotic genes in colorectal cancer may suppress the activity of the pro-apoptotic molecules Bax and Bak, contributing to cancer progression [162, 163]. Especially the overexpression of Mcl-1 as the main apoptosis regulator at the outer mitochondrial membrane was shown to directly correlate with tumor grade, tumor stage and metastasis in human colorectal tumors [162, 164, 165].

In contrast to the current knowledge described in the literature, I show a novel function of Mcl-1 in preventing tumorigenesis. Mcl-1 emerged as tumor-suppressor in the intestinal epithelium by suppressing epithelial cell death followed by a sequence of hyper-proliferation, malignant transformation and finally tumorigenesis without any further genotoxic stimulus.

Actually, Mcl-1 as well as Bcl-xl are well known to be frequently amplified in a variety of human cancers. Multiple copies of the Mcl-1 gene are often present at genomic level in tumors and correlate with chromosomal amplification of the Mcl-1 gene locus and subsequent chemotherapeutic resistance [166-168]. Mcl-1 is one of nine genes in an amplification peak in cytoband 1q21.2 with amplifications observed in 10.9% of cancers across multiple tissue types [168].

Thus, at the first glance it seems to be contradictory that the lack of Mcl-1 is promotes tumor

development. But by dissecting the phenotype of Mcl-1$^{\Delta IEC}$ mice in different parts, one could get an explanation for the tumor suppressing function and the new definition of Mcl-1 as environmental tumor suppressor in regenerating tissue.

First, the Mcl-1 deletion leads to fulminant enterocyte apoptosis and therefore to a leaky intestinal barrier and followed by the influx of microbiotic components and pathogens. This means Mcl-1 is required for tissue homeostasis and tissue integrity.

Second, leakiness is triggering a strong inflammatory response and a cytokine secretion. Thus, Mcl-1 also emerged as suppressor for intestinal inflammation by preventing intestinal barrier disruption. Significantly elevated cytokines found in Mcl-1$^{\Delta IEC}$ mice such as IL-22,IL-10 and IL-6 are well known tumor-promoting cytokines by driving STAT3/NF-kB activation and aberrant epithelium hyper-proliferation [169, 170]. Hence, not Mcl-1 itself or a related intracellular function but rather the loss of enterocytes and the disruption of the mucosal integrity are associated with the pathogenesis.

Third, the vicious circle of constant enterocyte apoptosis and regeneration promotes spontaneous genetic mutations, the accumulation of genetic defects and the malignant transformation [171]. Whereas hyper-proliferation was clearly observable in apoptotic intestinal tissue, genetic defect, exactly chromosomal aberrations and oncogene/tumor suppressor gene mutation were only detected in carcinoma and not in regenerative tissue. But due to technical limitations, for conventional Sanger sequencing as well as array-based comparative genomic hybridization (aCGH) this has to be analyzed in more detail on single cell level to gain better understanding.

Aberrant apoptosis signaling represents a main mechanism through which cancer cells are enabled acquire apoptosis resistance to survive therapy, i.e. chemotherapy or irradiation-induced cell death. In more detail, Bcl-xL expression levels were significantly higher in cancer tissue than in surrounding non-malignant tissue on protein and RNA level. Whereas Mcl-1 mRNA expression was significantly lower in malignant tissues, the protein expression was significantly increased as analyzed by immunohistochemistry and immunoblotting of cell lines derived from primary tumor tissue [165]. In line with these findings, it was experimentally shown that the knock-down of Bcl-xl or Mcl-1 in cell lines of colorectal origin leads to increased sensitivity towards chemotherapeutically induced cell death as well as increased sensitivity towards death receptor induced cell death by agonistic CD95 antibody treatment [165].

The above mentioned studies clearly implicate the anti-apoptotic activity of Bcl-2 family members, such as Bcl-xL and Mcl-1 are important components of the treatment resistance of colorectal cancer cells and efforts are in progress to find specific inhibitors against Bcl2 family members for anti-tumor therapy. Especially Mcl-1 and Bcl-xl are promising targets for future cancer therapies to treat chemotherapy resistant patients. Great efforts are in progress

to find small molecules and inhibitors to target Mcl-1 for cancer therapy. The first promising inhibitor on the market was developed by the Abbott Laboratories, ABT-737 is a small molecule Bcl-2 homology (BH)-3 domain mimetic that acts as a specific inhibitor of Bcl2,Bcl-xl and Bcl-w [172]. ABT-737 treatments were successful to some extent to treat lymphoma and other blood cancer but ABT-737 failed in general because it did not inhibit the compensatory upregaulted Mcl-1.

As described in the first part of this discussion, Mcl-1 is an essential protein for tissue homeostasis, especially in regenerative tissues like liver and intestine. The systemic depletion of Mcl-1 would have dramatic short term or long-term outcome and based on the published literature [173, 174] and my own experimental findings I would expect cardiac toxicity, liver damage and intestinal tissue disruption.

In summary, I demonstrated Mcl-1 is a key regulator in the intestinal epithelium for homeostasis and preventing intestinal inflammation and tumor development and can be reported as environmental tumor suppressor in regenerating organs.

5.4.4 Intestinal epithelial apoptosis and necroptosis drive colonopathy and tumorigenesis in mouse models

Recently, proteins regulating intestinal cell death, apoptosis as well as necroptosis came into the focus of IBD research. First, a critical role was shown for Caspase 8 in regulating necroptosis of IECs. Mice with a conditional deletion of Caspase 8 in the intestinal epithelium developed a phenotype reminiscent of human Crohn's disease showing terminal ileitis [129].It was shown that Caspase 8 deficient enterocytes spontaneously undergo TNFα-dependent and RIPK3-mediated necroptosis. Due to the strong apoptotic and inflammatory phenotype and premature death of $Casp8^{\Delta IEC}$ mice, the long-term outcome of constant intestinal necroptosis related to tumor development is not shown in this mouse model. In addition, evidence for increased necroptosis in the terminal ileum of patients with Crohn's disease was shown, suggesting a potential role of necroptosis in the pathogenesis of IBD [129]. This study described that necroptosis in the intestinal epithelium is crucial for intestinal tissue homeostasis and intestinal inflammation following epithelial cell death [129]. Interestingly, the same group published a second paper about the deletion Caspase 8 inhibitor cFLIP in the intestinal epithelium. The knock-out of cFLIP leads to embryonic lethality and when cFLIP was deleted from the intestinal epithelium of adult mice using tamoxifen-inducible knock-out mice, the animals died within a few days from severe tissue destruction, epithelial cell death, and intestinal inflammation [175]. As expected, the knock-out of the negative regulator of Caspase 8 leads to a strong Caspase 8 activation upon tamoxifen induction and a Caspase 8 dependent but RIPK3-independent cell death.

Conclusively, the anti-apoptotic cFLIP is required for intestinal tissue homeostasis by controlling Caspase 8 to promote survival of intestinal epithelial cells and prevent inflammation. Furthermore, it was show that under steady-state conditions, intestinal epithelial cells depend on constitutive signaling via Caspase 8 and activation of Caspase 8 is essential for epithelial homeostasis in the steady-state. But the degree of activation is tightly controlled by cFLIP to mediate survival of epithelial cells and intestinal immune homeostasis [175].

In line with this finding, mice with an IEC-specific knock-out of FADD developed intestinal epithelial cell necroptosis and IBD-like and MyD88- and microbiota dependent inflammation. The additional genetic knock-out of RIPK3 also prevented the development of intestinal inflammation in these mice, revealing the importance of RIPK3 mediated necroptosis in intestinal tissue homeostasis [130].

Most interestingly, two independent studies by Dannappel et al. and Takahashi et al. recently showed the effects of constant apoptotic epithelial cell death on intestinal tissue homeostasis, inflammation and tumorgenesis [176, 177]. Here, they show that RIPK1 suppresses epithelial cell apoptosis and necroptosis by preventing FADD/caspase-8-mediated apoptosis and RIPK3-dependent necroptosis. These findings, together with additional experimental data about antibiotic treatment and *ex vivo* organoids, suggest that RIPK1 is a master regulator of epithelial cell survival, homeostasis and inflammation in the intestine. Moreover, by using knock-in mice expressing the kinase-inactive RIPK1 they show that as well as promoting cell death, RIPK1 has a paradoxical function in supporting the survival of mouse epithelial cells that is independent of its kinase function [176-178].

Taken together what we learn from different mouse models for intestinal pathologies:. Caspase 8-independent and RIPK3 dependent necroptotic cell death as well as Caspase 8 dependent and RIPK3-independent apoptotic epithelial cell death drive massive intestinal tissue disruption leading to intestinal barrier loss, inflammation and premature death of knock-out mice. Not only necroptosis of enterocytes as described before is able to drive intestinal colonopathies, also constant apoptotic cell death of enterocytes is able to disturb intestinal homeostasis and drive IBD-like and microbiota-dependent inflammation and tumor lesions as already seen in the Mcl-1$^{\Delta IEC}$.

The Mcl-1$^{\Delta IEC}$ model represents an additional model to investigate the consequences of apoptotic epithelial cell death. In this project, we did not focus on the mechanisms of cell death. Although we observed Caspase 8 positive apoptotic enterocytes and also the histological analysis revealed no signs of necroptosis, we have no experimental evidence for the role of RIPK3 and RIPK1-dependent necroptotic cell death. The analysis of necroptosis in this mouse model remains elusive to better understand the molecular mechanisms driving the inflammatory and tumor phenotype.

5.4.5 Position-effect variegation and environmental factors lead to phenotypical patchyness

Interestingly, the organ site of interest showing the phenotype in the intestinal tract differs a lot between the different mouse models. Taken together, all groups used the same VillinCre deleter line, initially published in 2002 by Madison et al and they use lacZ and β-Gal reporter genes to show the expression of the VillinCre transgene in the entire intestinal epithelium of mice [139]. The same VillinCre delete line was used to establish the Mcl-1$^{\Delta IEC}$ in 2010.

Thus, the question remains elusive why different sites of the whole intestinal tract are affected to such a variable degree in the various knock-out mouse models?

Mice with a conditional deletion of Caspase 8 in the intestinal epithelium spontaneously develop inflammatory lesions in the terminal ileum and mice with a specific knockout of FADD spontaneously develop the inflammatory phenotype mostly in the colon [129, 130]. Mcl-1 $^{\Delta IEC}$ showed knock-out lesions and tumor development equally distributed throughout the whole intestine and no difference in phenotype between small intestine and colon. In our model, we have performed a detailed genetic analysis of the recombination event and uncovered a patchy phenotype which strongly correlated with the phenotypical outcome of mice. By using scrapings from intestinal FFPE section or laser micro-dissected lesion, we uncovered observed an incomplete recombination event for the floxed genomic Mcl-1 locus in unaffected regions. In line, mice with a deletion of Mcl-1 nearly through the whole intestinal tract did not survived whereas mice with only very few knock-out lesions, roughly less than 5% of the intestinal tract, did not show any pathological phenotype and showed a body weight and survival similar to wild-type mice.

Therefore we can speculate about the same patchy phenotype due to incomplete genetic recombination in other published models, but there are no published data officially available, only informal statements at conferences confirmed the patchyness at least in the Casp8$^{\Delta IEC}$ model.

Epigenetic silencing or spontaneous point mutations in the Cre transgene might limit the Cre expression and these modifications could be outbred during the last years in the different mouse cohorts. But one has not only to think about the VillinCre deleter line as source of patchy genetic phenotype. Also the exact genomic locus of the floxed gene of interest and the accessibility of the chromosomal region e.g. in heterochromatin or flanking regulatory sequences has to be taken into account. It is also known that genes in the tightly packed heterochromatin are poorly expressed and can lead to position-effect variegation [179] and are described knock-out mice generated with the Cre/loxP recombination system [180, 181].

Cre transgenic mouse strains are mostly generated by random integration of a DNA construct containing the cell or tissue specific promoter and the Cre cDNA into the host DNA. The random integration may lead to unspecified genetic interactions, e.g. transactivations at

the site of integration which lead to unspecific Cre expression in other cell types [180, 181]. Indeed, the Cre expression for the VillinCre deleter line was observed in the kidney by using the lacZ reporter mouse line [139]. Most likely, the random integration site of the VillinCre construct lead to position-effect variegation and to mosaic expression of the Cre-transgene. Interestingly, the integration site of the VillinCre transgene has never been analyzed or the mosaic expression published.

In the Mcl-1$^{\Delta IEC}$ mouse model, mice which had to be sacrificed due to body weight loss and symptoms of diarrhea, showed affected areas with signs of apoptosis and tissue damage almost throughout the whole intestinal tract in contrast to almost unaffected mice which reached the age of 12 months and older. Altogether, the patchy phenotype had clear benefits because mice with a 100% knock-out of Mcl-1 most probably would not have survived and the phenotype would be most probably embryonic lethal. In addition, intestinal pathology with affected and unaffected areas is more similar to the pathology of humans. The genetic patchyness provided an experimental window to let the tumorigenic phenotype develop stepwise and finally recapitulate the whole spectrum of the adenoma-carcinoma sequence.

Furthermore, due to the rescue of Mcl-1 $^{\Delta IEC}$ under germ-free conditions or antibiotic treatment we can show in two independent experiments that the inflammatory reaction and ILC-driven enteritis in Mcl-1 $^{\Delta IEC}$ depend on the microbiotic colonization and not exclusively on mouse genetics. Additionally, two different groups describing the same apoptotic and inflammatory phenotype of Ripk1$^{\Delta IEC}$ in the ileum and the colon show a different survival rate of mice and different success upon microbiota depletion experiments [176, 177]. But these phenotypical differences are most probably caused by the housing of mice in different mouse facilities and due to different colonization of the intestine. Therefore environmental factors substantially influence the phenotype of genetically-modified mice.

6 Material and Methods

Human material: Formalin-fixed, paraffin-embedded normal or tumor tissue was retrieved from the archives of the Institute of Surgical Pathology, University Hospital Zürich. Snap-frozen liver needle biopsies from the biobank were used to extract RNA and proteins for molecular analyses. A tissue microarray (TMA) with duplicates of 95 HCC and 58 non-neoplastic liver samples was used for immunohistochemical analysis as described [17]. Follow-up data for all patients were available. The study was approved by the local ethics committee ("Kantonale Ethikkommission Zürich", application number StV26/2005 and KEK-ZH-Nr. 2013-0382).) as described.

Human cohort studies: For evaluation of liver function tests as potential predictors of HCC development, HCV-positive patients with confirmed diagnosis of HCC and HCV positive patients with liver disease but without HCC were selected from the patient database as matched pairs according to MELD score for the given time point before the HCC diagnosis. The MELD score was chosen as the current international standard for assessment of severity of liver disease e.g. in liver transplant organ allocation and is based on laboratory values bilirubin, creatinine and INR. HCV-positive patients who underwent liver transplantation (Swiss Hepato-Pancreato-Biliary Center, UniversityHospital Zürich) due to liver tumors were chosen for the transplantation study and compared to HCV-positive which underwent liver transplantation but without liver tumors development.

Mice: Animals were maintained under specific pathogen-free conditions and experiments were approved in accordance to the guidelines of the Swiss Animal Protection Law, Veterinary Office, Canton Zürich. Generation of hepatocyte specific Mcl-1 knock-out (homozygous: AlbCre$^{tg/+}$/Mcl-1$^{flox/flox}$ (Mcl-1$^{\Delta hep}$), heterozygous AlbCre$^{tg/+}$/Mcl-1$^{flox/wt}$) was described previously [55]. TNFR1$^{-/-}$ and TNFR1/2$^{-/-}$ mice were purchased from Jackson Laboratories and TNFR1$^{-/-}$ mice intercrossed to Mcl-1$^{\Delta he}$ mice and bred in house. Xiap$^{-/-}$ and cFlip mice were kindly provided [182, 183]. Tak1$^{\Delta hep}$, Casp8$^{\Delta hep}$, Tak1/Casp8$^{\Delta hep}$ and Tak1$^{\Delta hep}$/RIP3$^{-/-}$ were described previously [49]. *Ikk*$\beta^{\Delta hep}$ mice [184], *Lt*β*r*$^{\Delta hep}$ mice and *JNK1/2*$^{\Delta hep}$ mice [generated by crossing of *JNK1/2*$^{loxP/loxP}$ [185] or *Lt*β*r*$^{loxP/loxP}$ [186] with Alb-Cre mice [187]] were bred in house. Ripk1$^{-/-}$/Ripk3$^{-/-}$/Casp8$^{-/-}$, Ripk3$^{-/-}$Casp8$^{-/-}$ and Ripk3$^{-/-}$ were kindly provided and have been described recently [188].

Animal experiments: Injections of Doxorubicin (Sigma) or vehicle (DMSO) were performed as previously described [189]. Shortly, intraperitoneally (15 mg/kg) on gender and age matched mice at 6-8 weeks of age. Mice were sacrificed 12 hr or 48h post injection and

littermates carrying the respective loxP-flanked alleles but lacking the Cre recombinase served as wild-type controls. The pan-Caspase inhibitor QVD-OPh (20mg/kg, Sigma) or the RIPK1 inhibitor Necrostatin1 (6 mg/kg, Sigma) were administered intraperitoneally 1h before doxorubicin injection and repeated after 24h. Induction of hepatocyte cell death was performed as described elsewhere [190]. Shortly, mice were injected i.p. with the liver-specific transcriptional inhibitor d-(+)-galactosamine (800 mg/kg, Sigma), followed by i.v. injection with lipopolysaccharide (5mg/kg, Sigma). Eventually, mice were pre-treated 30min prior LPS/DGal injections with QVD-OPH or Nec1. For irradiation experiments, mice were irradiated with 100Rad (1Gy) and sacrificed 30min post irradiation. Two-third partial hepatectomy was performed with mice of 6 to 8 weeks previously described [191]. After surgery, mice were injected subcutaneously with buprenorphine (Temgesic; 0.1 µg/g body weight; Essex Chemie AG, Luzern, Switzerland) for analgesia. At different time points after surgery, mice were sacrificed and remaining liver tissue was harvested. Livers removed during surgery served as controls. All mice were sacrificed by CO_2 inhalation. All animal experiments were approved by the Swiss Veterinary Office (134/2014, 217/2012, 63/2011 Zürich, Switzerland) and performed according to federal and institutional guidelines.

Germ free housing and antibiotic treatment: Mcl-1$^{\Delta IEC}$ mice were embryo transferred into the germ-free facility of Prof. Andrew Macpherson (University of Berne) and mice kept and bred under axenic conditions.

Mcl-1$^{\Delta IEC}$ mice at the age of four weeks were given drinking water supplemented with antibiotics to deplete the complete microbiota under SPF housing. The mixture of antibiotics was described previously [133] and drinking water and cage bedding was changed three times per week.

Table 2 Composition of antibiotics for supplemented drinking water

Antibiotic	**dose**	**efficiency**
Ciprofloxacin	200 mg/l	bactericide (gram-negative)
Ampicillin	1 g/l	bactericide (gram-positive)
Metronidazole	1 g/l	anaerobic bacteria
Vancomycin	500 mg/l	cocci

***Ex vivo* colon culture:** Murine intestinal tissue from Mcl-1$^{\Delta IEC}$ and control mice was incubated *ex vivo* in modified cell culture medium to collect and analyze secreted cytokines in cell culture supernatant [143]. Briefly, animals were sacrificed, small intestine and colon were excised, feces flushed out with ice-cold PBS. After that, payers patches removed, tissue was cut into 1 cm pieces, opened longitudinally and washed three times with PBS and

once with specific culture medium. At least one piece of tissue was incubated at 37°C and 5% CO_2 in freshly prepared 0.5 ml culture medium in a 24-well plate. After 48 hrs, medium was collected, centrifuged for 5 min at 1000g and the supernatant was directly used for ELISA.

Table 3 Medium conditions for *ex vivo* culture of intestinal murine tissue

	For 10 ml:	Final concentration
Click's Medium		
FBS	1 ml	10%
NEAA (100x)	100 µl	1x
Gentamicin/Amphotericin (500x)	100 µl	5x
Antibiotic/Antimicotic (100x)	200 µl	2x
L-Glutamin (100x)	100 µl	1x
$NaHCO_3$ (0.5 M)	500 µl	25 mM
Na Pyruvate (1 mM)	100 µl	0.01 mM

Flow cytometry for intrahepatic immune cells: Livers were minced, digested in 0.05% Collagenase IV and hepatic lymphocytes were purified using a Ficoll gradient. Antibody staining was done in presence of Fc receptor blockade (monoclonal antibody to mouse CD16-CD32 (eBioscience) in flow cytometry buffer. A FACSCanto II or Fortessa (BD Biosciences) and FlowJo sofware (TreeStar) were used for acquisition and data analysis. LIVE/DEAD Fixable Dead Cell Stain Kit (Invitrogen) was used for exclusion of dead cells. The following antibodies were used: CD45, CD3, B220, Ly6C (eBioscience) and CD11b, Ly6G (BD Bioscience).

Flow cytometry for DNA damage: Flow cytometry for the analysis of DNA damage in hepatocytes was performed as described previously (Forment JV Cytometry A. 2012). First, primary murine hepatocytes were isolated by the two-step collagenase perfusion method, purified by Percoll gradient and finally collected in RPMI 1640 medium for flow cytometry procedures. Next, hepatcytes were fixed and permeabilized, followed by incubation with antibodies against γH2AX (#9718; Cell Signaling Technology) and RPA (NA19L, Calbiochem) and suitable secondary antibodies. DNA was stained with 1 µg/ml DAPI. Samples were measured on a Cyan ADP flow cytometer (Beckman Coulter) and analyzed with Summit software v4.3 (Beckman Coulter).

Measurement of serum parameters: The analysis for aminotransferases (AST/ALT) and bilirubin was performed with mouse serum on a Roche Modular System (Roche Diagnostics) with a commercially available automated colorimetric system at the Institute of Clinical Chemistry at the University Hospital Zürich using a Hitachi P-Modul (Roche).

RNA isolation: Total RNA from snap-frozen human liver biopsies or mouse livers was isolated using RNeasy Mini Kit (Qiagen) according to the manufactures protocol. The quantity and quality of the RNA was determined spectroscopically using a Nanodrop (Thermo Scientific).

Real-time PCR: Total RNA (1 µg) was reversely transcribed into cDNA using Quantitect Reverse Transcription Kit (Qiagen) according to the manufacturer's protocol. For mRNA expression analysis real-time PCR was performed (reactions in duplicates) using Fast Start SYBR Green Master Rox (Roche). Primers were custom made by Microsynth. Real-time PCR was performed on an ABI PRISM 7900 HT and VIIA7 Fast Real-Time PCR System (AB). Data were generated and analyzed using SDS 2.4 and RQ manager 1.2 software. For human samples, mRNA expression levels were normalized to the housekeeping gene *HPRT* and *f*or murine samples to the housekeeping gene *GAPDH.* Expression profiling of murine liver tumors for a 16 gene array to cluster the tumors according to the proliferation or differentiation status was performed as described [59]. Primer sequences for oncogene and tumor-suppressor gene expression analysis were described before [46].

DNA extraction: DNA was isolated from unstained 2 µm sections of murine or human FFPE slides by scrapings or punching from paraffin blocks and tissue digested with Proteinase K overnight. After Proteinase K inactivation for 10min at 95°C the DNA concentration was determined spectroscopically using a Nanodrop (Thermo Scientific) and genomic DNA was directly used for PCR reactions in duplicates

Taqman copy number analysis: Taqman copy number analysis was carried out as multiplex PCR in duplicates with 20 ng DNA per reaction and *Ttert* as internal reference according to the manufacturer's protocol. *Wwox, Spata22, Fhit* were selected as described markers from common fragile sites in humans and *Fgfr1* and *Fgr* were selected as genes of interest in previously published areas of genetic instability in $Tak1^{\Delta hep}$ mice [46]. Data analysis was performed using Copy Caller Software (Life Technologies).

Fragment length analysis for allelic imbalance: For analysis of allelic imbalance the markers D3S1263 and D3S1289 at described common fragile sites were selected [53]. Four

distinct regions (non-inflamed) of interest per liver needle biopsy were identified by pathologists and gDNA isolated from 2 µm unstained consecutive sections. PCR products were separated by capillary electrophoresis using the ABI 3130XL Genetic Analyzer (Applied Biosystems) and results are analyzed with the help of GeneMapper software (Applied Biosystems). Allelic imbalance was identified by calculating the fluorescence ratios of heterozygous (informative) markers for each biopsy. The following primers were used: D3S1263-Fwd CTG TTG ACC CAT TGA TAC CC (FAM labeled), D3S1263-Rev TAA AAT CAC AGC AGG GGT TC, D3S1289-Fwd AAA GCA ACT TGT AAG AGA GCA (HEX labeled), D3S1289-Rev CTC CTA GAT ATA ATC ACT GGC A.

Pulse field electrophoresis: Pulse field gel electrophoresis was performed as published previously [192, 193]. Briefly, snap-frozen liver tissue was directly put into 4% formaldehyde without thawing and incubated for 10min at 37°C. Tissue was mechanically dissociated (gentleMACS Dissociator, Miltenyi Biotec), filtered through a 70 um cell strainer (Falcon) and 2.5×10^5 cell were embedded in a 0.8% agarose plus, digested in lysis buffer (100 mM EDTA, 1% [wt/vol] sodium lauryl sarcosyne, 0.2% [wt/vol] sodium deoxycholate, and 1 mg/ml proteinase K) at 37°C for 48 h, and washed in 10 mM Tris-HCl, pH 8.0, and 100 mM EDTA. Electrophoresis was performed at 14°C in 0.9% (wt/vol) Pulsed Field Certified Agarose (Bio-Rad Laboratories) containing Tris-borate/EDTA buffer in a CHEF DR III apparatus (9 h, 120°, 5.5 V/cm, 30–18 s switch time; 6 h, 117°, 4.5 V/cm, 18–9 s switch time; 6 h, 112°, 4 V/cm, 9–5 s switch time; Bio-Rad Laboratories). The gel was stained with ethidium bromide and imaged on an Alpha Innotech Imager.

Immunoblot analysis: Snap-frozen Liver tissue was dissociated (gentleMACS Dissociator, Miltenyi Biotec) and homogenates (10%) were prepared in RIPA buffer (50 mM Tris; 1% NP40; 0.25% Deoxycholic acid sodium salt; 150 mM NaCl; 1 mM EGTA) containing Halt Protease and Phosphatase Inhibitor Cocktail (Thermo Scientific). Quantification with a BCA protein assay kit (Thermo Scientific) according to the manufacturer's manual was followed by denaturation of 80µg protein in Laemmli buffer containing 5% β-mercaptoethanol and separated by gel electrophoresis (Mini Protean Gels, Bio Rad) and blotted by semi-dry blotting (Trans-Blot Turbo Transfer, Bio Rad) onto nitrocellulose membranes (Bio Rad) and tained with Ponceau Red. Membranes were blocked in 5% milk/PBST for at least 1hr at RT. Primary antibodies against γH2AX, p-p53, GAPDH, PCNA, p-ATM, p-CHK1, p-CHK2, p-ATR, pBRCA, claved-Casp3, cleaved-Casp8, RIPK1 (all Cell Signaling) and total-Casp8 (SantaCruz) were incubated at 4°C overnight under shaking conditions. Incubation with the secondary antibody (HRP-anti rabbit IgG, 1:5000; Promega) was performed under shaking conditions for 1 hr. Detection was achieved with Clarity Western ECL Substrate (Bio Rad)

using Stella 3200 imaging system (Raytech).

Histology and immunohistochemistry: Histology and immune stainings were performed as described before [194] with antibodies against the following proteins: glutamine synthetase (GS), 1:800 dilution (abcam); b-Catenin, 1:25 dilution (6B3, Cell Signaling Technology); A6, 1:20 dilution, kindly provided by Valentina Factor. Ki67, 1:200 dilution (SP6, NeoMarkers / Lab Vision Corporation), γH2AX, 1:300 dilution (Novus Biologicals). Human tissues: Bcl2A1, 1:500 dilution (EP517Y, abcam); Tpx2, 1:500 dilution (18D5-1, abcam); Tinag, 1:250 dilution (ptglab); Plk1, 1:100 dilution (F-8, Santa Cruz); p-cJUN, 1:100 (Abcam); cleaved-Caspase 8, 1:500; p-CHK1, 1:50 and p-CHK2, 1:500 (Novus Biologicals) and p-JNK ,1:500 dilution (Abcam). For virtual microscopy and archiving, histological and immunohistochemical images were digitalized using a Nano Zoomer C9600 Virtual Slide Light microscope scanner by Hamamatsu using NDP, View Software, version 1.2.36. TMA immuno scoring was performed on TMA spots. For statistical analysis of TMA staining, Fisher`s exact test was applied using SPSS software (IBM SPSS, Version 21).

Bead-based multiplex elisa: The Bio-Plex® Multiplex System (BIO-RAD) was used to detect and quantify multiple cytokines and chemokines in serum of mice and cell culture supernatant according to the manufacturer's protocol.

RNA Microarray: An Agilent one-color microarray-based gene expression analysis (Mouse DNA Microarray 4x 44K) was performed according to the manufacturer's protocol. 2- and 12-month-old mice were analyzed. For 12 months, HCC and corresponding non-tumor tissue (n=3) from the same animal (n=5) as well as livers from Cre-negative littermates as controls (n=3) were analyzed. For 2 months, Mcl-$1^{\Delta hep}$ (AlbCre-Mcl-$1^{flox/flox}$), hemizygous Albcre-Mcl-$1^{flox/wt}$ and Cre-negative controls were analyzed. Gene expression was quantified using Agilent Feature Extraction Software Version 9.5.3.1. Gene Ontology microarray data analysis: Lists of significantly differentially expressed genes were investigated in respect to enrichment of Gene Ontology categories using the Gene Ontology Browser as implemented in GeneSpring 7.3. A Fisher's exact test was used to show whether more genes belonging to a Gene Ontology category are found in the list under investigation than in a randomized gene list of the same size.

GSEA: Gene sets from the biological process gene ontology for GSEA analysis were downloaded from the Molecular Signatures Database (http://www.broadinstitute.org) or integrated manually into the GSEA for human HCV-induced hepatitis gene expression sets [195] or alcohol-induced hepatitis [196]. GSEA tests whether genes sets were

overrepresented in microarray expression data were performed with standard settings as described before [197].

Cell lines and *in vitro* experiments: U2OS were grown in DMEM containing 10% FBS and 1% penicillin/streptomycin. Cells were transfected with lentiviral particles for Caspase 8 (Santa Cruz, sc-29930-V) or control particles (Santa Cruz, sc-108080) according to the manufacturer's protocol and cells stably expressing the shRNA were isolated by puromycin selection (Santa Cruz). Cells were treated as indicated with Doxorubicin (Sigma) and for inhibition experiments, cells were pretreated for 4h with 10 μM of the ATM inhibitor Ku-55933 (Selleckchem) or pretreated with the JNK inhibitor (SP600125, Abcam) at 25 μM and Doxorubicin added and cells incubated for indicated time.

Statistical analysis: Statistical analysis was performed using GraphPad Prism software (version 5.0) or SPSS. All data are presented as mean ± SEM and were analyzed by ANOVA with Bonferroni correction. Analysis of two samples was performed with Student *t* test, statistics for HCC incidence were calculated using Fisher's Exact test. Statistical significance is indicated as follows: ****$p < 0.0001$; ***$p < 0.001$; **$p < 0.01$; *$p < 0.05$; n.s. not significant.

7 References

1. WHO. *Cancer Fact Sheet No 297*. 2011 2011-09-21]; Available from: http://www.who.int/mediacentre/factsheets/fs297/en/index.html.
2. Forner, A., J.M. Llovet, and J. Bruix, *Hepatocellular carcinoma.* Lancet, 2012. **379**(9822): p. 1245-55.
3. Stewart, B.W. and C.P. Wild, *World Cancer Report 2014*. 2014: WHO Press.
4. AmericanCancerSociety, *Cancer Facts & Figures.* 2007.
5. Bianchini, F., R. Kaaks, and H. Vainio, *Overweight, obesity, and cancer risk.* Lancet Oncol, 2002. **3**(9): p. 565-74.
6. Malhi, H. and G.J. Gores, *Cellular and molecular mechanisms of liver injury.* Gastroenterology, 2008. **134**(6): p. 1641-54.
7. Schattenberg, J.M., P.R. Galle, and M. Schuchmann, *Apoptosis in liver disease.* Liver Int, 2006. **26**(8): p. 904-11.
8. Tai, D.I., et al., *Long-term outcome of hepatitis B e antigen-negative hepatitis B surface antigen carriers in relation to changes of alanine aminotransferase levels over time.* Hepatology, 2009. **49**(6): p. 1859-67.
9. Ruhl, C.E. and J.E. Everhart, *Elevated serum alanine aminotransferase and gamma-glutamyltransferase and mortality in the United States population.* Gastroenterology, 2009. **136**(2): p. 477-85 e11.
10. Luedde, T., N. Kaplowitz, and R.F. Schwabe, *Cell Death and Cell Death Responses in Liver Disease: Mechanisms and Clinical Relevance.* Gastroenterology, 2014.
11. Kroemer, G., et al., *Classification of cell death: recommendations of the Nomenclature Committee on Cell Death 2009.* Cell Death Differ, 2009. **16**(1): p. 3-11.
12. Galluzzi, L., et al., *Essential versus accessory aspects of cell death: recommendations of the NCCD 2015.* Cell Death Differ, 2015. **22**(1): p. 58-73.
13. Akazawa, Y. and G.J. Gores, *Death receptor-mediated liver injury.* Semin Liver Dis, 2007. **27**(4): p. 327-38.
14. Guicciardi, M.E., et al., *Apoptosis and necrosis in the liver.* Compr Physiol, 2013. **3**(2): p. 977-1010.
15. Igney, F.H. and P.H. Krammer, *Death and anti-death: tumour resistance to apoptosis.* Nat Rev Cancer, 2002. **2**(4): p. 277-88.
16. Vanden Berghe, T., et al., *Regulated necrosis: the expanding network of non-apoptotic cell death pathways.* Nat Rev Mol Cell Biol, 2014. **15**(2): p. 135-47.
17. Cain, K., S.B. Bratton, and G.M. Cohen, *The Apaf-1 apoptosome: a large caspase-activating complex.* Biochimie, 2002. **84**(2-3): p. 203-14.
18. Fulda, S. and K.M. Debatin, *Extrinsic versus intrinsic apoptosis pathways in anticancer chemotherapy.* Oncogene, 2006. **25**(34): p. 4798-811.
19. Tait, S.W. and D.R. Green, *Mitochondria and cell death: outer membrane permeabilization and beyond.* Nat Rev Mol Cell Biol, 2010. **11**(9): p. 621-32.
20. Nanji, A.A. and S. Hiller-Sturmhofel, *Apoptosis and necrosis: two types of cell death in alcoholic liver disease.* Alcohol Health Res World, 1997. **21**(4): p. 325-30.
21. Malhi, H., G.J. Gores, and J.J. Lemasters, *Apoptosis and necrosis in the liver: a tale of two deaths?* Hepatology, 2006. **43**(2 Suppl 1): p. S31-44.
22. Zhou, W. and J. Yuan, *Necroptosis in health and diseases.* Semin Cell Dev Biol, 2014.
23. Peng, Y., et al., *Innate and adaptive immune response to apoptotic cells.* J Autoimmun, 2007. **29**(4): p. 303-9.
24. Chen, G.Y. and G. Nunez, *Sterile inflammation: sensing and reacting to damage.* Nat Rev Immunol, 2010. **10**(12): p. 826-37.
25. Kaczmarek, A., P. Vandenabeele, and D.V. Krysko, *Necroptosis: the release of damage-associated molecular patterns and its physiological relevance.* Immunity, 2013. **38**(2): p. 209-23.
26. Center, M.M. and A. Jemal, *International trends in liver cancer incidence rates.* Cancer Epidemiol Biomarkers Prev, 2011. **20**(11): p. 2362-8.

27. Flejou, J.F., *[WHO Classification of digestive tumors: the fourth edition].* Ann Pathol, 2011. **31**(5 Suppl): p. S27-31.
28. El-Serag, H.B., *Hepatocellular carcinoma.* N Engl J Med, 2011. **365**(12): p. 1118-27.
29. http://www.mylivercanceroptions.com, *mylivercanceroptions.* 2002.
30. Mazzaferro, V., et al., *Liver transplantation for the treatment of small hepatocellular carcinomas in patients with cirrhosis.* N Engl J Med, 1996. **334**(11): p. 693-9.
31. Bruix, J., G.J. Gores, and V. Mazzaferro, *Hepatocellular carcinoma: clinical frontiers and perspectives.* Gut, 2014. **63**(5): p. 844-55.
32. Llovet, J.M., et al., *Sorafenib in advanced hepatocellular carcinoma.* N Engl J Med, 2008. **359**(4): p. 378-90.
33. Keating, G.M. and A. Santoro, *Sorafenib: a review of its use in advanced hepatocellular carcinoma.* Drugs, 2009. **69**(2): p. 223-40.
34. Laurent-Puig, P. and J. Zucman-Rossi, *Genetics of hepatocellular tumors.* Oncogene, 2006. **25**(27): p. 3778-86.
35. Guichard, C., et al., *Integrated analysis of somatic mutations and focal copy-number changes identifies key genes and pathways in hepatocellular carcinoma.* Nat Genet, 2012. **44**(6): p. 694-8.
36. Parada, L.A., et al., *Frequent rearrangements of chromosomes 1, 7, and 8 in primary liver cancer.* Genes Chromosomes Cancer, 1998. **23**(1): p. 26-35.
37. Rowley, J.D., *Chromosomal patterns in myelocytic leukemia.* N Engl J Med, 1973. **289**(4): p. 220-1.
38. Zucman-Rossi, J., *Molecular classification of hepatocellular carcinoma.* Dig Liver Dis, 2010. **42 Suppl 3**: p. S235-41.
39. Villanueva, A., et al., *Genomics and signaling pathways in hepatocellular carcinoma.* Semin Liver Dis, 2007. **27**(1): p. 55-76.
40. Coleman, M.L., C.J. Marshall, and M.F. Olson, *Ras promotes p21(Waf1/Cip1) protein stability via a cyclin D1-imposed block in proteasome-mediated degradation.* Embo J, 2003. **22**(9): p. 2036-46.
41. Hanahan, D. and R.A. Weinberg, *The hallmarks of cancer.* Cell, 2000. **100**(1): p. 57-70.
42. Colotta, F., et al., *Cancer-related inflammation, the seventh hallmark of cancer: links to genetic instability.* Carcinogenesis, 2009. **30**(7): p. 1073-81.
43. Hanahan, D. and R.A. Weinberg, *Hallmarks of cancer: the next generation.* Cell, 2011. **144**(5): p. 646-74.
44. Weber, A., et al., *Chronic liver inflammation and hepatocellular carcinoma: persistence matters.* Swiss Med Wkly, 2011. **141**: p. w13197.
45. Hikita, H., et al., *Bak deficiency inhibits liver carcinogenesis: a causal link between apoptosis and carcinogenesis.* J Hepatol, 2012. **57**(1): p. 92-100.
46. Bettermann, K., et al., *TAK1 suppresses a NEMO-dependent but NF-kappaB-independent pathway to liver cancer.* Cancer Cell, 2010. **17**(5): p. 481-96.
47. Vucur, M., et al., *Mouse models of hepatocarcinogenesis: what can we learn for the prevention of human hepatocellular carcinoma?* Oncotarget, 2010. **1**(5): p. 373-8.
48. Weber, A., et al., *Hepatocyte-specific deletion of the antiapoptotic protein myeloid cell leukemia-1 triggers proliferation and hepatocarcinogenesis in mice.* Hepatology, 2010. **51**(4): p. 1226-36.
49. Vucur, M., et al., *RIP3 inhibits inflammatory hepatocarcinogenesis but promotes cholestasis by controlling caspase-8- and JNK-dependent compensatory cell proliferation.* Cell Rep, 2013. **4**(4): p. 776-90.
50. Ringelhan, M., et al., *Modeling human liver cancer heterogeneity: virally induced transgenic models and mouse genetic models of chronic liver inflammation.* Curr Protoc Pharmacol, 2014. **67**: p. 14 31 1-14 31 17.
51. Matsuda, Y., et al., *DNA damage sensor gamma -H2AX is increased in preneoplastic lesions of hepatocellular carcinoma.* ScientificWorldJournal, 2013. **2013**: p. 597095.
52. Kim, H., et al., *Large liver cell change in hepatitis B virus-related liver cirrhosis.* Hepatology, 2009. **50**(3): p. 752-62.
53. Gorgoulis, V.G., et al., *Activation of the DNA damage checkpoint and genomic instability in*

human precancerous lesions. Nature, 2005. **434**(7035): p. 907-13.
54. Bartkova, J., et al., *DNA damage response as a candidate anti-cancer barrier in early human tumorigenesis.* Nature, 2005. **434**(7035): p. 864-70.
55. Vick, B., et al., *Knockout of myeloid cell leukemia-1 induces liver damage and increases apoptosis susceptibility of murine hepatocytes.* Hepatology, 2009. **49**(2): p. 627-36.
56. Bosman, F., F. Carneiro, and R. Hruban, eds. *WHO Classification of Tumours of the Digestive System* 2010.
57. Imbeaud, S., Y. Ladeiro, and J. Zucman-Rossi, *Identification of novel oncogenes and tumor suppressors in hepatocellular carcinoma.* Semin Liver Dis, 2010. **30**(1): p. 75-86.
58. Zender, L., et al., *Identification and validation of oncogenes in liver cancer using an integrative oncogenomic approach.* Cell, 2006. **125**(7): p. 1253-67.
59. Cairo, S., et al., *Hepatic stem-like phenotype and interplay of Wnt/beta-catenin and Myc signaling in aggressive childhood liver cancer.* Cancer Cell, 2008. **14**(6): p. 471-84.
60. Subramanian, A., et al., *Gene set enrichment analysis: a knowledge-based approach for interpreting genome-wide expression profiles.* Proc Natl Acad Sci U S A, 2005. **102**(43): p. 15545-50.
61. Lim, H.Y., et al., *Prediction of disease-free survival in hepatocellular carcinoma by gene expression profiling.* Ann Surg Oncol, 2013. **20**(12): p. 3747-53.
62. Satow, R., et al., *Combined functional genome survey of therapeutic targets for hepatocellular carcinoma.* Clin Cancer Res, 2010. **16**(9): p. 2518-28.
63. Xie, P., et al., *Role of extracellular matrix renal tubulo-interstitial nephritis antigen (TINag) in cell survival utilizing integrin (alpha)vbeta3/focal adhesion kinase (FAK)/phosphatidylinositol 3-kinase (PI3K)/protein kinase B-serine/threonine kinase (AKT) signaling pathway.* J Biol Chem, 2011. **286**(39): p. 34131-46.
64. Batts, K.P. and J. Ludwig, *Chronic hepatitis. An update on terminology and reporting.* Am J Surg Pathol, 1995. **19**(12): p. 1409-17.
65. Wajant, H., K. Pfizenmaier, and P. Scheurich, *Tumor necrosis factor signaling.* Cell Death Differ, 2003. **10**(1): p. 45-65.
66. Hatano, E., *Tumor necrosis factor signaling in hepatocyte apoptosis.* J Gastroenterol Hepatol, 2007. **22 Suppl 1**: p. S43-4.
67. Ogrunc, M., et al., *Oncogene-induced reactive oxygen species fuel hyperproliferation and DNA damage response activation.* Cell Death Differ, 2014. **21**(6): p. 998-1012.
68. Klaunig, J.E., L.M. Kamendulis, and B.A. Hocevar, *Oxidative stress and oxidative damage in carcinogenesis.* Toxicol Pathol, 2010. **38**(1): p. 96-109.
69. Luedde, T., et al., *Deletion of NEMO/IKKgamma in liver parenchymal cells causes steatohepatitis and hepatocellular carcinoma.* Cancer Cell, 2007. **11**(2): p. 119-32.
70. Magdalou, I., et al., *The causes of replication stress and their consequences on genome stability and cell fate.* Semin Cell Dev Biol, 2014. **30**: p. 154-64.
71. Zeman, M.K. and K.A. Cimprich, *Causes and consequences of replication stress.* Nat Cell Biol, 2014. **16**(1): p. 2-9.
72. Barash, H., et al., *Accelerated carcinogenesis following liver regeneration is associated with chronic inflammation-induced double-strand DNA breaks.* Proc Natl Acad Sci U S A, 2010. **107**(5): p. 2207-12.
73. de Santibanes, E. and P.A. Clavien, *Playing Play-Doh to prevent postoperative liver failure: the "ALPPS" approach.* Ann Surg, 2012. **255**(3): p. 415-7.
74. Tacar, O., P. Sriamornsak, and C.R. Dass, *Doxorubicin: an update on anticancer molecular action, toxicity and novel drug delivery systems.* J Pharm Pharmacol, 2013. **65**(2): p. 157-70.
75. Pommier, Y., et al., *DNA topoisomerases and their poisoning by anticancer and antibacterial drugs.* Chem Biol, 2010. **17**(5): p. 421-33.
76. McIlwain, D.R., T. Berger, and T.W. Mak, *Caspase functions in cell death and disease.* Cold Spring Harb Perspect Biol, 2013. **5**(4): p. a008656.
77. Tenev, T., et al., *The Ripoptosome, a signaling platform that assembles in response to genotoxic stress and loss of IAPs.* Mol Cell, 2011. **43**(3): p. 432-48.
78. Wu, Z.H., et al., *Molecular linkage between the kinase ATM and NF-kappaB signaling in response to genotoxic stimuli.* Science, 2006. **311**(5764): p. 1141-6.

79. McCool, K.W. and S. Miyamoto, *DNA damage-dependent NF-kappaB activation: NEMO turns nuclear signaling inside out.* Immunol Rev, 2012. **246**(1): p. 311-26.
80. Sakamoto, K., et al., *Promotion of DNA repair by nuclear IKKbeta phosphorylation of ATM in response to genotoxic stimuli.* Oncogene, 2013. **32**(14): p. 1854-62.
81. Takahashi, N., et al., *Necrostatin-1 analogues: critical issues on the specificity, activity and in vivo use in experimental disease models.* Cell Death Dis, 2012. **3**: p. e437.
82. Chen, W., et al., *RIP1 maintains DNA integrity and cell proliferation by regulating PGC-1alpha-mediated mitochondrial oxidative phosphorylation and glycolysis.* Cell Death Differ, 2014. **21**(7): p. 1061-70.
83. Feoktistova, M., et al., *cIAPs block Ripoptosome formation, a RIP1/caspase-8 containing intracellular cell death complex differentially regulated by cFLIP isoforms.* Mol Cell, 2011. **43**(3): p. 449-63.
84. Biton, S. and A. Ashkenazi, *NEMO and RIP1 control cell fate in response to extensive DNA damage via TNF-alpha feedforward signaling.* Cell, 2011. **145**(1): p. 92-103.
85. Sluss, H.K. and R.J. Davis, *H2AX is a target of the JNK signaling pathway that is required for apoptotic DNA fragmentation.* Mol Cell, 2006. **23**(2): p. 152-3.
86. Picco, V. and G. Pages, *Linking JNK Activity to the DNA Damage Response.* Genes Cancer, 2013. **4**(9-10): p. 360-8.
87. Giunta, S., R. Belotserkovskaya, and S.P. Jackson, *DNA damage signaling in response to double-strand breaks during mitosis.* J Cell Biol, 2010. **190**(2): p. 197-207.
88. Shiloh, Y., *ATM: Expanding roles as a chief guardian of genome stability.* Exp Cell Res, 2014.
89. Ofengeim, D. and J. Yuan, *Regulation of RIP1 kinase signalling at the crossroads of inflammation and cell death.* Nat Rev Mol Cell Biol, 2013. **14**(11): p. 727-36.
90. Kerr, J.F., et al., *The nature of piecemeal necrosis in chronic active hepatitis.* Lancet, 1979. **2**(8147): p. 827-8.
91. Luedde, T., N. Kaplowitz, and R.F. Schwabe, *Cell death and cell death responses in liver disease: mechanisms and clinical relevance.* Gastroenterology, 2014. **147**(4): p. 765-783 e4.
92. Chen, C.F., et al., *Changes in serum levels of HBV DNA and alanine aminotransferase determine risk for hepatocellular carcinoma.* Gastroenterology, 2011. **141**(4): p. 1240-8, 1248 e1-2.
93. Tomasetti, C. and B. Vogelstein, *Cancer etiology. Variation in cancer risk among tissues can be explained by the number of stem cell divisions.* Science, 2015. **347**(6217): p. 78-81.
94. Weng, S.Y., et al., *Synergism between p53 and Mcl-1 in protecting from hepatic injury, fibrosis and cancer.* J Hepatol, 2011. **54**(4): p. 685-94.
95. Pinyol, R., et al., *Molecular profiling of liver tumors: classification and clinical translation for decision making.* Semin Liver Dis, 2014. **34**(4): p. 363-75.
96. Lecona, E. and O. Fernandez-Capetillo, *Replication stress and cancer: It takes two to tango.* Exp Cell Res, 2014. **329**(1): p. 26-34.
97. Gao, G. and D.I. Smith, *Very large common fragile site genes and their potential role in cancer development.* Cell Mol Life Sci, 2014. **71**(23): p. 4601-15.
98. Schrock, M.S. and K. Huebner, *WWOX: A fragile tumor suppressor.* Exp Biol Med (Maywood), 2014.
99. Waters, C.E., et al., *FHIT loss-induced DNA damage creates optimal APOBEC substrates: Insights into APOBEC-mediated mutagenesis.* Oncotarget, 2014.
100. Green, D.R., et al., *RIPK-dependent necrosis and its regulation by caspases: a mystery in five acts.* Mol Cell, 2011. **44**(1): p. 9-16.
101. Weinlich, R. and D.R. Green, *The Two Faces of Receptor Interacting Protein Kinase-1.* Mol Cell, 2014. **56**(4): p. 469-480.
102. Kang, T.B., et al., *Caspase-8 blocks kinase RIPK3-mediated activation of the NLRP3 inflammasome.* Immunity, 2013. **38**(1): p. 27-40.
103. Gurung, P., et al., *FADD and caspase-8 mediate priming and activation of the canonical and noncanonical Nlrp3 inflammasomes.* J Immunol, 2014. **192**(4): p. 1835-46.
104. Roth, S. and J. Ruland, *Caspase-8: clipping off RIG-I signaling.* Immunity, 2011. **34**(3): p. 283-5.

105. Shalini, S., et al., *Old, new and emerging functions of caspases.* Cell Death Differ, 2014.
106. Salvesen, G.S. and C.M. Walsh, *Functions of caspase 8: the identified and the mysterious.* Semin Immunol, 2014. **26**(3): p. 246-52.
107. Liedtke, C., et al., *Loss of caspase-8 protects mice against inflammation-related hepatocarcinogenesis but induces non-apoptotic liver injury.* Gastroenterology, 2011. **141**(6): p. 2176-87.
108. Yu, J., et al., *Methylation profiling of twenty promoter-CpG islands of genes which may contribute to hepatocellular carcinogenesis.* BMC Cancer, 2002. **2**: p. 29.
109. Cho, S., et al., *Epigenetic methylation and expression of caspase 8 and survivin in hepatocellular carcinoma.* Pathol Int, 2010. **60**(3): p. 203-11.
110. Haggar, F.A. and R.P. Boushey, *Colorectal cancer epidemiology: incidence, mortality, survival, and risk factors.* Clin Colon Rectal Surg, 2009. **22**(4): p. 191-7.
111. Fearon, E.R. and B. Vogelstein, *A genetic model for colorectal tumorigenesis.* Cell, 1990. **61**(5): p. 759-67.
112. Fodde, R., R. Smits, and H. Clevers, *APC, signal transduction and genetic instability in colorectal cancer.* Nat Rev Cancer, 2001. **1**(1): p. 55-67.
113. Cancer-Genome-Atlas-Network, *Comprehensive molecular characterization of human colon and rectal cancer.* Nature, 2012. **487**(7407): p. 330-7.
114. Ekbom, A., et al., *Ulcerative colitis and colorectal cancer. A population-based study.* N Engl J Med, 1990. **323**(18): p. 1228-33.
115. Vereecke, L., R. Beyaert, and G. van Loo, *Enterocyte death and intestinal barrier maintenance in homeostasis and disease.* Trends Mol Med, 2011. **17**(10): p. 584-93.
116. Miron, N. and V. Cristea, *Enterocytes: active cells in tolerance to food and microbial antigens in the gut.* Clin Exp Immunol, 2012. **167**(3): p. 405-12.
117. Nunes, T., C. Bernardazzi, and H.S. de Souza, *Cell Death and Inflammatory Bowel Diseases: Apoptosis, Necrosis, and Autophagy in the Intestinal Epithelium.* Biomed Res Int, 2014. **2014**: p. 218493.
118. Hocker, M. and B. Wiedenmann, *Molecular mechanisms of enteroendocrine differentiation.* Ann N Y Acad Sci, 1998. **859**: p. 160-74.
119. Abreu, M.T., *Toll-like receptor signalling in the intestinal epithelium: how bacterial recognition shapes intestinal function.* Nat Rev Immunol, 2010. **10**(2): p. 131-44.
120. Potten, C.S., et al., *The stem cells of small intestinal crypts: where are they?* Cell Prolif, 2009. **42**(6): p. 731-50.
121. Edelblum, K.L., et al., *Regulation of apoptosis during homeostasis and disease in the intestinal epithelium.* Inflamm Bowel Dis, 2006. **12**(5): p. 413-24.
122. Marchiando, A.M., et al., *The epithelial barrier is maintained by in vivo tight junction expansion during pathologic intestinal epithelial shedding.* Gastroenterology, 2011. **140**(4): p. 1208-1218 e1-2.
123. Renehan, A.G., S.P. Bach, and C.S. Potten, *The relevance of apoptosis for cellular homeostasis and tumorigenesis in the intestine.* Can J Gastroenterol, 2001. **15**(3): p. 166-76.
124. Hagiwara, C., M. Tanaka, and H. Kudo, *Increase in colorectal epithelial apoptotic cells in patients with ulcerative colitis ultimately requiring surgery.* J Gastroenterol Hepatol, 2002. **17**(7): p. 758-64.
125. Iwamoto, M., et al., *Apoptosis of crypt epithelial cells in ulcerative colitis.* J Pathol, 1996. **180**(2): p. 152-9.
126. Di Sabatino, A., et al., *Increased enterocyte apoptosis in inflamed areas of Crohn's disease.* Dis Colon Rectum, 2003. **46**(11): p. 1498-507.
127. Kaser, A., et al., *XBP1 links ER stress to intestinal inflammation and confers genetic risk for human inflammatory bowel disease.* Cell, 2008. **134**(5): p. 743-56.
128. Greten, F.R., et al., *IKKbeta links inflammation and tumorigenesis in a mouse model of colitis-associated cancer.* Cell, 2004. **118**(3): p. 285-96.
129. Gunther, C., et al., *Caspase-8 regulates TNF-alpha-induced epithelial necroptosis and terminal ileitis.* Nature, 2011. **477**(7364): p. 335-9.
130. Welz, P.S., et al., *FADD prevents RIP3-mediated epithelial cell necrosis and chronic intestinal inflammation.* Nature, 2011. **477**(7364): p. 330-4.

131. Pierdomenico, M., et al., *Necroptosis is active in children with inflammatory bowel disease and contributes to heighten intestinal inflammation.* Am J Gastroenterol, 2014. **109**(2): p. 279-87.
132. Nenci, A., et al., *Epithelial NEMO links innate immunity to chronic intestinal inflammation.* Nature, 2007. **446**(7135): p. 557-61.
133. Grivennikov, S.I., et al., *Adenoma-linked barrier defects and microbial products drive IL-23/IL-17-mediated tumour growth.* Nature, 2012. **491**(7423): p. 254-8.
134. Li, Y., et al., *Gut microbiota accelerate tumor growth via c-jun and STAT3 phosphorylation in APCMin/+ mice.* Carcinogenesis, 2012. **33**(6): p. 1231-8.
135. Helbling, M., et al., *Investigation of IL-23 (p19, p40) and IL-23R identifies nuclear expression of IL-23 p19 as a favorable prognostic factor in colorectal cancer: a retrospective multicenter study of 675 patients.* Oncotarget, 2014. **5**(13): p. 4671-82.
136. Burri, E. and C. Beglinger, *Faecal calprotectin -- a useful tool in the management of inflammatory bowel disease.* Swiss Med Wkly, 2012. **142**: p. w13557.
137. Turgeon, N., et al., *HDAC1 and HDAC2 restrain the intestinal inflammatory response by regulating intestinal epithelial cell differentiation.* PLoS One, 2013. **8**(9): p. e73785.
138. McAlpine, C.A., et al., *Intestinal-specific PPARgamma deficiency enhances tumorigenesis in ApcMin/+ mice.* Int J Cancer, 2006. **119**(10): p. 2339-46.
139. Madison, B.B., et al., *Cis elements of the villin gene control expression in restricted domains of the vertical (crypt) and horizontal (duodenum, cecum) axes of the intestine.* J Biol Chem, 2002. **277**(36): p. 33275-83.
140. Boivin, G.P., et al., *Pathology of mouse models of intestinal cancer: consensus report and recommendations.* Gastroenterology, 2003. **124**(3): p. 762-77.
141. Vogelstein, B., et al., *Cancer genome landscapes.* Science, 2013. **339**(6127): p. 1546-58.
142. Michor, F., et al., *Can chromosomal instability initiate tumorigenesis?* Semin Cancer Biol, 2005. **15**(1): p. 43-9.
143. Zenewicz, L.A., et al., *Innate and adaptive interleukin-22 protects mice from inflammatory bowel disease.* Immunity, 2008. **29**(6): p. 947-57.
144. Karczewski, J., et al., *[Role of Th17 lymphocytes in pathogenesis of colorectal cancer].* Postepy Hig Med Dosw (Online), 2014. **68**: p. 42-7.
145. De Nitto, D., et al., *Targeting IL-23 and Th17-cytokines in inflammatory bowel diseases.* Curr Pharm Des, 2010. **16**(33): p. 3656-60.
146. Gladiator, A., et al., *Cutting edge: IL-17-secreting innate lymphoid cells are essential for host defense against fungal infection.* J Immunol, 2013. **190**(2): p. 521-5.
147. Diefenbach, A., M. Colonna, and S. Koyasu, *Development, differentiation, and diversity of innate lymphoid cells.* Immunity, 2014. **41**(3): p. 354-65.
148. De Simone, V., et al., *Role of T17 cytokines in the control of colorectal cancer.* Oncoimmunology, 2013. **2**(12): p. e26617.
149. Moser, A.R., et al., *ApcMin: a mouse model for intestinal and mammary tumorigenesis.* Eur J Cancer, 1995. **31A**(7-8): p. 1061-4.
150. Moser, A.R., H.C. Pitot, and W.F. Dove, *A dominant mutation that predisposes to multiple intestinal neoplasia in the mouse.* Science, 1990. **247**(4940): p. 322-4.
151. Fodde, R., et al., *A targeted chain-termination mutation in the mouse Apc gene results in multiple intestinal tumors.* Proc Natl Acad Sci U S A, 1994. **91**(19): p. 8969-73.
152. Oshima, M., et al., *Loss of Apc heterozygosity and abnormal tissue building in nascent intestinal polyps in mice carrying a truncated Apc gene.* Proc Natl Acad Sci U S A, 1995. **92**(10): p. 4482-6.
153. Babaei-Jadidi, R., et al., *FBXW7 influences murine intestinal homeostasis and cancer, targeting Notch, Jun, and DEK for degradation.* J Exp Med, 2011. **208**(2): p. 295-312.
154. Davis, H., et al., *Investigation of the atypical FBXW7 mutation spectrum in human tumours by conditional expression of a heterozygous propellor tip missense allele in the mouse intestines.* Gut, 2014. **63**(5): p. 792-9.
155. Barderas, R., et al., *Sporadic colon cancer murine models demonstrate the value of autoantibody detection for preclinical cancer diagnosis.* Sci Rep, 2013. **3**: p. 2938.
156. Thaker, A.I., et al., *Modeling colitis-associated cancer with azoxymethane (AOM) and dextran*

sulfate sodium (DSS). J Vis Exp, 2012(67).
157. Kirchberger, S., et al., *Innate lymphoid cells sustain colon cancer through production of interleukin-22 in a mouse model.* J Exp Med, 2013. **210**(5): p. 917-31.
158. Ermann, J., et al., *Nod/Ripk2 signaling in dendritic cells activates IL-17A-secreting innate lymphoid cells and drives colitis in T-bet-/-.Rag2-/- (TRUC) mice.* Proc Natl Acad Sci U S A, 2014. **111**(25): p. E2559-66.
159. Longman, R.S., et al., *CX(3)CR1(+) mononuclear phagocytes support colitis-associated innate lymphoid cell production of IL-22.* J Exp Med, 2014. **211**(8): p. 1571-83.
160. Gores, G.J. and S.H. Kaufmann, *Selectively targeting Mcl-1 for the treatment of acute myelogenous leukemia and solid tumors.* Genes Dev, 2012. **26**(4): p. 305-11.
161. Nakamura, Y., et al., *Mutations of the adenomatous polyposis coli gene in familial polyposis coli patients and sporadic colorectal tumors.* Princess Takamatsu Symp, 1991. **22**: p. 285-92.
162. Henderson-Jackson, E.B., et al., *Correlation between Mcl-1 and pAKT protein expression in colorectal cancer.* Int J Clin Exp Pathol, 2010. **3**(8): p. 768-74.
163. Krajewska, M., et al., *Elevated expression of Bcl-X and reduced Bak in primary colorectal adenocarcinomas.* Cancer Res, 1996. **56**(10): p. 2422-7.
164. Krajewski, S., et al., *Immunohistochemical analysis of Mcl-1 protein in human tissues. Differential regulation of Mcl-1 and Bcl-2 protein production suggests a unique role for Mcl-1 in control of programmed cell death in vivo.* Am J Pathol, 1995. **146**(6): p. 1309-19.
165. Schulze-Bergkamen, H., et al., *Bcl-x(L) and Myeloid cell leukaemia-1 contribute to apoptosis resistance of colorectal cancer cells.* World J Gastroenterol, 2008. **14**(24): p. 3829-40.
166. Wei, G., et al., *Chemical genomics identifies small-molecule MCL1 repressors and BCL-xL as a predictor of MCL1 dependency.* Cancer Cell, 2012. **21**(4): p. 547-62.
167. Perciavalle, R.M. and J.T. Opferman, *Delving deeper: MCL-1's contributions to normal and cancer biology.* Trends Cell Biol, 2013. **23**(1): p. 22-9.
168. Beroukhim, R., et al., *The landscape of somatic copy-number alteration across human cancers.* Nature, 2010. **463**(7283): p. 899-905.
169. Yu, L.Z., et al., *Expression of interleukin-22/STAT3 signaling pathway in ulcerative colitis and related carcinogenesis.* World J Gastroenterol, 2013. **19**(17): p. 2638-49.
170. De Simone, V., et al., *Th17-type cytokines, IL-6 and TNF-alpha synergistically activate STAT3 and NF-kB to promote colorectal cancer cell growth.* Oncogene, 2014.
171. Lievre, A., H. Blons, and P. Laurent-Puig, *Oncogenic mutations as predictive factors in colorectal cancer.* Oncogene, 2010. **29**(21): p. 3033-43.
172. Chauhan, D., et al., *A novel Bcl-2/Bcl-X(L)/Bcl-w inhibitor ABT-737 as therapy in multiple myeloma.* Oncogene, 2007. **26**(16): p. 2374-80.
173. Wang, X., et al., *Deletion of MCL-1 causes lethal cardiac failure and mitochondrial dysfunction.* Genes Dev, 2013. **27**(12): p. 1351-64.
174. Thomas, R.L., et al., *Loss of MCL-1 leads to impaired autophagy and rapid development of heart failure.* Genes Dev, 2013. **27**(12): p. 1365-77.
175. Wittkopf, N., et al., *Cellular FLICE-like inhibitory protein secures intestinal epithelial cell survival and immune homeostasis by regulating caspase-8.* Gastroenterology, 2013. **145**(6): p. 1369-79.
176. Takahashi, N., et al., *RIPK1 ensures intestinal homeostasis by protecting the epithelium against apoptosis.* Nature, 2014. **513**(7516): p. 95-9.
177. Dannappel, M., et al., *RIPK1 maintains epithelial homeostasis by inhibiting apoptosis and necroptosis.* Nature, 2014. **513**(7516): p. 90-4.
178. Chan, F.K., *Cell biology: A guardian angel of cell integrity.* Nature, 2014. **513**(7516): p. 38-40.
179. Elgin, S.C. and G. Reuter, *Position-effect variegation, heterochromatin formation, and gene silencing in Drosophila.* Cold Spring Harb Perspect Biol, 2013. **5**(8): p. a017780.
180. Schulz, T.J., et al., *Variable expression of Cre recombinase transgenes precludes reliable prediction of tissue-specific gene disruption by tail-biopsy genotyping.* PLoS One, 2007. **2**(10): p. e1013.
181. Lloyd, V.K., et al., *Different patterns of gene silencing in position-effect variegation.* Genome, 2003. **46**(6): p. 1104-17.

182. Schattenberg, J.M., et al., *Ablation of c-FLIP in hepatocytes enhances death-receptor mediated apoptosis and toxic liver injury in vivo.* J Hepatol, 2011. **55**(6): p. 1272-80.
183. Olayioye, M.A., et al., *XIAP-deficiency leads to delayed lobuloalveolar development in the mammary gland.* Cell Death Differ, 2005. **12**(1): p. 87-90.
184. Maeda, S., et al., *IKKbeta couples hepatocyte death to cytokine-driven compensatory proliferation that promotes chemical hepatocarcinogenesis.* Cell, 2005. **121**(7): p. 977-90.
185. Das, M., et al., *The role of JNK in the development of hepatocellular carcinoma.* Genes Dev, 2011. **25**(6): p. 634-45.
186. Wang, Y., et al., *Lymphotoxin beta receptor signaling in intestinal epithelial cells orchestrates innate immune responses against mucosal bacterial infection.* Immunity, 2010. **32**(3): p. 403-13.
187. Haybaeck, J., et al., *A lymphotoxin-driven pathway to hepatocellular carcinoma.* Cancer Cell, 2009. **16**(4): p. 295-308.
188. Dillon, C.P., et al., *RIPK1 blocks early postnatal lethality mediated by caspase-8 and RIPK3.* Cell, 2014. **157**(5): p. 1189-202.
189. Bopp, A., et al., *Rac1 modulates acute and subacute genotoxin-induced hepatic stress responses, fibrosis and liver aging.* Cell Death Dis, 2013. **4**: p. e558.
190. Jost, P.J., et al., *XIAP discriminates between type I and type II FAS-induced apoptosis.* Nature, 2009. **460**(7258): p. 1035-9.
191. Bohm, F., et al., *FGF receptors 1 and 2 control chemically induced injury and compound detoxification in regenerating livers of mice.* Gastroenterology, 2010. **139**(4): p. 1385-96.
192. Neelsen, K.J., et al., *Deregulated origin licensing leads to chromosomal breaks by rereplication of a gapped DNA template.* Genes Dev, 2013. **27**(23): p. 2537-42.
193. Neelsen, K.J., et al., *Oncogenes induce genotoxic stress by mitotic processing of unusual replication intermediates.* J Cell Biol, 2013. **200**(6): p. 699-708.
194. Wolf, M.J., et al., *Metabolic activation of intrahepatic CD8+ T cells and NKT cells causes nonalcoholic steatohepatitis and liver cancer via cross-talk with hepatocytes.* Cancer Cell, 2014. **26**(4): p. 549-64.
195. Sarasin-Filipowicz, M., et al., *Interferon signaling and treatment outcome in chronic hepatitis C.* Proc Natl Acad Sci U S A, 2008. **105**(19): p. 7034-9.
196. Affo, S., et al., *Transcriptome analysis identifies TNF superfamily receptors as potential therapeutic targets in alcoholic hepatitis.* Gut, 2013. **62**(3): p. 452-60.
197. Mootha, V.K., et al., *PGC-1alpha-responsive genes involved in oxidative phosphorylation are coordinately downregulated in human diabetes.* Nat Genet, 2003. **34**(3): p. 267-73.

8 Curriculum vitae

Home Address:	Wolfbachstrasse 25 8032 Zürich
Mobile:	+41 78 857 4531
E-Mail:	y.boege@googlemail.com
Birthday:	19th October 1983
Birth name:	Yannick Thimotheus Böge
Nationality:	German
Civil status:	unmarried

since 10/2010	PhD candidate in Molecular Biology, University of Zürich University Hospital Zürich/ Institute of Surgical Pathology and Institute of Neuropathology Enrolled in the PhD program ”Cancer Biology”
01/2009 - 09/2010	Master Studies in Molecular and Cell Biology, University of Zürich Master of Science
10/2005 - 12/2008	Studies in Molecular Life Science, University of Lübeck/Germany Bachelor of Science
2004 - 2005	Military Service
2003	A-levels (German Abitur), Kaiser-Karl-Gymnasium Itzehoe/Germany

8.1 Conferences and awards

Oral and poster presentation, Keystone Symposium "*Cell Death Signaling in Cancer and the Immune System*" in Sao Paolo/Brazil, 2014
**travel grant by Hartmann-Müller Foundation and Cancer Network Zürich*

Oral presentation, *"Day of Clinical Research",* UniversityHospital Zürich/Switzerland, 2014

Oral presentations, "*Lab Retreat*", Institute of Virology/Helmholtz Center Munich, 2011-2014
**best presentation, 2014*

Poster presentation, *"Breakthroughs in Cancer Research and Therapy"*, 11th Brupbacher Symposium, UniversityHospital Zürich/Switzerland, 2013

Oral presentation, *"97. Jahrestagung der Deutschen Gesellschaft für Pathologie"*, DGPath in Heidelberg/Germany, 2013

Poster presentation, *"Annual Meeting of the Swiss and Austrian Societies of Pathology*", SGPath in Baden/Switzerland, 2013
**poster prize*

Poster presentation, *"International Liver Cancer Meeting",* EASL in Heidelberg/Germany, 2012
**poster prize, together with Dr. Friederike Böhm*

Oral presentations, "*Hepatobiliary and Gastrointestinal Research Retreat*", Institute of Visceral and Transplantation Surgery, UniversityHospital Zürich in Vulpera/Switzerland, 2011-2014

Poster presentations, *"Day of Clinical Research",* UniversityHospital Zürich/Switzerland, 2011-2013
**poster prize, together with Dr. Friederike Böhm, 2012*

Poster presentation, *"Hallmarks & horizons of cancer"*, ISREC in Lausanne/Switzerland, 2011

8.2 Teaching

Supervising of Ursula Brack, master thesis and experimental work for 4 months, 2013
"Genetic and mutation analysis of the Mcl-1$^{\Delta IEC}$ mouse model"

Supervising of Simone Büehler, master thesis and experimental work for 6 months, 2012
"*Characterization of RNA/protein expression and mutation analysis in the Mcl-1$^{\Delta IEC}$ mouse model for apoptosis- and inflammation-induced intestinal tumorigenesis*"

Teaching assistant on selected days during the block course "*Medical Immunology*", University of Zürich, BIO430, 2011-2013

Teaching assistant during the block course "*Classical and Molecular Genetics*", University of Zürich, BIO111 by Prof. M. Hengartner, 2011

8.3 Certificates

LTK Module 1: "*Introductory Course in Laboratory Animal Science"*

LTK Module 3: "*Generation of Transgenic Animals"*

LTK Module 4: "*Surgery and Anesthesia"*

Flow Cytometry Facility, University of Zürich: *"Comprehensive course in flow cytometry"*

Life Science Graduate School: "*Scientific Writing, Clinical Cancer Research, Molecular and Cell Biology of Cancer, Ethics in Science"*

Life Science Graduate School, Cancer Network Zürich: "*Organization of the 5th Student Retreat of the Cancer Biology PhD Program"*

Graduate Campus, University of Zürich: *"Project management for research", "Writing grants for research and academia"*

Functional Genomics Center Zürich, University of Zürich: *"Next-Generation Sequencing – a practical course on technologies, applications and data analysis"*

8.4 Publication list

Yannick Boege, Mohsen Maleh Mir, Akshay Ahuja, Monika Wolf, Mihael Vucur, Friederike Böhm, Lukas Frick, Joachim Mertens, Beat Müllhaupt, Holger Moch, Regina Boger, Henning Schulze-Bergkamen, Tobias Speicher, Susagna Padrissa-Altés, Sabine Werner, Christiane Koppe, Tom Lüdde, Massimo Lopes, Ricardo Weinlich, Douglas Green, Christopher Dillon, Emmanuel Dejardin, Mathias Heikenwälder* and Achim Weber*

"A novel RIPK1/c-FLIP/CASP8-dependent damage response pathway in hepatocytes is mediated by JNK signaling"

Submission in preparation

Monika Julia Wolf, Arlind Adili, Kira Piotrowitz, Zeinab Abdullah, Yannick Boege, Kerstin Stemmer, Marc Ringelhan, Nicole Simonavicius, Michèle Egger, Dirk Wohlleber, Anna Lorentzen, Claudia Einer, Sabine Schulz, Thomas Clavel, Ulrike Protzer, Christoph Thiele, Hans Zischka, Holger Moch, Matthias Tschöp, Alexei V. Tumanov, Dirk Haller, Kristian Unger, Michael Karin, Manfred Kopf, Percy Knolle, Achim Weber and Mathias Heikenwalder

"Metabolic activation of intrahepatic CD8+ T cells and NKT cells causes nonalcoholic steatohepatitis and liver cancer via cross-talk with hepatocytes"

Cancer Cell. 2014 Oct 13;26(4):549-64.

Achim Weber, Yannick Boege, Florian Reisinger, Mathias Heikenwalder

"Chronic liver inflammation and hepatocellular carcinoma: persistence matters"

Swiss Med Wkly. , 2011 141:w13197. doi: 10.4414/smw.2011.13197.

Kira Bettermann, Mihael Vucur, Johannes Haybaeck, Christiane Koppe , Jörn Janssen, Felix Heymann, Achim Weber, Ralf Weiskirchen, Christian Liedtke, Nikolaus Gassler, Michael Müller, Rita de Vos, Monika Julia Wolf, Yannick Boege, Gitta Maria Seleznik, Nicolas Zeller, Daniel Erny, Thomas Fuchs, Stefan Zoller, Stefano Cairo, Marie-Annick Buendia, Marco Prinz, Shizuo Akira, Frank Tacke, Mathias Heikenwalder, Christian Trautwein and Tom Luedde

"TAK1 suppresses a NEMO-dependent but NF-kappaB-independent pathway to liver cancer"

Cancer Cell. 2010 May 18;17(5):481-96.

9 Acknowledgement

For providing lots of help and support to make this work successful I am grateful to many people:

First of all, I would like to thank Mathias Heikenwälder and Achim Weber for all the support and encouragement during the years of my thesis, for giving me the opportunity to work on these very interesting projects, for intensive scientific discussions, for never-ending enthusiasm, and for many suggestions & ideas and finally for the opportunity to perform my PhD thesis.

I would like to thank Adriano Aguzzi for the opportunity to start my PhD thesis, for discussions, suggestions and critical questions on my projects and for his constant push to perform thorough and well-controlled experiments.

I would like to thank everybody involved in the liver project, especially Monika Wolf, Mohsen Malemir, Friederike Böhm, Renaud Maire and Marion Bawohl. Many thanks for all of your support and sharing and exchanging ideas, knowledge and experiments. Many thanks to all co-workers in the Heikenwälder group, in particular to Daniel Kull, Ruth Hillermann, Barbara Zadnich, Florian Reisinger and Arlind Adili for lots of help and support during the past years.

Furthermore, I would like to thank everybody involved in the intestine project, especially Simone Büehler and Ursula Brack for their encouragement and support during their master theses, also Lubor Borsig, Katya Kurakevich, Andrew Macpherson, Kathy McCoy, Andreas Diefenbach and Christoph Klose.

I would like to thank all collaboration partners Beat Müllhaupt, Joachim Mertens, Mihael Vucur, Tom Lüdde and Christopher Dillon, Ricardo Weinlich and Douglas Green for many cutting-edge discussions, input and providing mice. I would like to thank especially Akshay Ahuja, Raquel Herrador and Massimo Lopes for excellent and purposeful input, support and providing reagents.

Many thanks to all co-workers in the Surgical Pathology, Institute of Neuropathology and BZL for their support during the last more than five years, in particular to Mirzet Delic, Victor Escalante, Petra Schwarz, Marianne König, Peter Schramel, Martina Storz, Dieter Zimmermann, Holger Moch, Lukas Frick, Juliane Friemel, Susanne Dettwiler, André Fritsche and Peggy Tzscheetzsch.

This work was supported by grants from the Schweizerischer Nationalfond (SNF, 3/0030-146940/1) and Krebsliga Zürich (to A.W.).

Finally, I would like to thank all members of my PhD committee, Adriano Aguzzi, Mathias Heikenwälder, Achim Weber and Ian Frew for very constructive discussions, suggestions and support.